Sedimentary response to tectonism and rifting in basins on the Norwegian shelf and onshore Norway

Atle Folkestad

Thesis for the degree of Doctor Philosophiae (dr. philos.)
University of Bergen, Norway
2021

UNIVERSITY OF BERGEN

Sedimentary response to tectonism and rifting in basins on the Norwegian shelf and onshore Norway

Atle Folkestad

Thesis for the degree of Doctor Philosophiae (dr. philos.)
at the University of Bergen

Date of defense: 10.09.2021

Year: 2021

Title: Sedimentary response to tectonism and rifting in basins on the Norwegian shelf and onshore Norway

Name: Atle Folkestad

Print: Skipnes Kommunikasjon / University of Bergen

Preface to the dissertation

This dissertation is submitted for fulfilment of the degree Doctor Philosophiae at the Department of Earth Science at the University of Bergen. This dissertation consists of published studies carried out by the author as an employee in Statoil ASA, now Equinor ASA. Thus, the requirement for the Doctor Philosophiae of an independent study without supervision outside an academic institution, is fulfilled.

This dissertation consists of five published papers in international journals, four abstracts of studies presented at the American Associations of Petroleum Geologist Annual meetings (USA) and a contribution to the Norwegian Geological Society publication: *Making of the land*. All papers and abstracts have been peer reviewed. The papers and abstracts are based on individual datasets for each study, from different geographical areas and from different geological periods. Permission for reprint is obtained from all publishers.

This dissertation consists of three parts. The first part contains an introduction to the dissertation with statement of objectives, a description of the geological setting covering the five papers and a review of development in sedimentary models for stratal accumulation and methods applied. The second part consists of the five papers with an introduction and summary of each paper. The third part synthesizes the findings within the papers in the context of the aims of the dissertation.

Table of contents

Acknowledgements

My family have accepted and perhaps found it amusing that I have spent so much of my time writing in the evenings and weekends. Still, they have given me the freedom to do so and sometimes even encouraged me. For this I am grateful. I want to thank Marit and my daughters, Marianne and Frida.

At Equinor, I have the pleasure of working with many skill-full geologists, geophysicists and petrophysicists. It is an inspiring environment that has influenced much of my work that is part of this dissertation. Equinor ASA is acknowledged for allowing me to conduct these studies and let me publish them. The graphic department is acknowledged for assistance with my drawings.

I would like to thank my co-authors for being willing to go the long road with me to publish a study. As many of you know, it has not been a walk in the park. Whatever challenge the reviewers have handed us for whatever reason, we have endured and dealt with it. I have enjoyed integrating my sedimentological interpretations with structural geology and biostratigraphy which has resulted in a final interpretation on a higher level.

In addition to my co-authors, there are several people who has taken their time to advise and help me out during the process of completing these studies. To you I am in debt. Thanks to:

Kyrre Breivik

Haakon Fossen

Robert Gawthorpe

John Gjelberg

Erik P. Johannessen

James MacEachern

Ben Roger Nordås

Tore Odinsen

Signe Ottesen

Linn Orre

Martin Pearce

Paul Roberts

Arnfinn Rømuld

Tore Skar

Tor Sømme

Nicholas Satur

Ronald J. Steel

Jan Tveranger

Zbynek Veselovsky

Abstract

The Norwegian sedimentary basins offshore and onshore have in variable degree been influenced by tectonism as rifting and faulting during deposition. This stems from post-Caledonian extensional events that affected both the Devonian and Mesozoic sedimentary basins in Norway. The Mesozoic northern North Sea region experienced well-known multiple rift-phases with intervening intervals of reduced tectonic activity. This resulted in a complex sedimentary infill of the basin. However, the significance of the tectonic influence in the stratigraphy of the sedimentary basin has, to some extent, been downplayed. In many cases, this is caused by the application of the sequence stratigraphic method which conventionally has placed greatest and dominating weight on eustatic sea level changes. Among other things, this has led to the interpretation of many of the sedimentary units offshore Norway as being deposited during tectonic quiescence.

This dissertation documents and discusses the sedimentary response to tectonism based on several case-studies offshore and onshore Norway at three levels of scale: at basinal scale, at the infill style and architectural scale, and at local fault-induced depositional environment scales. At basinal scale, the impact of tectonism must be distinguished from the impact of other allogenic forces such as climate or eustasy, not least because tectonic changes cause changes in both supply and accommodation. Basins at various stages of rifting show different infill styles dependent on the interplay between accommodation space and the sediment supply. This is sometimes reflected in the depositional environments in terms of wave and fluvial influence in relative open, shallow seascapes of overfilled basins, typically during proto- and rift-initiation stages. Underfilled rift basins are sometimes dominated by tidal depositional environments, typically during syn-rift stage when rapid burial and topography allows good preservation of tidal signals. The sequence stratigraphic method can be applied to the sedimentary infill of a rift basin where parts of fault blocks have been subjected to near uniform subsidence. This implies that the method has some important limitations. At local scale, fault movement has a direct impact on the depositional environment by creating local depressions or elevating fault-footwall crests.

It is suggested that the results herein benefit our understanding of: modern sedimentary basins in terms of environmental challenges and hazards; the subsurface parts of sedimentary basins with regard to hydrocarbon exploration, production and CO_2 storage; and the general geological evolution of these sedimentary basins in Norway with application to other areas.

Authorship statement and list of papers

(The publications presented in this dissertation are the products of collaboration between the listed authors. Interpretations and conclusions in this dissertation reflect the view of the candidate, who therefore bears the responsibility of omissions and misinterpretations. An overview of the contributions of the candidate and the co-authors is presented below. Contributions by other than the authors are acknowledged at the end of each paper.

Paper 1: *Folkestad, A. & Steel, R. J. 2001. The alluvial cyclicity in Hornelen basin (Devonian Western Norway) revisited: a multiparameter sedimentary analysis and stratigraphic implications. Norwegian Petroleum Society Special Publications,* ***10****, 39-50.*

The candidate was responsible for collecting all logs and sedimentary data, interpretation and design of method with regard to quantification with analysis of the sedimentary data, and the novel sequence stratigraphic approach. The candidate wrote the paper. The study was conceptualized by R.J. Steel who provided discussions and assisted in reviewing the manuscript.

Paper 2: *Orre, L.T.E. & Folkestad A. 2019. Depositional environments of the Early to Middle Triassic Northern North Sea in a syn-rift to a post-rift setting. Geological Society, London, Special Publications,* ***64****. pp 21.*

The candidate was responsible for conceptualization of the study, description and interpretation of the Teist Formation. He also wrote the introduction, geological setting and discussion, as well as the revision of the description and interpretations of the Lomvi Formation, and revisions of the manuscript during reviews. L.T.E Orre wrote the initial manuscript - initiated, analyzed and interpreted the petrographic study of the Lomvi Formation, logged, described and interpreted the Lomvi Formation.

Paper 3: *A. Folkestad, Z. Veselovsky, P. Roberts, 2012a. Utilising borehole image logs to interpret delta to estuarine system: a case study of the subsurface Lower Jurassic Cook Formation in the Norwegian northern North Sea; Marine and Petroleum Geology,* ***29,*** *pp. 255-275.*

The candidate was responsible for conceptualization of the study, description and interpretation of the Cook Formation using the slabbed cores and wireline logs. He wrote the introduction, geological setting and discussion. Z. Veselovsky collected and interpreted the image-log data. The sedimentological interpretation of the image-log and integration with the cored strata and wireline-logs were done by the candidate with support from Z. Veselovsky. Revisions of the manuscript during reviews were done by the candidate (lead) with support of Z. Veselovsky. P. Roberts built the reservoir model which is not included in the paper.

Paper 4: *Folkestad, A., Odinsen T. H. Fossen, Pearce, M.A. 2014. Tectonic influence on the Jurassic sedimentary architecture in the northern North Sea with focus on the Brent Group. International Association of Sedimentologists. Special Publication,* ***46****, 389–416.*

The candidate was responsible for initiating and conceptualization of the study, sedimentological description and interpretation of the Brent Group of cores and wireline logs and wrote the manuscript. Biostratigraphic description and interpretation were done by M.A. Pearce. Structural geology description and interpretation of seismic data were done by Tore Odinsen with support from Haakon Fossen. Integration of the different disciplines and the discussion were done by the candidate with support from the co-authors.

Paper 5: *Folkestad, A. & Satur, N. 2008. Regressive and transgressive cycles in a rift-basin: depositional model and sedimentary partitioning of the Middle Jurassic Hugin Formation, Southern Viking Graben, North Sea. Sedimentary Geology,* ***207****, 1-21.*

The candidate was responsible for initiating and conceptualization of the study, sedimentological description and interpretation of the Hugin Formation and wrote the manuscript with support from Nicholas Satur. The candidate built the sequence stratigraphic model including the use of the sediment partitioning method. The discussion part and the revision of the paper during reviews were done equally by the candidate and Nicholas Satur.

Appendix 1a. *Folkestad, A., Ottesen, S. & Rømuld, A. 2005. Reservoirs in a structurally controlled estuary: the Jurassic Snøhvit gas condensate Field, Barents Sea, Norway. Abstract presented at the American Association of Petroleum Geologists Annual Meeting Calgary, Alberta, 19–22 June.*

The candidate (lead) was responsible for the sedimentological part, S. Ottesen for the structural geology and A. Rømuld for the biostratigraphy.

Appendix 1b. *Folkestad, A. 2008. The Snøhvit Field. In: Ramberg I.B., Brynhni I., Nøttvedt A. & Rangnes K. (eds.). The making of a land—geology of Norway. Trondheim: Geological Society of Norway, 380p.*

The candidate prepared and wrote this contribution based on an internal study conducted by the candidate, in Statoil ASA.

Appendix 1c. *Ottesen, S., Folkestad, A., Gawthorpe, R., 2005. Tectono-stratigraphic development of the Hammerfest Basin (Northern Norway) during the Jurassic to Cretaceous. Abstract presented at the American Association of Petroleum Geologists Annual Meeting Houston, Texas, 9-12 April.*

The candidate was responsible for the sedimentological part, S. Ottesen (lead) for the structural geology with support from R. Gawthorpe. Integration and interpretation of the results: equal with S. Ottesen.

Appendix 2. *Folkestad, A., Skar, T., Pearce, M., A., 2012b. Using sedimentology, bio-stratigrapy and tectonics to interpret a complex rift-graben: The Middle-Late Jurassic South Viking Graben, North Sea. Abstract presented at the American Association of Petroleum Geologists Annual Meeting Long Beach, California, 22-25 April.*

The candidate (lead) was responsible for the sedimentological part, T. Skar for the structural geology and M. A. Pearce for the biostratigraphy. The candidate was responsible for the integration and interpretation of the results with support from the co-authors.

Appendix 3. *Folkestad, A., Johannessen, E.P., Steel, R.J., 2015. Variation in stacking style of delta-estuary couplets and associated deep-marine fans: An example from the Eocene Central Basin of Spitsbergen. Abstract presented at the American Association of Petroleum Geologists Annual Meeting Denver, Colorado, 1-3 June.*

The candidate was responsible for initiating and conceptualization of the study, collecting all logs and description and interpretation of them. The candidate built the correlation panel of the three clinoforms and interpreted the sequence stratigraphic model. E.P. Johannessen and R.J. Steel provided comments to the interpretations.

1. Introduction

The stratigraphic infill and architecture of the sedimentary basins onshore and offshore Norway are the responses and product of interplay between the allogenic forces i.e. tectonics, climate and eustasy, as well as the more local and smaller scale autogenic responses within the basins. These sedimentary basins show a variety of depositional environments, internal stratigraphic stacking patterns, and perhaps also a stratigraphic cyclicity at various time scales due to different influencing roles and impact of the allogenic forces. However, there has been a tendency among studies of the sedimentary infill of these basins to relate stratigraphic changes primarily to changes in eustasy, thereby downplaying the significance of other allogenic forces. Therefore, the motivation for this dissertation is to documents and discuss the sedimentary responses to faulting and tectonism, herein interpreted as an important allogenic force in the infilling of these basins.

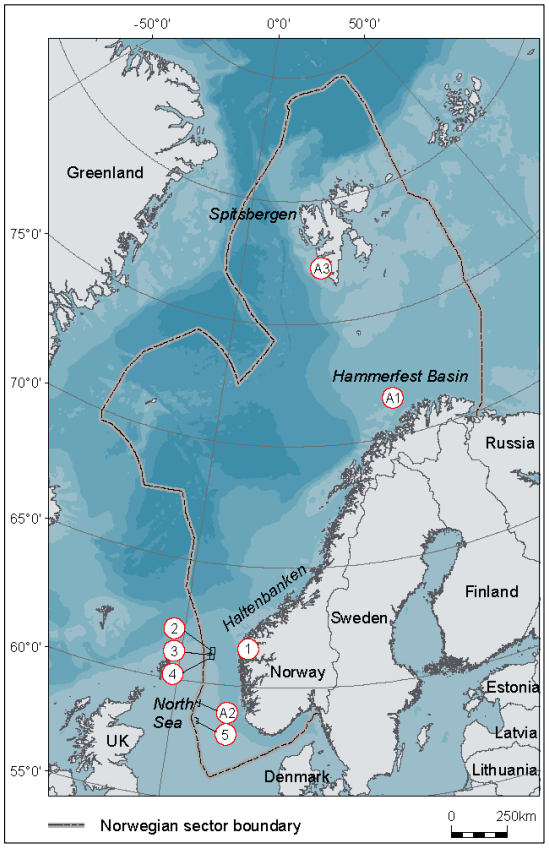

Figure 1. Location of the studies presented in this dissertation - onshore and offshore Norway. Numbers refer to paper-numbering and ´A´ refers to appendices. Modified from Kartverket.no.

In the current dissertation, a series of case studies are presented ranging from intra-cratonic alluvial to continental-margin fluvial and shallow-marine deltaic and tidal deposits. These studies have a common theme as they all address the influence of tectonism on sedimentation and sediment accumulation on various scales in different geological settings. The studies are, in a broad sense, genetically and tectonically linked in time and space from the post-

Caledonian extensional collapse that created Devonian stratigraphy along Western Norway to later reactivation of inherited weakness zones of the old Caledonian suture during subsequent lithospheric extension and rift-episodes controlling the architecture of the offshore Mesozoic margin stratigraphy. Within these examples of onshore and offshore sedimentary basins (Fig. 1), variable tectonic activity caused uplift or subsidence and formed the basins, affecting the sediment supply via topographic relief and depositional environments via geometry of accommodation space, and sometimes induced climatic changes across topographic barriers The aim of this dissertation is to demonstrate and discuss the sedimentary response to tectonic forces and active rifting based on the findings within the papers of this dissertation. The sedimentary responses are tied to different time and space scales and thus this dissertation is divided into three themes as:

1) The allogenic forces acting on the sedimentary basins were commonly dominated by tectonics, climate or eustasy; however, these factors can act in near concert. The time scales between these forces, however, can be different as tectonic processes such as thrusting and the formation of mountain ranges occur on longer time scales, typically on 1Myr or more. This time scale may also be important for long-term climate change, whereas eustatic changes in the studied basins commonly occur on a scale of about 3-400Kyr (Ravnås et al., 2000). Intra-cratonic basins, such as the Devonian Hornelen Basin (Folkestad & Steel, 2001) (Paper 1), are excluded from eustatic influence which leaves tectonic and climate as the controlling allogenic factors. In offshore basins, however, with shallow-marine conditions, eustasy has traditionally been regarded as the main control (Van Wagoner, 1995; Hampson et al., 2004), but in some cases the tectonic events and fault movements can move at a rate that masks a fluctuating eustatic sea-level signal (Folkestad & Satur, 2008, Paper 5; Folkestad et al., 2014) (Paper 4).

2) The second theme has a focus on how rifting and fault-movements may have influenced the infill of the sedimentary basins. The reasoning behind what affects the different depositional environments on local and basin-scale has changed through time as methods have become fashionable but later criticized and evolved or replaced with new methods. The break-through as regards the stratigraphic organization of

sedimentary units in a systematic way arrived with the concept of sequence stratigraphy (Vail et al., 1977) and this has dominated how shallow-marine depositional environments have been interpreted for decades. Unfortunately, this has also led to a tendency to interpret the evolution of the Jurassic sedimentary basins offshore Norway with overemphasis on eustatic fluctuations and downplay of tectonics. For example, the shallow-marine Middle Jurassic Brent Group has generally been interpreted as deposited prior to the Middle-Late Jurassic rift phase, in a tectonically quiet basin controlled by eustasy with evenly thick basinwide sand units (Helland-Hansen et al., 1992; Hampson et al., 2004; Bullimore et al., 2009; Went, et al., 2013).

In the subsurface, the identification of syn-rift sedimentary units has commonly been done by interpreting reflection seismic data (Prosser, 1993) which is limited by decreasing seismic resolution with depth. In stratigraphic successions buried at depths with reduced seismic imaging, identification of the rift initiation and early rift-stage can be challenging whereas the main rift-stage is often better defined. To overcome the resolution issue in seismic data, the rift-stages are more easily recognized in well-correlations via asymmetric-shaped stratigraphic thickness increase towards faults and through lateral changing facies interpretations from cored intervals as documented in the Brent Group by Folkestad et al., (2014) (Paper 4). These findings are important in the understanding of the evolution of a rift phase using sub-surface data.

3) The third theme focus is on the depositional environment response to fault activity, i.e. in terms of fault-induced depositional environments. Extensional fault activity and rifting creates increased accommodation with the effect of promoting transgression of the shallow-marine, shoreline system at that location. During fault-block rotation, a segregation of depositional environments occurs as the accommodation space becomes relatively low or negative (erosion) along the footwall crest areas whereas the hangingwall areas will have increased and higher accommodation space. Such a variation in accommodation space results in different depositional environments in the deeper hangingwall sites compared to the up-dip footwall sites. Extensional faulting and very rapid subsidence can cause transgression with a significant landward retreat of the shallow-marine depositional environment. In such a setting, tidal processes can

easily dominate in the coastal estuaries and outer reaches of rivers as the tidal currents will reach farther inland, at least through the backwater zone (Swenson et al., 2005). A consequence of such a transgression is a gradual landward shift of sedimentation locus, accompanied by increased thickness of the transgressive tract landward, opposite to the seaward thickening of the regressive tract. This gives a characteristic opposite skew to the thickness distribution of the transgressive and regressive units within a syn-rift sequence over relatively short distances at times (see Folkestad & Satur, 2008) (Paper 5).

In this dissertation the three themes above are referred to as:

- **Theme 1)** Allogenic forces: tectonics – climatic - eustatic controls
- **Theme 2)** Basin-wide infill style, rift-stages and sequence stratigraphic implications
- **Theme 3)** Intra-basinal fault induced depositional environments

2. Geological setting

After the formation of the prominent Caledonian Mountain range in Palaeozoic, many of the sedimentary basins onshore and offshore Norway became affected by tectonic events. The Caledonian Mountain range was formed by the collision between the Fennoscandian Shield and Greenland in Ordovician and Silurian time. The Caledonian orogenic belt extends over most of Norway today and forms the crystalline basement below the offshore sedimentary basins (Ziegler, 1990; Gabrielsen et al., 2010). The formation of this mountain range occurred through contractional forces and was followed by gravitational collapse and extension in Devonian time with formation of collapse and pull-apart basins (Steel, 1976; Folkestad & Steel, 2001) (Paper 1) (Figure 2). These pull-apart basins became imprinted onto the Caledonian crust (Beach, 1985) and they were formed by lateral movements of shear zones cutting across the northern North Sea from Norway into Scotland (Fossen et al., 2016) (Fig. 2). These basins and shear-zones had an important influence on subsequent tectonics in the region, at least in the Mesozoic (Coward, 1993).

The Caledonian Mountain range (both in Norway and Scotland) became the prominent sediment source-area for the Devonian intra-cratonic pull-apart basins. These are found along the west-coast of Norway and were filled with alluvial fans, lakes and fluvial depositional systems (Steel & Gloppen, 1980). The exposed Devonian Hornelen Basin (Folkestad & Steel, 2001) (Paper 1) (Fig. 2), shows only the roots of the Devonian deposits that became buried down to depth of greenschist facies, i.e. at depth of 8-50 km (Blatt & Tracey, 1996). The Caledonian rocks continued to act as sediment source area for the offshore sedimentary basins throughout the Triassic and Jurassic (Steel, 1993; Gabrielsen et al., 2010). As pointed out by Orre & Folkestad (2019) (Paper 2), the original burial depth (8-50 km) of the Devonian basins that are exposed today, indicates an uplift and exhumation of Norway with vast amounts of clastic sediment supplied into the adjacent basins predominately during the Mesozoic. This aligns with the suggestion of Roberts et al., (1999) that post-Devonian uplift of western Norway was in the order of 60 km due to the occurrence of basement eclogites in that area. The Mesozoic epoch was dominated by Greenhouse conditions (Nøttvedt et al., 2008)

which typically promotes high sediment yield from the sediment source areas (Carvajal et al., 2009).

In Mesozoic time, the break-up of the super-continent Pangaea commenced with the development of the Artic-North Atlantic rift in Permo-Triassic time. The rift propagated from the Barents region and southward to the North Sea Basin (Ziegler & Van Hoorn, 1989; Roberts et al., 1999) and probably followed the old Caledonian suture (Dorè et al., 1997; Nøttvedt et al., 2008) and cut across the (east-west oriented) Caledonian lineaments (Ziegler, 1990; Fossen et al., 2016) (Fig. 2). The rifting reached a climax phase in the Early Triassic in the northern North Sea with fault-orientation running north-south (Ziegler, 1990; Coward, 1993; Færseth, 1996; Odinsen et al., 2000). The Permo-Triassic rift axis was located under the Horda Platform (Færseth, 1996) (Fig. 2). In this part of the rift, the period between Middle Triassic and Early Jurassic is by several authors termed a post-rift phase (Nøttvedt et al., 1995; Ryseth, 2000; Bullimore & Helland-Hansen, 2009).

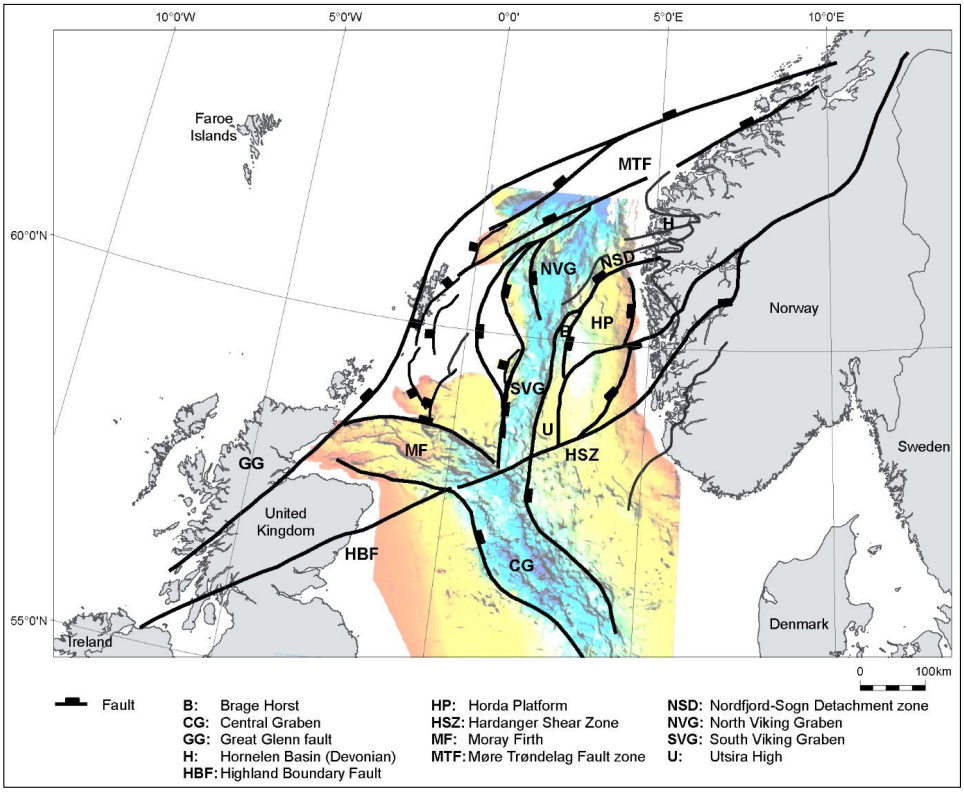

Figure 2. The northern North Sea with sub-basins indicated. The faults and lineaments of post-Caledonian extension are of Devonian origin and resembles pull-apart basins in places. Modified from Fossen et al., (2017); Orre & Folkestad (2019); Zanella & Coward, (2003). The seismic map shows Base Cretaceous Horizon and indicates the NVG, SVG, MF and CG basins. Modified from Fraser et al., (2003).

Ravnås et al., (2000), however, suggest that this period represents an inter-rift phase before the main Arctic-North Atlantic rift became reactivated again in Middle-Late Jurassic. Ziegler (1990) suggested that the rift zone became more active in the Jurassic, which implies that the rift was to some extent active through Triassic and Jurassic as an inter-rift phase, and the rift propagated again southwards in the Jurassic. This southward propagation is reflected in the development of a rift-branch in the Hammerfest Basin with syn-rift phase in Early Jurassic (Wennberg et al., 2008), rift-initiation phase in Pliensbachian in the Haltenbanken (Martinius et al., 2001) and with subsequent rift-propagation into the northern North Sea with rotation of the Permo-Triassic fault-blocks in Middle Jurassic (Bajocian) time (Folkestad et al., 2014)

(Paper 4) and farther into the South Viking Graben (Fig. 2) in Late Jurassic (Dorè et al., 1997; Folkestad & Satur, 2008) (Paper 2). The rift became a failed rift (Rattey & Hayard, 1993) and died out at the triple junction of the South Viking Graben, Moray Firth and Central Graben. Coward (1993) suggested that the Mesozoic rift-phases reactivated the old Devonian pull-apart basins in the northern North Sea and influenced the fault configuration of the Mesozoic rift-phases. This was followed up by Orre & Folkestad (2019) (Paper 2) who pointed out that the curved fault-ridges of the Mesozoic rift-basins in the northern North Sea (Lee & Hwang, 1993) resembles shapes of pull-apart basins of probably Devonian origin (Fig. 2). This would be the Devonian basins imprinted onto the Caledonian crust as suggested by Beach (1985).

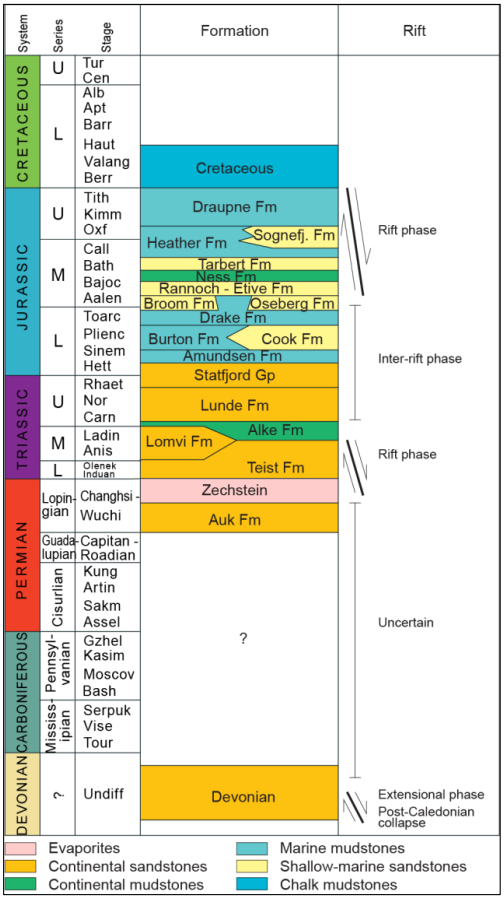

Figure 3. Stratigraphic column of the North Viking Graben.

The break-up of Pangaea in the Late Permian and Triassic was associated with volcanic activity and release of huge volumes of CO_2 giving a warming climate (Nøttvedt et al., 2008). This caused increased precipitation and weathering of the sediment source areas where the sediment yield and climatic influence is reflected in the stratigraphy and depositional environments in the Triassic (Orre & Folkestad, 2019) (Paper 2). The Permo-Triassic rifting in the northern North Sea occurred within an arid continental setting. The Triassic strata are represented by the Hegre Group (Fig. 3) which consists of the Teist, Lomvi, Alke and Lunde formations comprising fluvial channels, lakes, braided stream units, aeolian deposits and floodplain deposits

(Fig. 3). The lower Triassic succession reflects a syn-rift setting (Odinsen et al., 2000) with rotated fault-blocks filled in with lakes and fluvial deposits in the hanging wall depressions (Teist Formation) and with aeolian sands (Lomvi Formation) restricted to the elevated footwall highs (Orre & Folkestad, 2019) (Paper 2). These environments became drowned in the post-rift phase by the floodplains of the Alke Formation. The Alke Formation is the distal (mud-dominated) part of the large alluvial sedimentary wedge represented by the Lunde Formation (Middle Triassic) (Fig. 3). The Lunde Formation consists of fluvial channels, braided streams and meters-thick red-coloured overbank fines. This formation built out from Norwegian mainland and Scotland into the northern North Sea Basin and covered the whole basin. This increased sediment influx during the Triassic was caused by basin margin uplift (Nøttvedt et al., 2008) combined with high rates of precipitations and weathering due to a monsoonal effect (Orre & Folkestad, 2019) (Paper 2).

The Hegre Group is succeeded by the fluvial to shallow-marine Statfjord Group, deposited during the Late Triassic-Early Jurassic transition (Nystuen & Fält, 1995) (Fig. 3). The Statfjord Group became transgressed from the south by the Tethys Sea through the northern North Sea due to fault movements (Færseth & Ravnås, 1998) which led to the formation of the Early Jurassic Seaway (Dorè et al., 1997). This seaway followed the weakness zone of the older Artic rift-zone, being the proto-Viking Graben (Fig. 2) in the northern North Sea (Coward et al., 2003). This narrow seaway established a connection between the southern Tethys Sea and the artic Boreal Sea in the north (Gjelberg et al., 1987; Ziegler, 1990; Dorè et al., 1997). The formation of the seaway was caused by fault-activity in this period (Færseth & Ravnås, 1998), strongly suggesting that the interval of Middle Triassic to Early Jurassic represents an inter-rift phase (Færseth & Ravnås, 1998; Ravnås et al., 2000). The narrow and elongated shape of the seaway (Dorè et al., 1997) suppressed wave-action and favored instead the building of fluvio-tidal dominated deltas into the seaway as the Cook Formation (Folkestad et al., 2012a) (Paper 3) (Fig. 3). The seaway is also named ´The Viking Corridor´ by Baroni et al., (2018) and the protected basinal setting facilitated the generation of organic rich source-rocks during the ´Toarcian Anoxic Event´ (Baroni et al., 2018).

Gjelberg et al., (1987) demonstrated the link between the Early Jurassic formations in Haltenbanken and in the Hammerfest Basin and their comparable depositional evolution within the Early Jurassic Seaway. A similar comparison can be made towards the south. In the Early Jurassic, a rift-branch developed into the Hammerfest Basin with deposition of the tidal-dominated Stø formation during syn-sedimentary faulting (possibly rift initiation) (Folkestad et al., 2005, Appen. 1a; Folkestad, 2008; Appen. 1c; Ottesen et al., 2006, Appen. 1b; Wennberg et al., 2008). This evolution shows similarities to the Early Jurassic Seaway in the northern North Sea where the Pliensbachian Cook Formation accumulated with some syn-sedimentary faulting (Livbjerg & Mjøs, 1989; Folkestad et al., 2012a) (Paper 3).

The Cook Formation was subsequently drowned by offshore shales of the Drake Formation in Toarcian time (Fig. 3). This tranquil offshore environment became disrupted by a rapid build-out of Gilbert-type deltas of the Broom Formation from the East Shetland Platform during the Aalenian. Simultaneously, the Oseberg Formation built out from the Norwegian coast directed towards the Viking Graben (Fig. 3). According to Underhill & Partington (1994), the build-out of the Broom and Oseberg formations was immediately followed by an uplift of the triple junction of Central Graben, Moray Firth and South Viking Graben to the south in Aalenian time (Fig. 2). This initiated the rapid northward advancement of the Middle Jurassic Brent ´Delta´ through the Viking Graben (Helland-Hansen et al., 1992) (Fig. 2 and 4). The Brent Delta entered a slightly northward-descending ramp in the northern North Sea (Nøttvedt et al., 1995) as a consequence of the formation and deepening of the Møre Basin across the Møre-Trøndelag Fault Zone in Toarcian-Aalenian time (Brekke, 2000) (Fig. 2). This resulted in a broad wave-dominated delta front of the lower Brent Delta (Fjellanger et al., 1996; Folkestad et al., 2014) (Paper 4). The progradation of the Brent Delta halted due to an overextended delta-front (Muto & Steel, 1992) combined with the initiation of the Middle-Upper Jurassic rift phase with increased subsidence (Folkestad et al., 2014) (Paper 4) (Fig 4).

Increasing rift activity during the deposition of the Brent Group caused a change in depositional style from wave-dominance in the lower regressive part (Rannoch-Etive

formations) (Fig. 4) to overall transgressive estuaries, tidal bars and dune-fields, and spit-development in the Tarbert Formation (Folkestad et al., 2014) (Paper 4). The rifting led to a southward retreat of the transgressive depositional environments with the main rift axis placed in the Viking Graben (Fig 2). This brought the shallow-marine tidally dominated environment (Hugin Formation) (Fig. 4) into the South Viking Graben (Fig. 2) in Bathonian time, while footwall islands with attached sandstones of the Tarbert Formation, existed in the northern Viking Graben (Folkestad et al., 2012b, Appen. 2; Folkestad et al., 2014). The Middle-Late Jurassic rift-phase initiated in the Viking Graben and spread laterally outwards through time (Folkestad et al., 2014) (Paper 4) and affected (to a lesser extent) the adjacent areas as the Horda Platform in the Late Jurassic (Duffy et al., 2015). In Late Jurassic, deltaic sand sheets built out from Norway onto the relative tectonically stable Horda Platform with the Oxfordian Sognefjord Formation ´Delta´ covering most of the northern Horda Platform (Dreyer et al., 2005).

In the South Viking Graben (Fig. 2), fault-block rotation in the Middle-Late Jurassic gave a similar arrangement of the depositional environments as within the Brent Group in the North Viking Graben (Folkestad et al., 2012b, Appen. 2; Folkestad et al., 2014; Paper 4). In both areas, the deepening of the hanging walls sites facilitated the deposition of sedimentary gravity-flow deposits and the organic-rich Upper Jurassic claystones of the Draupne Formation (Fig. 4). The northern North Sea experienced its main syn-rift stage with fault-block rotation in the Late Jurassic (Callovian-Oxfordian) with some of the footwall highs lifted above sea-level and exposed to erosion. The footwall highs became thereafter straddled by the Base Cretaceous Unconformity. This was followed by thermal subsidence of the basin in a post-rift stage in Cretaceous and a general drowning of the footwall ridges (Roberts et al., 2019) that culminated with the highest sea-level in Mesozoic time.

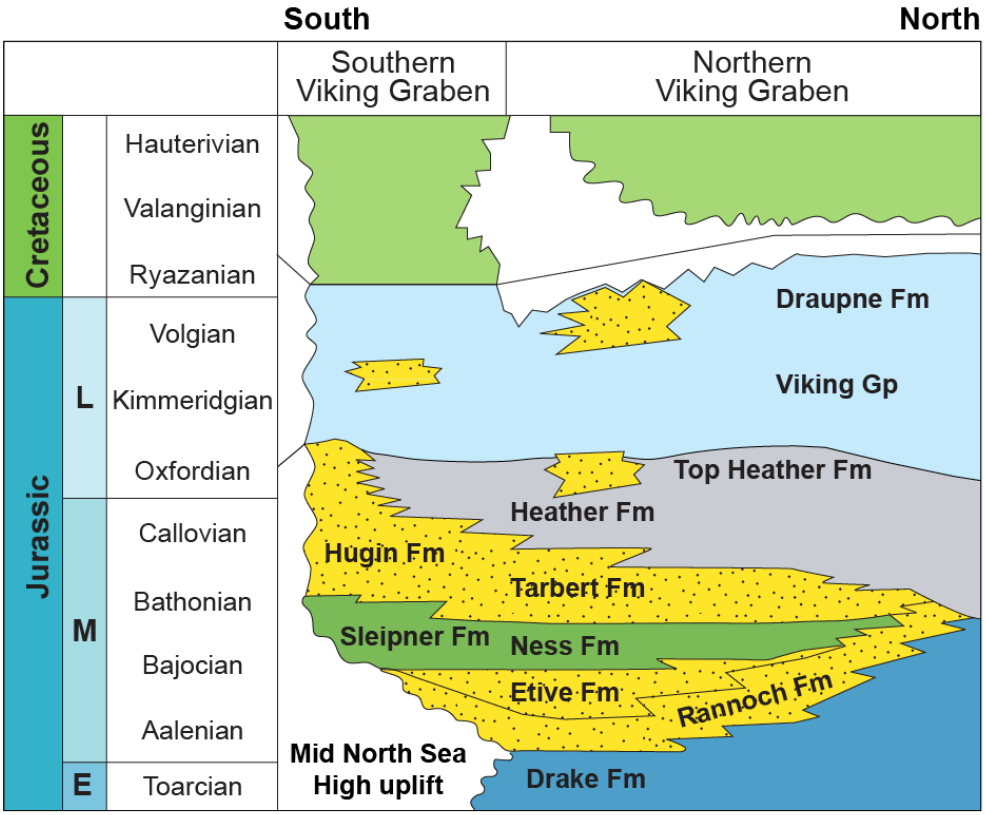

Figure 4. Stratigraphic column of the Early Jurassic to Early Cretaceous shown as a south - north transect within the Viking Graben. The Brent Group is genetically related to the Sleipner and Hugin formations in the South Viking Graben. Modified from Gradstein et al., (2010).

3. Development in sedimentary models for stratal accumulation

Sedimentology has had a series of key breakthroughs in understanding process regimes from bed-scale to basin-wide organized strata. The first step was the introduction of the concept of facies (Gressley, 1838) which enabled sedimentologists to group sedimentary strata into genetic units based on how modern environments change their facies, both along depositional strike and down depositional dip. Secondly, by using the technique that the 'present is the key to the past' (Lyell, 1830) it was possible to understand and infer the depositional system of the genetic unit by describing the vertically changing facies in the rock unit. This method became popular in the 1960`s and 70`s and was developed into the concept of 'depositional systems' and 'facies tracts' (Frazier et al., 1974) which grouped facies into successions (Walker, 1984). The third breakthrough came with the introduction of the sequence stratigraphic method (Vail et al., 1977) which enabled sedimentologists to systematize the facies successions into orderly stacking patterns within a conceptual framework bounded by basin-wide surfaces, where the basin-wide surfaces are controlled by allogenic force(s).

Vail et al., (1977) developed their new method in the shelfal part of the Gulf of Mexico by describing and interpreting seismic stratigraphy within the coastal and marine environment. In that part of the clastic sedimentological spectrum, the stratigraphic stacking pattern consists of prograding or advancing deltaic units and subsequent drowned delta-tops and shoreline retreat. The Gulf of Mexico has a wide shelf with a low tectonic subsidence rate working on long time-scale (>1Myr) and a relatively low-gradient river valley of the Mississippi. It became obvious that changes in eustatic sea-level, commonly working on timescale of 100`s Kyr, was the allocyclic (driving) force that controlled the stacking pattern. Eustatic sea-level variations arise from the variable volume of water in the global ocean linked to expanding and contracting ice-caps at the poles (Miller et al., 1998). Eustasy has, therefore, the largest impact on shallow-marine depositional systems in areas with stable shelfs where rising sea-level pushes the coastline towards the land, and seaward when its falls, even beyond the shelf edge.

It became prevalent to interpret the evolution of shallow-marine sedimentary systems and the infilling of basins with only changes in eustasy, largely ignoring or downplaying the effects of changing sediment supply, and the role of tectonics and climate in controlling both sediment supply and accommodation. This tended to dominate the sedimentological papers in the 80-90`s within the shallow-marine realm. Typically, a sequence was interpreted as two seaward stepping sand-tongues, namely the falling-stage (forced regression) to lowstand and the later highstand tongues (Hunt & Tucker, 1992) separated by a flooding surface in the middle. Unfortunately, this promoted a lacking or poor recognition of the transgressive tract as an important sedimentary package. This approach left the transgressive tract either ignored or portrayed just as a surface, and the transgression-related tidal deposits were typically downplayed in the papers on shallow-marine sequence stratigraphy as in the northern North Sea (see Hampson et al., 2004; Kiefs et al., 2010; Went et al., 2013).

Response to tectonic forces in sedimentary basins involving subsidence or uplift challenged the idea of eustasy as the unique allogenic driving force within sequence stratigraphy. This was solved by introducing the term `relative sea-level` where sea-level rise or fall is the combined product of basinal subsidence or uplift and eustatic changes (Hunt & Tucker, 1992). Modern, coastal areas with active tectonism experience typically a combined tectonic and compactional subsidence with subsidence rates of 17mm/year along the Louisiana coast (Dokka, 2006), 5mm/year in Venice (Teatini et al., 2011) and 8mm/year at Jakarta (Sarah & Soebowo, 2018). Hence, tectonic and compactional subsidence combined with eustasy gives the modern day relative sea-level rise that certain areas experience.

Tectonic forces have commonly been assumed to act on long timescales of >1 Myr whereas climatic forces act on >100Kyr (Posamentier & Allen, 1988). More recent studies (Gawthorpe et al., 1994; Catuneanu, 2002; Davis & Gibling, 2003) suggest that the tectonic subsidence can act on shorter timescale less than 1 Myr. In this way the timescale of the tectonic process may become closer towards the timescale of both eustatic cyclicity and the climatic cyclicity and mask the signal of the most dominating allogenic force. However, as cyclicity forms mainly at two different time scales

(100Kyr and at Myr) it is likely that the two different time scales require two different generating mechanisms.

The Book Cliffs of Utah and Colorado within the Cretaceous Sevier foreland basin became (and still is) the prime field location to demonstrate sequence stratigraphy with eustatic control of the sedimentary sequences (Van Wagoner, 1995). This was followed up with papers arguing for climatic glacio-eustatic control of these Cretaceous sequences in the foreland basin (Plint & Kreitner, 2007; Chen et al., 2015). Van Wagoner`s (1995) interpretations of the Book Cliff sequences were boldly challenged by Yoshida et al., (1996) who instead inferred a tectonic control of foreland basin strata as the foreland basin was formed by repeated thrusting during deposition of the strata on comparable timescales as defined by the sequences. From this, two schools of thoughts formed in the debate of eustatic (Van Wagoner, 1995; Van Wagoner, 1998; Plint & Kreitner, 2007; Hampson, 2000; Chen et al., 2015) versus tectonic (Yoshida et al., 1996; Liu & Nummedal., 2004; Fielding, 2011) control of the sedimentary sequences of the Book Cliffs and the debate is still ongoing (Fielding, 2011). The study of Yoshida et al., (1996) is one of many papers of that time that illustrate the change from the habit of having eustasy as the allocyclic control towards documenting a tectonic impact on the sedimentary infill on basin scale. The allogenic control of sequences of the Cretaceous Book Cliffs remains an open question as both climate-eustasy and tectonism may act on same timescale (Aschoff & Steel, 2011).

Within the debate on the causes of the cyclic sedimentary stacking pattern and the popularity of using eustasy as an explanation for the stratal cyclic pattern, the effects of climate became a natural component in the discussion and highlighted the sediment supply aspect (Steckler et al., 1993; Helland-Hansen & Gjelberg, 1994). Climate, in terms of temperature and precipitation (along with tectonic relief), has a clear influence on the erosion of the sediment source area and the sediment input to the receiving basins (Syvitski & Milliman, 2007). Assuming a constant subsidence rate, the prograding and retrograding stratal packages can be interpreted as variation in sediment influx, controlled by wetter (progradation) and drier (retrogradation) climate (Van Houten, 1974; Simpson & Castelltort, 2012). Climate has in addition an impact on the

depositional systems as it exerts a major control on organic productivity, where wet climate promotes vegetation and peat-formation and dryer climate promotes evaporites. Further, in fluvial systems vegetation cover is important as the sediment yield broadly varies inversely with vegetation covers (Abbink et al., 2004).

These considerations became important when the sequence stratigraphic method was also used for accumulation of continental strata. In order to adapt to the eustasy-driven sequence stratigraphic model of the coastal areas, the concept of base-level (Sloss, 1963; Wheeler, 1964) was brought forward (Shanley & McCabe, 1994) to describe the preservation of deposits. Base-level changes were formulated as the interplay between accommodation and sediment supply (Schlager, 1993; Folkestad & Steel, 2001) (Paper 1). The sedimentary stacking pattern (and its preservation) can be described by these two parameters in all depositional environments as they are not tied to a specific allocyclic process. Within the continental depositional environment, it was common for sequence stratigraphic models to acknowledge the influence of tectonism and climate as important allogenic drivers as well (Shanley & McCabe, 1994; Carroll & Bohacs, 1999).

When moving from basin-wide scale (>100 km) to intra-basinal scale (>1 km), the sedimentary response to fault activity and rifting gives local variation in the accommodation space. This can be recognized by stratal thickness differences observed in seismic, in well-correlations and in lateral difference in the style of the depositional environment. Prosser (1993), Nøttvedt et al., (1995), Færseth & Ravnås (1998), Gawthorpe & Leeder (2000) and Folkestad et al., (2014) (Paper 4) provide a list of generic key-points to identify the different stages during the development a rift. Using the thickness distribution of sedimentary units and shape of the stratal package (given a relative homogenous lithology) this can be arranged according to a pre- to syn-rift stage as:

- Proto-rift stage: Tabular units are un-affected by fault movements but can have variable thicknesses from fault block to fault block, indicative of differential subsidence or sag with minor fault-movements.

- Rift-initiation: Fault movements creates depressions at the down-faulted side which acts as local depositional centers. A scattered distribution of these fault-induced depressions indicates rift initiation. This is associated with fault propagation and linkage, initial wedge-shaped strata and initial footwall flexing.
- Main rift stage: Wedge-shaped stratal units represents the main syn-rift phase and are formed during rotation of fault blocks, experiencing lithospheric extension. This stage includes increased fault linkage, fault-death and footwall flexing. The growth strata can occur as thickening of layers or with adding of layers. Expanded growth-strata at the fault plane indicates the rate of fault-movement. Emerged fault block crest may occur.
- Late rift stage and into the post rift stage: Reduced block-rotation and emerged fault block crest occurs which can be exposed to erosion giving tilted strata cut by an angular-discordance at the top, subsequent submerged fault-block crests.

The infill of rift basins is the product of the interplay between subsidence-rate, climate, sediment supply and eustasy (Leeder & Gawthorpe, 1987). It can be challenging to separate potential climatic induced sea-level rise from rift-induced subsidence, whereas the term ´accommodation space´, and its companion sediment supply factor (Schlager, 1993), can describe the infill in temporal and spatial terms. The sediment supply is the product of the climate, tectonics and the exhumed hinterland physiography, lithology and drainage pattern. The ratio between accommodation space generation (A) and the rate and volume of sediment supply (S), shortened to A/S ratio, can be applied beyond the reach of the sea-level fluctuations in the continental environment and even be applied to aeolian deposits.

According to Nøttvedt et al., (1995) and Ravnås et al., (2000), rift-basins can further be divided into three types based on the subsidence rate (accommodation space) versus the sediment supply as:

- overfilled (A<S) where the sedimentary system is dominantly regressive and can build into adjacent basins
- balanced (A=S) where both factors are near equal and gives a vertical stack of strata
- underfilled (A>S) where the sedimentary system is dominantly transgressive, and the rift basin becomes drowned

The A/S ratio will vary within a sedimentary basin and maybe most interestingly, in a proximal to distal profile where regressive units will differ from transgressive units, both spatially and volumetrically. This is best described with the concept of sediment partitioning (Cant, 1995) within sequence stratigraphy which dictates that a regressive unit will have its thickest part basinward whereas the companion transgressive unit will become thickest landward (Fig. 5). The behavior of a deltaic to estuarine sequence can illustrate the effects of sediment partitioning (Fig. 5). The deltaic unit builds out basinward during regression due to a higher sediment supply versus accommodation space. As the delta builds out, it faces more accommodation space and at some point, the budget of sediment supply becomes exhausted and regression ceases. The shape of the regressive unit is thin landward due to limited accommodation space, thickest basinward, and thin in the very distal part due to lack of sediment supply in that location. The transgressive unit above will experience added accommodation space landward during transgression and thereby thicken landward whereas the distal part will experience sediment starvation. Hence, the regressive and transgressive units are skewed oppositely within a sequence in terms of shapes (Fig. 5). This feature is demonstrated within the sequences with deltaic-estuary couplets in the Hugin Formation (Folkestad & Satur, 2008) (Paper 5), in the Iles Formation in the Western Interior Seaway (Gomez & Steel, 2010) and within the shallow-marine clinothems of the Battfjellet Formation Spitsbergen (Folkestad et al., 2015, Appen. 3). The regressive unit commonly differ from the transgressive unit in terms of depositional environment and reservoir properties.

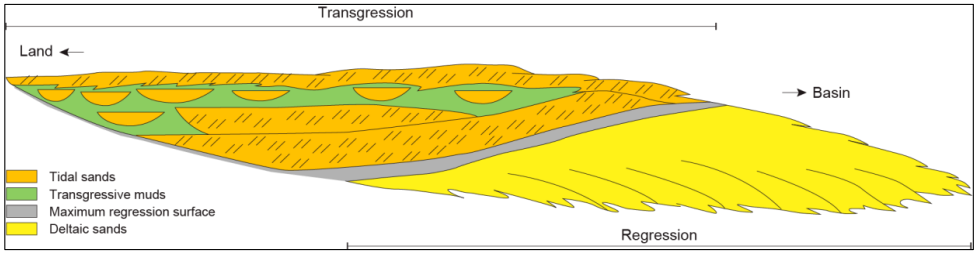

Figure 5. The concept of sediment partitioning. The regressive unit thins landward due to lack of accommodation space and thickens basinward. The distal part of the regressive unit thins and pinch-out due to lack of sediment supply at that location. The transgressive unit experiences added accommodation space landward during transgression and trap the supplied sediments there. Distally, the transgressive unit thins due to sediment starvation.

4. Introduction to the papers of this dissertation

This dissertation is built around 5 papers published in international journals and supported by 4 abstracts of presentations given at the American Association of Petroleum Geologist Annual Meetings. All papers and abstracts have been peer-reviewed. The data-types of these papers range from outcrops, cored material, wireline and image logs, biostratigraphy, seismic reflection data and petrography. Below, an introduction to each paper is given with focus on:

- purpose of the study
- key findings assigned to one of the themes
- relevance for other areas or stratigraphic units

The abstracts are referred to in connection to relevant key findings in the papers. The papers are organized in a geologic chronological order which illustrate the concept of geological inheritance.

4.1 Paper 1

Folkestad, A. & Steel, R. J. 2001. The alluvial cyclicity in Hornelen basin (Devonian Western Norway) revisited: a multiparameter sedimentary analysis and stratigraphic implications. Norwegian Petroleum Society Special Publications, ***10****, 39-50.*

The purpose of this study was to apply the sequence stratigraphic methodology to strata in a continental basin. The continental realm lacks eustatic sea-level control and therefore Shanley & McCabe (1994) suggested to use the concept of base-level (Wheeler, 1964) as the sum of the allogenic forces in continental strata. Base-level changes reflect the interplay between accommodation space generation and sediment supply. These two parameters are often used to describe sequence stratigraphic models in the shallow-marine environment (Helland-Hansen & Gjelberg, 1994) and in this way create the link into the continental sequence stratigraphic application (Shanley & McCabe, 1994).

The alluvial and fluvial Devonian Hornelen Basin on the west-coast of Norway (Fig. 1) was formed as a post-Caledonian collapse or pull-apart basin bound by a low-angle detachment zone related to the Caledonian Nordfjord-Sogn lineament (Fig. 2). The basin has a 25 km stratigraphic infill organized in about 200 upward-coarsening to fining cyclothems formed from repeated movements on the basin-bounding low-angle detachment fault. The large stratigraphic thickness and the numerous cyclothems illustrates a basinal setting with high accommodation and high sediment supply within each cyclothem, which is typical for pull-apart basins (Hempton & Dunne, 1984). The Hornelen Basin was regarded as a suitable place to interpret changing accommodation space versus sediment supply rate (A/S ratio) through the cyclothems and in this way establish a sequence stratigraphic framework. Besides interpretation of facies and facies successions, the changes in A/S ratio were interpreted from quantification of multiple sedimentary parameters which divided each cyclothem into a four-fold A/S ratio system.

This paper points out that the previous papers on the Hornelen Basin had been mainly concerned with understanding the facies and facies successions of the basin (Steel et

al., 1977). Folkestad & Steel (2001) (Paper 1) added a stratigraphic framework of each cyclothem on a more basinal scale, and thus shifted focus towards sequence stratigraphy in a continental setting (**Theme 2)**. The tectonic impact on the sedimentary infill is obvious and the most likely interpretation for the cyclic nature is repeated stress-release and slip on the basin-bounding faults (**Theme 1)**. The faults at the basin margin were part of the larger strike-slip system that formed and controlled the Devonian basins within the Scotland, North Sea to Norway transect (Coward, 1993) (Fig. 2). An anti-model would be to regard the subsidence as constant with fluctuating sediment supply. Anderson & Cross (2001) suggested a combined climatic and tectonic control of the sedimentary infill of the Devonian Hornelen Basin without being specific of which parameter was mainly responsible for the cyclicity.

The northern North Sea basins rest on a Caledonian crust that probably have Devonian pull-apart basins imprinted on to it (Beach, 1985). These offshore basins may have a similar sedimentary infill-style as described in this paper. It is worth mentioning that the bounding-faults of the Hornelen Basin are part of the system of the Caledonian lineaments cutting across the North Sea from Norway and into Scotland. These lineaments are measured to be in the order of 100 km`s of lateral movements (Fossen et al., 2016).

The alluvial cyclicity in Hornelen Basin (Devonian western Norway) revisited: a multiparameter sedimentary analysis and stratigraphic implications

Atle Folkestad and Ronald J. Steel

Accommodation space and sediment supply are the main factors controlling the spatial and stratigraphic pattern of the infill of sedimentary basins. The interaction of these factors, over periods of time, can be identified in the basin-fill succession by the changes of, for example, grain size, bed thicknesses and erosion-surface frequency, which are parameters easily measurable in outcrops as well as in cores and on image logs of subsurface successions. This study demonstrates how this approach can be used to recognise changes in the accommodation-space/sediment-supply ratio, based on an analysis of the alluvial succession in the Devonian Hornelen Basin of western Norway. Four of the basin-fill cyclothems have been logged (a total of 525 m of the basin-fill) with a systematic quantification of such parameters as grain size, bed thicknesses, erosion-surface density, occurrence of intraformational clasts and extraformational clasts, clast position within beds, and the degree of soft-sediment deformation. The analysis leads to a new understanding of the cyclicity and style of sedimentation in the Hornelen Basin.

The deposits of the alluvial succession can be divided into three facies associations: (1) fluvial channels; (2) channel-mouth splays; and (3) distal floodbasin deposits. The dynamics of basin infilling can be expressed as an interplay of stratigraphic accommodation-space creation (A) and sediment supply (S), commonly expressed as the A/S ratio. In broad terms, an increasing A/S ratio implies increasing preservation potential of sediment infill, whereas a decreasing A/S ratio signifies a decrease of preservation potential and an increasing probability of sediment bypass or erosion. Because of the critical importance of erosion in the A/S ratio concept, cycles in the A/S ratio for the succession can be identified by using peaks in the frequency of occurrence of erosion surfaces (quantified as "erosion-surface frequency") to pick A/S ratio minima, and minima of erosion surfaces to pick A/S ratio maxima.

One of the more interesting results from the study shows that peaks in grain size occur somewhat after A/S ratio minima, the offset being caused by continued high levels of sediment supply and flow competence despite a relative increase in A where the offset represents a time-lag. Bed thicknesses show low values close to the A/S ratio maxima and minima, and peak where A approaches S. The effect can be compared with the depositional pattern along the length of a clinoform with a low-angle trajectory. In a proximal position the clinothem, after a certain time period, is thin due to low A/S ratio conditions, in the distal part it is thin due to a high A/S ratio conditions, whereas the greatest thicknesses are recorded in between these two extremes. The soft-sediment deformation parameter follows the pattern of the bed thickness parameter and is thus interpreted as being linked to the bed thickness. The clast parameters (intra-, extra-formational clasts and clast position within the beds) follow the pattern of grain-size and erosion-surface frequency parameters where increasing clast occurrence reflects lower A/S ratio and decreasing clast occurrence indicates higher A/S ratio.

The approach described here can be applied easily to subsurface successions. In cored intervals, parameters such as grain size, erosion surfaces and bed thicknesses can be extracted. The same approach has been used on a Formation Micro Image Log from a well in the North Sea where bioturbation, erosion-surface density, set density and angle of lamination were quantified and cross-analysed in terms of shallowing and deepening trends.

Introduction

The dynamics of a basinal stratigraphic system can be described in terms of the changing ratio of the rate of accommodation-space development and the rate of sediment supply (referred to below as the A/S ratio) as done by Shanley and McCabe (1994). Bars, hydraulic bedforms and other geomorphic elements of a depositional system are likely to be better preserved when the A/S ratio is high, but poorer preserved when this ratio is low. Erosion and sediment bypass may prevail in the latter case.

In an alluvial basin such as the Old Red Hornelen Basin in Norway, where the sediment accumulation rates are estimated to have been as high as 2 m/ka (Steel et al., 1977), it is appropriate to consider the accumulation/preservation potential of sediments in terms of A/S ratio changes. The conceptual A/S ratio defines the dynamic state of the sedimentary system, whether it evolves towards a higher degree of preservation (maximum A/S) or a greater degree of erosional destruction (minimum A/S) of the deposits (Fig. 1) (see also Shanley and McCabe, 1994). Consequently, it can be expected, as a working hypothesis,

Sedimentary Environments Offshore Norway – Palaeozoic to Recent edited by O.J. Martinsen and T. Dreyer. NPF Special Publication 10, pp. 39–50, Published by Elsevier Science B.V., Amsterdam.

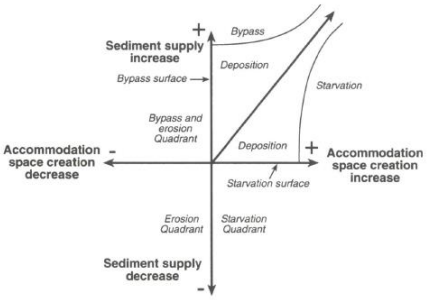

Fig. 1. Conceptual relationship between the changes in the rates of accommodation-space creation (A) and sediment supply (S). The A/S ratio defines conditions of sediment erosion, deposition and bypass (non-deposition). The negative axis of the accommodation-space creation represents erosion, whereas the negative axis of sediment supply is included to account for the mass-balance of the system; when deposition occurs in one area, erosion must occur elsewhere. The equilibrium line 1:1 in the diagram represents equal rates of accommodation-space creation and sediment supply ($A = S$). The area of bypass in the positive quadrant of the diagram ($A > 0$, $S < 0$), is meant to indicate the condition of non-deposition in a situation where the rate of sediment supply is disproportional higher than the rate of accommodation-space creation. Similarly, the area of starvation in the same quadrant indicates conditions where the rate of accommodation-space creation grossly exceeds the rate of sediment supply.

that some measurable sedimentary parameters reflecting variation in the degree of sediment preservation may indicate changes in the A/S ratio in a stratigraphic succession (see also Gardner, 1995). If this is the case, this crucial aspect of a depositional system's dynamics might then be deciphered from the sedimentary succession. The aim of the present study is to evaluate this hypothesis through an analytic approach in identifying time-trends in the A/S ratio and their turn-around points (i.e. changes from a decreasing to an increasing trend, or vice versa) in a thick, representative portion of the alluvial succession in the Hornelen Basin. The basin is probably ideal for testing such ideas because of its high but variable rates of sediment accumulation and its very thick stratigraphic succession. The quantitative method used for this purpose was originally developed by Folkestad (1995) and is presented here in a refined form.

Tectonic and stratigraphic setting

The Hornelen Basin is a small (<2000 km^2), E–W oriented, oblong basin in southwestern coastal Norway. The basin-fill has a huge stratigraphic thickness (about 25 km), consisting of conglomerates, sandstones, mudstones and siltstones, and is probably of Middle Devonian age (Steel et al., 1977; Steel, 1988). Alluvial fans, and local fan deltas developed along the margins (Steel et al., 1977; Larsen and Steel, 1978; Steel and Gloppen, 1980; Anderson, 1997) whereas a westward-directed, sandy fluvial system developed along the basin axis with a terminal floodbasin in the western part (Steel and Aasheim, 1978) (Fig. 2).

The Hornelen Basin is bounded by a low-angle listric fault in the east and high-angle normal faults to the north and south. The basin-fill succession is gently folded, with several east–west trending axes, and generally tilted towards the east, except of the northern margin where the strata tend to be deformed and often occur in a vertical position (Steel and Aasheim, 1978). The surrounding and underlying basement rocks are Precambrian gneisses and Cambro–Silurian schists, metagreywackes, metabasalts, granodiorite and gabbro of the Caledonian orogen (Bryhni, 1964; Steel et al., 1977).

The basin probably originated by gravitational collapse of the Caledonian orogen during the final stage of the orogeny (Hossack, 1984; Seguret et al., 1989). The Caledonian crust along the Fennoscandian border is thought to have been excessively thickened by the folding and thrusting, but returned to its normal (present-day) thickness by a reactivation of some of the thrusts as listric, normal detachment faults (Norton, 1986; Steel, 1988; Seranne et al., 1989; Fossen and Rykkelid, 1992). The Hornelen sedimentary succession, which developed syntectonically on a west-gliding, hanging-wall basement block, slid discontinuously westwards while rotating slightly eastwards during the extensional collapse. A clear evidence of this development can be seen along the low-angle normal fault at the eastern edge of the basin, where the basin-infill strata show a systematic eastward onlap of the footwall through time. This syntectonic and migratory aspect of the basin was first recognised by Bryhni (1964) and documented in greater detail by Steel et al. (1977) and Steel and Gloppen (1980). Steel (1988) has demonstrated that the alluvial-fan wedges along the transfer faults of the northern and southern basin margins are geometrically skewed eastwards, opposite to the direction of the tectonic displacement, supporting the extensional model for the origin of the basin. By the mid-80s, an early notion that the basin was formed purely due to strike-slip tectonics (Steel et al., 1977; Steel and Gloppen, 1980) had been replaced by the gravitational collapse model (Hossack, 1984; Steel, 1988; Seguret et al., 1989; Seranne et al., 1989). However, more recent structural research (Osmundsen et al., 1998) has re-emphasised the importance of strike-slip faulting interacting with the regional extension.

The thick infill of the Hornelen Basin is organised into more than 200 basin-wide cyclothems, 100–200 m in thickness (Fig. 3). These cyclothems, orig-

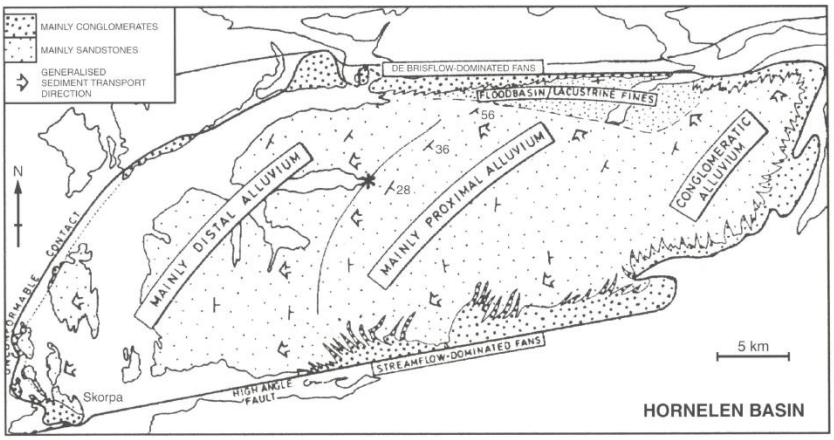

Fig. 2. Sketch map of the Hornelen Basin, showing generalised palaeo-flow direction and facies distribution (from Steel, 1988). The location of the study area is indicated by the asterisk.

inally distinguished solely on the basis of facies and grain size, have been interpreted to reflect the changing subsidence rate of the basin floor during the gravitational collapse, with the maximum rates of accommodation-space development corresponding to the fine-grained parts of the cyclothems (Steel, 1988). The cyclothems are generally asymmetrical as far as the upward change in grain size is concerned. This asymmetry is well displayed at the southern margin, where relatively thick coarsening-upward parts are capped by much thinner fining-upward parts. At the northern margin, cyclothems are less asymmetrical, with the fining-upward part constituting up to 35% of a cyclothem thickness (Gloppen and Steel, 1981; Steel, 1988). In the axial area of the basin, the cyclothems are often nearly symmetrical in terms of grain-size trend motif and facies stacking pattern, and also show abundant soft-sediment deformation (Steel and Aasheim, 1978).

The alluvial succession

The sedimentary succession of the Hornelen Basin consists of conglomeratic alluvial fan and fan delta deposits, sandy braided-stream deposits, sandy to silty floodbasin deposits and silty to muddy lacustrine deposits. The fans at the northern margin are characteristically small and steep, debris-flow dominated systems, whereas those at the southern margin are stream-flow dominated, with greater radii and gentler slopes (Gloppen and Steel, 1981) (Fig. 2). The axial part of the basin-fill succession was deposited by an extensive, sand-prone fluvial system debouching westwards and northwards into a floodbasin/lacustrine area, rendering it a kind of basin-axis terminal fan, or lacustrine braid-plain delta. The alluvium of the axial fluvial system shows a downstream lateral facies change, with trough cross-stratified coarse pebbly sandstones and conglomerates giving way to finer-grained sandstones characterised by planar cross-stratification and further passing into an assemblage of alternating fine-grained sandstones, siltstones and mudstones, dominated by ripple cross-lamination (Steel and Aasheim, 1978). The palaeo-current measurements in the axial alluvium are consistent with a westerly transport, but with secondary deviations towards both northwest and southwest (Fig. 2).

The representative portion of the axial alluvial succession selected for the present study is in the western, relatively distal part of the basin (Fig. 2). The sedimentary succession logged is 525 m thick and comprises four sections, labelled 1–4 (Fig. 3). Four 2-D panels (Figs. 4 and 5) showing the sedimentary architecture of the alluvium have been constructed on the basis of section 2 (Fig. 3) to illustrate the character of facies associations, the stacking patterns of facies and the lateral persistence of beds and bed sets. The deposits have been grouped into three facies associations, interpreted to be floodbasin facies, channel-mouth splay facies, and fluvial channel facies. The three facies associations are described briefly below, and their broader basinal context and more detailed description are given by Steel and Aasheim (1978), and Folkestad (1995).

Fig. 3. An oblique eastward aerial view of the axial part of the Hornelen Basin, showing the spectacular basin-wide cyclothems 100–200 m thick, represented by the morphological steps. The measured Sections 1–4 are indicated by the white bars, with a total thickness of 525 m. Courtesy of Bremanger Kommune©.

The *fluvial channel* facies association consists of mainly medium-grained sandstones dominated by an alternation of planar tabular cross-stratification and tangential low-angle cross-stratification, with multiple erosion surfaces (Fig. 4C). The cross-stratified sandstones tend to be overlain by slightly finer-grained sandstones with medium-scale trough cross-stratification and/or planar-parallel stratification (commonly showing parting lineation), but this trend is less obvious where frequent erosion surfaces occur. Soft-sediment deformation is relatively rare in this facies association. The multiple erosional surfaces, the stratification types and the sheet-like geometry of the bed sets suggest relatively broad and shallow braided streams, possibly flashy and ephemeral, dominated by transverse and longitudinal bars (see also Cant and Walker, 1978; Miall, 1985). The planar-parallel stratification indicates channel shoaling, whereas the occasional occurrences of trough cross-stratification scoured into the bar tops suggest some cross-cutting minor channels, formed at the falling stage of stream flood. The lack of vegetation in Devonian time is likely to have promoted the development of such a fluvial system (Schumm, 1968; Macnaughton et al., 1997).

The *channel-mouth splay* facies association is dominated by fine-grained, low-angle stratified sandstones with subordinate, but occasionally relatively thick, planar cross-stratified sets, accompanied by very fine-grained sandstones with planar-parallel stratification and abundant soft-sediment deformation features (Fig. 4B,C and Fig. 5). Sandstone units with trough cross-stratification and ripple cross-lamination, commonly convoluted, are minor components of this facies association. The ripple cross-lamination occasionally indicates wave action. The depositional units are characterised by a coarsening-upward transition from mudstone and siltstones or very fine-grained, wave ripple-laminated sandstone to fine-grained, low-angle cross-stratified sandstone, and eventually to planar cross-stratified, fine-grained sandstones (Fig. 4C and Fig. 5). The latter is typically a solitary cross-set, sigmoidal or top-truncated, tangential, often strongly deformed. This coarsening- and thickening-upward motif is followed in turn by a fining-upward trend of a fine-grained, low-angle strat-

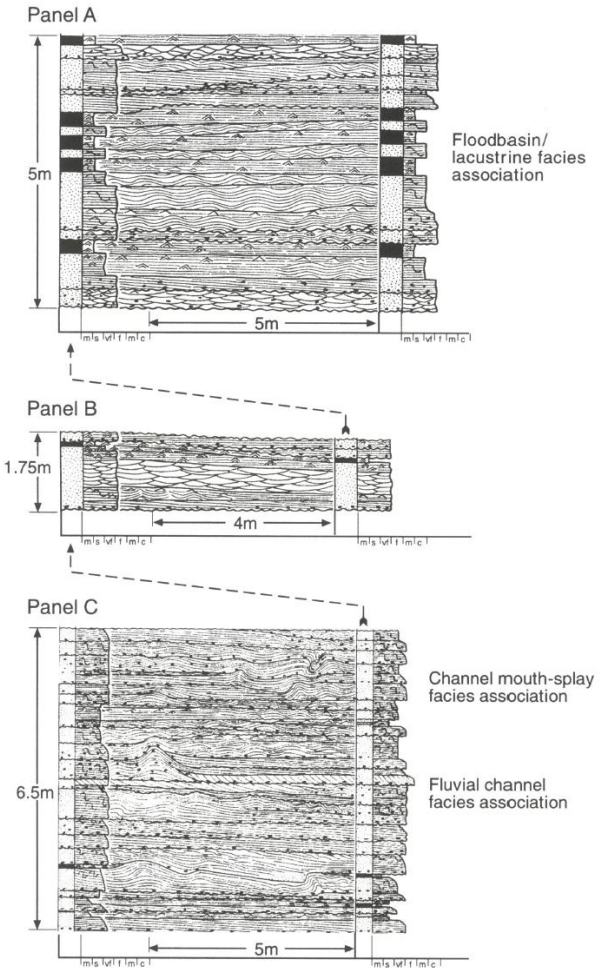

Fig. 4. Field-measured stratigraphic logs and facies distribution panels. Panels A and B show the channel-mouth splay and floodbasin/lacustrine facies associations, and panel C show the fluvial channel-mouth splay facies associations. The three panels A–C are located in the lower half of outcrop Section 2 (see Figs. 3 and 6), with panel A showing the fine-grained part of an alluvial cyclothem.

ified or trough cross-stratified sandstone overlain by very fine-grained, ripple-laminated sandstone, plane-parallel stratified sandstone and siltstone or mudstone (Fig. 5).

The thicker coarsening-upward lower part of such units, with an outstanding set of planar cross-strata and soft-sediment deformation, overlain by the fining-upward motif of a waning flow, suggest jointly the progradation and abandonment of a mouth-bar form, or a splay, in the area of terminal flow expansion (see also Elliott, 1974; Miall, 1985; Fielding, 1986; Pulham, 1989; Macnaughton et al., 1997). The wave-ripple cross-lamination in the alternating mudstone/siltstone deposits indicates a standing water environment, probably a floodbasin pond or shallow lake.

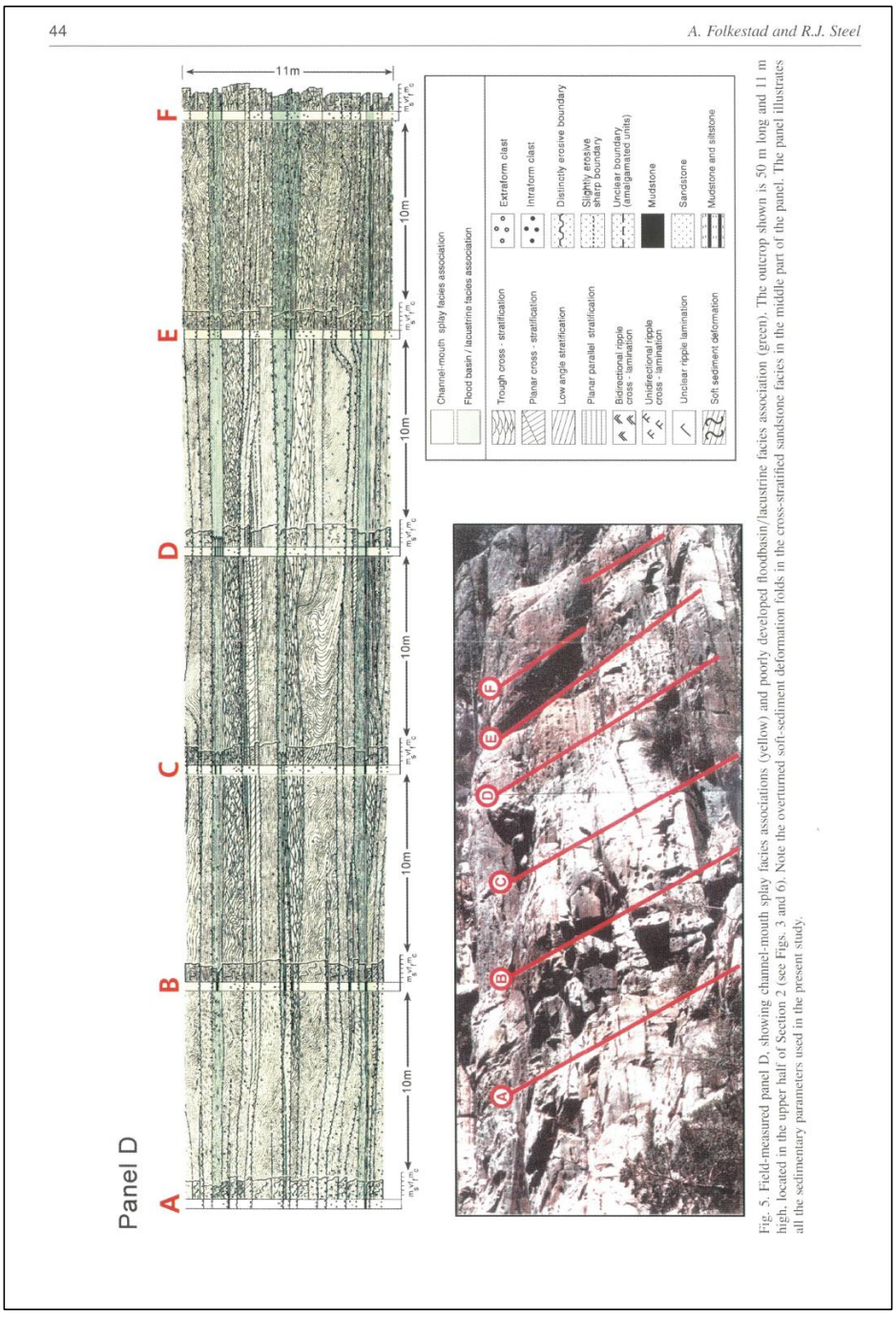

Fig. 5. Field-measured panel D, showing channel-mouth splay facies associations (yellow) and poorly developed floodbasin/lacustrine facies association (green). The outcrop shown is 50 m long and 11 m high, located in the upper half of Section 2 (see Figs. 3 and 6). Note the overturned soft-sediment deformation folds in the cross-stratified sandstone facies in the middle part of the panel. The panel illustrates all the sedimentary parameters used in the present study.

The *floodbasin/lacustrine* facies association consists of mudstones and siltstones thinly interbedded with very fine-grained, planar-parallel stratified sandstones (Fig. 4A and Fig. 5). The mudstone and siltstone layers show an alternation of uneven, subhorizontal parallel lamination and ripple cross-lamination, occasionally with convolutions, water-escape structures and desiccation cracks. The sandstones occur as isolated sheet-like layers, sharp-based or erosive, with plane-parallel stratification (showing parting lineation), ripple cross-lamination or low-angle parallel stratification, common normal grading, occasional desiccation cracks and local basal mudclasts. A common motif in these sandstone units is low-angle cross-stratification passing upwards into planar stratification, capped by ripple cross-lamination and siltstone/mudstone. The motif is often repeated in the form of composite, amalgamated units several metres thick (Fig. 4), traceable laterally for more than 50 m (Fig. 5). The individual sandstone sheets are thought to represent successive flood events in an area of shallow standing water. The desiccation cracks suggest ephemeral floodbasin ponds, occasionally turning into a shallow lake (e.g. see Elliott, 1974; Tunbridge, 1984).

In the measured cyclothems, with their characteristic fining- and coarsening-upward trends (Steel and Aasheim, 1978), the facies associations show a stacking pattern where fluvial channels are succeeded by channel-mouth splays and floodbasin deposits in the fining-upwards part of a cyclothem. In the coarsening-upward part of a cyclothem, the facies associations are stacked as floodbasin deposits succeeded by channel-mouth splays and fluvial channels above (see Fig. 6).

Multiparametric analysis

Stratigraphic changes in the A/S ratio are thought to be reflected in the variation of a number of sedimentological parameters, whose monitoring in the sedimentary basin-fill succession has been attempted in the present case. The selected parameters included mean grain size, intraformational and extraformational clasts occurrences, degree of soft-sediment deformation, bed thickness, erosion-surface frequency, and scour relief, all of which can be objectively measured and monitored through a sedimentary succession. An understanding of how the sedimentary parameters are related to the framework of the A/S ratio changes is crucial to an understanding of the depositional environment and associated allocyclic processes. The parameters measured are a continuous quantitative or semiquantitative variables of the sedimentary succession, with the values determined and averaged for each 0.5 m and 2 m. Each parameter was then plotted as two graphs (Fig. 6), with the exception of bed thickness, which was only averaged over 2 m intervals.

Mean grain-size parameter of sediment was determined visually for each 0.5 m interval and quantified as follows: coarse sandstone = 6; medium-grained sandstone = 5; fine-grained sandstone = 4; very fine-grained sandstone = 3; siltstone = 2; mudstone = 1; unexposed interval = 0. *Intraformational and extraformational clasts* were recorded in terms of the maximum particle size (MPS) and the dominant size for each 0.5 m interval was considered; separate graphs were made for intraformational clasts and for extraformational clasts. *The basal-lag or dispersed clasts* parameter indicates whether the intraformational clasts and extraformational clasts are concentrated as a lag at the lower bed boundary or scattered within the bed associated with a lag at the lower bed boundary. Intervals with no gravel clasts were given the value of 0, those containing a bottom lag were given a value of 1 and those with scattered clasts were given the value of 2. *Soft-sediment deformation* is a common type of sedimentary structure in the succession, and its intensity, or "degree", has been determined visually and averaged for each 0.5 m interval. *Erosion-surface frequency* was determined as the number of erosion surfaces per 0.5 m thickness interval. *Bed thicknesses* were measured and a mean thickness was calculated for each 2 m interval. *Scour relief* of the erosion surfaces was measured wherever significant, but the scours were mainly broad and shallow with little or no determinable relief.

The sedimentary parameters were plotted, analysed individually for possible trends, and defined as systematic stratigraphic changes of either an increasing or a decreasing type. The scour relief parameter was not used due to the scarcity of (non-zero) data. The trends were determined by visual inspection for each parameter (Fig. 6).

The A/S ratio cycles

Since the A/S ratio describes whether the sedimentary system moves towards a higher degree of preservation (maximum A/S) or a greater degree of erosional destruction (minimum A/S) of the deposits, the erosion-surface frequency parameter gives a good approximation of the changes of the A/S ratio. In times with a high degree of preservation of the deposits, little erosion takes place whereas during erosional destruction of the deposits, erosional processes dominates. Thus the large-scale trends of the erosion-surface frequency parameter is here interpreted to be equal to the large-scale changes of the

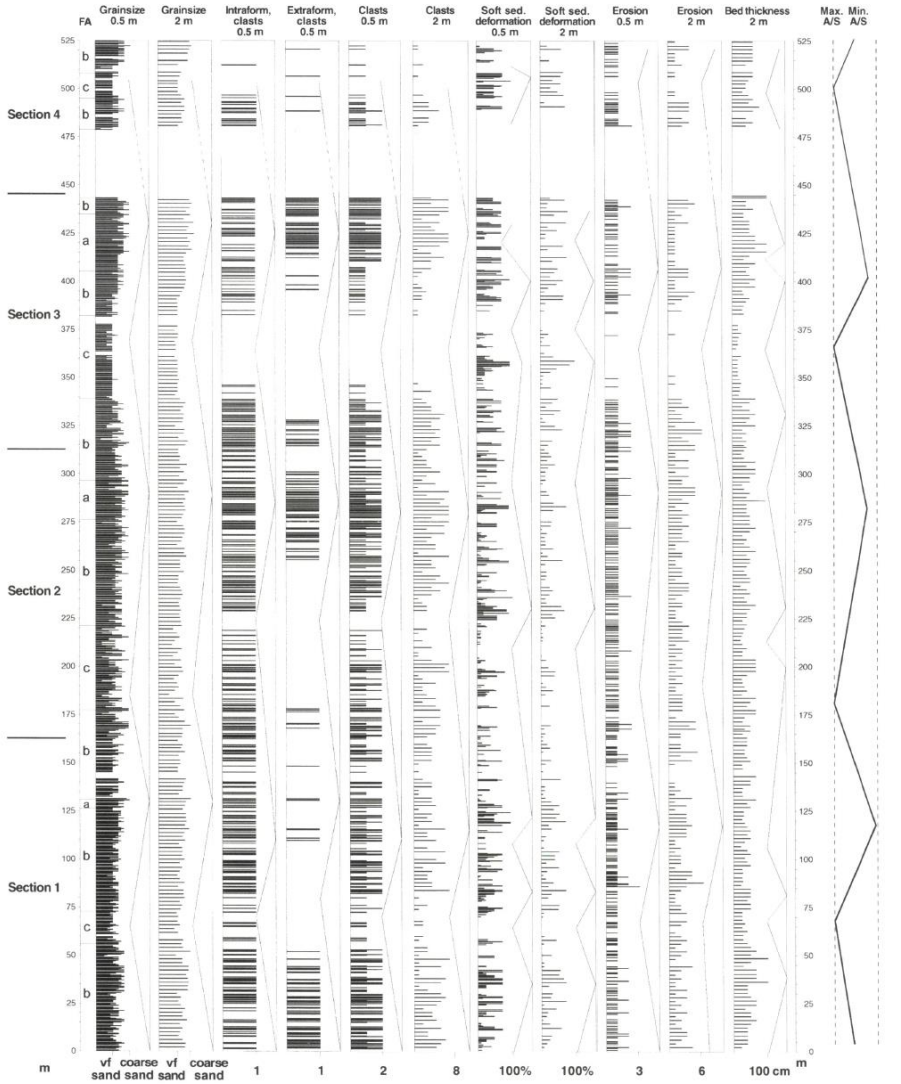

Fig. 6. The stratigraphic plots of the various sedimentary parameters measured in outcrop Sections 1–4 (Fig. 2) with the interpreted cycles of the A/S ratio. The sedimentary parameters were analysed individually for possible trends. Concentration of repeated high or low parameters values within a field were favoured over the occurrence of occasional extreme high or low values. The visually determined trends of each parameter is shown on the side of each graph. On the left hand side, the stacking pattern of the facies associations (*FA*) is shown, where: a = fluvial channel; b = channel-mouth splay; c = floodbasin. The lower part of Section 4 represents an unexposed interval.

A/S ratio within the measured cyclothems (Fig. 6). The identification of the turn-around points of the A/S ratio minima and maxima allows a subdivision of each cyclothem, within a 2-D framework, into two parts: a trend of an increasing A/S ratio, from a minimum to a maximum, and a trend of a decreasing

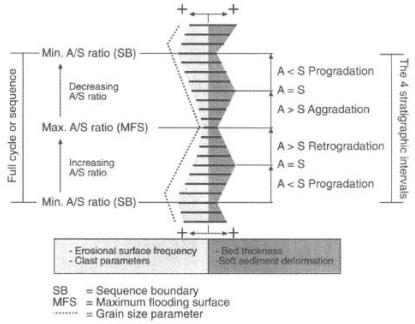

Fig. 7. A generalised summary of the changes in sedimentary parameters and the A/S ratio in one complete cycle. Note the asymmetric trend of the grain-size parameter within the A/S ratio cycle.

A/S ratio, from the maximum to the next minimum (Figs. 6 and 7).

Interestingly, the observed grain-size trend does not necessarily correspond strictly with the trend of the A/S ratio (Fig. 6). The coarsest sediment apparently tends to occur stratigraphically somewhat higher than the turn-around point of the A/S ratio minimum (Figs. 6 and 7). A possible explanation for the offset is that when the A/S ratio was reaching a minimum, coarse sediment was still being supplied to the upstream part of the depositional system, due to continued erosion and a time lag between the delivery of the sediment and its dispersal by the system. Consequently, coarse sediment continued to be deposited, extending the system's progradational signature, while the A/S ratio had already begun to increase. The geometric pinch-out, or architectural turn-around point, of the alluvial clastic wedge thus occurs at a higher stratigraphic level than the actual turn-around point of the A/S ratio in the succession. A similar observation has been reported by Wood et al. (1993) from a study of base-level fluctuations in sedimentation tank experiments. The latter authors used the base-level concept of Gary et al. (1972), equating base level with sea level, and observed that deposition of coarse sediment persisted into the early phase of base-level rise, rather than ceasing at the end of the base-level fall. The base-level minimum in that case can be said to correspond to a minimum A/S ratio, if the notion of this latter term is slightly simplified. A similar mismatch between the sediment grain-size maximum and the maximum regression level at a sequence boundary, is implicit in the sequence-stratigraphic models of Hunt and Tucker (1992) and Helland-Hansen and Gjelberg (1994).

The stratigraphic distribution and mode of occurrence of gravel-size clasts, both intra- and extraformational, seem to follow the pattern of the A/S ratio changes without any significant or systematic offset. The increasing-upward abundance of these clasts is interpreted to reflect the decreasing A/S ratio. However, some other parameters, such as the intensity of soft-sedimentary deformation and bed thicknesses, show a notably different trend than the trend of the A/S ratio in a cyclothem. The latter two parameters tend to have low values at the turn-around points of the A/S ratio and higher values between these points (Figs. 6 and 7). The low values of these parameters at the A/S ratio minima support the notion of greater erosion efficiency and a decreased rate of accommodation-space creation at this turn-around point. At the turn-around point related to the A/S ratio maximum, the rate of the accommodation-space creation is high, but the sediment supply is low, resulting in deposition of thin beds, with bed-shear stresses (sand load) low enough to prevent substratum deformation. Between the turn-around points, the two parameters assume higher values because the A/S ratio approaches an equilibrium state, with the rate of sediment supply keeping pace with the rate of the accommodation-space creation (Fig. 1). An equilibrium state comparable to the one considered here has been discussed by Schlager (1993), Shanley and McCabe (1994), and Gardner (1995).

In terms of the cyclic changes in the A/S ratio, an alluvial cyclothem in the Hornelen Basin can thus be divided into four parts, or stratigraphic intervals: a lower interval characterised by an increasing-upward trend of the A/S ratio (Fig. 7), with the $A < S$ relation meaning system progradation, culminating in a transient state of equilibrium ($A = S$) and turning into the state of retrogradation ($A > S$) in the second interval; and a third interval recording the system's aggradation ($A > S$) towards another transient state of equilibrium ($A = S$), with the fourth interval representing renewed progradation ($A < S$), but within the context of decreasing rather than increasing A/S ratio compared to the first (lowermost) segment. These four stratigraphic intervals of an alluvial cyclothem can be considered in terms of the conventional sequence-stratigraphic models (e.g. Helland-Hansen and Gjelberg, 1994) within a 2-D framework.

Sequence-stratigraphic interpretation of the cyclic changes in the A/S ratio

The application of the concept of sequence stratigraphy to continental sedimentary successions has become common in the recent years. However, it has mostly been applied to continental successions where

the sedimentation was controlled by changes in sea level (Shanley and McCabe, 1994; Burns et al., 1997; Willis, 1997; McCarthy et al., 1999). Sedimentation in the Hornelen Basin took place in an intra-cratonic basin (Steel et al., 1977) and involved no sea-level control. This renders the conventional concept and terminology of sequence stratigraphy non-applicable to this basin's alluvial succession (see also Olsen et al., 1995; Martinsen et al., 1999).

It is worth noting that the four stratigraphic intervals of an alluvial cyclothem identified in the present study are comparable to the genetic sedimentary units (or systems tracts) used in sequence-stratigraphic models (Helland-Hansen and Gjelberg, 1994). Since the changes in sediment-preservation potential are a key aspect of both the A/S ratio cycles and the conventional stratigraphic sequences, an interesting comparison can be made between the former and the sequence-stratigraphic models (Fig. 7). The subaerial unconformity and its correlative conformity bounding a stratigraphic sequence (sensu Van Wagoner et al., 1990) correspond to the phase of lowest sediment-preservation potential. With regard to the present study, this phase corresponds to a minimum of the A/S ratio. Furthermore, the maximum flooding surface (or condensed section) coincides with the phase of maximum sediment-preservation potential, which in comparison within the present study equals a maximum of the A/S ratio. The stratigraphic levels of minimum and maximum preservation potential represent the sedimentary system's maximum and minimum energy levels, respectively, recorded by the stratigraphic sequence or an alluvial basin-fill cyclothem. The equilibrium ($A = S$) point of the increasing-upward (minimum to maximum) trend of the A/S ratio divides the lower part of the cyclothem into a progradational interval passing into a retrogradational interval. In a coastal setting, these two intervals could be referred to as the lowstand prograding wedge (sensu Hunt and Tucker, 1992) and the transgressive systems tract, respectively. Similarly, the equilibrium point ($A = S$) of the decreasing-upward trend of the A/S ratio divides the upper part of the alluvial cyclothem into an aggradational interval followed by a progradational interval. As the A/S ratio begins to decrease and the sediment supply is barely sufficient to fill the available accommodation space, an aggradational style of deposition prevails in the system. But when the sediment supply eventually exceeds the rate of accommodation-space creation, the systems begins to prograde in a basinward-stepping pattern. In a coastal setting, this type of stacking pattern, following a maximum flooding phase, is referred to as a highstand systems tract in conventional sequence stratigraphy (Posamentier et al., 1988). A possible fifth segment, analogous to the forced regressive systems tract in a shoreline setting (Hunt and Tucker, 1992), is difficult to envisage in the sedimentary succession of a purely alluvial basin, except perhaps in incised valleys.

Discussion and conclusions

The dynamic behaviour of an alluvial sedimentary system controlled by pulses of tectonic subsidence tends to show cyclic phases of progradation and retrogradation, with the corresponding decrease (minimum A/S ratio) and increase (maximum A/S ratio) of the sediment preservation potential. This oscillating behaviour results in systematic changes in the morphology and sedimentary characteristics of the depositional system, such as the upward coarsening and fining of the sediment grain size, due to the increasing and decreasing A/S ratio. A range of quantitative and semiquantitative sedimentary parameters appears to reflect changes in the A/S ratio controlling the depositional system, and the stratigraphic plots of these measurable characteristics can thus be used to recognise cyclic changes in the A/S ratio. On this basis, an alluvial succession can be analysed by a "sequencing" approach analogous to that used in conventional sequence stratigraphy. The full cycle of changes in the A/S ratio can be devised into four intervals, or phases, including progradation, retrogradation, aggradation and some "remnant" progradation.

The cyclicity in the Hornelen Basin was previously defined on the basis of facies and grain-size changes alone. The present method documents a stratigraphic offset of the maximum grain-size points with respect to the turn-around points of minimum A/S ratio. This is interpreted in terms of a time lag between the A/S ratio minimum and the peak of the alluvial system progradation. The study shows that although the grain-size maximum and minimum in an alluvial succession may be a good proxy of the system's peak progradation and peak retrogradation, respectively, the grain-size parameter alone is insufficient to detect accurately the stratigraphic pattern of allocyclic changes in the A/S ratio. The resolution of the stratigraphic record appears to be improved when a wider range of sedimentary parameter are used.

The bed thickness and soft-sediment deformation parameters show higher values between the A/S ratio minima and maxima, when the system passes through an equilibrium between the rates of accommodation-space creation and sediment supply. This effect can be compared to the longitudinal pattern of deposition along a clinoform with a low-angle trajectory. The clinothem tends to be thin in the source-proxi-

mal part due to the low A/S ratio and in the distal part due to the high A/S ratio, while reaching the greatest thickness in the middle part, between the two extremes. The intensity of soft-sediment deformation follows the pattern of the bed thickness changes and is thought to be related to the latter parameter, probably by the specific sediment discharge controlling both the bed morphology and the bed shear stresses.

The measured sections represent an 1-D data set that alone is insufficient to describe 3-D stratigraphic changes in the basin. However, in combination with the well-established palaeo-flow direction of the axial part of the basin (Steel and Aasheim, 1978) (Fig. 2), predictions of A/S ratio trends becomes feasible away from the measured 1-D profile. The A/S ratio maxima and minima represent correlatable zones and predictions about the A/S ratio trends in adjacent areas can be tested by measuring more sections.

The approach described here can readily be applied to subsurface sedimentary successions, because parameters such as grain size, soft-sediment deformation, frequency of erosion surfaces and bed thicknesses can be determined from cores. A modified version of the technique has been applied to a Formation Micro Image Log from a North Sea well (Folkestad, 1999), where the degree of bioturbation, the frequency of erosion surfaces, the bed thickness and the angle of lamination were determined for half-metre intervals. The trends shown by these parameters were compared and used to recognise longer-term shallowing- and deepening-upwards cycles in the marine sedimentary succession.

Acknowledgements

The authors wish to thank Jan Tveranger for discussions and improvements on the early versions of the manuscript. The NPF referees Wojtec Nemec and Michael Gardner are thanked for their very constructive criticism and suggestions for improvements. The authors would like to acknowledge the University of Bergen for their funding of the fieldwork. Liv Ims and Eden Potter have given technical assistance in the preparation of figures.

References

Anderson, D.S., 1997. Sedimentary responses to base-level change in linked alluvial fan, lake and braidplain strata, Hornelen Basin, Western Norway. Unpublished Ph.D. Thesis, Colorado School of Mines, Golden, 269 pp.

Bryhni, I., 1964. Sediment structures in the Hornelen series. Nor. Geol. Tidsskr., 5: 486–488.

Burns, B.A., Heller, P.L., Marzo, M. and Paola, C., 1997. Fluvial response in a sequence stratigraphic framework: example from the Montserrat fan delta, Spain. J. Sediment. Res., 67: 311–321.

Cant, D.J. and Walker, R.G., 1978. Fluvial processes and facies sequences in the sandy braided South Saskatchewan River, Canada. Sedimentology, 25: 625–648.

Elliott, T., 1974. Interdistributary bay sequences and their genesis. Sedimentology, 21: 611–622.

Fielding, C.R., 1986. Fluvial channel and overbank deposits from the Westphalian of the Durham Coalfield, Northeastern England. Sedimentology, 33: 119–140.

Folkestad, A., 1995. Cyclicity in Hornelen Basin (Devonian), Norway. Unpublished Candidatus Scientiarum Thesis, University of Bergen, Norway, 96 pp.

Folkestad, A., 1999. Compilation of sedimentological parameters from Formation Micro Image logs (FMI) to identify stratigraphic patterns. In: O.J. Martinsen and T. Dreyer (Editors), Sedimentary Environments Offshore Norway. Norwegian Petroleum Society (NPF) Extended Abstracts, 37.

Fossen, H. and Rykkelid, E., 1992. Postcollisional extension of the Caledonide orogen in Scandinavia: structural expressions and tectonic significance. Geology, 20: 737–740.

Gardner, M.H., 1995. Tectonic and eustatic controls on the architecture of mid-Cretaceous, stratigraphic sequences, Central Western Interior Foreland Basin of North America. In: S.L. Dorobek and G.M. Ross (Editors), Stratigraphic Evolution in Foreland Basins. Soc. Econ. Paleontol. Mineral. Spec. Publ., 52: 243–281.

Gary, M., McAffee, R. Jr. and Wolf, C.L., 1972. Glossary of Geology. American Geological Institute, Washington DC, 805 pp.

Gloppen, T.G. and Steel, R.J., 1981. The deposits, internal structure and geometry in six alluvial fan-fan delta bodies (Devonian, Norway): a study in the significance of bedding sequences in conglomerates. In: F.G. Etheridge and R. Flores (Editors), Recent and Ancient Non-Marine Depositional Environments: Models for Exploration. Soc. Econ. Paleontol. Mineral. Spec. Publ., 31: 49–56.

Helland-Hansen, W. and Gjelberg, J., 1994. Conceptual basis and variability in sequence stratigraphy: a different perspective. Sediment. Geol., 92: 31–52.

Hossack, J.R., 1984. The geometry of listric normal faults in the Devonian basins of Sunnfjord, Western Norway. J. Geol. Soc., London, 141: 629–637.

Hunt, D. and Tucker, M.E., 1992. Stranded parasequences and the forced regressive wedge systems tract: deposition during base-level fall. Sediment. Geol., 81: 1–9.

Larsen, V. and Steel, R.J., 1978. The sedimentary history of a debris flow-dominated alluvial fan: a study of textural inversion. Sedimentology, 25: 37–59.

Macnaughton, R.B., Dalrymple, R.W. and Narbonne, G.M., 1997. Early Cambrian braid-delta deposits, MacKenzie Mountains, northwestern Canada. Sedimentology, 44: 587–609.

Martinsen, O.J., Ryseth, A., Helland-Hansen, W., Flesche, H., Torkildsen, G. and Idil, S., 1999. Stratigraphic base level and fluvial architecture: Ericson Sandstone (Campanian), Rock Springs Uplift, southwest Wyoming, USA. Sedimentology, 46: 235–263.

McCarthy, P.J., Faccini, U.F. and Plint, G., 1999. Evolution of an ancient coastal plain: palaeosols, interfluves and alluvial architecture in a sequence stratigraphic framework, Cenomanian Dunvegan Formation, northeastern Columbia, Canada. Sedimentology, 46: 861–891.

Miall, A.D., 1985. Architectural-element analysis: a new method of facies analysis applied to fluvial deposits. Earth-Sci. Rev., 22: 261–308.

Norton, M.G., 1986. Late Caledonian extension in Western Norway: a response to extreme crustal thickening. Tectonics, 5: 195–204.

Olsen, T., Steel, R.J., Høgseth, K., Skar, T. and Røe, S.-L., 1995. Sequential architecture in a fluvial succession: sequence stratigraphy in the Upper Cretaceous Mesaverde Group, Price Canyon, Utah. J. Sediment. Res., B65: 265–280.

Osmundsen, P.T., Andersen, T.B., Markussen, S. and Svendby, A.K., 1998. Tectonics and sedimentation in the hanging wall of a major extensional detachment: the Devonian Kvamshesten basin, Western Norway. Basin Res., 10: 213–234.

Posamentier, H.W., Jervey, M.T. and Vail, P.R., 1988. Eustatic controls on clastic deposition, I. Conceptual framework. In: C.K. Wilgus, B.S. Hastings, C.G.St.C. Kendall, H.W. Posamentier, C.A. Ross and J.C. Van Wagoner (Editors), Sea Level Change: An Integrated Approach. Soc. Econ. Paleontol. Mineral. Spec. Publ., 42: 109–124.

Pulham, A.J., 1989. Controls on internal structures and architecture of sandstone bodies within Upper Carboniferous fluvial-dominated deltas, County Clare, Western Ireland. In: M.K.G. Whatley and K.T. Pickering (Editors), Deltas: Sites and Traps for Fossil Fuels. Geol. Soc. Spec. Publ., 41: 179–203.

Schlager, W., 1993. Accommodation and supply — a dual control on stratigraphic sequences. Sediment. Geol., 86: 111–136.

Schumm, S.A., 1968. River adjustment to altered hydrologic regime: the Murumbridge River and paleochannels, Australia. U.S. Geol. Surv. Prof. Pap., 598, 65 pp.

Seguret, M., Seranne, M., Chauvet, A. and Brunel, M., 1989. Collapse basins: a new type of extensional sedimentary basin from the Devonian of Norway. Geology, 17: 127–130.

Seranne, M., Chauvet, A., Seguret, M. and Brunel, M., 1989. Tectonics of the Devonian collapse-basins of Western Norway. Bull. Soc. Geol., Fr., 8: 489–499.

Shanley, K.W. and McCabe, P.J., 1994. Perspectives on the sequence stratigraphy of continental strata. Am. Assoc. Pet. Geol. Bull., 78: 544–568.

Steel, R.J., 1988. Coarsening-upward and skewed fan bodies: symptoms of strike-slip and transfer fault movement in sedimentary basins. In: W. Nemec and R.J. Steel (Editors), Fan Deltas: Sedimentology and Tectonic Setting. Blackie and Son, Glasgow, pp. 75–83.

Steel, R.J. and Aasheim, S., 1978. Alluvial sand deposition in a rapidly subsiding basin (Devonian, Norway). In: A.D. Miall (Editor), Fluvial Sedimentology. Can. Soc. Pet. Geol., Mem., 5: 385–413.

Steel, R.J. and Gloppen, T.G., 1980. Late Caledonian (Devonian) basin formation, Western Norway: signs of strike-slip tectonics during infilling. In: H.G. Reading and P.F. Ballance (Editors), Sedimentation in Oblique-Slip Mobile Zones. Int. Assoc. Sedimentol. Spec. Publ., 4: 79–103.

Steel, R.J., Mæhle, S., Røe, S.-L., Spinnanger, Å. and Nilsen, H.R., 1977. Coarsening-upwards cycles in the alluvium of Hornelen Basin (Devonian), Norway. Sedimentary response to tectonic events. Geol. Soc. Am. Bull., 88: 1124–1134.

Tunbridge, I.P., 1984. Facies models for a sandy ephemeral stream and clay playa complex; the Middle Devonian Trentishoe Formation of North Devon, U.K. Sedimentology, 31: 697–715.

Van Wagoner, J.C., Mitchum, R.M., Campion, K.M. and Rahmanian, D., 1990. Siliciclastic sequence stratigraphy in well logs, cores and outcrops: concepts for high-resolution correlation of time and facies. Methods in Exploration Series 7, American Association of Petroleum Geologists, Tulsa, OK, 55 pp.

Willis, B.J., 1997. Architecture of fluvial-dominated valley-fill deposits in the Cretaceous Fall River Formation. Sedimentology, 44: 735–757.

Wood, L.J., Ethridge, F.G. and Schumm, S.A., 1993. The effects of rate of base level fluctuation on coastal plain shelf and slope depositional systems: an experimental approach. In: H.W. Posamentier, C.P. Summerhayes, B.U. Haq and G.P. Allen (Editors), Sequence Stratigraphy and Facies Associations. Int. Assoc. Sedimentol. Spec. Publ., 18: 43–53.

A. FOLKESTAD *Statoil Research and Technology, Department of Reservoir Characterisation, N-4035 Stavanger, Norway*
R.J. STEEL *University of Wyoming, Department of Geology and Geophysics, Laramie, WY 82071, USA*

4.2 Paper 2

Orre, L.T.E. & Folkestad A. 2019. Depositional environments of the Early to Middle Triassic Northern North Sea in a syn-rift to a post-rift setting. Geological Society, London, Special Publications, 64. pp 21.

The Early to Middle Triassic represents an interesting and poorly documented epoch in the evolution of the northern North Sea sedimentary basin. This period was strongly influenced by the break-up of Pangaea and the associated Artic rift system that entered the North Sea Basin and initiated the Permo-Triassic rift phase. This study documents the sedimentary infill of rotated fault blocks during syn-rift (Early Triassic) and the start of the inter-rift (Middle Triassic) (**Theme 2)**. The aeolian deposits are restricted to the elevated footwall highs above the lake level, formed in response to the interplay between rifting and sedimentation in the North Sea Basin (**Theme 3)**. This paper suggests that the aeolian deposits came into existence at the change from syn- to post/inter-rift stage with elevated and drained fault ridges that allowed aeolian dunes to form at those locations. The aeolian deposits are interpreted as loess due to their massive character and the results of the petrographic analysis. In this case, the wind strength creates the accommodation space for the aeolian sands and provides the sediment flux **(Theme 2)**.

The paper suggests that the Devonian pull-apart basins in the northern North Sea (Beach, 1985) became reactivated during the Permo-Triassic rift phase. Reactivation of these tectonic features occurred again in the Middle to Late Jurassic rift phase, which would explain the structural features as curved ridges seen in Jurassic seismic maps (Fraser et al., 2003) (Fig. 2) in the northern North Sea. Further, this adds to the understanding of the subsidence pattern in the northern North Sea in Mesozoic time and forms the link between the Devonian sedimentary basins and the Triassic and Jurassic sedimentary basins (**Theme 1)**. The paper solved an old problem with the enigmatic depositional environment of the Lomvi Formation. This formation has been termed as `cryptic aeolian` by McKie & Williams (2009) whereas this paper demonstrates that these sandstones are loess.

4.3 Paper 3:

Folkestad, A., Veselovsky, Z., Roberts, P. 2012. Utilising borehole image logs to interpret delta to estuarine system: a case study of the subsurface Lower Jurassic Cook Formation in the Norwegian northern North Sea; Marine and Petroleum Geology, ***29****, 255-275.*

The Cook Formation belongs to the Early Jurassic Dunlin Group and is a secondary reservoir in the northern North Sea. This formation was analyzed in the Kvitebjørn and Valemon fields (Fig. 1) to establish a sedimentological model, as input for a reservoir model, using a limited sedimentological subsurface database of cored material and electrical image logs. The image logs (also known as dip-meter logs) can be used in sedimentological interpretation if structural tilt of the strata has been removed correctly. Image logging in wells is often performed if coring is difficult or too expensive. This log-type, therefore, acts as a substitute for core-data. The resolution of these logs is down to 5mm which gives a coarser view of the sedimentary strata compared to core material. When this paper was published, papers on sedimentological interpretations of image logs were scarce and a workflow for sedimentological interpretation of these data was lacking. This paper presents a novel method in describing and interpreting sedimentary strata from image logs in an objective manner designed to avoid over-interpreting of the sedimentary strata. This paper is often referred to in other papers focusing on sedimentological interpretation of image logs and the paper is partly reprinted in Pyrcz & Deutsch (2014) book on Geostatistical Reservoir Modeling.

In the study area, the Cook Formation is analyzed using cores and image logs and interpreted as a tidal deltaic unit succeeded by a wave-dominated estuary above. The formation shows a westward thickening as an asymmetrical stratal wedge, which documents syn-sedimentary fault activity. Based on a regional interpretation of the Cook Formation as a wave-dominated deltaic coastline (Dreyer & Wiig, 1995; Charnock et al., 2001), a seaward barrier attached to a footwall high of this fault is inferred **(Theme 3).** The inferred barrier shielded the interpreted tidal delta in the study

area from the otherwise wave-dominated shoreline of the Cook Formation as interpreted by Dreyer & Wiig (1995) and Charnock et al., (2001). Apart from the syn-sedimentary aspect, the fault activity and the asymmetrical stratal wedge of the Cook Formation contribute to the debate whether the Early Jurassic in the northern North Sea represents a post-rift phase (Charnock et al., 2001) or an inter-rift phase (Ravnås et al., 2000) **(Theme 2)**. Comparably, the time equivalent and transgressive Stø Formation (Hess et al., 2014) in the Hammerfest Basin (Barents Sea) was deposited as an estuary system in a fault-induced depression (Folkestad et al., 2005, Appen. 1a; Folkestad, 2008; Appen. 1c) which suggest that the Norwegian shelf experienced some tectonic activity in the Early Jurassic.

Marine and Petroleum Geology 29 (2012) 255–275

Contents lists available at ScienceDirect

Marine and Petroleum Geology

journal homepage: www.elsevier.com/locate/marpetgeo

Utilising borehole image logs to interpret delta to estuarine system: A case study of the subsurface Lower Jurassic Cook Formation in the Norwegian northern North Sea

Atle Folkestad [a,*], Zbynek Veselovsky [b], Paul Roberts [c]

[a] Statoil ASA, Dept. of Sedimentology and Biostratigraphy, Box 7200, Bergen 5020, Norway
[b] Eriksfiord AS, Postboks 8034, Stavanger 4068, Norway
[c] Statoil Gulf Services LLC, Gulf of Mexico Exploration, Houston, USA

ARTICLE INFO

Article history:
Received 6 November 2009
Received in revised form
4 May 2011
Accepted 13 July 2011
Available online 29 July 2011

Keywords:
Tidal delta
North Sea
Lower Jurassic
Image logs
Wire-line logs
Estuary
Cook Formation

ABSTRACT

The Lower Jurassic Cook Formation forms a regressive and transgressive sandstone wedge of shallow marine reservoir sandstones. It is distributed mainly in the Norwegian sector of the northern North Sea and the formation has proven to be hydrocarbon bearing. A case study of this formation from the Tampen Spur area presents a methodology for reconstructing depositional environments in areas of scarce data coverage and poor seismic quality using limited core-coverage, wire-line logs and borehole image logs. The core material and image logs are from different wells. The latter offer interesting opportunities for sedimentological descriptions and interpretations both in cored and uncored sections, particularly as the resolution of the tool (mm-scale under optimal conditions) enables identification of sedimentary structures. In order to avoid over-interpretation, a system of descriptive, simple and robust image facies was established for this study. These include: horizontal lamination, low-angle lamination, cross-stratification, as well as mottled and deformed strata.

The Cook Formation is interpreted here as a regressive tidal-fluvial delta to transgressive wave-dominated estuary couplet with offshore shale above and below. The tidal-fluvial delta of the regressive part seems to be at odds with the regional context as the regressive part of the Cook Formation in the Tampen Spur area is interpreted as a wave-dominated delta system. Internally, the regressive part of the Cook Formation thickens westwards with 68% which is unusual for the otherwise tabular regressive Cook Formation in the Tampen Spur area. Both the thickness and depositional environment difference of the regressive part of the Cook Formation can be explained with temporary fault movement of a blind fault located basinward during basin infill. This could have created a fault-induced monocline that led to wave sheltering of the tidal-fluvial delta system. A spit-barrier system was probably associated with the monocline sourced by longshore drift from the otherwise wave-dominated coast of the regressive Cook Formation. After basin infill and removal of basin relief, the subsequent transgression resulted in the formation of a wave-dominated estuary.

1. Introduction

The Kvitebjørn Field and the adjacent Valemon area, located 20 km southeast of the Gullfaks Field and 130 km off the West Norwegian coast (Fig. 1), lie on a down-faulted terrace adjacent to the deeply subsided Viking Graben to the east (Odinsen et al., 2000). It is situated in a structurally complex area as a result of several rift phases. The Cook Formation varies in thickness from about 65 m to 87 m over a distance of 13 km in the study area.

The Kvitebjørn Field produces gas and condensate from the Brent Group and also from now the Cook Formation (Toarcian age) following the discovery of gas in the 34/11-A - 6 well. In order to aid the future and ongoing gas production of the Cook Formation a sedimentological study was initiated to provide input to reservoir characterisation and reserve estimates for both the Kvitebjørn Field (production license 193) and Valemon area (production license 050). The database consists of five wells (34/10 - 23, 34/10 - 35, 34/11 - 1, 34/11 - A - 6 and 34/11 - A - 10) with wire-line logs, one partly cored Cook Formation well (34/10 - 35) and two wells (34/11 - A - 6 and 34/11 - A - 10) with borehole image logs (Formation Micro Image log – FMI). The base of the Cook Formation is set at the level

* Corresponding author. Tel.: +47 41409194; fax: +47 55995852.
E-mail address: atlef@statoil.com (A. Folkestad).

0264-8172/$ – see front matter © 2011 Elsevier Ltd. All rights reserved.
doi:10.1016/j.marpetgeo.2011.07.008

where the gamma-log values decrease upwards in comparison to the continuous high values of the underlying Burton Formation. This break in gamma-ray log response is easily identified in the other wells and is a pragmatic approach to define the base of the Cook Formation.

Seismic interpretation of the Cook Formation in the Tampen Spur area is difficult due to the weak impedance contrast of the shales above and below, and the relatively low frequencies at these great depths of reservoir (in this case from about 3930 m (below sea floor) in 34/10 - 35 to about 4380 m in 34/10 - 23). As a result no surfaces of the Cook Formation or the Dunlin Group are recognisable in seismic data. With this limited database it was important to take full advantage of the available data. The aim of this study is to describe and interpret the borehole image logs, wire-line logs and the available cores and combine them to establish depositional environments, palaeo sediment transport directions within these environments, and the stratigraphic development of the formation based on sequence stratigraphic principles within a biostratigraphically calibrated framework. The results were used as input for reservoir evaluation purposes, however this aspect is not discussed here.

2. Geological setting

The Cook Formation belongs to the Dunlin Group (Pliensbachian – Toarcian; Vollset and Doré, 1984; Charnock et al., 2001) and is bound by the offshore Burton Formation below and the offshore Drake Formation above in the Tampen Spur area. It has been described as a succession of relatively shallow marine deposits (Ager, 1975; Gage and Doré, 1986; Dreyer and Wiig, 1995; Marjanac and Steel, 1997). In the study area, the Cook Formation is of Toarcian age and is time-equivalent with the Cook Formation found in the Gullfaks Field (Fig. 2). The formation was sourced from the eastern basin margin and prograded westwards due to the Late Pliensbachian rift margin uplift (Charnock et al., 2001; Husmo et al., 2003) and shows a maximum westerly extent into the Statfjord Field (33/12) (Dreyer and Wiig, 1995) (see Husmo et al. (2003) for palaeogeographical maps of the Cook Formation in the northern North Sea). The Cook Formation was deposited at a time when marine waters had transgressed over parts of the Triassic and Lower Jurassic sediments mainly fluvial Statfjord Formation in the northern North Sea (Steel, 1993) and formed a narrow seaway (Husmo et al., 2003). The Cook Formation can be divided into two distinct units, a lower (regressive) and an upper (transgressive) unit of the Cook Formation (Steel, 1993) and this study also uses this nomenclature.

The northern North Sea experienced rifting and extension in the Late Permian to Early Triassic epoch with development of north–south trending faults (Fig. 1), and was followed by general post-rift thermal cooling and subsidence (Gabrielsen et al., 1990; Yielding et al., 1992; Steel, 1993). These Permo – Triassic faults are also

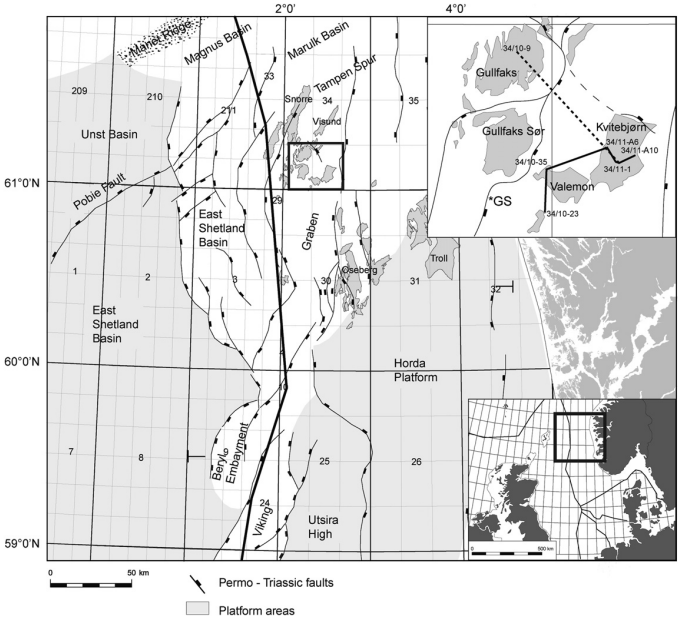

Figure 1. Basin configuration map of the northern North Sea, modified from Færseth (1996). Indent map show the study area with blocks 34/10 and 34/11 and Permo – Triassic fault pattern (modified from Rouby et al., 1996) with the position of the well-correlation panel in Fig. 16 and the seismic cross-section in Fig. 17. Dashed line indicates the well correlation shown in Fig. 2. Note the indicated Gullfaks Sør (GS) fault which is discussed later in the text.

found in the study area (Fig. 1). A following rift phase occurred in the Middle-Late Jurassic to Early Cretaceous with a dominant extension orientated in a northwest (NW) to southeast (SE) direction and was followed by crustal contraction and thermal subsidence throughout Cretaceous and Cenozoic (Yielding et al., 1992; Færseth, 1996; Odinsen et al., 2000). The Cook Formation was deposited during a phase of general tectonic inactivity and subsidence after the Permo – Triassic rift phase. However, mild extensional tectonics in the Early Jurassic period (Rhaetian – Toarcian) (Færseth and Ravnås, 1998) led to the development of wedge-shaped stratal packages that are suggested as fault-related (i.e. Livbjerg and Mjøs, 1989; Gabrielsen et al., 1990; Steel and Ryseth, 1990; Ravnås et al., 2000). The faults of the Permo – Triassic rift phase, with a spacing of 15–50 km (Lervik et al., 1989; Gabrielsen et al., 1990; Odinsen et al., 2000), was suggested by Charnock et al. (2001) to probably have also controlled the subsequent Lower Jurassic subsidence and hence the thickness distribution of the Dunlin Group in the northern North Sea (see also Fig. 1). A tectonic influence of the Cook Formation in the study area may also have had an influence on the thickness distribution and will be discussed below.

3. Database and methodology

This study is based on results from the description and interpretation of core material from well 34/10 - 35, wire-line logs from wells 34/10 - 23, 34/10 - 35, 34/11 - 1, 34/11 - A - 6 and 34/11 - A - 10 and borehole images from 34/11 - A - 6 and 34/11 - A - 10. The core and the borehole images were acquired from different wells and could not be directly correlated. Therefore these datasets were first described and interpreted separately and subsequently integrated into one final interpretation. This interpretation led to the subdivision of the Cook Formation following the definition of Steel (1993) with a lower shallowing part and an upper deepening part.

The cored interval of well 34/10 - 35 has been described and divided into three facies associations based on: lithology, grain-size trends, internal structures, colour, bioturbation (bioturbation index scheme of Taylor and Gawthorpe, 1993), bed boundaries, debris content and cementation. In addition, it is important to note that the upper part of the Cook Formation was not cored in this well.

One seismic line from the 3D seismic survey ST06M06 has been used as tie between the Kvitebjørn, Valemon and Gullfaks wells. Inline direction is east–west with a line spacing of 12.5 m, and

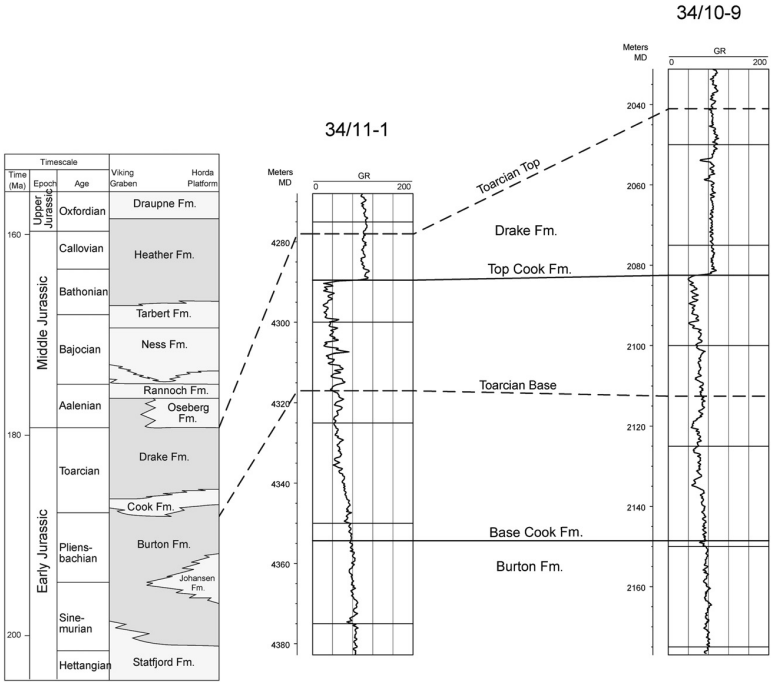

Figure 2. Chronostratigraphy of wells 34/11 - 1 and 34/10 - 9 illustrating the Pliensbachian – Toarcian age of the Cook Formation (dashed lines are time-lines) and the time equivalence between the study area and the nearby Gullfaks Field (34/10 - 9) (see Fig. 1 for location). Stratigraphic position of studied section indicated. Stratigraphic column modified from Husmo et al. (2003).

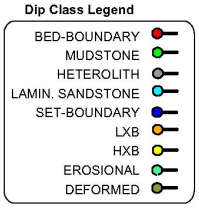

Figure 3. Dip class legend for all following examples presenting BHI results. HXB – cross-stratified sandstone planes; LXB – low-angle laminated sandstone planes.

cross-line direction is north–south with line spacing of 25 m. The vertical seismic resolution (reflection separation) is depth-dependent and varies throughout the area from ~20 ms TWT to ~50 ms TWT at a depth of 3500 ms TWT. Lateral resolution is dependent on line spacing and depth and would typically be 200–300 m at 3500 ms TWT. The seismic lines have not been depth-converted since they are used to show relative lateral thickness variations of the sedimentary strata. However, velocity well data have been utilized for both time and depth migration of the seismic surveys, and show that the velocity field is relatively laterally uniform for regional (kilometre-scale) interpretation or depth conversion purposes. Hence, the thickness variations in time reflect true thickness variations. Time-to-depth relationships are derived from well data, and show that the equivalent true vertical depth (TVD) at 3500 ms TWT is approximately 4000 m. Interpretation of the seismic data was based on correlation with the well data. Chrono-and lithostratigraphically significant surfaces identified from the interpretation of core samples, electrical logs and biostratigraphic information were tied to the seismic volumes using velocity log data.

Borehole image tools (BHI) such as the Fullbore Formation MicroImager (FMI) measure micro-resistivity fluctuations around the borehole wall and significantly contribute to geological

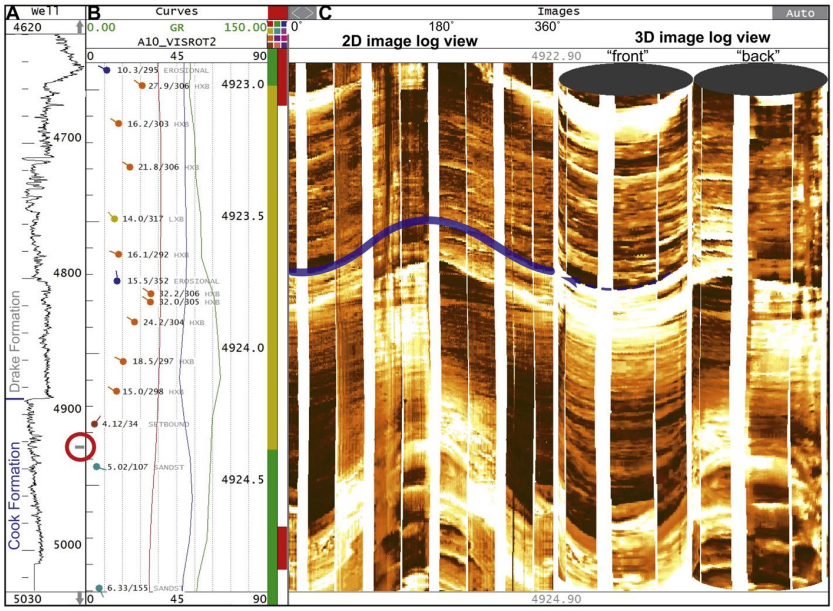

Figure 4. Borehole image log display in the interactive dip and facies picking screen of Recall (Petris Technologies). Example from well 34/11 - A - 6. A) GR (Gamma Ray) overview of the entire well, with a grey bar (marked by a red circle) indicating the position of the displayed image (B and C) within the logged section. B) Each picked plane is characterised by a tadpole showing the true dip angle (0°–45°–90° scale at top and base) and azimuth as well as the assigned dip type (such as mud lamination or erosive surface; see colour coding legend in Fig. 3). Additionally petrophysical curves are plotted together with the depth annotations on the right side (depth in mMD): GR (green), ROBB (Bulk Density – blue) and TNPH (Neutron Porosity – red). Colour bars to the far right of B (here yellow and green) refer to the image facies zonation. Reduced image quality is indicated by red bars. C) BHI tools record a cylindrical image of the borehole wall, displayed in a 3D image log view visualizing the principle and showing the front and back of the recorded cylinder (right side – 3D image log view). The white vertical gaps result from areas not covered by the image tool pads and flaps. For interpretation and dip picking, the cylinder is unrolled (left side – 2D image log view) and all planes intersecting the borehole are represented as sine waves (blue line). The amplitude of an individual sine wave depends on the dip and azimuth of the plane relative to the borehole. The brownish colours are a function of the formation resistivity variations (dark – conductive, bright – resistive). Precise top and base of the displayed window are given above and below the BHI.

understanding and interpretation of logged intervals (see Hoecker et al., 1990; Luthi, 2001; Rider, 2004; Donselaar and Schmidt, 2005; Poppelreiter et al., 2005; Xu, 2007 or Hansen and Weihe, 2008 for a more detailed description and use of BHI). The FMI image logs used in this study display variations of micro-resistivity with 192 electrodes located on eight pads/flaps. The borehole coverage is a function of borehole diameter and amounts to approximately 80% in an 8.5 inch borehole. The oriented image log has a vertical resolution down to 5 mm under optimal conditions and provides far greater resolution in comparison to traditional wire-line resistivity tools. In the displayed FMI examples resistive rocks are bright, whereas conductive material is dark (normal polarity). The directional information and position of the tool in space is calculated using inclinometer measurements (accelerometers and magnetometers). Geological planes (e.g. faults, erosive surfaces, cross-stratification, see Fig. 3) will appear on the BHI as sine waves, with the amplitudes of the sine waves reflecting the dip relative to the borehole (see erosional surface at 4923.7 mMD in Fig. 4). The dip/azimuth values that are stored in the database are corrected for the borehole orientation and are true values relative to the current horizontal plane/geographical North. All depths given for the BHI results refer to metres measured depth of the FMI tool (mMD). A manual point-to-point method was used for picking all planar features on the BHI, due to its higher accuracy and reliability compared to automated methods. Due to the difficult logging conditions in the HP/HT Kvitebjørn Field, the BHI tools in both logged wells experienced minor tool sticking. The latter occurs when the arms of the tool get stuck in the borehole, e.g. due to borehole wall washout/breakout or too high pad pressure. As the tool is continuously pulled uphole, it is eventually released due to increasing cable tension and jumps with a higher speed upwards. These periodical tool sticking events result in parts of the image being compressed (where the tool does not move or moves at a slower speed) or stretched (where the tool travels at a higher speed due to built up cable tension). Speed correction using high-resolution accelerometer data normally resolves these image artefacts, however, significant tool sticking may result in image distortion or complete data loss. In 34/11 - A - 6 and 34/11 - A - 10 such intervals can be occasionally observed on decimetre scale and are excluded from interpretation due to unreliable orientation of the observed sine waves.

3.1. Structural de-rotation

Since the BHI log is oriented, palaeo sediment transport and palaeo-slope (slump/slide) directions can be interpreted. Subsequently depositional systems and individual sand bodies can be oriented for reservoir characterisation. To determine sediment transport directions, the structural tilt of the stratigraphic section needs to be compensated for. The estimation of structural tilt is based upon measurements of stable dip intervals of strata that were deposited close to palaeohorizontal, as for example coal layers. In this case coal layers within the Cook Formations were lacking and therefore the shelfal mudstones of the Burton Formation below and the Drake Formation above were used for de-rotation. After removing the structural tilt, 9° south - southeast (SSE) in well 34/11 - A - 10 and 4° east–northeast (ENE) in well 34/11 - A - 6, the dip planes of cross-stratified sandstones record palaeocurrent transport direction depending on whether downstream or lateral accretion is present. However, due to a complex structural setting and image quality issues (the direct contact between the Cook and Drake Formations was concealed by tool sticking in well 34/11 - A - 6) the removal of structural tilt was not optimal in this study, so palaeocurrent directions were treated in terms of trends and not for individual sand bodies.

3.2. Image facies subdivision

Donselaar and Schmidt (2005) recommended calibration of the image logs with the corresponding outcrop rocks or cores in order to correctly recognize the sedimentary structures that are seen in the BHI images. This reduces the uncertainty in the interpretation of the sedimentary features. In the current study, cores were not retrieved from wells with BHI information due to drilling operational issues. This is not optimal, but a pragmatic approach with identification of primary sedimentary structures down to, but not including ripple scale was chosen. Therefore, a system of descriptive, simple and robust image facies was established based on identification of the following internal structures: horizontal lamination, low-angle lamination, cross-stratification and mottled and deformed strata (Fig. 5). These lithological classes from the BHI were combined with conventional logs: GR – Gamma Ray, ROBB – Bulk Density, TNPH – Neutron Porosity, DT – Delta-T (Sonic Slowness). The image facies defined in this study are provided in Chapter 6 and descriptions and interpretations of the cored facies associations and the image facies are given below.

4. Description and interpretation of the cored interval of well 34/10 - 35

4.1. Facies association F1: planar bedded mudstones and sandstone

Description: These deposits range in grain-size from mudstones and siltstones to fine grained sandstones in a coarsening-upward trend (Fig. 6) with some thin beds of medium-grained sand (Fig. 7A). The internal structures include: lenticular and flaser bedding with variable grain-size distribution, horizontal lamination, symmetrical and asymmetrical ripples (Fig. 7A). The lenticular and flaser bedded sands show either asymmetrical or symmetrical ripples or appear structureless. Some of the asymmetrical ripples show bidirectional palaeocurrents. Sharp-based structureless upward-fining sand units with rippled tops occur and show an increase in stratigraphic occurrence upwards. Mudstone drapes are prominent and have thicknesses of up to 2 cm, sometimes seen in pairs. Beds are typically of 2–10 cm thick, commonly with alternating sand and mud layers. Some structureless sand units contain considerable amounts of coal fragments (0.2 cm) and mica, often with asymmetrical ripples at the top. Zones of calcite cementation (>1 m) with some shell material were observed. Bioturbation is common with variable intensity and traces of *Planolites*, thin *Diplocraterion*, *Phycosiphon* and *Palaeophycus* with a general decrease

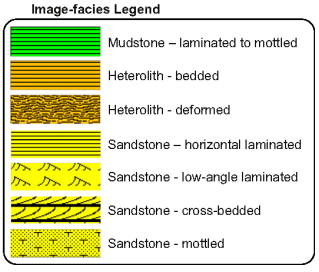

Figure 5. Image facies types established from both FMI logs in wells 34/11 - A - 6 and 34/11 - A - 10.

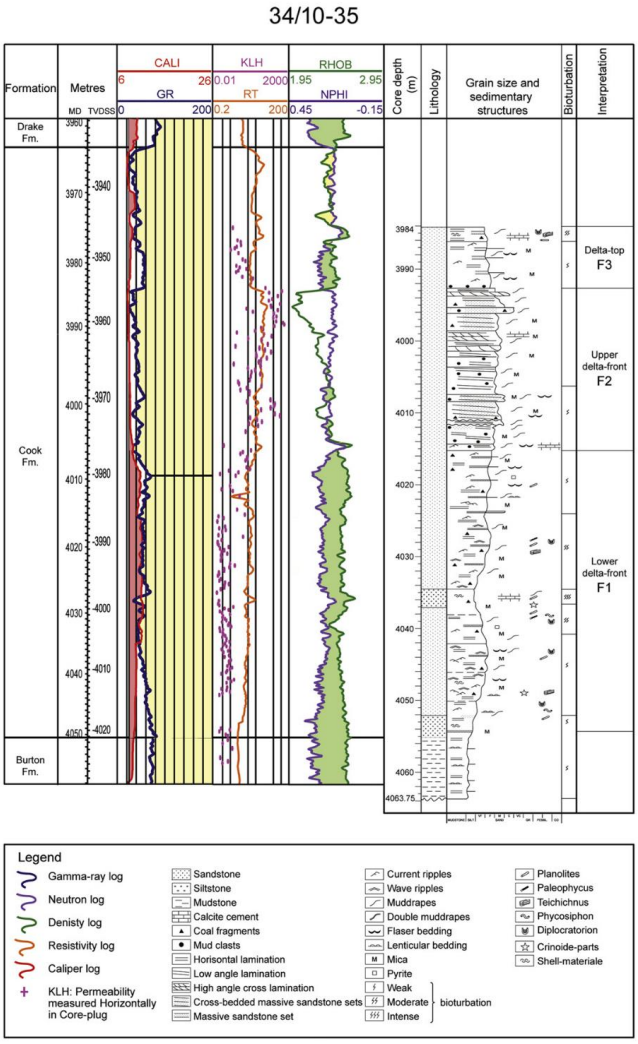

Figure 6. Sedimentary log of well 34/10 - 35 aligned with the wire-line logs. Due to core-shift the depths of the wire-line logs and the core are offset against each other.

in occurrence upwards. In addition, pyrite nodules occur along with a few shell and crinoid fragments. These deposits show a gradual transition to the overlying stratigraphic unit.

Interpretation: The coarsening-upward trend from mudstones to fine grained sandstones with a change from lenticular to flaser bedding upwards indicates shallowing and progradation of this facies association. In the lower part of this unit, the grain-size, style of bioturbation, horizontal and lenticular sand beds in muddy strata with shell fragments, crinoid fragments and wave ripples indicates deposition in a low-energy environment with marine conditions. The sharp-based structureless beds with coal fragments and abundant mica, capped by asymmetrical ripples indicate decelerating waning flows from river mouths as the flow changes from confined to unconfined (Bhattacharya and Walker, 1991) or as dilute turbiditic currents (Ambrose et al., 2009). These episodic gravity sandstone units with coal material are characteristic of delta front mouthbar deposits within fluvial deltas related to flood events in the fluvial sediment delivery system (e.g. Olariu and Bhattacharya, 2006). They may represent low-density hyperpicnal flows as they contain organic material and have sharp but not erosive bases (Lowe, 1982; Plink-Björklund et al., 2001; Petter and Steel, 2006). Similar event-flood units within marine bioturbated mudstones have been described by Myrow and Southard (1996) within a lower-delta front environment where these units originate from river input. The common occurrence of mudstone drapes in this unit, in pairs or in lenticular and flaser bedding (Fig. 7A) and the bidirectional asymmetrical ripples (current ripples), indicate tidal currents and reworking of the sediments (Visser, 1980). The thickness of mudstone drapes (up to 2 cm) indicates flocculation of mud in a brackish water environment (Nio and Yang, 1991) and they probably represent fluid muds that can be found in tidal deltas (Dalrymple et al., 2003). This alternation between rapid and episodic deposition and periods of fall-out from muddy suspension indicates a tidal-deltaic environment (Martinius et al., 2001). The limited number of trace fossil types indicates a stressed environment and this

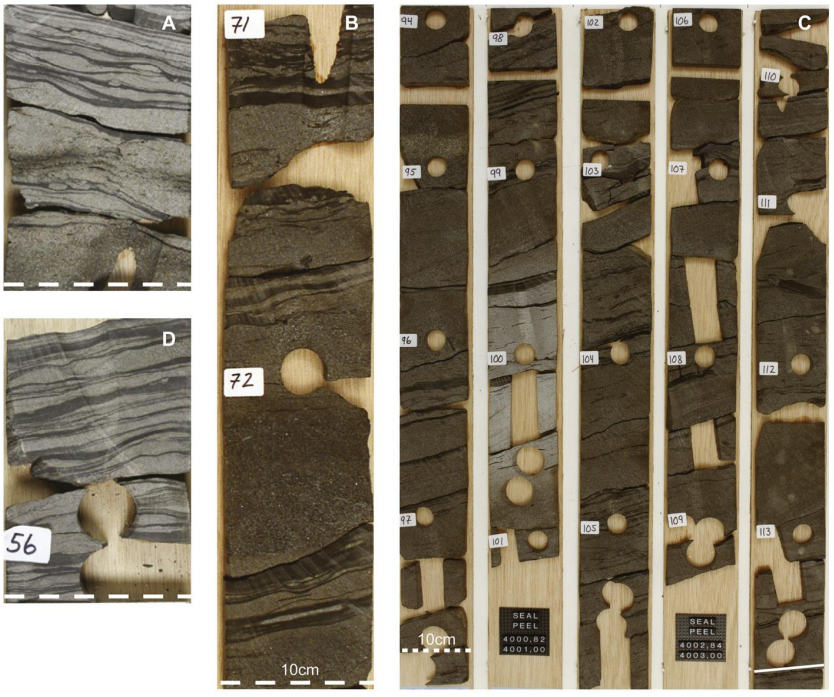

Figure 7. Core photos of the facies association of the Cook Fm, well 34/10 - 35. Dashed lines indicate scale (10 cm). A) Structureless medium-grained sandstone with coal and mud clasts seen as pulses – as well as asymmetrical ripples and 1–2 cm thick structureless sandstone pulses with mudstone drapes and *Planolites* burrows; 4023.50 mMD. B) Structureless sandstones showing fining upward trend and capped by weakly to structureless mudstones (up to 2.5 cm thick). C) Stacked structureless and cross-stratified sandstone beds with an increase in angle of bed stacking. The white line indicates the palaeohorizon. D) Alternating mudstones and very fine and fine grained sandstone with structureless sandstone pulses, asymmetrical ripples and mud drapes; 3989.20 mMD.

bioturbation suite can be found in brackish environments (MacEachern and Bann, 2008). This facies association probably represents part of a delta system, building out into marine or brackish waters, dominated by river-derived mass-flow units that are subsequently tidally reworked. The laminated sand and silts of this unit with lenticular and flaser bedding with mud drapes and bioturbation possibly represents the more common and everyday deposition whereas the mass-flow units represent the flood events. Based on the sedimentary features of this unit a lower-delta front of fluvial-tidal dominated delta is suggested.

4.2. Facies association F2: cross-stratified and massive sandstones

Description: These deposits are coarse-grained (Fig. 7B) to fine grained sandstone beds (5–60 cm thick) that are internally structureless or show high-angle tangential cross-stratified, low-angle cross-stratified and horizontal lamination. These beds show a fining upward trend in grain-size and are capped by weakly laminated to partly structureless mudstone (up to 2.5 cm thick, see Fig. 7B). The structureless beds range from 5 to 25 cm in thickness and the cross-stratified beds range from 20 to 60 cm. Asymmetrical ripples, flaser bedding and reactivation surfaces occur. Mudstone drapes are common, occasionally with organic material. The lower boundaries are generally sharp but one boundary is seen as erosive. Coal fragments (max 1 cm), mica and mud clasts (max 3 cm and angular) are common within these deposits. The stacking of beds, both structureless and laminated beds, show an increase in angle upwards (Fig. 7C) forming a cross-stratified co-set. Calcite cemented intervals are also present. Within the upper part of the structureless mudstones, bioturbation of *Planolites* occur in a few places with low intensity. The beds of these deposits show a general upward-coarsening trend (Fig. 6).

Interpretation: The coarsening-upward trend of successions of these beds and the increase in bed angle of the bed stacking indicates basinward progradation and shallowing conditions of this unit. The fining upward motif of the sandstone beds capped by ripples and centimetre thick mud layers indicate waning flow conditions. The high and low-angle cross-stratification with mudstone drapes suggest traction currents by tidal currents (Kreisa and Moiola, 1986; Plink-Björklund, 2005) forming tidal dunes, whereas the structureless beds loaded with mica minerals and coal fragments represent rapid deposits of mass-flow pulses from rivers (Bhattacharya and Walker, 1992). This suggests that both tidal and fluvial currents were active during deposition. The centimetre thick weakly laminated to structureless mudstones that cap the sandstone beds indicate flocculation of mud particles in brackish waters. The lack of lamination may indicate rapid deposition but their thickness suggests that they can be fluid mud units found in tidal deltas (Dalrymple et al., 2003). The bioturbation style observed, such as low intensity suspension feeders also suggests an environment with high sedimentation rates (Martinius et al., 2001). The bed stacking with inclined sandstone beds (both the cross-laminated and structureless type) appears to form a type of cross-stratified bed set, probably migrating 2-D dunes, that appear to be similar to what Olariu and Bhattacharya (2006) interpreted as terminal distributary channels in the delta front part of fluvial deltas. The erosive base of one unit probably represents a short-lived shallow channel where avulsion occurs rapidly due to high sedimentation rates and these shallow channels occur within the terminal distributary channel complex. The calcite cement is probably sourced from the shell material that is found in the formation. Based on these sedimentary features and stacking style of beds, an upper delta front depositional environment is suggested with influence from both fluvial rivers and tidal currents.

4.3. Facies association F3: flaser bedded sandstones

Description: These deposits range from medium to very fine grained sand, but are dominated by fine to very fine grained sandstone. Flaser bedding is the most prominent feature with asymmetrical (Fig. 7D), bidirectional ripple lamination, horizontal laminated beds and occasionally thin beds (1–5 cm thick) of structureless sandstone. Mudstone drapes occur frequently with thicknesses of up to 1 cm, sometimes in pairs. Bed thicknesses can be up to 30 cm but most beds vary from 2 to 10 cm thick with sharp lower boundaries. Near the base of this facies association a lag of mud clasts is seen above a sharp surface. The clasts are elongated (4 cm) and occur both as matrix and clast-supported. Coal fragments and mica minerals are common in these beds and some intervals are calcite cemented. Bioturbation with traces of *Diplocraterion* occur occasionally in the fine to very fine grained part and the largest traces recorded are 8 cm in width and 20 cm long. This facies association occurs above facies association F2.

Interpretation: The frequent occurrence of mudstone drapes, sometimes in pairs and in flaser bedding, and the bidirectional nature of the asymmetrical (current) ripples, suggests tidal processes were important during deposition of these sediments. The alternation between mudstones and sandstones suggests rapid changes in current strength, a feature commonly found in tidal environments. The structureless sandstone beds and the presence of mica minerals and coal fragments suggests an association to fluvial rivers, where the structureless beds are probably related to flood events. The style and type of the bioturbation within this interval suggest brackish water in a low-energy environment. A tidal flat depositional environment is proposed for these sediments (Reineck and Singh, 1980) and the mud clast lag may represent a tidal gully within such an environment (Dalrymple et al., 1991). Taking into account the stratigraphic position of this facies association, a delta top environment is inferred for these deposits. The similarities between F3 and F2 in terms of structureless sandstone units rich in mica and coal fragment and mudstone drapes underline the relationship between these two facies associations.

5. Depositional model for the cored section of well 34/10 - 35

The stacking of facies associations F1 and F2 shows a coarsening-upward trend (Fig. 6) in grain-size that suggests shallowing and progradation of either a shoreface or a deltaic depositional environment. However, the lack of wave-reworked structures, such as hummocky and swaley cross-stratification for example, renders the shoreface possibility as unlikely. A tidal signature is a clear sedimentary feature within this succession indicated by the abundant mud drapes in cross and flaser bedding and the bidirectional ripples (Kreisa and Moiola, 1986). However, the river-derived structureless gravity beds, often with mica minerals and coal fragments, are the other prominent feature of these cores suggesting a strong fluvial influence. With both of these processes present, this delta is thought to represent a mixed tidal and fluvial delta with a possible emphasis on the tidal aspect. A tidal delta would be dominated by tidal dunes (Mellere and Steel, 1996) whereas in this case fluvial deposits are also clearly present. These structureless sandstone beds show an increase in both thickness and occurrence upwards through F1 and F2, which suggests that the gravity mass-flow units are deposited at the delta front (F2) and pinch out in the lower-delta front (F1). The irregular occurrence of these mass-flow pulses indicates variable river-flow discharge (Bhattacharya and Walker, 1991). The low intensity bioturbation with horizontal traces in the delta front part points towards rapid sedimentation rates (Harris et al., 1992). Wave action appears to be

of less importance within these deposits, with wave ripples only recorded in the lower-delta front part (F1) and also occasionally in the top of the structureless sandstone beds in F1. Taking these aspects into consideration, it is suggested that these strata represent a deltaic environment deposited from tidal and fluvial conditions in a wave-sheltered setting with high deposition rates which is typical of river and tidal deltas (Coleman et al., 1970). The tidal flat deposits (F3) show that tides dominated the delta top environment and the tides probably reached far inland in such a flat and extensive environment (Dalrymple and Choi, 2007). Therefore, we interpret that the tides were the dominant process but with extensive fluvial influence.

6. Sedimentology of the Cook Formation as seen from BHI in wells 34/11 - A - 6 and 34/11 - A - 10

The BHI in both wells are described from base to top in terms of: a) classification of individual image facies types, b) stacking patterns of the image facies and c) the acquired dip patterns. Palaeocurrent directions are inferred only from dip patterns in cross-stratified units and in some cases also in sandstones with low-angle lamination. All dip angles and azimuths given are corrected for structural tilt.

6.1. Image facies types

The image facies types defined in this study are summarized in Table 1 and illustrated by examples for each individual facies type (Figs. 8–12). The image facies stacking pattern in wells 34/11 - A - 6 and 34/11 - A - 10 define two units with different styles of image facies stacking: 1) From base and uphole there is a change from horizontal laminated strata to low-angle laminated and cross-stratified sandstones. This unit shows an overall shallowing-upward trend, followed by bedded heteroliths (IF 2), which subdivide both units. 2) In the unit above the heteroliths, image facies are stacked from cross-stratified to low and horizontal laminated sandstones in a general deepening trend. A description of these two image facies stacking patterns is given below, accompanied by stereographical projections of the genetically related palaeocurrent directions (Fig. 13 and 14). All sedimentological findings are summarised in a correlation panel in Fig. 15.

6.2. Image facies stacking patterns and associated palaeocurrent trends

The correlation panel in Fig. 15 displays the dip, petrophysical log and image facies stacking patterns as well as measured palaeocurrent directions from the shallowing and deepening Cook Formation units in wells 34/11 - A - 6 and 34/11 - A - 10. As the palaeocurrent trends and their changes are genetically related to the individual facies units they were measured in, they are described together in order to avoid confusion.

6.2.1. Shallowing-upward unit

The transition between the offshore mudstones of the Burton Formation and the sand-rich Cook Formation does not show any structural disturbance in well 34/11 - A - 10. The same interval in

Table 1
Description and interpretation of image facies types based on wells 34/11 - A - 6 and 34/11 - A - 10.

Image facies type	BHI and petrophysical response	Interpretation
IF 1: Mudstone – laminated (Fig. 8)	Well-developed lamination in mm to cm scale, conductive (dark colour) spots with variable abundance may follow single laminae and lead to a mottled pattern with faint lamination. High to very high GR and TNPH values, moderate to high DT and ROBB values.	Suspension fall-out deposits. Blurred conductive spots may represent bioturbation with variable abundance. Sharply delimited spots with high conductivity (black) may represent pyrite nodules. This image facies is recorded in the Burton Formation below the Cook Formation and in the overlying Drake Formation.
IF 2: Heterolith – bedded (Fig. 9)	Parallel to irregular laminated, strong variation in image-resistivity contrast between the laminae/beds on cm scale. Conductive spots common (mm to cm scale); may gradually pass into laminated sandstones (IF 3). Irregular dip patterns up to 20° in dip angle occur in 34/11 - A - 10. In comparison to the mudstones of IF 1, GR and DT readings are slightly decreased.	Alternating traction currents to suspension fall-out deposits. Intercalated muddy/silty and sandy beds/lamina. Conductive spots probably represent bioturbation. Irregular dip patterns may indicate soft sediment deformation (heterolith – deformed). This image facies is seen within F1 and F3.
IF 3: Sandstone – horizontal laminated (Fig. 10)	Parallel to wavy lamination (<7° in dip angle) clear to faint in cm to dm scale, conductive spots to mottled pattern observed (sandstone – mottled); can gradually pass into laminated heterolithic strata IF2 (with increased amount of conductive laminae) or steepen into low-angle laminated sandstones IF4; gradual or sharp boundaries.	Deposited by traction currents. The wavy lamination may represent ripples. Thin conductive lamina can be interpreted as mud drapes (regular thickness and spacing). Variable bioturbation may be responsible for partly mottled image patterns. This image facies occurs within the facies associations F1, F2 and F3.
IF 4: Sandstone – low-angle laminated (Fig. 11)	Laminated sandstones with dip angles between 7° and 15° organized in 0.2–3.5 m thick beds with 0.2–0.8 m thick sets. Units of uni-modal dip patterns dominate but bimodal packages occur. Some patches or beds show higher resistivity (cementation); gradual or sharp boundaries (set or bed boundaries); can gradually steepen into cross-stratified sandstones IF 5, conductive spots and laminae are present.	Low-angle dip patterns suggest deposition by traction currents. The conductive spots may indicate bioturbation whereas the conductive lamina may represent mudstone drapes. Units with bimodal dip directions may indicate tidal influence. This image facies is found in the facies associations F1, F2 and F3.
IF 5: Sandstone – cross-stratified (Fig. 12)	Units of steeply dipping laminated sandstones (>15° in dip angle) range between 0.3 and 1.2 m in thickness; bed boundaries are mostly sharp but erosive boundaries are also present. Low GR, ROBB/TNPH closure variable. Exaggerated dip angles of up to 30° in two intervals are due to minor uncertainties during structural tilt removal.	Migration of 2D and 3D dunes. This image facies is seen within the facies association F2.

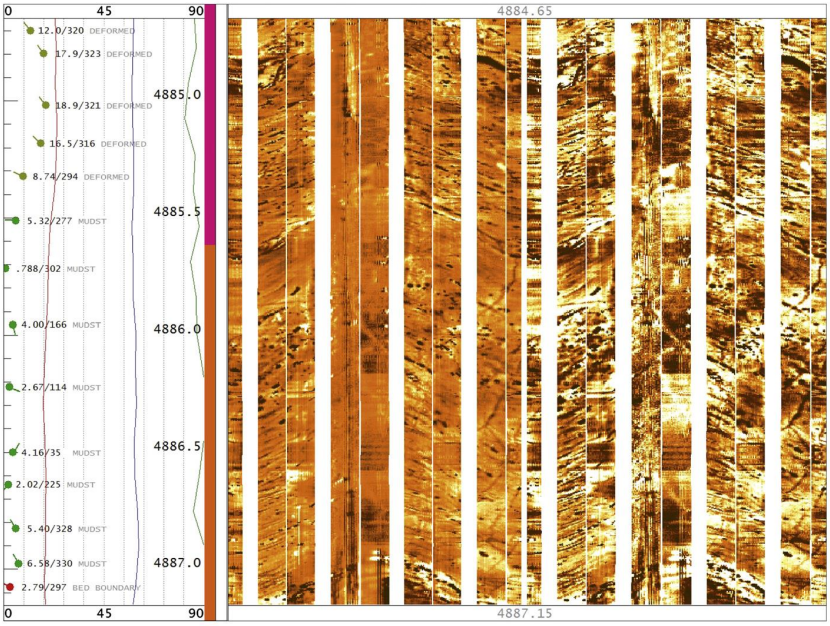

Figure 8. Laminated mudstone – IF 1 (34/11 - A - 10; Drake Formation): Well to faintly laminated mudstone (orange bar) showing conductive spots interpreted as burrows and/or pyrite nodules. Note that some mudstone beds are basically unaffected (e.g. at 4885.7 mMD). The upper part of the screenshot shows soft-sedimentary deformed mudstones with dip angles of up to 19° (after removing structural tilt, magenta bar). The petrophysical curves indicate high GR and a large positive separation of the ROBB and TNPH. As for all following examples the right-hand BHI image is dynamic normalized, while the left-hand image is static normalized (less contrast). (For interpretation of the references to colour in this figure legend, the reader is referred to the web version of this article.)

well 34/11 - A - 6 is concealed, however petrophysical logs indicate a gradual coarsening-upward trend from the underlying Burton Formation (see overview GR in Fig. 13).

The lowermost part of the shallowing-upward unit of the Cook Formation consists of alternating planar laminated mudstones (IF 1, Fig. 8) and scarce low-angle laminated sandstone intervals (IF 4, Fig. 11) in well 34/11 - A - 6. In contrast, well 34/11 - A - 10 shows dominant heterolithic strata (IF 2, Fig. 9) and two interbedded low-angle laminated sandstone beds (IF 4) with 1–2.5 m in thickness. The latter display up to 1 m thick sets with sharp set boundaries and stable east-southeast (ESE) dipping surfaces. Deformation in a heterolithic interval is caused by the presence of a small scale fault at 4947 mMD. Few palaeocurrent readings in well 34/11 - A - 6 (in beds ranging in thickness between a few decimetres up to 1 m) indicate a northwest (NW) to north–northwest (NNW) direction.

Further uphole (above 4938 mMD), well 34/11 - A - 6 consists of approximately 60% plane parallel laminated sandstones (IF 3, Fig. 10 and 15). Interbedded sandstone beds are low-angle laminated (IF 4) arranged in decimetre to 1.5 m thick beds with well-defined boundaries. Cross-stratified sandstones of image facies type IF 5 are characterized by decimetre scale to 1 m thick sets, often delimited by sharp to erosional set boundaries. Well 34/11 - A - 10 becomes progressively sandier, with plane parallel (IF 3) and low-angle laminated sandstones (IF 4). Minor disturbances in dip patterns are due to the presence of small scale faults. Overall, dip directions are to the NW (slightly scattered in well 34/11 - A - 6). The latter well also shows one metre thick interval with southeast (SE) dips (IF 4) in the middle of this section (4925 mMD). A weak bimodal NW–SE distribution can be inferred around 4935 mMD in well 34/11 - A - 10, however with a dominant NW direction (lower part of Fig. 15).

Towards the upper part of this unit, rhythmical, centimetre scale, conductive laminae become visible in well 34/11 - A - 6. Well 34/11 - A - 10 is characterized by plane-parallel laminated sandstones (IF 3) with interbedded units of IF 4 (1 – 3 m thick) and IF 5 (0.8–1.5 m thick, Fig. 15) and NW directed dip directions (see example at 4924 mMD, Fig. 12 and 15). Sharp to clearly erosional set boundaries (e.g. 4923.7 mMD, Fig. 12) are visible and cross-stratified sets (IF 5) seldom exceed a couple of decimetres in thickness (up to 1 m). The uppermost part of this unit is characterised by heterolithic laminated beds (IF 2, Fig. 9) in both wells. It is

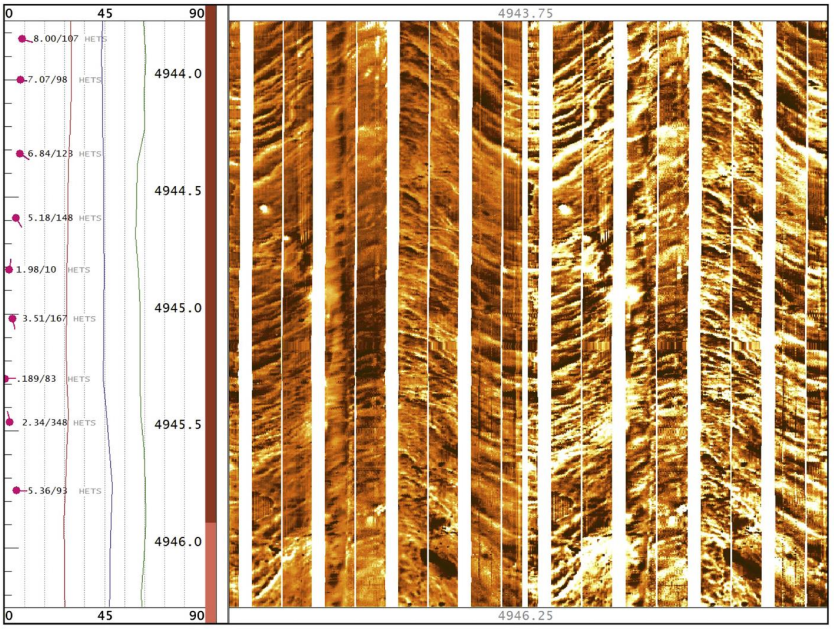

Figure 9. Bedded to laminated heterolith – IF 2 (34/11 - A - 10) with thin resistive and conductive laminae (brown bar). The wavy, flaser pattern can be interpreted as small scale ripple lamination. In comparison to the mudstones increased GR and closer ROBB and TNPH. (For interpretation of the references to colour in this figure legend, the reader is referred to the web version of this article.)

better defined in well 34/11 - A - 10 (Fig. 15). There is no indication of bioturbation in the range of the tool resolution. The overall stacking pattern of this unit and the described main NW dip direction of the cross beds (Figs. 13 and 14) suggest progradation of a delta in a NW direction. The heterolithic upper part probably represents the delta top of the delta system. Bimodal palaeocurrents indicate tidal influence.

6.2.2. Deepening-upward unit

This unit is best visible in well 34/11 - A - 10 in comparison to well 34/11 - A - 6 (Fig. 15). The deepening-upward unit in well 34/11 - A - 10 can be split into two sub-units, each measuring some 14 m in thickness: (i) The lower sub-unit is made up of high-angle cross-stratified (IF 5) as well as low-angle laminated (IF 4) sets (0.4 – 1.2 m in thickness), interbedded with horizontal laminated sandstones (IF 3) in the lowermost part. Sharp to erosional set boundaries are common in the cross-stratified sandstones (e.g. 4912 mMD and 4889.4 mMD). They display more regular dip patterns in comparison to the low-angle and plane-parallel laminated sandstones. The latter are irregularly laminated with fluctuating azimuths in some intervals. In terms of palaeo transport the lowermost part of the deepening unit shows highly variable directions, with northwest (NW), south–southeast (SSE) and a few west (W) directions (Fig. 14). (ii) The upper sub-unit shows only four cross-stratified (IF 5) to low-angle laminated (IF 4) beds (0.2–0.8 m in thickness), encased in dominantly plane-parallel laminated sandstones (IF 3, Fig. 15). Dip directions are bimodal WNW–ESE with a stronger influence of SE directions to the top (Fig. 14).

The deepening-upward unit in well 34/11 - A - 6 is characterized mainly by low-angle laminated (IF 4) and horizontal laminated sandstones (IF 3), as well as rare, decimetre thick, cross-stratified intervals (IF 5) with sets at decimetre scale (Fig. 15). The sandstones contain periodic conductive and resistive intervals, arranged in 20–25 cm thick plane parallel laminated packages (IF 3). In the upper part a more mottled unit (IF2) is seen below a unit of IF4 as a bright image which indicates clean sandstones. Sandstone dip directions show an overall bimodal, NW–SE trending pattern, again with a stronger SE influence towards the top (Fig. 13).

The deepening-upward unit in both wells is characterized by stacked cross-beds with bimodal palaeocurrents. The NW–SE directions suggest an estuarine environment for this unit in comparison to the deltaic unit below with dominant NW palaeocurrent directions. The planar laminated (IF3) and low-angle laminated sandstones (IF4) in the upper part of this unit (below the offshore Drake Formation) show a resistive appearance (bright

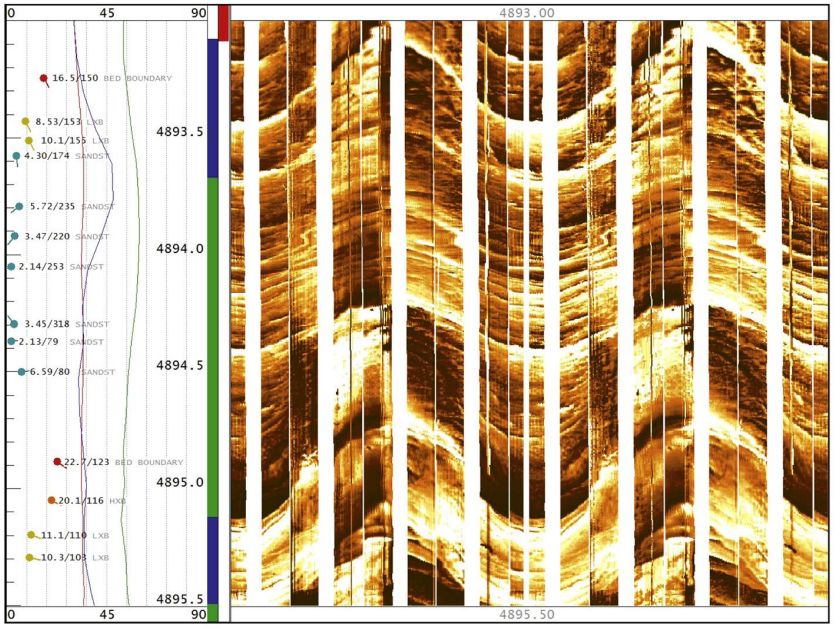

Figure 10. Horizontally laminated sandstone (green bar) – IF 3 (34/11 - A - 10) encased in low-angle cross-laminated sandstone packages (blue bar). The low dip angles show a considerable scatter in azimuth. Note the internal, sharp boundaries. (For interpretation of the references to colour in this figure legend, the reader is referred to the web version of this article.)

colours in 34/11 - A - 6), possibly suggesting well-sorted, wave-reworked sandstones. The mottled sandstones (IF2) seen below this wave-reworked unit in well 34/11 - A - 6 represent most likely a bioturbated interval. A stacking pattern starting with an estuary unit which is overlain by a bioturbated unit and above a wave-reworked sandstone at the top may suggest a wave-dominated estuary environment. The mottled and bioturbated interval possibly represents a back-barrier environment below the wave reworked beach-barrier environment. The latter is covered by offshore shales of the Drake Formation.

6.3. Top Cook Formation/base Drake Formation

The top of the Cook Formation in well 34/11 - A - 10 is a sharp boundary, covered by well laminated mudstones (IF 1) of the Drake Formation. However, comparable structural mean values (structural tilt) from the Drake Formation and the lowermost Cook Formation point to a conformable contact without any significant structural disturbance. In well 34/11 - A - 6 the Drake Formation is composed mainly of laminated mudstones (IF 1) with abundant conductive spots, possibly representing intense bioturbation and/or pyrite nodules.

7. Depositional environments of the Cook Formation by integrating image facies and cored facies association

The depositional interpretation of the Cook Formation is based on aligning the interpretations from the wire-line logs of the wells, the cored section of well 34/10 - 35 (Fig. 6) and the image logs in wells 34/11 - A - 6 and 34/11 - A - 10 (correlation panel in Fig. 15). A summary is given below.

The base of the Cook Formation is set at the level 4050.5 mMD in 34/10 - 35 where the gamma-log values decrease upwards from uniform and continued high values of the underlying Burton Formation. This break in gamma-ray log response is easily identified in the other wells (Fig. 16) and is a pragmatic approach to define the base of the Cook Formation. Above, the Cook Formation shows a gradual coarsening-upward trend from marine mudstones of the Burton Formation below to heterolithic sandstones and mudstones as shown in the cored section with facies association F1 and IF 1 in the image logs. This unit is interpreted as a part of a lower-delta front environment and is similar to the Cook 1 unit of Dreyer and Wiig (1995).

Above, the Cook Formation continues the coarsening-upward trend and the image logs show a change from dominantly horizontal lamination (IF 3) to more low-angle (IF 4) and cross-

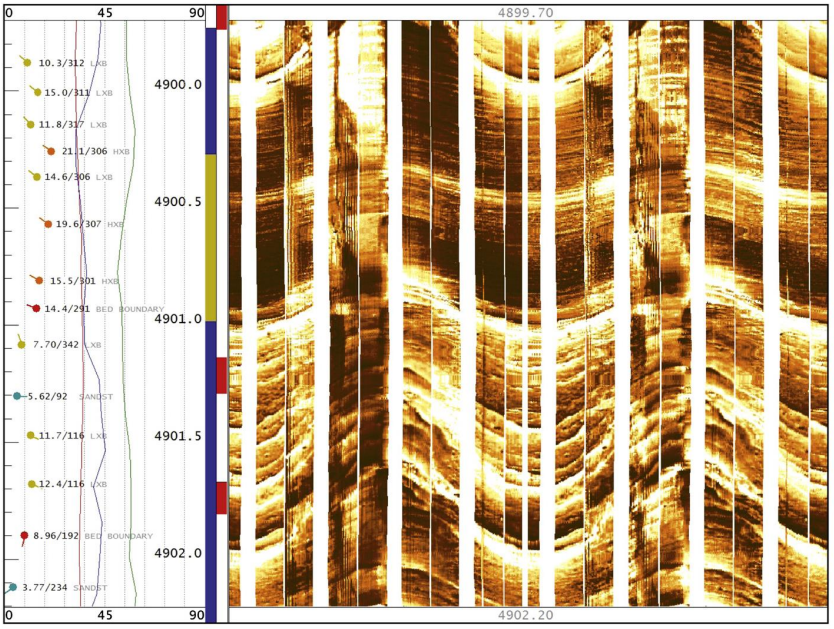

Figure 11. Low-angle cross-laminated sandstone (blue bar) – IF 4 (34/11 - A - 10) can have relatively variable resistivity patterns, being finely and regularly laminated (upper part) or rather wavy bedded (lower part). The latter pattern may be due to ripple lamination also causing less stable dip patterns. The upper part shows a gradual transition into cross-stratified sandstones (yellow bar). Both are limited by sharp to erosive (e.g. at 4900 mMD) bed boundaries. (For interpretation of the references to colour in this figure legend, the reader is referred to the web version of this article.)

stratified image facies (IF 5) upwards, suggesting the build-out of a delta with palaeocurrents indicating a NW transport direction but with bimodal palaeocurrent directions (inferred tidal currents, see also Kreisa and Moiola, 1986) seen in the image logs. This corresponds with the observations in the cored interval of facies association F2 in well 34/10 - 35 interpreted as a tidal-fluvial interaction delta. This interpretation is inferred to be valid also for the other wells without cores or image logs as the wire-line logs show a similar appearance.

Facies association F3 in the cored interval of well 34/10 - 35 is interpreted as a tidal dominated delta top environment, as the delta had built up to near sea level. This facies association has an erratic log signature in the wire-line logs and a heterolithic appearance in the image logs. The tidally influenced delta top environment interpretation is assumed valid for the other wells, especially as the image logs in this interval indicate mottling, probably caused by bioturbation.

The unit above the facies association F3 in well 34/10 - 35, up to the top of the formation, is not cored and the depositional interpretation is based in the image and wire-line logs. The wire-line logs strongly suggest a sandy unit and the image logs show that the lower part of this unit consists of stacked sets of cross-stratified sandstones (IF5) interpreted as tidal dunes, with low-angle (IF4) and horizontally laminated strata (IF3) in the upper part (Fig. 15). Here, palaeocurrent directions in the image logs show a general southern direction and a preferred SE direction with secondary bipolar palaeocurrents in well 34/11 - A - 6 (4898–4885 mMD) and 34/11 - A - 10 (4901–4888 mMD) suggesting tidal flood and ebb currents (see also Nio and Yang, 1991). An estuary environment is interpreted for this upper unit of the Cook Formation. This takes into account the thickly stacked sets of cross-stratified sandstones in this unit, the reversed (southerly direction opposed to NW of the delta below) and bipolar palaeocurrents in the upper part of this unit and the flat lamination at the top of this unit (below the mudstones of the offshore Drake Formation) as well as the tidal-fluvial influenced deltaic interpretation of the Cook Formation below. The upper part of this unit shows clean and well-sorted sands with horizontal lamination (IF 3) and indicates reworking by a wave-ravinement process and an associated barrier complex. This suggests that the estuary probably was a wave-dominated estuary type (sensu Dalrymple et al., 1992) and the transition into offshore mudstone environment above (Drake Formation) points to a final drowning of the Cook Formation. Charnock et al. (2001) interpreted the upper part of the contemporary Cook Formation in the Gullfaks

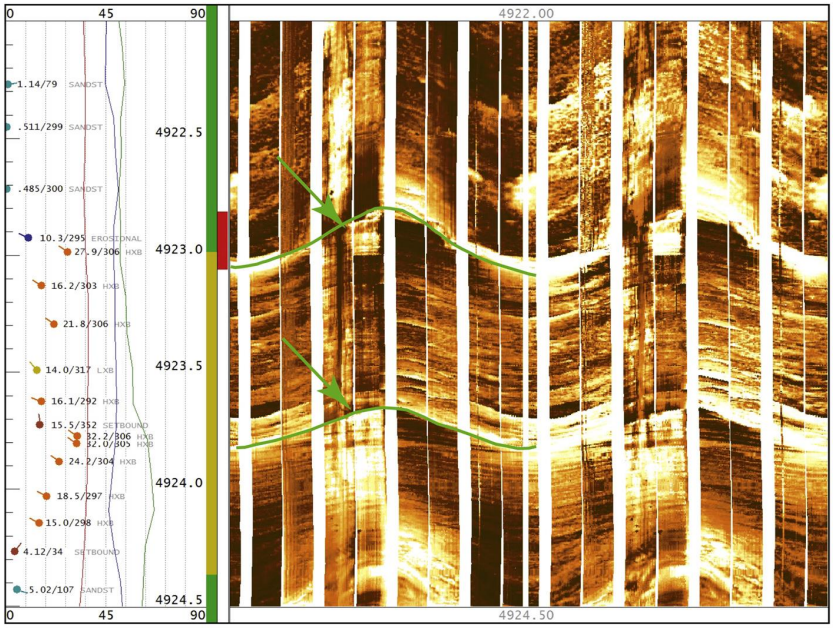

Figure 12. Cross-stratified sandstones – IF 5 (34/11 - A - 10) are characterised by steep dip angles with stable dip azimuths (yellow bar), as well as steepening upwards dip patterns (e.g. around 4924 mMD). Some cross-set boundaries (green planes) are clearly erosive and cut the underlying lamination (e.g. 4923.7 and 4923 mMD; green arrows). The erosive set boundaries limit an approx. 80 cm thick cross-set. The cross-sets are overlain by horizontal, faintly laminated sandstones (green bar). (For interpretation of the references to colour in this figure legend, the reader is referred to the web version of this article.)

area (Fig. 2) as estuary deposits, which is consistent with our interpretation here. The base of the estuary unit is not cored in the wells of the study area but the image log in well 34/11 - A - 10 suggests an erosive base, making this surface a potential (tidal) transgressive surface at the base of the estuary. The deltaic to estuary couplet interpretation of the Cook Formation corresponds to the regressive to transgressive subdivision for the Cook Formation by Steel (1993).

8. Thickness distribution within the Cook Formation

In Fig. 16, the Cook Formation shows a thickening trend of approximately 30% from 34/11 - A - 10 (65 mTVD) to the wells 34/10 - 35 (87 mTVD) and 34/10 - 23 (84 mTVD). Internally, the regressive (deltaic facies association F1 - 2 - 3) of the formation shows a thickening trend westward of approximately 68% from 34/11 - A - 10 (45 mTVD) to the wells 34/10 - 35 (76 mTVD) and 34/10 - 23 (73 mTVD). Such a thickness difference has not been reported within the deltaic part of the Cook Formation in the Tampen Spur (Dreyer and Wiig, 1995; Charnock et al., 2001; Husmo et al., 2003) and it appears to be at odds with the general tabular thickness distribution of the Cook Formation on field scale (Charnock et al., 2001; Husmo et al., 2003).

An east–west seismic cross-section is shown in Fig. 17 with well-ties of 34/11 - A - 10 to 34/10 - 35 of the correlation panel and further to well 34/10 - 9 in the Gullfaks Field to the northwest (Figs. 1 and 2). At these depths of >4000 m below the sea floor, the seismic resolution and quality is unfortunately poor. The Cook Formation (top and base) surfaces in the wells are tied to the seismic but it is challenging to impossible to interpret these surfaces between the wells. A fault is identified between well 34/10 - 35 and well 34/10 - 9 in this seismic cross-section. According to Færseth (1996) and Odinsen et al. (2000) this fault is a Permo – Triassic fault and is here named the Gullfaks South (GS) fault (see Fig. 1). The 34/10 - 9 well is located on the footwall side of this Permo – Triassic fault (Fig. 1) and has a similar thickness to well 34/11 - 1 (see Fig. 2) which illustrates the general tabular appearance of the Cook Formation in this area. Therefore, the added thickness of the Cook Formation in wells 34/10 - 23 and 34/10 - 35 appears to be of local significance.

One possibility to explain the stratal east–west wedge-shape of the regressive part (Fig. 16) is to assume movement of the GS fault (Fig. 17) during deposition. Such an interpretation would fit with

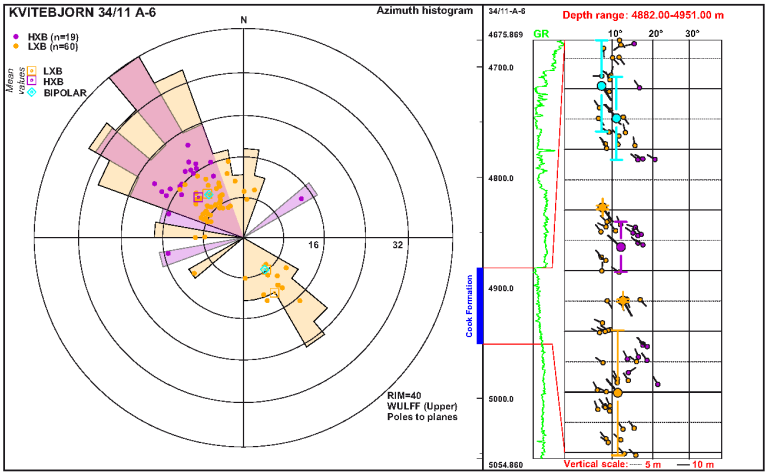

Figure 13. Stereographic summary (left) and depth plot (right) of all measured cross-stratified and low-angle laminated sandstones in the entire Cook Formation (blue bar) in well 34/11 - A - 6 (the overview GR is given for consistency with remaining figures as well as to depict the transition to adjacent formations). The rim of the stereonet (Wulff upper hemisphere projection of poles to planes) is limited to 40° in order to increase detail. Each vertical line in the depth plot displayed to the right accounts for 10° in dip angle (showing 0°–40°). HXB – cross-stratified sandstones of IF 5; LXB – low-angle laminated sandstones of IF 4, bipolar-dipping sandstone laminae interpreted as influenced by tidal currents. (For interpretation of the references to colour in this figure legend, the reader is referred to the web version of this article.)

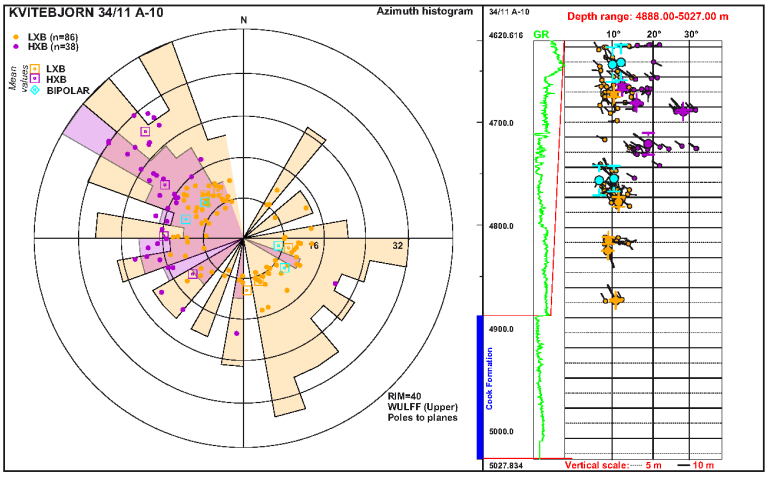

Figure 14. Stereographic summary and depth plot of all measured cross-stratified and low-angle laminated sandstones in the entire Cook Formation (blue bar) in well 34/11 - A - 10. See Fig. 13 for further detail. (For interpretation of the references to colour in this figure legend, the reader is referred to the web version of this article.)

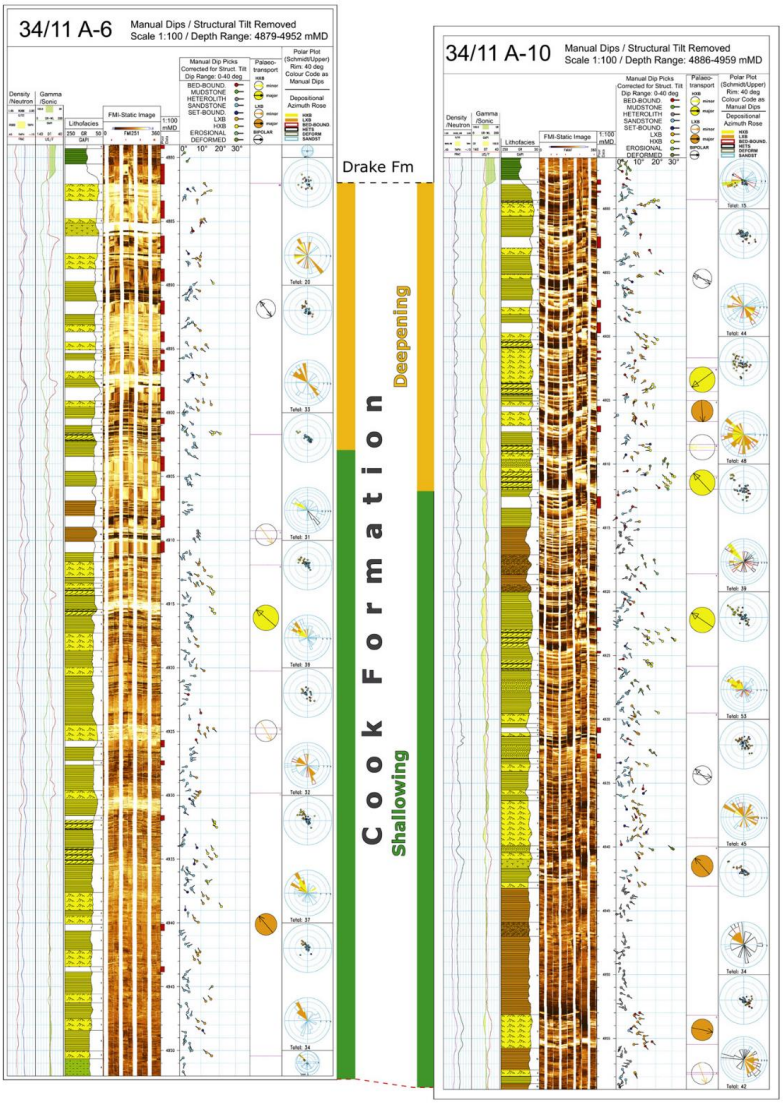

Figure 15. Correlation panel of wells 34/11 - A - 6 and 34/11 - A - 10, showing facies stacking and dip patterns (in dip track and stereographic projection) as well as calculated palaeocurrent directions (coloured arrows) and the petrophysical log response (GR, ROBB/TNPH). See Fig. 5 for image facies legend.

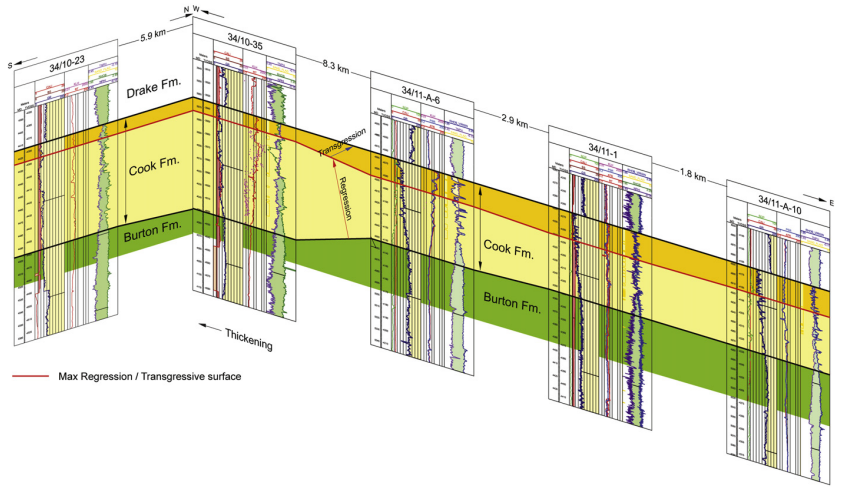

Figure 16. Correlation of the Cook Formation in the Kvitebjørn and Valemon areas. East–west and north–south oriented correlation of the wells used in this study. Well spacing is not to scale. Note the thickness trends of the regressive versus the transgressive part of the formation.

the observed local added thickness of the regressive part. An assumption of fault movement of this Permo – Triassic fault is a relevant model as some of these Permo – Triassic faults showed activity throughout the Jurassic (Hampson et al., 2004) and others show sporadic movements in the Early Jurassic epoch (Færseth, 1996; Færseth and Ravnås, 1998). Charnock et al. (2001) suggested from their regional study of the Cook Formation that the Permo – Triassic faults had an influence on the subsidence pattern. However, the poor quality of the seismic cross-section (Fig. 17) allows for no examination of stratal growth on the GS fault plane within the Cook Formation.

The westward increase in thickness towards the wells 34/10 - 35 and 34/10 - 23 could be explained by a westward deepening of the basin floor. This interpretation would render a rather steep angle of the basin floor. As a logical consequence, the basinward well 34/10 - 9 would be expected to have a thicker Cook Formation. Fig. 2 shows that well 34/10 - 9 has the same thickness as well 34/11 - 1, illustrating the tabular nature of the Cook Formation in this area. This contradicts a steep basin floor interpretation which is here regarded as less likely. The authors have not found alternative interpretations to explain the westward thickening of the regressive Cook Formation.

9. Discussion

The overall stratigraphic development of the Cook Formation in the study area represents the growth of a tidal-fluvial interaction delta, shallowing upwards to a delta top at near sea level and capped by a surface of maximum regression (sensu Helland-Hansen and Martinsen, 1996). Thus the accommodation space was filled and the delta front was forced to prograde further basinward (Fig. 18). At some point, as a result of reduced sediment supply, increased tectonic subsidence or simply auto-retreat (Muto and Steel, 2002), the coastline started to step landwards, initiating a transgression that finally drowned the Cook Formation in the study area. During this transgression, the sea invaded the delta top environment and probably transformed the distributary rivers into estuaries, possibly in a similar manner as described by Plink-Bjørklund (2008), with tidal erosion and subsequent expansion of the size of the channels (Fig. 19). The base of the estuary is termed a transgressive, tidal ravinement surface (sensu Catuneanu, 2002) that coincides with the maximum regressive surface. This surface will correspond to the regional unconformity surface proposed by Steel (1993) separating the regressive lower Cook Formation from the transgressive upper Cook Formation. Such a delta-estuary couplet is often seen within shallow marine sand units as a result of changing accommodation space versus sediment supply rates creating transgressive and regressive cycles (Schellpeper, 2000; Mellere et al., 2002; Folkestad and Satur, 2008; Steel et al., 2008). The tidal-fluvial influenced delta was deposited under highstand conditions due to a significant rise in base level during regional tectonic subsidence whereas the estuary was deposited within the transgressive system tract.

Both Dreyer and Wiig (1995) and Charnock et al. (2001) have described the deltaic part of the Cook Formation in the Tampen Spur area as being wave-dominated. This stands in contrast to the tidal-fluvial dominated delta regressive unit of this study. However, a tidal-fluvial delta can occur in a sheltered position in an otherwise wave-dominated coast. With the proposed model of fault movement of the GS fault, explaining the added thickness of the Cook Formation, one can speculate that the GS fault did not breach the sea floor surface as the added stratal thickness is limited (68%). According to Ford et al. (2007) a substantial part of the total fault movement will occur in the subsurface before the fault breaches

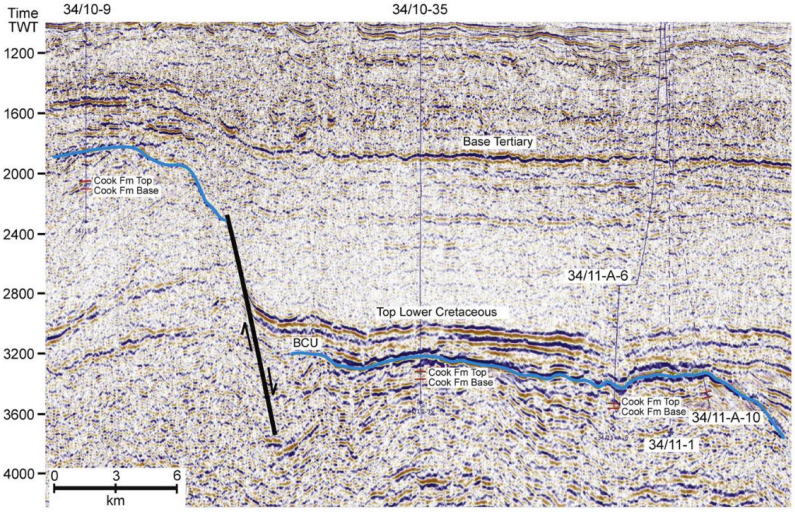

Figure 17. East–west seismic cross-section in time-depth. The section is parallel to most of the well correlation panel (Fig. 16). The wells are tied to the seismic (see Fig. 1 for locations) but the quality of the seismic is too poor to allow interpretation of surfaces between the wells below the Base Cretaceous Unconformity (blue surface). A major fault (GS, see Fig. 1 for location) can be seen. According to Færseth (1996) and Odinsen et al. (2000) it is a Permo – Triassic fault. (For interpretation of the references to colour in this figure legend, the reader is referred to the web version of this article.)

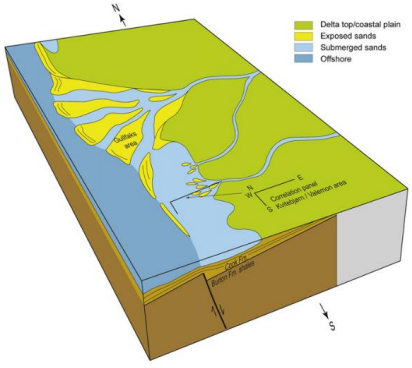

Figure 18. The coarsening-upward or the regressive part of the Cook Formation is proposed as a regressive tidal-fluvial dominated delta with: numerous mudstone drapes, horizontal bioturbation, cross-stratification and bedsets of structureless sandstones followed by current ripples and mudstone drapes. The image logs indicate a NW sediment transport direction (basinward) with some bipolar (tidal) currents. The unit shows a general lack of wave structures. These observations suggest a tidal-fluvial delta deposited in a sheltered setting facilitated by a proposed monocline with an attached barrier. The delta top environment is assumed to be a more drained coastal plain type of depositional environment landward.

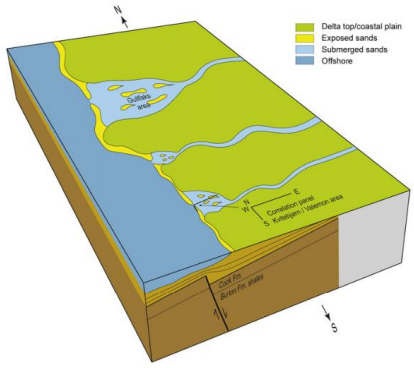

Figure 19. The upper part of the Cook Formation is not cored and the interpretation is constrained by the interpretation of image facies and conventional logs. This unit is interpreted as stacked cross-stratified sandstones with SE (landward) sediment transport direction and overlain by planar laminated sandstones. It is interpreted as a wave-dominated estuary deposited during transgression and subsequent drowning of the Cook Formation.

the surface. A blind fault would form a monocline above the fault plane (Fig. 20), creating a bathyal topographic high. Such a bathyal high may have attracted sands fed from longshore drift from the adjacent wave reworked deltas, as for example in the adjacent Gullfaks area (Dreyer and Wiig, 1995; Charnock et al., 2001). Sands deflected longshore in a similar manner as described by Bhattacharya and Giosan (2003) would create a spit system (see also Dreyer et al., 2005) that can extend for tens of kilometres (Nielsen and Johannessen, 2009). A monocline with an attached spit system would create a sheltered sub-basin that the tidal-fluvial delta of the study area built into (Fig. 18). The well 34/10 - 9 (Fig. 1) located on the footwall side of the GS fault was described and interpreted as shoreface in the regressive part of the Cook Formation by Charnock et al. (2001). This interpretation fits with a proposed spit-model associated with the GS fault.

This model involves several assumptions in order to integrate the observed stratal wegde-shaped regressive unit with the tidal-fluvial delta depositional environment within the context of a regional, tabular wave-dominated deltaic unit (Dreyer and Wiig, 1995; Charnock et al., 2001). However, other examples of structurally protected deltas have been reported which makes the current model likely. A somewhat similar setting for a tidal delta within a micro tidal range regime was described by Lambiase et al. (2003) from the NW coast of Borneo. There a tidal delta built out into a structurally controlled coastal embayment bordered by a sill at the mouth of the bay which thus sheltered the bay from the open sea. In addition syn-sedimentary fault activity, producing sedimentary wedges, within the Cook Formation has been reported by Livbjerg and Mjøs (1989) in block 30/6 that is to the southeast of this study area.

The formation of the delta top environment suggests complete infill of the basinal topography and the following transgression occurred across a relatively flat coastal plain. The transgressive part of the Cook Formation shows a gentle eastwards thickening trend (Fig. 16), an opposite trend to that seen in the regressive part. This is probably related to the change from regressive deltas to transgressive estuaries, where sediments were trapped landwards due to added accommodation space caused by a rising relative sea level with a climbing (landward) shoreline trajectory. Similar landward increases in thickness of the transgressive phase units have earlier been reported in other studies by Mellere and Steel (1996), Ravnås et al. (1997) or Folkestad and Satur (2008). The transgressive ravinement process can scour down into the strata below, thus creating a landward-thickening transgressive unit. However the relatively tabular and thick delta top facies association contradicts that. It is possible that the thickness difference of the estuary unit can be related to differential subsidence, but it seems unlikely that the fault block should dip the opposite way, without being associated with an active fault.

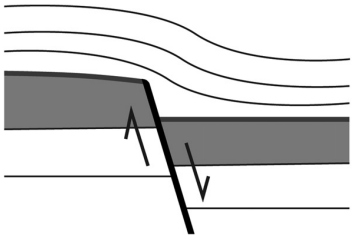

Figure 20. Movement of a blind fault will produce a monocline above the fault plane. Modified from Ford et al. (2007).

10. Conclusions

From descriptions and interpretations of cores, wire-line and borehole image logs the Cook Formation in the Kvitebjørn/Valemon area (blocks 34/10 and 34/11) of the North Sea is interpreted as a mixed-energy, tidal-fluvial delta capped by a wave-dominated estuary. With only one cored well in this study, the use of borehole image logs proved to be of great importance for understanding the depositional environments. As the cored well did not have any image log, a direct calibration between the cores and image logs was not possible. Therefore a simple and objective description approach of the sedimentary structures was chosen to limit the uncertainties in the interpretation of the image facies association. Despite these challenges, the use of image logs in this study provided sediment transport directions for the prograding delta and the overlying retreating estuary and supported the interpretation of tidal processes from bidirectional palaeocurrents. The image logs played a key role in interpreting the uncored estuary unit with the identification of thickly stacked sets of cross-stratified sandstone interpreted as bars or dunes on tidal sandflats. Added to the landward-directed palaeocurrents, a sandy, transgressive estuary environment is proposed for this upper part of the Cook Formation.

The deltaic part of the Cook Formation shows a significant thickening trend westwards, interpreted to have been caused by movements on an active fault. The syn-sedimentary tectonic explanation for this feature is likely, as syn-sedimentary tectonics have earlier been reported in the Cook Formation in the Oseberg area (Block 30/6) (Livbjerg and Mjøs, 1989) and fault-associated sedimentary wedges are recorded in the Lower Jurassic in the northern North Sea (Ravnås et al., 2000). The delta was deposited in a sheltered basin and it lacks signs of wave reworking. This sheltering is inferred to have been caused by a basinward barrier attached to the crest of an active fault. The barrier was fed from the coeval wave-dominated delta at the adjacent Gullfaks Field (Dreyer and Wiig, 1995; Charnock et al., 2001) by deflection and longshore drift of sands along the coast. The proposed estuary in the upper part of the formation is interpreted from wire-line and image logs based on the recognition of thick stacked sets of cross-stratified sandstones that migrated landward. Thus the Cook Formation here represents a delta-estuary couplet of a type commonly recorded elsewhere in shallow marine regressive-transgressive cycles.

Acknowledgements

The authors would like to thank the partners in the Kvitebjørn Licence for permission to publish: Statoil, Petoro, Enterprise Norway Oil, and Total. Tore Odinsen, Martin A. Pearce and Nicholas Satur are thanked for their assistance and discussion, Wenche Bødtker and Linda Dyrkolbotn for graphical assistance and Naomi Veselovsky for proof reading of the text. In addition Ronald Steel is thanked for his comments on an early version of this manuscript. The suggestions and improvements of the anonymous reviewers are also appreciated.

References

Ager, D.V., 1975. The Jurassic world ocean (with reference to the North Atlantic): Jurassic Northern North Sea Symposium, Stavanger, pp. 1–43.

Ambrose, W.A., Hentz, T.F., Bonnaffé, F., Loucks, R.G., Brown Jr., L.F., Wang, F.P., Potter, E.C., 2009. Sequence-stratigraphic controls on complex reservoir architecture of highstand fluvial-dominated deltaic and lowstand valley-fill deposits in the Upper Cretaceous (Cenomanian) Woodbine Group, East Texas field: regional and local perspective. Bulletin of American Association of Petroleum Geologists 93, 231–269.

Bhattacharya, J., Walker, R.G., 1991. River and wave-dominated depositional systems of the Upper Cretaceous Dunvegan Formation, Northwestern Alberta. Bulletin of Canadian Petroleum Geology 39, 165–191.

Bhattacharya, J., Walker, R.G., 1992. Deltas. In: Walker, R.G., James, N.P. (Eds.), Facies Models: Response to Sea-Level Change. Geological Association of Canada, pp. 157–177.

Bhattacharya, J., Giosan, L., 2003. Wave-influenced deltas: geomorphological implications for facies reconstruction. Sedimentology 50, 187–210.

Catuneanu, O., 2002. Sequence stratigraphy of clastic systems: concepts, merit, and pitfalls. Journal of African Earth Science 35, 1–43.

Charnock, M.A., Kristiansen, I.L., Ryseth, A., Fenton, J.P.G., 2001. Sequence stratigraphy of the Lower Jurassic Dunlin Group, northern North Sea. In: Martinsen, O.J., Dreyer, T. (Eds.), Sedimentary Environments Offshore Norway – Palaeozoic to Recent. Norwegian Petroleum Society, Special Publication, vol. 10, pp. 145–174.

Coleman, J.M., Gagliano, S.M., Smith, W.G., 1970. Sedimentation in a Malaysian high tide tropical delta. In: Morgan, J.P. (Ed.), Deltaic Sedimentation: Modern and Ancient. Society of Economic Paleontologists and Mineralogists Special Publication, vol. 15, pp. 185–197.

Dalrymple, R.W., Yasuhiko, M., Zaitlin, B.A., 1991. Temporal and spatial patterns of rhythmite deposition on mud flats in the macrotidal Cobequid Bay-Salmon River estuary, Bay of Fundy, Canada. In: Smith, D.G., Reinson, G.E., Xaitlin, B.A., Rahmani, R.A. (Eds.), Clastic Tidal Sedimentology. Canadian Society of Petroleum Geologists Memoirs 16, pp. 3–28.

Dalrymple, R.W., Zaitlin, B.A., Boyd, R., 1992. Estuarine facies models: conceptual basis and stratigraphic implications. Journal of Sedimentary Petrology 62, 1130–1146.

Dalrymple, R.W., Baker, E.K., Harris, P.T., Hughes, M.G., 2003. Sedimentology and Stratigraphy of a tide-dominated, foreland-basin delta (Fly River, Papua New Guinea). In: Sidi, F.H., Nummedal, D., Imbert, P., Darman, H., Posamentier, H.W. (Eds.), Tropical Deltas of Southeast Asia-Sedimentology, Stratigraphy, and Petroleum Geology. Society of Economic Paleontologists and Mineralogists Special Publication, vol. 76, pp. 147–173.

Dalrymple, R.W., Choi, K., 2007. Morphology and facies trends through the fluvial-marine transition in tide-dominated systems: a schematic framework for environmental and sequence-stratigraphic interpretation. Earth-Science Reviews 81, 135–174.

Donselaar, M.E., Schmidt, J.M., 2005. Integration of outcrop and borehole image logs for high-resolution facies interpretation: example from a fluvial fan in the Ebro Basin, Spain. Sedimentology 52, 1021–1042.

Dreyer, T., Wiig, M., 1995. Reservoir architecture of the Cook Formation on the Gullfaks field based on sequence stratigraphic concepts. In: Steel, R.J., Felt, V., Johannessen, E.P., Mathieu, C. (Eds.), Sequence Stratigraphy of The Northwest European Margin. Norwegian Petroleum Society, Special Publication, vol. 5, pp. 109–142.

Dreyer, T., Whitaker, M., Dexter, J., Flesche, H., Larsen, E., 2005. From spit system to tide-dominated delta: integrated reservoir model of the Upper Jurassic Sognefjord Formation on the Troll West Field. In: Dore, A.G., Vinning, B. (Eds.), Petroleum geology: North-West Europe and Global Perspectives. Proceedings of The 6th Petroleum Geology Conference. Geological Society, London, pp. 1–27.

Folkestad, A., Satur, N., 2008. Regressive and transgressive cycles in a rift-basin: depositional model and sedimentary partitioning of the Middle Jurassic Hugin Formation, Southern Viking Graben, North Sea. Sedimentary Geology 207, 1–21.

Ford, M., Le Carlier de Veslud, C., Bourgeois, O., 2007. Kinematic and geometric analysis of fault-related folds in a rift setting: the Dannemarie basin, Upper Rhine Graben, France. Journal of Structural Geology 29, 1811–1830.

Færseth, R., 1996. Interaction of Permo – Triassic and Jurassic extensional fault-blocks during the development of the northern North Sea. Journal of the Geological Society, London 153, 931–944.

Færseth, R.B., Ravnås, R., 1998. Evolution of the Oseberg fault-block in context of the northern North Sea structural framework. Marine and Petroleum Geology 15, 467–490.

Gabrielsen, R.H., Færseth, R.B., Steel, R.J., Idil, S., Kløvjan, O.S., 1990. Architectural styles of basin fill in the northern Viking Graben. In: Blundell, D.J., Gibbs, A.D. (Eds.), Tectonic Evolution of the North Sea Rifts. Oxford University Press, Oxford, pp. 158–179.

Gage, M.S., Doré, A.G., 1986. A regional geological perspective of the Norwegian offshore exploration provinces. In: Spencer, A.M., Campbell, C.J., Hanslien, S.H., Holter, E., Nelson, P.H.H., Nysæther, E., Ormaasen, E.G. (Eds.), Habitat of Hydrocarbons on the Norwegian Continental Shelf, pp. 21–38. London, Graham and Trotman.

Hampson, G.J., Sixsmith, P.J., Johnson, H.D., 2004. A sedimentological approach to refining reservoir architecture in a mature hydrocarbon province: the Brent Province, UK North Sea. Marine and Petroleum Geology 21, 457–484.

Hansen, B., Weihe, T., 2008. The control of geomechanics on reservoir properties of the upper sarir sandstone formation. An Nakhlah oil field, Hameimat Trough, East Sirt Basin, Libya. In: Salem, M.J., Aburawi, R.M., Misallati, A.A. (Eds.), Geology of East Libya 2, pp. 309–318.

Harris, P.T., Pattiaratchi, C.B., Cole, A.R., Keene, J.B., 1992. Evolution of subtidal sandbanks in Moreton Bay, eastern Australian. Marine Geology 103, 225–247.

Helland-Hansen, W., Martinsen, O.J., 1996. Shoreline trajectories and sequences; description of variable depositional-dip scenarios. Journal of Sedimentary Research 66, 670–688.

Hoecker, C., Eastwood, K.M., Herweijer, J.C., Adams, J.T., 1990. Use of dipmeter data in clastic sedimentological studies. Bulletin of American Association of Petroleum Geologists 74, 105–118.

Husmo, T., Hamar, G.P., Høiland, O., Johannessen, E.P., Rømuld, A., Spencer, A.M., Titterton, R., 2003. Lower and Middle Jurassic. In: Evans, D., Graham, C., Armour, A., Bathurst, P. (Eds.), The Millenium Atlas: Petroleum Geology of the Central and Northern North Sea. Geological Society of London, pp. 129–155.

Kreisa, R.D., Moiola, R.J., 1986. Sigmoidal tidal bundles and other tide-generated sedimentary structures of the Curtis Formation, Utah. Geological Society of America Bulletin 97, 381–387.

Lambiase, J.J., Razak Damit, A., Simmons, M.D., Abdoerrias, R., Hussin, A., 2003. A depositional model and the stratigraphic development of modern and ancient tide-dominated deltas in NW Boreno. In: Tropical Deltas of South East Asia. Sedimentology, Stratigraphy and Petroleum Geology. Society of Economic Paleontologists and Mineralogists Special Publication, vol. 76, pp. 109–123.

Lervik, K.S., Spencer, A.M., Warrington, G., 1989. Outline of Triassic stratigraphy and structure in the central and northern North Sea. In: Collinson, J.D. (Ed.), Correlation in Hydrocarbon Exploration. Outline of Triassic Stratigraphy and Structure. Norwegian Petroleum Society, pp. 173–189.

Livbjerg, F., Mjøs, R., 1989. The Cook Formation, an offshore sand ridge in the Oseberg area, northern North Sea. In: Collinson, J.D. (Ed.), Correlation in Hydrocarbon Exploration. Norwegian Petroleum Society, Graham and Trotman, London, pp. 299–312.

Lowe, D.R., 1982. Sediment gravity flows: II. Depositional models with special reference to the deposits of high-density turbidity currents. Journal of Sedimentary Petrology 52, 279–297.

Luthi, S.M., 2001. Geological Well Logs: Their Use in Reservoir Modelling. Springer, 373 p.

MacEachern, J., Bann, K., 2008. The role of ichnology in refining shallow marine facies models. In: Hampson, G.J., Steel, R.J., Burgess, P.M., Dalrymple, R.W. (Eds.), Recent Advances in Models of Siliciclastic Shallow-Marine Stratigraphy. Society of Economic Paleontologists and Mineralogists Special Publication, vol. 90, pp. 73–116.

Marjanac, T., Steel, R.J., 1997. Dunlin Group sequence stratigraphy in the northern North Sea, a model for Cook Sandstone deposition. Bulletin of American Association of Petroleum Geologists 81, 276–292.

Martinius, A.W., Kaas, I., Næss, A., Helgesen, G., Kjærefjord, J.M., Leith, D.A., 2001. Sedimentology of the heterolithic and tide-dominated Tilje Formation (Early Jurassic, Halten Terrace offshore mid-Norway). In: Martinsen, O., Dreyer, T. (Eds.), Sedimentary Environments Offshore Norway – Paleozoic to Recent. Norwegian Petroleum Society, Special Publication, vol. 10, pp. 103–144.

Mellere, D., Plink-Björklund, P., Steel, R.J., 2002. Anatomy of shelf deltas at the edge of a prograding Eocene shelf margin, Spitsbergen. Sedimentology 49, 1181–1206.

Mellere, D., Steel, R.J., 1996. Tidal sedimentation in the Inner Hebrides half grabens, Scotland: the mid-Jurassic Bearreraig Sandstone Formation. In: De Batist, M., Jacobs, P. (Eds.), Siliciclastic Shelf Seas. Geological Society, London, Special Publication, vol. 117, pp. 49–79.

Muto, T., Steel, R.J., 2002. Role of autoretreat and A/S changes in the understanding of deltaic shoreline trajectory: a semi-quantitative approach. Basin Research 14, 303–318.

Myrow, P.M., Southard, J.B., 1996. Tempestite deposition. Journal of Sedimentary Research 66, 875–887.

Nielsen, L.H., Johannessen, P.N., 2009. Facies architecture and depositional processes of the Holocene – recent accretionary forced regressive Skagen spit system, Denmark. Sedimentology 56, 935–968.

Nio, S.D., Yang, C.S., 1991. Diagnostic attributes of clastic tidal deposits: a review. In: Smith, D.G., Reinson, G.E., Zaitlin, B.A., Rahmani, R.A. (Eds.), Clastic Tidal Sedimentology. Canadian Society of Petroleum Geologists, Memoir 16, pp. 3–28.

Odinsen, T., Christianson, P., Garbielsen, R.H., Faleide, J.I., Berge, A.M., 2000. The geometries and deep structures of the northern North Sea rift system. In: Nøttvedt, A. (Ed.), Dynamics of the Norwegian Margin. Geological Society of London, Special Publications, vol. 167, pp. 41–57.

Olariu, C., Bhattacharya, J.P., 2006. Terminal distributary channels and delta-front architecture of river-dominated delta systems. Journal of Sedimentary Research 76, 212–233.

Petter, A.L., Steel, R.J., 2006. Hyperpicnal flow variability and slope organization on an Eocene shelf margin, Central Basin, Spitsbergen. Bulletin of American Association of Petroleum Geologists 90, 1451–1472.

Plink-Björklund, P., Mellere, D., Steel, R.J., 2001. Turbidite variability and architecture of sand-prone, deepwater slopes: eocene clinoforms of the Central Basin, Spitsbergen. Journal of Sedimentary Research 71, 897–914.

Plink-Björklund, P., 2005. Stacked fluvial and tide-dominated estuarine deposits in high-frequency (fourth-order) sequences of the Eocene Central Basin, Spitsbergen. Sedimentology 52, 391–428.

Plink-Bjørklund, P., 2008. Wave-to-tide facies change in a Campanian shoreline complex, Chiney Rock Tounge, Wyoming–Utah, U.S.A. In: Hampson, G.J., Steel, R.J., Burgess, P.M., Dalrymple, R.W. (Eds.), Recent Advances in Models of Siliciclastic Shallow-Marine Stratigraphy. Society of Economic Paleontologists and Mineralogists Special Publication, vol. 90, pp. 265–292.

Poppelreiter, M., Balzarini, M.A., De Sousa, P., Engel, S., Galarraga, M., Hansen, B., Marquez, X., Morell, J., Nelson, R., Rodriguez, F., 2005. Structural control on sweet-spot distribution in a carbonate reservoir: concepts and 3-D models (Cogollo Group, Lower Cretaceous, Venezuela). Bulletin of American Association of Petroleum Geologists 89, 1651–1676.

Ravnås, R., Bondevik, K., Helland-Hansen, W., LømoLeif, D., Ryseth, A., Steel, R.J., 1997. Sedimentation history as an indicator of rift initiation and development: the Late Bajocian – Bathonian evolution of the Oseberg – Brage area, northern North Sea. Norsk Geologisk Tidskrift 77, 205–232.

Ravnås, R., Nøttvedt, A., Steel, R.J., Windelstad, J., 2000. Syn-rift sedimentary architectures in the northern North Sea. In: Nøttvedt, A., Larsen, B.T., Olaussen, S., Tørudbakken, B., Skogseid, J., Gabrielsen, R.H., Brekke, H., Birkeland, Ø. (Eds.), Dynamics of the Norwegian Margin. Geological Society of London, Special Publications, vol. 167, pp. 133–177.

Reineck, H.E., Singh, I.B., 1980. Depositional Sedimentary Environments, second ed. Springer, 549 p.

Rider, M., 2004. The Geological Interpretation of Well Logs, second ed. Rider-French Consulting, 280 p.

Rouby, D., Fossen, H., Cobbold, P.R., 1996. Extension, displacement, and block rotation in the larger Gullfaks area, northern North Sea: determined from map view restoration. Bulletin of American Association of Petroleum Geologists 80, 875–890.

Schellpeper, M. E., 2000. Basin analysis of the Central Tertiary Basin and sequence stratigraphy of an Eocene clinoform in the Battfjellet Formation, Spitsbergen. MSc Thesis, Department of Geology and Geophysics, University of Wyoming, 63 p.

Steel, R.J., 1993. Triassic – Jurassic megasequence stratigraphy in the Northern North Sea: rift to post-rift evolution. In: Parker, J.R. (Ed.), Petroleum Geology of Northwest Europe: Proceedings of the 4th Conference. Geological Society, London, pp. 299–315.

Steel, R.J., Ryseth, A., 1990. The Triassic – Early Jurassic succession in the northern North Sea: megasequence stratigraphy and intra-Triassic tectonics. In: Hardman, R.F.P., Brooks, J. (Eds.), Tectonic Events Responsible for Britain's Oil and Gas Reserves. Geological Society, London, Special Publications, vol. 55, pp. 139–168.

Steel, R.J., Carvajal, C., Petter, A., Uroza, C., 2008. In: Recent Advances in Models of Siliciclastic Shallow-Marine Stratigraphy. Society for Sedimentary Geology, Special Publication, vol. 90, pp. 47–72.

Taylor, A.M., Gawthorpe, R.L., 1993. Application of sequence stratigraphy and trace fossils analysis to reservoir description; examples from the Jurassic of the North Sea. In: ParkerJ.R. (Ed.), Petroleum Geology of Northwest Europe: Proceedings of the 4th Conference. The Geological Society of London, pp. 317–335.

Visser, M.J., 1980. Neap-spring cycles reflected in Holocene subtidal large-scale bedform deposits: a preliminary note. Geology 8, 543–546.

Vollset, J., Doré, A.G., 1984. A revised Triassic and Jurassic lithostratigraphic nomenclature for the Norwegian North Sea. Norwegian Petroleum Directorate Bulletin 3, 2–53.

Xu, C., 2007. Interpreting shoreline sands using borehole images: A case study of the Cretaceous Ferron Sandstone Member in Utah. Bulletin of American Association of Petroleum Geologists 91, 1319–1338.

Yielding, G., Badley, M.E., Roberts, A.M., 1992. The structural evolution of the Brent Province. In: Morton, A.C., Haxeldine, R.S., Giles, M.R., Brown, S. (Eds.), Geological Society Special Publication, vol. 61. Geology of the Brent Group, pp. 27–43.

4.4 Paper 4:

Folkestad, A., Odinsen T. H. Fossen, Pearce, M.A. 2014. Tectonic influence on the Jurassic sedimentary architecture in the northern North Sea with focus on the Brent Group. International Association of Sedimentologists. Special Publication, ***46****, 389–416.*

The Brent Group has been described and interpreted in numerous papers from the 1980`s and onwards. Simultaneously, the sequence stratigraphic method became popular and this influenced the interpretation of the Brent Group (see Van Wagoner et al., 1993). The paper of Helland-Hansen et al., (1992) interpreted the Brent Group to be deposited prior to the Middle-Late Jurassic rift-phase and the sequences of the Brent Group were controlled by eustatic fluctuations without any tectonic influence. This interpretation prevailed in several papers (e.g. Hampson et al., 2004, Bullimore & Helland-Hansen, 2009; Went et al., 2013) in which the Jurassic rift-phase was ascribed to the Late Jurassic associated with deposition of the mudstones of the Heather and Draupne formations (Fig. 4).

The postulated tabular nature of the Brent Group from the sequence stratigraphic-focused papers was not seen in east-west well correlations within the Brent Group in the Kvitebjørn and Gullfaks area (Fig. 1). Paper 4 shows several well correlations orientated perpendicular to the former Permo-Triassic fault blocks. The correlations display clear asymmetric stratal wedges in the Brent Group within the Ness-Tarbert formation succession. These findings demonstrate the initiation of the Middle-Late Jurassic rift-phase within the Brent Group in the northern North Sea (**Theme 2**). The results contrast the previous papers on the Brent Group (Helland-Hansen, 1992; Hampson et al., 2004; Bullimore & Helland-Hansen, 2009), who interpreted the Brent Group as being part of the post-rift phase (after the Permo-Triassic rift phase) and controlled by eustatic changes or relative sea-level (if basinwide tectonic subsidence is inferred) (**Theme 1**).

The paper demonstrates the rift initiation phase with the development of local depressions filled with stacked tidal bars and wedge-shaped stratal units of the Brent

Group. The units display both lithological variations and facies segregation and reveal an undulating coastline defined by the underlying Permo-Triassic fault-blocks. The paper illustrates how the reactivation of the Artic rift zone in the Middle Jurassic contributed to surplus accommodation space, which led to a southward retreat of the Ness-Tarbert formations in the Viking Graben with estuaries in the hangingwall and spit deposits along the footwall high of rotated fault blocks (**Theme 3**). The paper points out that the Ness-Tarbert formations are equivalent to the Sleipner - Hugin formations in the South Viking Graben (Fig. 4) and is a continuation of the Middle-Late Jurassic rift propagation southwards through time (Fraser et al., 2003) (Fig. 2). The South Viking Graben experienced rifting with rotation of fault blocks during deposition of the Hugin Formation in Middle-Upper Jurassic time (Folkestad et al., 2012b; Appen. 2) with estuaries in the hangingwalls and wave-reworked strata as spits at the footwall highs.

4.5 Paper 5:

Folkestad, A. & Satur, N. 2008. Regressive and transgressive cycles in a rift-basin: depositional model and sedimentary partitioning of the Middle Jurassic Hugin Formation, Southern Viking Graben, North Sea. Sedimentary Geology, ***207****, 1-21.*

This paper proposes a sequence stratigraphic model of the Hugin Formation in the South Viking Graben (Fig. 2). The study was finally used as input to the reservoir model for production purposes at the Sleipner Field. The sequences are stacked in a retrogradational manner due to the drowning of the basin caused by rifting at that time (Fraser, et al., 2003; see also Folkestad et al., 2012b, Appen. 2) **(Theme 1)**. Well-correlations show sedimentary wedges illustrating the tectonic influence and syn-sedimentary tectonic characteristics of this formation.

In addition to the deltaic to estuarine depositional environments identified in this paper, it is probably one of the first papers to demonstrate the concept of sedimentary partitioning (within sequence stratigraphy) in a subsurface study (see Steel & Milliken, 2013) **(Theme 2)**. The sequences were interpreted to consist of alternating highstand and transgressive system tracts without the lowstand or forced regressive system tracts. This differ from the study of Hampson et al., (2009) of the same formation, who interpreted the deltaic or regressive units to include forced regression.

The transgressive unit of the sequences is well-developed with a similar thickness to the adhering regressive unit. This differ from the tendency within sequence stratigraphic models where the transgressive unit is portrayed just as a surface (Hampson et al 2004; Bullimore & Helland-Hansen 2009; Kiefts et al., 2010; Went et al., 2013). Instead, the transgressive and the regressive units within a sequence show a skewed distribution with the regressive unit thickening towards the basin and the transgressive unit thickening towards land (Fig. 5), illustrating the concept of sedimentary partitioning. Similar, skewed thickness patterns of deltaic and estuary units within sequences illustrating sedimentary partitioning, are identified in the shallow-marine part of the clinoforms in the Battfjellet Formation, Spitsbergen (Folkestad et al., 2015; Appen. 3). The clinoforms of the Battfjellet Formation

developed in a foreland basin with an active thrust belt nearby shedding sediments into the basin.

The stack of the deltaic and estuary sequences with the internal skewed thicknesses in the Hugin Formation, is shown in a north-south correlation panel (Fig. 8 in Paper 5) running along the strike of the footwall high of a major fault-block. This illustrates that sequence stratigraphy can be performed along dip-orientated sections in a syn-rift basin. However, on basin-scale it is challenging or not possible to trace regional surfaces across the basin as the rate of block rotation will be different from block to block, i.e. different rates of accommodation space generation. An early version of this study is published in the Millennium Atlas (Husmo et al., 2003).

Sedimentary Geology 207 (2008) 1–21

Contents lists available at ScienceDirect

Sedimentary Geology

journal homepage: www.elsevier.com/locate/sedgeo

Regressive and transgressive cycles in a rift-basin: Depositional model and sedimentary partitioning of the Middle Jurassic Hugin Formation, Southern Viking Graben, North Sea

Atle Folkestad [a,*], Nicholas Satur [b]

[a] StatoilHydro ASA, N-5020 Bergen, Norway
[b] StatoilHydro ASA, N-4035 Stavanger, Norway

ARTICLE INFO

Article history:
Received 8 September 2006
Received in revised form 29 February 2008
Accepted 12 March 2008

Keywords:
Shallow marine
Facies
Sequence stratigraphy
Sediment partitioning
Middle Jurassic
North Sea
Hugin Formation

ABSTRACT

The Jurassic Hugin Formation consists of shallow-marine sandstones that belong to a significant hydrocarbon reservoir in the Sleipner area in the Norwegian North Sea. The formation encompasses coarsening-upward units of mouth bar and shoreface facies, interpreted to record delta outbuilding during regression; and fining-upward units with tidal channel, dune, and tidal flat facies interpreted as part of an estuary environment during transgression. The correlations reveal that the studied part of the Hugin Formation consists of 8 sequences, each with a transgressive and a regressive unit, representing the transgressive systems tract and the highstand systems tract respectively. The sequences are stacked retrogradationally landward as a result of rapid tectonic subsidence and rifting of the Viking Graben. Rifting led to the development of an elongate graben where tidal currents were amplified, wave-action damped and longshore drift (as sediments supply) reduced or absent. Lowstand and forced regressive systems tracts are not identified, and their absence is interpreted to reflect suppression of relative sea level falls in a rapidly subsiding basin where the basin subsidence rate outpaced any potential fall in eustatic sea level. Through facies interpretation and sequence-stratigraphic correlations between wells, these regressive and transgressive units are shown to exhibit characteristic thickness trends in the form of sigmoidal-shaped wedges, stacked in an offset manner in a landward to basinward orientation. These thickness trends illustrate sediment partitioning within the sequences and are explained by the relationship between accommodation versus sediment supply in terms of mass-balance. During regression, the focus of sedimentation was pushed basinward, and during transgression it was pushed landward as sediments were trapped there. The mapping of these sequence-stratigraphic units serves as input to reservoir models and to help increase recovery and identify new exploration targets.

1. Introduction

Hydrocarbon production from sandstone reservoirs deposited in transgressive, shallow-marine settings is economically important, for example in the transgressive part of the Brent system (Graue et al., 1987; Fält et al., 1989; Fjellanger et al., 1996; Hampson et al., 2004), the hydrocarbon-bearing, transgressive Stø Formation of the Snøhvit Field in the Barents Sea (Gjelberg et al., 1987), the upper Jurassic Fulmar Formation in the south Central Graben (Howell et al., 1996) and the Sacha Field in Ecuador (Shanmugam et al., 2000). Sedimentological facies analysis followed by the construction of sequence-stratigraphic models of the reservoirs serves as input to drainage strategy-planning, enables more accurate estimates of recoverable reserves and can highlight potential new hydrocarbon prospects.

* Corresponding author. Fax: +47 55143119.
E-mail address: atlef@statoilhydro.com (A. Folkestad).

0037-0738/$ – see front matter © 2008 Elsevier B.V. All rights reserved.
doi:10.1016/j.sedgeo.2008.03.006

The Jurassic Hugin Formation (Callovian–early Oxfordian) is a sand-rich, shallow-marine formation (Vollset and Dòre, 1984) and forms the main hydrocarbon reservoir unit in the south Viking Graben, productive in the Sleipner area (blocks 15/9 and 15/6: Fig. 1). The Hugin Formation was deposited during a large-scale transgression of the Viking Graben within Middle to Late Jurassic times (Cockings et al., 1992; Sneider et al., 1995; Husmo et al., 2003) (Fig. 2). The Hugin Formation has been linked to the retreat and drowning of the older shallow-marine Brent system in the northern part of the Viking Graben, and the Hugin Formation is interpreted to be the southern extension of the Tarbert Formation of the Brent Group (Graue et al., 1987; Fält et al., 1989; Mitchener et al., 1992, Cockings et al., 1992; Sneider et al., 1995; Milner and Olsen, 1998). The transgression of the Viking Graben was caused by the rapid deepening of a developing rift system initiated in the Late Bathonian (Hodgson et al., 1992; Cockings et al., 1992) and which caused progressive onlap of strata towards the graben margins (Sneider et al., 1995).

The Hugin Formation has previously been interpreted as a marine shoreface with beach barrier, lagoonal and associated coastal plain

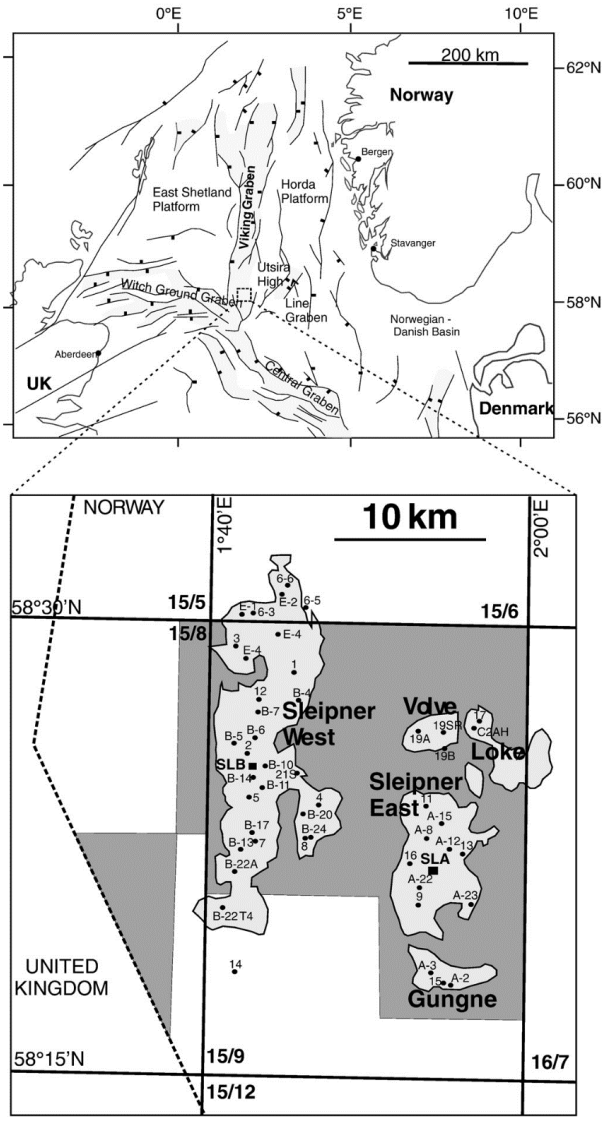

Reprinted with permission from Elsevier, whose permission is required for further use.

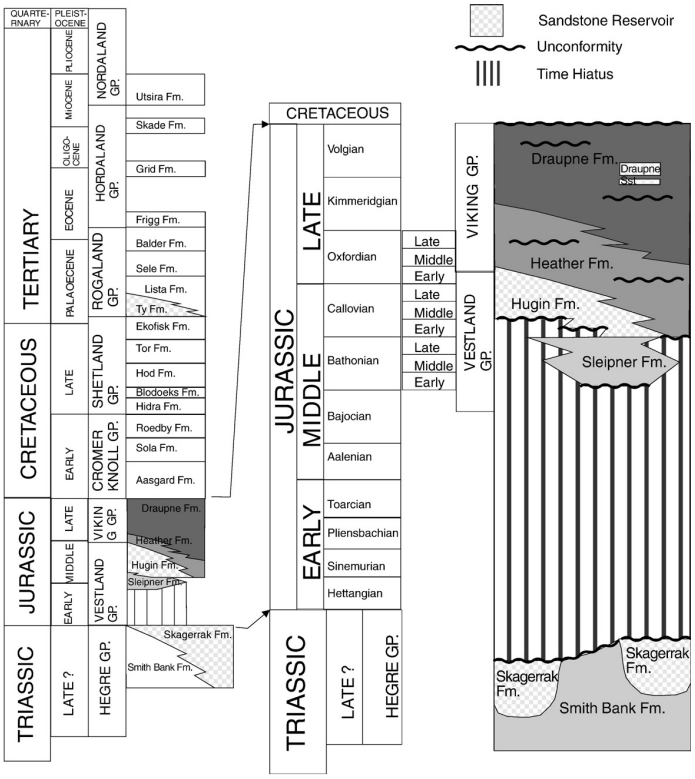

Fig. 2. Stratigraphic column of the southern Viking Graben highlighting the Triassic and Jurassic formations in the Sleipner area.

deposits (Milner and Olsen, 1998), or as delta-plain and delta-front deposits (Cockings et al., 1992) arranged in several back-stepping regressive–transgressive cycles as the coastline retreated southwards through the Viking Graben (Sneider et al., 1995). However, core examination from new production wells in the Hugin Formation now suggests an important tidal influence which is at odds with the previous interpretation (Cockings et al., 1992; Milner and Olsen, 1998). This study therefore updates and revises the sedimentological interpretation of the vertically stacked units of the Hugin Formation in the Sleipner area, with the following aims: 1) to present updated sedimentological descriptions and interpretations from the Hugin Formation; 2) to achieve a better understanding of the facies association architecture within the Hugin Formation; 3) to identify and correlate key sequence-stratigraphic surfaces and to describe and interpret the geometry of the stratal packages bounded by these sequence-stratigraphic surfaces; 4) to provide input to updated reservoir models and 5) to aid increased recovery of hydrocarbons from the reservoir and predict new exploration targets in the area with improved geological prediction of interwell areas.

2. Geological setting

During the Middle Jurassic, the south Viking Graben formed a relatively elongate, narrow and north–south oriented basin (Fig. 1), (Sneider et al., 1995). This basin was characterised by rift-related faulting and block rotation, and additionally was affected by movements of the underlying Zechstein salt (Cockings et al., 1992). The initial phase of rifting in the Sleipner area probably commenced in the early Permian with the deposition of the coarse-grained clastic Rotliegends Group, followed by the carbonates and evaporites of the

Fig. 1. Geographical map with mid-Jurassic structural features of the North Sea area with the Sleipner area located in the southern part of the Viking Graben. Insert illustrates the location of the studied wells within the Sleipner area.

Upper Permian Zechstein Group (Cockings et al., 1992). This rifting was followed by thermal subsidence from the mid-Triassic onwards (Steel and Ryseth, 1990; Yielding et al., 1992; Steel, 1993; Thomas and Coward, 1996; Husmo et al., 2003). Triassic deposits consist of continental mudstones of the Smith Bank Formation and the continental, sand-dominated Skagerrak Formation (Fig. 2) with accommodation influenced by salt movement.

The next phase of extension in the Viking Graben commenced in the Late Bathonian and continued through to the Oxfordian (Steel, 1993; Thomas and Coward, 1996; Husmo et al., 2003). In the Sleipner area, the coastal plain Sleipner Formation (Vollset and Dòre, 1984) has a variable thickness distribution and reflects the initiation of extensive rifting in the area (Richards, 1991; Sneider et al., 1995). The rifting was accompanied by a relative rise in sea level (Graue et al., 1987, Fält et al., 1989)

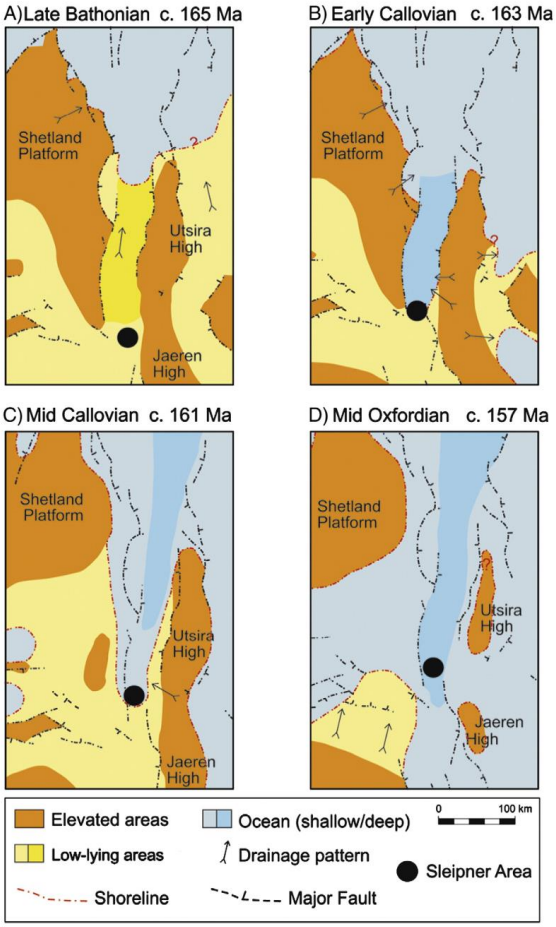

Fig. 3. Tectono-stratigraphical development of the Viking Graben from Late Bathonian (A) to mid Oxfordian (D) times. The location of the Sleipner area is highlighted. These maps illustrate the changes from alluvial to shallow marine to deep marine sedimentation in the study area through this time period as subsidence in the Viking Graben continued with flooding. Modified from Cope et al. (1992). Note the elongate nature of the Viking Graben which at the time of deposition of the Hugin Formation was approximately 30 km wide and 100 km long.

which caused a general southwards retreat of the Brent system in mid- to- Late Bathonian times (Fig. 3), (Fjellanger et al., 1996), with an overall transgression in the Sleipner area (Fig. 2). This resulted in the deposition of shallow-marine facies (Hugin Formation) in Early Callovian time in the Sleipner area (Fig. 3), interfingering and replacing the coastal plain and coal swamp deposits of the Sleipner Formation (Skarpnes et al., 1980; Milner and Olsen, 1998). The contemporaneous mid-Jurassic thermal dome (Ziegler, 1990) probably supplied sediments to the Viking Graben and adjacent basins of the thermal dome.

Through Middle Callovian to Early Oxfordian time, marginal to shallow-marine clastic sediments of the Hugin Formation continued to be deposited in the Sleipner area (Fig. 3), along with the distally coeval offshore mudstones of the Heather Formation (Cockings et al., 1992; Sneider et al., 1995; Milner and Olsen, 1998; Husmo et al., 2003). Eventually, the southern Viking Graben was flooded in the Middle Oxfordian period resulting in widespread deposition of marine mudstones of the Heather Formation and later the Draupne Formation (Cockings et al., 1992) (Fig. 3).

At the time of deposition of the Hugin Formation in the south Viking Graben, the graben itself was a depression, approximately 100 km long and 30 km wide (Sneider et al., 1995) with high ground to the east (Utsira High) and west (Shetland Platform), a coastal plain area to the south and an open marine connection to the north (Cockings et al., 1992; Sneider et al., 1995; Milner and Olsen, 1998). The palaeogeographical maps of the Middle Jurassic Viking Graben by Cope et al. (1992), (Fig. 3) illustrate the shape of the Viking Graben at that time. These maps also suggest a pause in the southward retreat of the shallow-marine system in the Sleipner area during early to Middle Callovian times, before the graben was drowned in the Middle Oxfordian.

3. Study area

The sedimentological and reservoir properties of the Hugin Formation have been studied in the Sleipner area. This formation forms a productive reservoir in the Sleipner area within blocks 15/9 and 15/6 (Fig. 1). The Sleipner area encompasses the Sleipner Vest, Sleipner Øst, Loke, Gungne and Volve fields (Fig. 1). These fields produce gas condensate with the exception of Volve where oil has been discovered. The main reservoir interval is the Jurassic Hugin Formation but hydrocarbon production also comes from the Triassic Skagerrak Formation, the upper Jurassic Draupne Formation and the Palaeocene Ty Formation (Fig. 2). The Hugin Formation ranges in thickness between 5 and 200 m in the area covered by wells but seismic data indicates it can be significantly thicker off-structure, and absent on structurally high areas due to post-depositional erosion. This thickness variation of the Hugin Formation reservoir is primarily controlled by the amount of available accommodation generated from rifting and salt tectonics, depositional pinch-out and/or later erosion from structural highs. The wells from the Sleipner Vest Field (Fig. 1) are the main focus for this study as they provide the most complete dataset.

The Hugin Formation in the Sleipner area can be divided into two units. The lower unit (Hugin 1), above the alluvial Sleipner Formation, has variable thickness and has been influenced by syn-sedimentary tectonics that indicates the start of more active rifting of the Viking Graben (Sneider et al., 1995). The upper unit of the Hugin Formation (Hugin 2) shows an aggrading to retrograding stacking pattern as illustrated by Cockings et al. (1992) after most of the irregular topography associated with early rifting in the area had been infilled by the Hugin 1 unit. This study focuses on the depositional environment and sequence-stratigraphic pattern of the Hugin 2 unit in the Sleipner area.

4. Database and methods

This study is based upon description and interpretation of 1600 m of cores from 31 wells and interpretation of wire-line logs from 43 wells in the Sleipner area (i.e. within block 15/9 of the North Sea). Several facies associations have been identified based upon lithology, primary sedimentary structures, colour, bedding contacts with overlying and underlying units, and bioturbation type and intensity (using the bioturbation index scheme of Taylor and Gawthorpe, 1993) of the cores. From the vertical stacking pattern of the facies associations and their internal relationship, the facies associations have been grouped into 7 broader facies association units (Figs. 4–6).

The vertical stacking pattern and lateral distribution of facies associations is the basis for the sequence-stratigraphic analysis in this study. Key sequence-stratigraphic surfaces with potential for semi-regional correlations were identified from changes in the stacking pattern of the facies associations and discontinuities in cores and wire-line logs. Biostratigraphic analysis was consulted for consistency with the identified key sequence-stratigraphic surfaces. Detailed facies association architecture panels with sequence-stratigraphic interpretations have been constructed in north–south depositional dip and east–west, depositional strike directions.

5. Facies associations

The Hugin Formation consists of a range of facies associations representing offshore mudstones, shallow-marine sandstones and coastal plain deposits. These are described and interpreted below. Based on the interpretation of the facies associations and their internal relationships, the facies associations are grouped into depositional environments representing either transgressive or regressive units (Figs. 4–6).

6. Regressive or coarsening-upward facies associations

6.1. Offshore mudstones (Fig. 4A)

6.1.1. Description

This facies association consists of claystones with thin (<1 cm) siltstone laminations. They are greyish-black to black in colour with horizontal laminae. The laminae are poorly defined or destroyed in some intervals (10–40 cm thick) with bioturbation index of 3 to 6. Abundant *Chondrites* traces give rise to a mottled appearance and traces of *Terebellina*, *Planolites*, *Cylindrichnus* and *Thalassinoides* are common. Red coloured siderite concretions occur locally. The lower and upper boundaries are gradual or sharp.

6.1.2. Interpretation

The laminated claystones were deposited by suspension fallout in the relatively quiet setting of the offshore shelf environment. The absence of sedimentary structures other than the horizontal lamination (Fig. 4A) suggests that oscillatory or unidirectional flow was not important. The fine-grained sediments were probably set into suspension in fluvial/shallow-marine environments, transported offshore and deposited during fair-weather conditions (Walker and Plint, 1992). The occurrence of *Terebellina* and *Chondrites*, *Planolites*, *Cylindrichnus* and *Thalassinoides* trace fossils can indicate an offshore marine environment (Bromley, 1996). A depositional environment of offshore mudstones is proposed for these sediments and they are regarded as coeval with the offshore mudstones of the Heather Formation.

6.2. Shoreface (Fig. 4B)

6.2.1. Description

These deposits consist of well-sorted siltstones and very fine- to medium-grained sandstones with fine- and very fine-grained sand being the predominant grain-size. Beds range in thickness from 0.3 to 1.0 m and the vertical stacking of beds shows a coarsening-upward grain-size trend (Fig. 7A). These coarsening-upward units range in thickness from 3 to 25 m. Primary sedimentary structures are

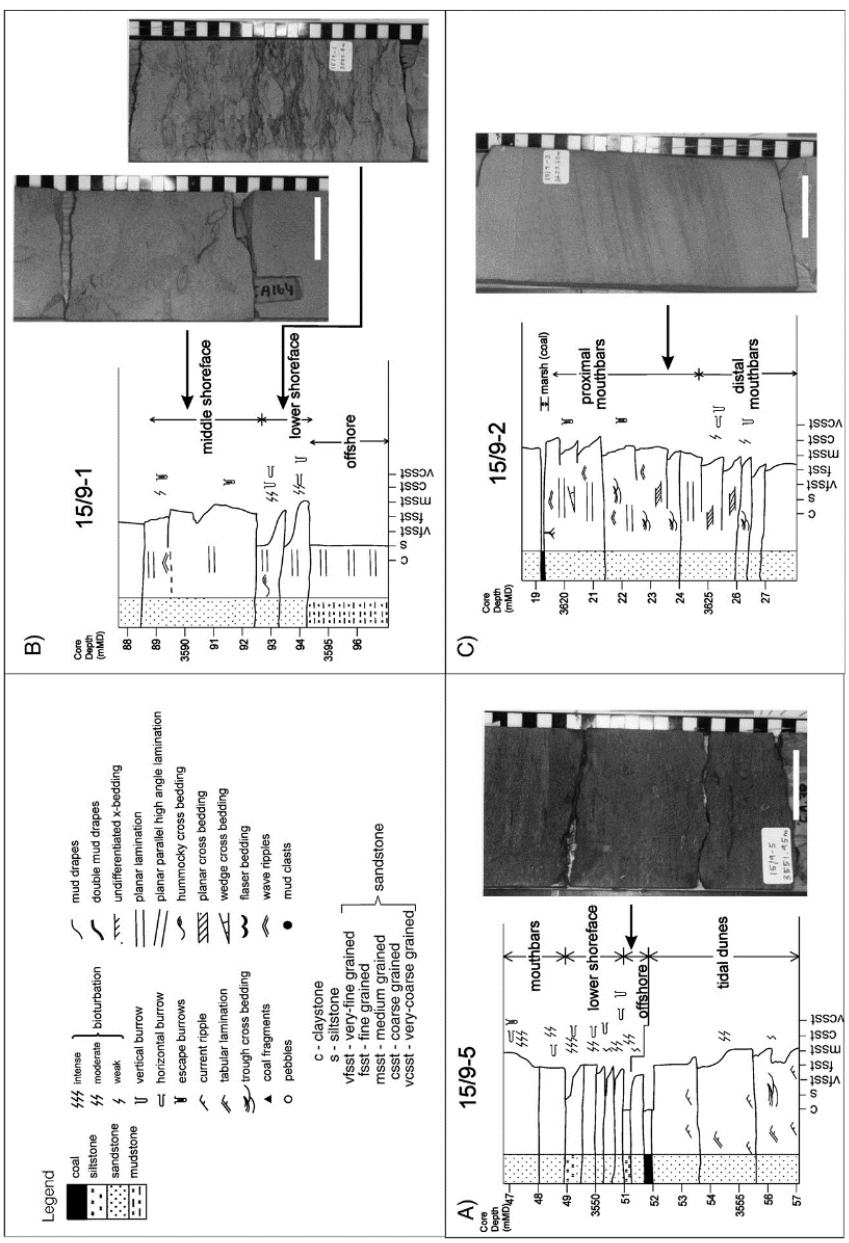

Fig. 4. Description and core photographs of facies within the coarsening upwards or regressive facies associations: A) Offshore mudstone facies association. Note the presence of *Terebellina* and *Chondrites* trace fossils; B) Very fine- to fine-grained, well-sorted sandstones of the shoreface facies association. The log shows coarsening upwards with loss of the finer-grained more bioturbated parts of the beds. Note traces of *Ophiomorpha nodosa*; C) Coarsening- upward cross-bedded sandstones of the mouthbar facies association. White bar for scale (3 cm) also indicating paleo-horizontal.

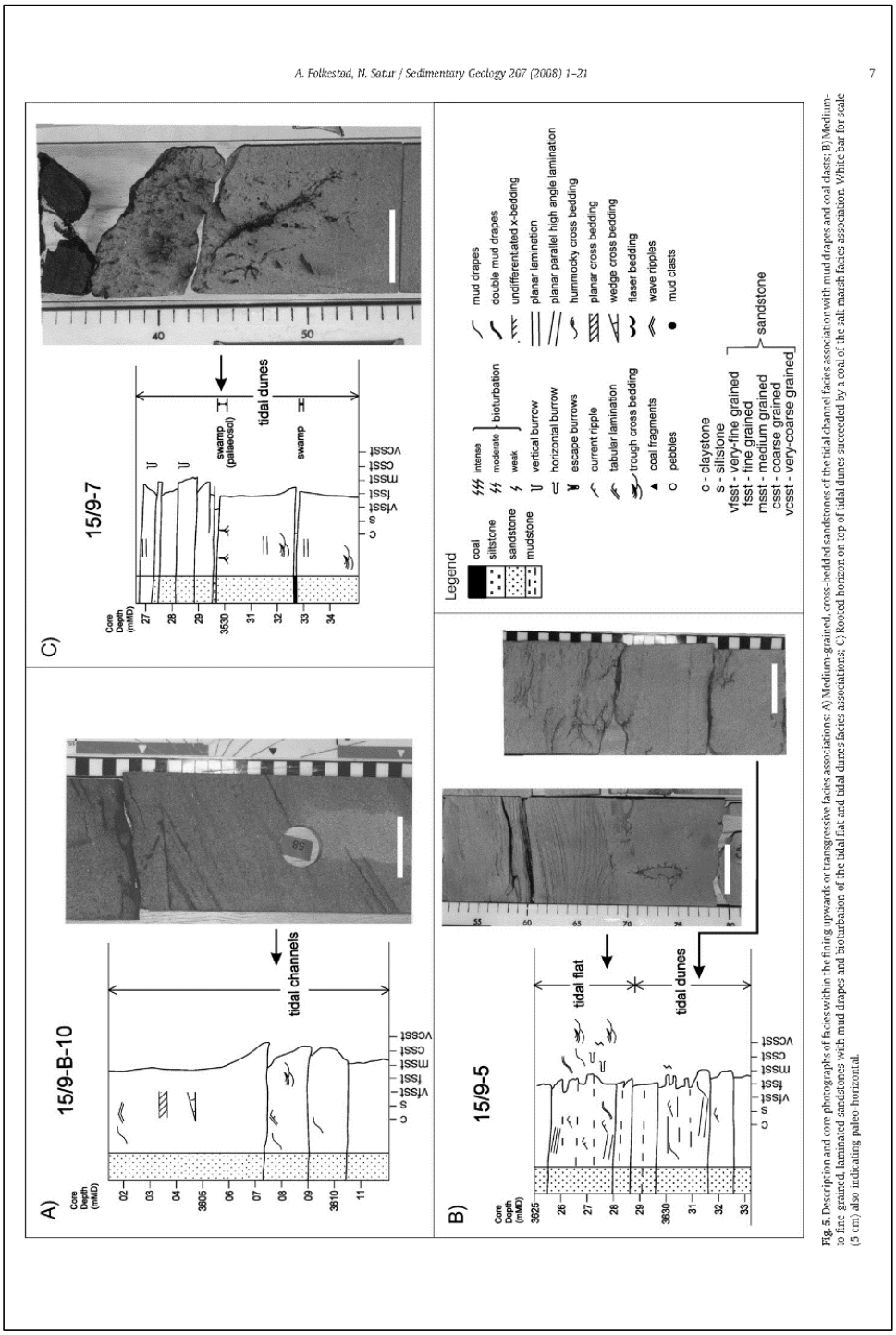

Fig. 5. Description and core photographs of facies within the fining upwards or transgressive facies associations: A) Medium-grained, cross-bedded sandstones of the tidal channel facies association with mud drapes and coal clasts; B) Medium- to fine grained, laminated sandstones with mud drapes and bioturbation of the tidal flat and tidal dunes facies associations; C) Rooted horizon on top of tidal dunes succeeded by a coal of the salt marsh facies association. White bar for scale (5 cm) also indicating paleo horizontal.

Reprinted with permission from Elsevier, whose permission is required for further use.

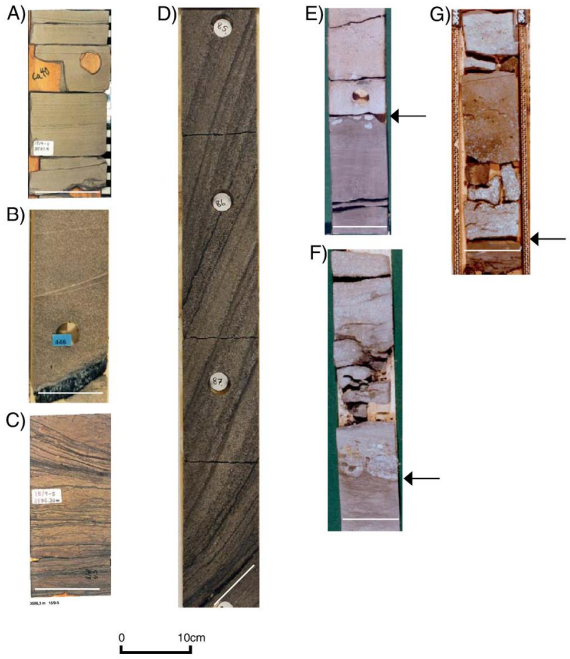

Fig. 6. Selected core photos of sedimentary facies identified in the Hugin 2 unit. White bar shows paleo-horizontal. A) Shoreface sandstone consisting of very fine-grained, well-sorted, mm scale, horizontal laminated sandstones; C) Tidal flat deposits consisting of very fine-grained sandstones and siltstones, planar laminated strata followed by cross-beds, with mud drapes and *Planolites* trace fossils; B) Fine- to medium-grained cross-bedded sandstones of the mouthbar facies association with a large coaly clast, probably a coalified branch; D) Coarse- to medium-grained cross-bedded sandstones of the tidal channel facies association with mud and organic-rich drapes. This well is deviated. E) Base of the Hugin unit 2 in 15/9-1 showing *Glossifungites* ichnofacies associated with a transgressive surface (indicated by the black arrow) below tidal channel sandstones. F) Base of the transgressive unit of sequence 5 in 15/9-2 showing a transgressive surface (indicated by the black arrow) with associated lag of coarse-grained material. G) Base of the Hugin 2 in 15/9-1 indicated by black arrow, showing a transgressive lag with pebbles and coal clasts above a coal layer and organic-rich mudstones (see also Fig. 7A).

horizontal (Fig. 6A) to low-angle lamination, hummocky and swaley cross-stratification, with some trough cross-bedding and wave ripples. Some intervals appear homogeneous and local shell fragments are observed scattered in these sandstones. Bed boundaries are sharp or slightly erosional. These coarsening-upward units show an upward change in sedimentary structures from hummocky cross-stratification and horizontal lamination to swaley cross-stratification and low-angle lamination with some wave ripples and occasional trough cross-stratification. The coarsening-upward units also show an upward decrease in bioturbation intensity (Fig. 7A). In the very fine- to fine-grained parts, the intensity of bioturbation has an index of 3 to 6 with traces of *Skolithos*, *Palaeophycus*, *Thalassinoides* and *Planolites* that locally obscure the primary structures. In the fine- to medium-grained parts, the bioturbation intensity has an index of 0 to 2 with *Ophiomorpha nodosa* being the most common trace and less abundant *Planolites*, *Palaeophycus* and *Skolithos*.

6.2.2. Interpretation

The sedimentary structures and the clean and well-sorted nature of these sandstones suggest deposition during frequent reworking by waves under fair-weather conditions and storms (Hunter and Clifton, 1982; Walker and Plint, 1992). The coarsening-upward trends of these units and the vertical change in sedimentary structures suggest progradation and shallowing of a shoreface environment. The fine- to very fine-grained sandstones and siltstones with intense bioturbation were probably deposited below fair-weather base, occasionally interrupted by storms producing hummocky cross-strata. The swaley structures and trough cross-bedded sandstones in the upper part indicate prevailing fair-weather conditions. The sedimentary structures, the occurrence and type of trace fossils suggest a shoreface environment (Bromley, 1996).

6.3. Mouthbars (Fig. 4C)

6.3.1. Description

This facies association is dominated by medium-grained sand and grain-size ranges from very fine- to very coarse-grained sandstones and granules. Bed thicknesses vary from 10 to 75 cm and the vertical stacking of beds in this facies association shows a coarsening-upwards grain-size trend (Fig. 7B). The colour varies from brown–grey to brown–red in the coarser parts to grey in the finer parts, and sorting varies from poor to

well-sorted. The internal structures are horizontal, planar cross-bedding, low-angle lamination, trough cross-bedding, with current and wave-ripple lamination. Some homogeneous intervals are recorded. Mud drapes occur in the very fine-grained part often associated with intense bioturbation that locally overprints primary structure. Coarse sand and gravel occur as 0.5 cm to 25 cm thick stringers on foresets or as homogeneous intervals. Coal fragments (0.2–8 cm), igneous clasts (0.2–1 cm) and rare mudclasts (4 cm) occur scattered within the beds (Fig. 6B). Dewatering structures, micro-faults and load structures are locally present at the base of some units. At the top of these coarsening-upward units, rooted horizons occur with roots penetrating up to 0.5 m down into the underlying strata (Fig. 4C). Bioturbation has an index of 1 to 3 and the bioturbation occurs in the finer-grained sections with traces of *O. nodosa*, *Arenicolites*, *Diplocraterion*, *Skolithos*, *Palaeophycus*, *Planolites*, *Cylindrichnus* and *Rhizocorallium*.

6.3.2. Interpretation

The coarsening-upward motif of these sandstones indicates a shallowing and progradational origin for this unit. The internal structures indicate traction currents, and the clast types and the coarse-grained sand-stringers on the foresets suggest an association with fluvial streams. The coarsening-upward motif and the internal structures suggest a mouthbar depositional environment for these deposits (Coleman and Prior, 1982; Elliott, 1986). The degree and style of bioturbation may occur within a mouthbar environment (MacEachern et al., 2005). The rooted horizons on top of some of these coarsening-upward mouthbars indicate that the bar built upwards to sea level with periods of subaerial exposure and temporary colonization by vegetation. The occurrence of mud drapes in the finer-grained parts may indicate some tidal influence (Willis, 2005).

7. Transgressive or fining-upwards facies associations

7.1. Tidal channel (Fig. 5A)

7.1.1. Description

These sandstones range in grain-size from fine to very coarse sand, and are moderately to poorly sorted and light grey in colour. The vertical stacking of beds produces fining-upward units up to 23 m in thickness. The internal structures are trough, tangential tabular and low-angle cross-bedding, often with single or double mud (or organic-rich) drapes (Fig. 6D). Flaser bedding occurs and reactivation surfaces have been recorded in the cross-bedded sandstones. No wave-generated structures are observed. The lower boundary of this unit is either erosional or sharp, locally associated with a *Glossifungites* ichnofacies assemblage below (Fig. 6E), and internal erosion surfaces are also present (Fig. 7B). Intervals of matrix-supported coal fragments (0.2–6 cm) occur along with rounded igneous clasts (0.2– 2 cm), with the latter occurring both as isolated matrix-supported clasts and as basal lags associated with erosional boundaries. Shell material and thin (up to 1 m thick) carbonate-cemented layers and concretions are also present. These sandstones are for the most part unbioturbated, but where burrows are present with a bioturbation index of 1 to 2, traces of *O. nodosa*, *Thalassinoides*, *Planolites* and *Palaeophycus* are recorded.

7.1.2. Interpretation

The abundance of current-generated structures such as trough and tabular cross-bedding and the absence of wave-generated structures, the coarse grain-size, the erosional base and associated basal lag of these fining-upward units indicate channel deposition. The occurrence of mud drapes, locally in pairs, reactivation surfaces and flaser bedding in the finer-grained parts suggests tidal current conditions with rapid and repetitive variations in energy conditions and water depths (Visser, 1980; Smith, 1988; Dalrymple et al., 1990). Cross-bedded sandstones with erosional bases, basal lags, and fining-upward grain-size trends and the association of flaser bedding and heterolithic deposits were interpreted by Elliott (1986) as estuarine tidal channels. Therefore, an estuarine tidal channel depositional environment is proposed for these sediments. The stacked, erosionally based fining-upward units indicate that more than one episode of channel fill has been preserved. Coaly debris entered the tidal channels by erosion of coastal plain marshes in the landward parts of the system and indicates a proximity to rivers (Rahmani, 1988) whereas the shell debris indicates an association with marine conditions and was brought into the channels by tidal currents (Reinson, 1992). The suite and style of trace fossils may indicate a stressed marine environment with highly variable energy conditions and perhaps variable salinities and is consistent with a tidal channel environment (Bromley, 1996).

7.2. Tidal dunes (Fig. 5B)

7.2.1. Description

This facies association ranges in grain-size from very fine- to medium-grained sandstones. They are generally moderately sorted but both poor and well-sorted intervals are recorded. The colour ranges from light to dark grey. The internal structures are cross-bedding, horizontal lamination and locally wavy bedding in the fine- to very fine-grained sections. The lower boundaries are mostly sharp but some erosional boundaries also occur. The individual beds fine upward and can be up to several meters in thickness, and the stacking of the beds produces fining-upward trends (Fig. 7A, B). The cross-bedded sandstones show local mud drapes on tangential foresets and some laminated sandstones have mud drapes on the laminae. The mud drapes locally occur in pairs and the thickness of the mud drapes reaches up to 0.2 cm. Matrix-supported igneous clasts occur with a range in size from 0.2 to 0.5 cm, often at the base of beds with an erosional lower contact. Other bed boundaries are sharp. Coal fragments (0.5–4 cm) occur scattered within the beds. Bioturbation occurs in the upper part of the beds and bioturbation index ranges from 2 to 6 with traces of *O. nodosa*, *Planolites*, *Palaeophycus*, *Diplocraterion*, *Rhizocorallium* and *Cylindrichnus*. The occurrence and intensity of the bioturbation generally increase upwards in these fining-upward units (Fig. 7A, B).

7.2.2. Interpretation

The grain-size and internal structures of these sediments suggest primary deposition by traction currents. The presence of mud drapes in sandstones, sometimes in pairs, suggests tidal processes occurring during deposition (Shanmugam et al., 2000) where the mud drapes are formed during slack water conditions between the tides (Dalrymple et al., 1990). Therefore, tidal dunes are proposed for the origin of these deposits. The concentration of igneous clasts at the lower bed boundary indicates erosive processes prior to deposition of the dunes where the igneous and coal clasts were material derived from landward fluvial distributary system. The bioturbation of the upper part of the beds indicates a less energetic environment after deposition of the dunes, allowing biological activity. The fining-upward motif of the stacked beds and the increase of bioturbation suggest an increase in water depth due to transgression and introduction of more marine conditions. The stacking of these tidal dunes may produce a compound tidal dune unit (Dalrymple et al., 1990) during transgressive conditions.

7.3. Tidal flat (Fig. 5B)

7.3.1. Description

This facies association ranges in grain-size from mudstones to fine-grained sandstones. In the sandy part, the internal structures are low-angle and horizontal lamination, wavy bedding, flaser and lenticular bedding, and wave and current ripples. Current ripples are seen as climbing in some places and both the current and wave ripples are associated with flaser and lenticular bedding. Mud drapes occur frequently in pairs (Fig. 7B) with thickness up to 1 cm. Rhythmic bedding of sandstones and mud layers is common (Fig. 6C). The bed thickness is up to meter-scale and the bed boundaries are sharp. Coal

fragments, up to 8 cm long, occur both concentrated at the base of beds and scattered within beds of medium- to very fine-grained sandstones. Mudclasts (3 cm) occur locally and a range in bioturbation index from 2 to 6 is recorded with traces of *Planolites*, *Teichichnus*, *Palaeophycus*, *Diplocraterion* and *Rhizocorallium*. Carbonate concretions occur with a thickness variation of 1–25 cm within the muddier part of this facies association. Also present are load structures, convolute bedding and water escape structures, and micro-faults.

7.3.2. Interpretation

The common occurrence of mud drapes, in pairs and with a maximum thickness of 1 cm indicates a clear involvement of tidal processes in the formation of this facies (Visser, 1980). The mix of wave and current ripples occurring as flaser bedding in the sandier part or as lenticular bedding in the mud-dominated part, suggests a tidal flat environment (Reineck and Wunderlich, 1968; Willis, 1997). The combination of trace fossils described above may occur in such an environment (Pemberton et al., 1992). The rhythmic alternations of the sandstones and mudstones in tidal flat environments have been interpreted to represent tidal influence on inner estuary sediments (Kuecher et al., 1990). Therefore, the tidal flat is here interpreted to flank the estuary channels and also dominate the inner part of the estuary. The climbing current ripples and soft-sediment deformation structures indicate rapid deposition of sand. This association with the coal fragments indicates fluvial sediment pulses into this environment.

7.4. Salt marsh (Fig. 5C)

7.4.1. Description

This facies association consists of interbedded coal layers (up to 10 cm thick) and organic-rich mudstones. There are some indications of horizontal lamination in the mudstones but generally they are homogeneous. Reddish brown, sub-angular concretions up to 14 cm thick occur commonly. Pyrite mineralization occurs locally in zones of 0.5 to 10 cm thickness within the coal layers and mudstones. Rooted horizons occur with associated mottling of the strata below the coal beds up to 0.5 m into underlying sediments interpreted as mouthbars. The organic-rich mudstones and coal layers commonly overlie the tidal flat facies association.

7.4.2. Interpretation

Coal deposits originate from extensive accumulations of plant material in swamps and mires with a low input of clastic material, followed by relatively rapid burial to prevent decomposition. The mudstones contain a high amount of organic material as indicated by their black appearance, which suggests a proximity to vegetated areas. These mudstones were mostly deposited in anoxic standing water with a high supply of organic material. A salt marsh environment is proposed for these sediments. This is supported by the close association with the tidal flat facies association. The presence of pyrite indicates occasionally anoxic conditions. The mottled appearance of the underlying sediments is due to churning of the sediments by root activity. The root activity suggests a horizon exposed to vegetative processes, most likely in a subaerial setting in a palaeosol (McCarthy and Plint, 2003). The close association between the palaeosols and the coal layers and the observation that palaeosols occur on top of sandbodies, such as the mouthbar facies, suggest that the palaeosols formed under subaerial conditions prior to the deposition of the coal beds.

8. Depositional setting and facies model

8.1. Coarsening-upward facies successions: deltaic depositional environment

This succession of facies associations shows a distinct coarsening-upward motif along with an upward decrease in bioturbation intensity (Figs. 4, 7A (3609–3597 and 3582–3559 mMD) and B (3561–3547 mMD)). This coarsening-upward succession consists of offshore mudstones followed by shoreface deposits and succeeded by mouthbars (Figs. 7–9). The coarser-grained mouthbars contain coal, mud- and rounded igneous clasts indicating an association with fluvial distributary channel systems in more landward areas. The mouthbars extend basinward into shoreface deposits and the shoreface deposits show a coarsening-upwards trend from offshore mudstones below through silty and very fine-grained bioturbated lower shoreface to fine-grained, less bioturbated and unbioturbated upper shoreface (Figs. 7–9). These deposits are interpreted to represent outbuilding of a mixed fluvial- and wave-dominated deltaic environment (Bhattacharya and Walker, 1992; Fig. 10A) and form a regressive phase of a regressive–transgressive sequence. The preservation of the mouthbars indicates that the wave influence was not strong enough to rework the major part of the mouthbars. This observation provides some insight into the influence of the elongate and narrow shape of the Viking Graben (Fig. 3), which appears to have suppressed marine wave influence and also prevented longshore drift as a sediment supply mechanism. Without longshore drift as the sediment source mechanism and sediment supplied instead from rivers, the coarsening-upward units as described here most likely represent deltaic depositional environments and are in accordance with observations from Bhattacharya and Giosan (2003). The coastline is interpreted to have been oriented roughly east–west, perpendicular to the axis of the Viking Graben, based on the trends of facies successions and the shape of the Viking Graben at that time (see also Cockings et al., 1992; Sneider et al., 1995). Palaeosols occur locally on top of the more landward part of mouthbars, probably lateral to sand conduits, indicating expansion of the area of little available accommodation space during the regressive phase.

8.2. Fining-upward facies associations: estuary depositional environment

The stacking of the tidal facies associations produces a fining-upward trend in grain-size and an increase in bioturbation intensity upwards (Figs. 5, 7A (3622–3610 and 3587–3582 mMD) and B (3588–3562 and 3547–3519 mMD)). This indicates upward more marine and calm conditions during deposition (Figs. 5, 9 and 10B) and the top of these units displays the most bioturbated and marine influenced levels in the package. These observations suggest that these strata were deposited during transgressive phases of the system. The presence of mud drapes in these deposits (Figs. 5B, 6C and D) suggests tidal reworking of sediments. The tidal channel deposits fine upwards to either tidal dunes or tidal flat deposits that may be overlain by salt marsh facies (Figs. 5 and 7). The erosional bases with basal lag of the tidal channel facies (Fig. 6E, F and G) probably represents tidal ravinement surfaces (Hwang and Heller, 2002). The basinward part of these deposits is dominated by the tidal dunes whereas the landward part is dominated by both tidal flat and tidal dunes (Fig. 8). The tidal channels extend basinward into tidal dunes and both landward and laterally into tidal flats and salt marshes (Fig. 10B). In its distal location, this succession is overlain by offshore mudstones. The fining-upward trend of the tidal facies and the lateral change down depositional dip from salt marshes to tidal flat into tidal channel complexes is interpreted to represent an estuary depositional setting formed during the transgressive phase of a sequence (*sensu* Elliott, 1986; Dalrymple et al., 1992), (Fig. 10B).

9. Sequence stratigraphy

9.1. Key sequence-stratigraphic surfaces

The facies associations have been grouped into genetic units of chronostratigraphic significance (Posamentier et al., 1988), in this case as transgressive and regressive units defined by the facies character and stacking pattern. The mapping of these individual transgressive and regressive units reflects the shoreline trajectory. Changes in the shoreline trajectory in terms of shoreline migration either basinward as regression, landward as transgression or near-vertically as aggradation occur across key sequence-stratigraphic surfaces (Helland-Hansen and Gjelberg,

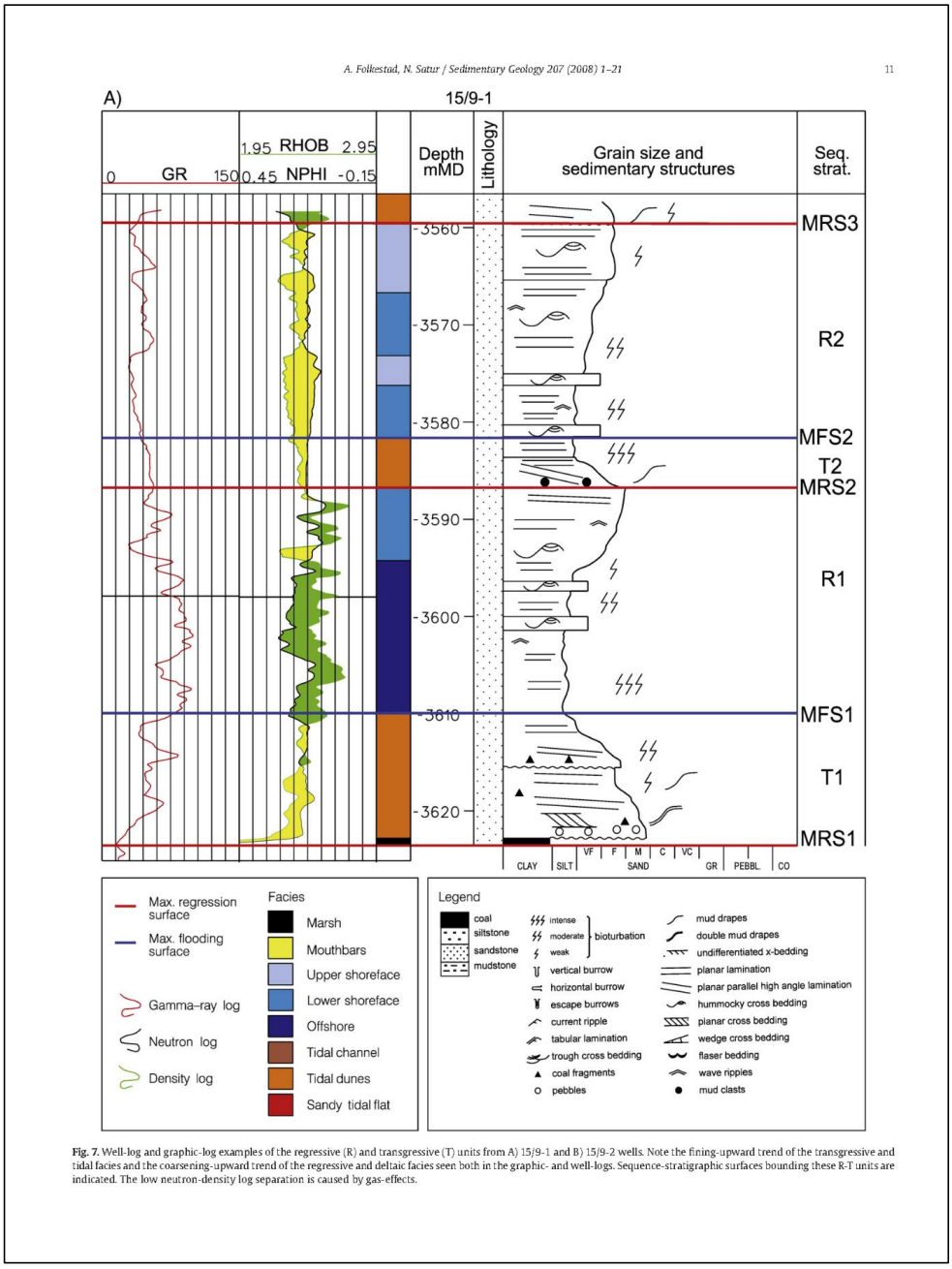

Fig. 7. Well-log and graphic-log examples of the regressive (R) and transgressive (T) units from A) 15/9-1 and B) 15/9-2 wells. Note the fining-upward trend of the transgressive and tidal facies and the coarsening-upward trend of the regressive and deltaic facies seen both in the graphic- and well-logs. Sequence-stratigraphic surfaces bounding these R-T units are indicated. The low neutron-density log separation is caused by gas-effects.

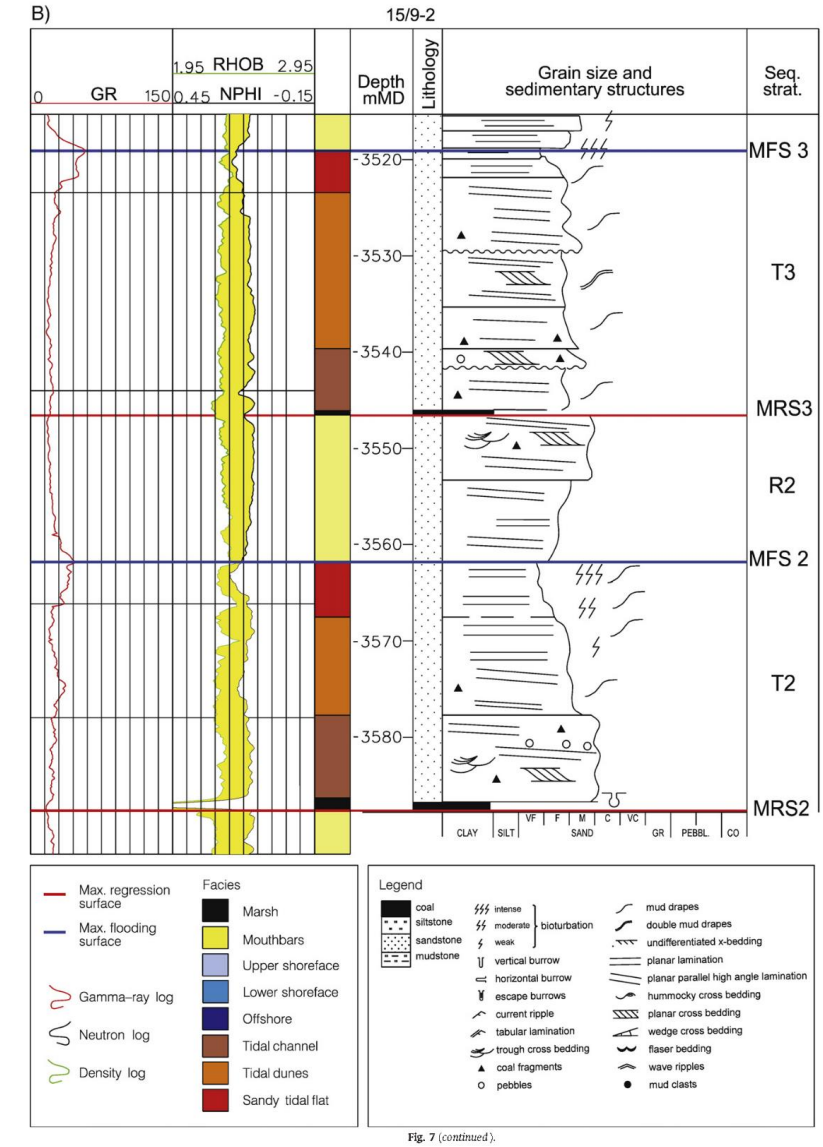

Fig. 7 (*continued*).

A. Folkestad, N. Satur / Sedimentary Geology 207 (2008) 1–21

pp. 13–14

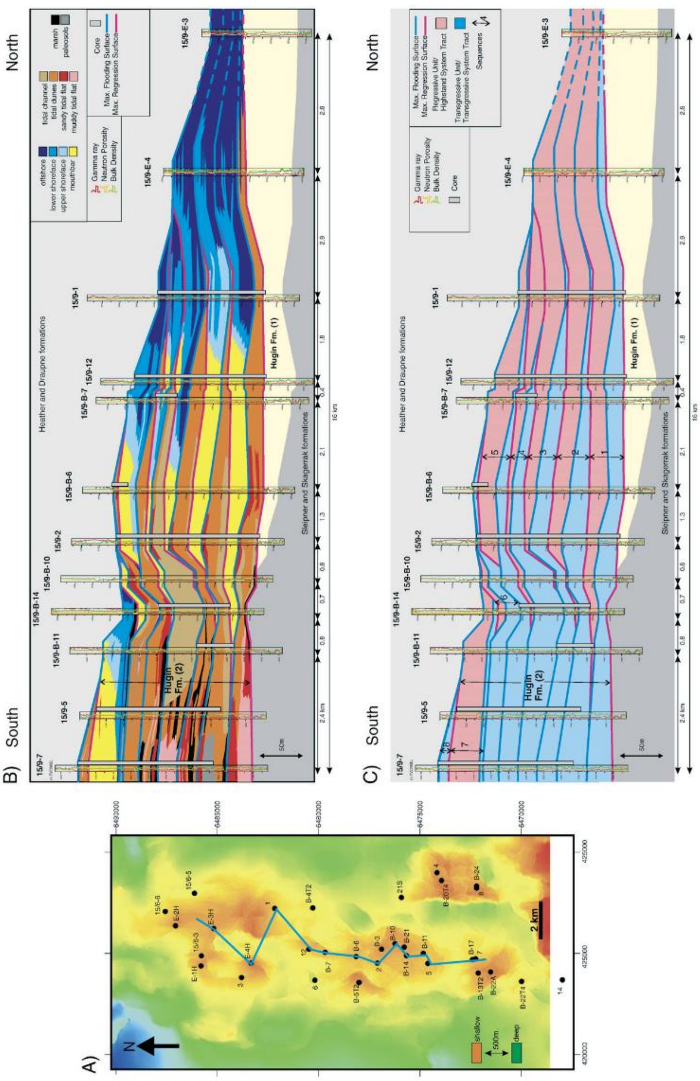

Fig. 8. A) Structural depth map of the Sleipner Vest area, warm colours indicate shallower depths. B and C) North to south (depositional dip) correlation diagram of the Hugin Formation, unit 2. The upper figure (B) illustrates the facies architecture within the wells and the extrapolation of these facies in the interwell areas. The lower figure (C) shows the same wells with the sequence-stratigraphic units (regressive and transgressive units) and surfaces (maximum flooding surfaces and maximum regressive surfaces) interpreted. Note the vertical stacking of the sequences which show an aggradational to back-stepping pattern through time. The pattern of each system tract displays an overall sigmoidal pattern, thin in both the most distal (north) and proximal (south) locations and expanding in thickness in the mid section. This pattern is a reflection of the interplay between accommodation and sediment supply within each systems tract. During regression the focus of sedimentation is forced basinward due to a lack of accommodation in the landward areas and a surplus of supplied sediments. During transgression the focus of sedimentation is moved landward due to added accommodation and trapping of sediments at that location, and sediment starvation prevails in the basinward areas.

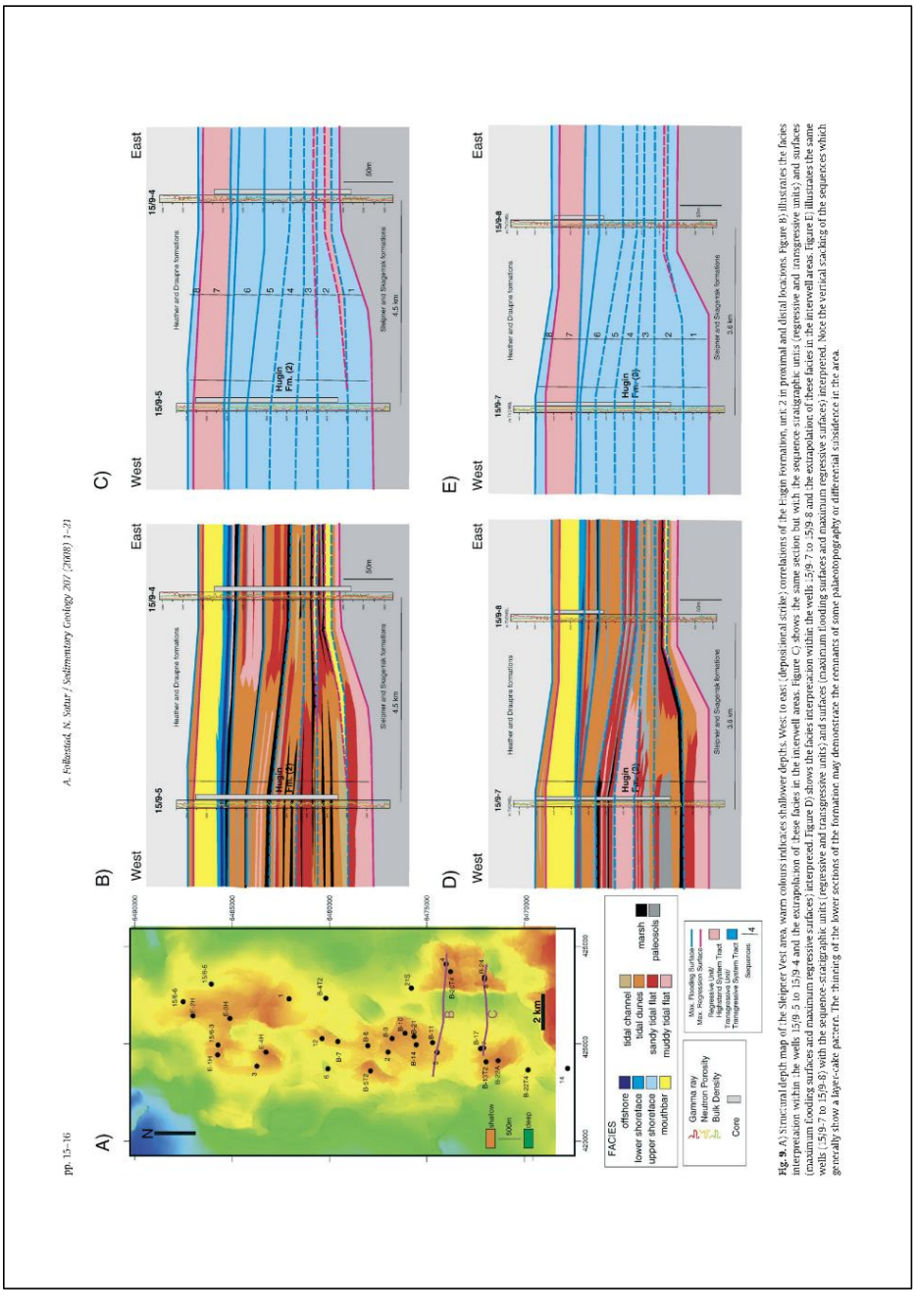

Fig. 9. A) Structural depth map of the Skeppet Vest area, warm colours indicates shallower depths. West to east (depositional strike) correlations of the Hugin Formation, unit 2 in proximal and distal locations. Figure B) illustrates the facies interpretation within the wells 15/9-5 to 15/9-4 and the extrapolation of these facies in the interwell areas. Figure C) shows the same section but with the sequence stratigraphic units (regressive and transgressive units) and surfaces (maximum flooding surfaces and maximum regressive surfaces) interpreted. Figure D) shows the facies interpretation within the wells 15/9-7 to 15/9-8 and the extrapolation of these facies in the interwell areas. Figure E) illustrates the same wells (15/9-7 to 15/9-8) with the sequence-stratigraphic units (regressive and transgressive units) and surfaces (maximum flooding surfaces and maximum regressive surfaces) interpreted. Note the vertical stacking of the sequences which generally show a layer-cake pattern. The thinning of the lower sections of the formation may demonstrate the remnants of some palaeotopography or differential subsidence in the area.

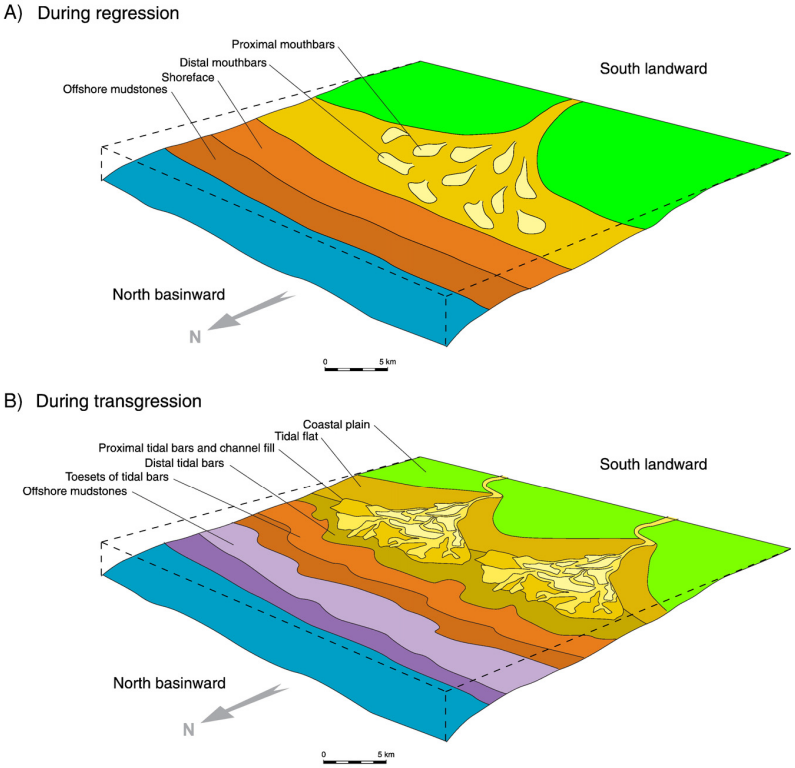

Fig. 10. Depositional models for the Hugin 2 unit. The overall coastline in the Sleipner area is east–west but there are most likely variations to this orientation in areas close to the margins of the Viking Graben. A) During regression, a mixed fluvial and wave-dominated delta environment existed with mouthbar and shoreface facies predominant. B) During transgression, an estuarine environment existed with tidal flats, dunes and channels.

1994). In this respect, the regressive-to-transgressive turnaround point is here termed a maximum regressive surface (*sensu* Helland-Hansen and Martinsen, 1996) as this level represents a marked change in the shoreline trajectory, shift of facies (Figs. 8, 9) and maximum basinward shoreline position (Saito, 1994). Similarly, the turnaround from the transgressive to regressive units is termed a maximum flooding surface due to the change of shoreline trajectory and the shift in facies at the top of the fining-upward facies succession (Catuneanu, 2002). Such a surface is characterised by the most intensely bioturbated and most seaward facies within a vertical section of a sequence (Figs. 7–9).

9.2. Sequence architecture

The identification of key stratal surfaces and their correlative deposits allows the Hugin 2 unit to be divided into 8 sequences (Figs. 8 and 9). Seven sequences contain a transgressive and regressive unit whereas the uppermost sequence has only a transgressive unit. Biostratigraphic analysis indicates the time-span of these 8 sequences is about 3 million years (Husmo et al., 2003), which would make them 4th order sequences according to Van Wagoner et al. (1990). For each sequence, the maximum regressive surface (MRS), transgressive unit (T), maximum flooding surfaces (MFS), and regressive unit (R) are described in this order with reference to Figs. 8 and 9. The well correlation panels approximate dip- and strike-sections through the Hugin Formation. In the dip section, north is basinwards and south in the landward direction.

9.2.1. Sequence 1

The maximum regressive surface of sequence 1 (MRS1) is placed at the base of the Hugin 2 unit and is overlain by the tidal deposits of the transgressive unit 1 (T1). In the area from 15/9-2 and 15/9-E-4 the MRS1 is marked by a coal-layer capping the Hugin unit 1 and from 15/9-B-10 to 15/9-7 the base of this sequence is marked by the top of the coastal plain Sleipner Formation, also often represented by a coal. The T1 unit comprises stacked tidal dune deposits in the distal part, tidal dunes,

channels and flat deposits in the middle part and is dominated by tidal flat with some dunes in the proximal part. In 15/9-E-4 and southward to 15/9-B-7 the MFS 1 caps tidal dunes. The T1 unit shows a thickening trend from 15/9-E-4 to 15/9-12 and has a general uniform thickness southward from 15/9-12. In 15/9-5 the MFS1 coincides with the maximum regressive surface of sequence 2 (MRS2) as R1 has pinched out at this southward position. Above the MFS1 the regressive unit (R1) consists of alternating offshore mudstones and shoreface deposits in 15/9-E-4, offshore mudstones and shoreface deposits in 15/9-1 (Fig. 7A) and mouthbars in 15/9-2 and southward to 15/9-B-11. The R1 unit pinches out southward of 15/9-B-11 and thickens northward to 15/9-E-4. The alternating offshore mudstones and shoreface deposits in 15/9-E-4 indicate that a pinch-out of the shoreface sands of R1 occurs northward of 15/9-E4. Both the T1 and R1 units are projected into 15/9-E-3.

9.2.2. Sequence 2

The maximum regressive surface (MRS2) marks the change from the mouthbars and shoreface deposits of R1 below into tidal deposits of the transgressive unit (T2) of sequence 2 above. In 15/9-1 to 15/9-B-7 the MRS2 is capped by tidal dune facies of T2, from 15/9-B-6 to 15/9-B-11 by tidal channel deposits and in 15/9-5 and 15/9-7 by tidal flat deposits. In 15/9-E-4 the T2 unit is not found and a pinch-out of the T2 unit is interpreted northward of 15/9-1. From 15/9-1 (Fig. 7A) to 15/9-5 the MFS2 generally caps tidal dune facies. From 15/9-12 to 15/9-B-14 the MFS2 marks the change from tidal dunes of T2 below to mouthbar deposits of R2 above with shorefaces in 15/9-1 (Fig. 7A) and 15/9-E-4. Between 15/9-B-11 and 15/9-7 the R2 unit has pinched out and MFS2 coincides with the base of T3 above. From 15/9-B-14 to 15/9-1 the thickness of R2 increases northward. However, from 15/9-1 to 15/9-E-4 the sandstones of R2 show a drastic thinning. The R2 is projected into the offshore shale of 15/9-E-3.

9.2.3. Sequence 3

The maximum regressive surface of sequence 3 (MRS3) is placed in 15/9-1 at the change from shoreface deposits belonging to R2 below to tidal dune facies of the T3 unit above (Fig. 7A). In 15/9-E-4 the MRS3 is placed on top of the shoreface deposits of R2. In 15/9-12 and 15/9-B-7 the MRS3 marks the change from mouthbar deposits of R2 below to tidal dunes of T3 above, whereas in 15/9-B-6 and -2 the change is into tidal channel deposits above. The erosional base of the tidal channel body may be interpreted as a tidal ravinement surface. From 15/9-B-10 to 15/9-B-14, MRS3 is placed on top of mouthbar deposits (R2) with a change into overlying tidal flat deposits (T3). As mentioned in sequence 2, MRS3 coincides with MFS2 in 15/9-B-11 to 15/9-7. T3 comprises a stack of tidal dunes in the distal part, some tidal channels but mostly tidal dunes in the middle part, and tidal dunes and mostly tidal flat in the proximal part. MFS3 marks the change from tidal dunes below (T3) to offshore mudstones in 15/9-1 to 15/9-B-7 above. In 15/9-2 (Fig. 7B) and 15/9-B-10, MFS3 marks the change from the tidal flat deposits of T3 below into mouthbar deposits of R3 above. From 15/9-B-10 to 15/9-B-14, the mouthbar deposits pinch-out and R3 is not recorded in 15/9-B-14. Thus MFS3 coincides with MRS4 in 15/9-B-14 and southward to 15/9-7. Above MFS3 in 15/9-1 and southward to 15/9-B-7, there are offshore mudstones with diminishing bioturbation upwards which grade upwards into shoreface and mouthbar deposits. In the uncored 15/9-E-4 well, the log indicates that the R3 consists of alternating offshore mudstones and shoreface deposits. In 15/9-B-6 and southward to 15/9-B-10, R3 consists of mouthbars that thin towards 15/9-B-10. From 15/9-B-10, the mouthbars of R3 pinch-out before 15/9-B-14, such that MRS4 coincides with MFS3 in 15/9-B14 and southward in 15/9-7.

9.2.4. Sequence 4

MRS4 is placed at the change from the mouthbar and shoreface deposits of R3 to the tidal deposits of T4 in sequence 4. 15/9-1 and 15/9-E-4 are exceptions to this as MRS4 caps the shorefaces of R3 and is overlain by offshore mudstones in unit R4. The T4 unit is not recorded at those locations. In 15/9-12, MRS4 divides the mouthbars of R3 below from the tidal dunes of T4 above, and from 15/9-B-7 to 15/9-B-11 tidal channel deposits cap MRS4, and tidal flat deposits in 15/9-5 and 15/9-7. In 15/9-1 and 15/9-E-4, no tidal deposits of T4 are recorded and thus MFS4 coincides with MRS4. The MFS4 caps tidal dunes in 15/9-12 to 15/9-7, except in 15/9-2 where tidal flat deposits underlie MFS4. In 15/9-12 and 15/9-B-7, MFS4 is overlain by shoreface and mouthbar deposits of R4. In 15/9-B-6 to 15/9-B-14, MFS4 is overlain by mouthbar deposits of R4. R4 thins towards 15/9-B-14 and is absent in 15/9-B-11, demonstrating a pinch-out at this location. Thus MFS4 coincides with the overlying MRS5 in 15/9-B-11 and southward to 15/9-7.

9.2.5. Sequence 5

MRS5 is overlain in 15/9-1 by offshore mudstones belonging to the R5 unit, in 15/9-12 to 15/9-B-10 by tidal dunes, and in 15/9-B-14 and southward to 15/9-7 by tidal flat deposits. In 15/9-1, MFS5 coincides with MRS5 and from 15/9-12 to 15/9-5 MFS5 caps tidal dunes except in 15/9-B-10 and 15/9-7 where it caps tidal flat deposits. The T5 unit shows a gentle thickening from 15/9-12 and southward to 15/9-7. Offshore mudstones occur above MFS5 in 15/9-E-4 and southward to 15/9-2, and are overlain by shoreface deposits in 15/9-12 and 15/9-B-7. In 15/9-B-6 and 15/9-2 the shoreface deposits are overlain by mouthbar facies. The R5 unit pinches out between 15/9-2 and 15/9-B-10 in a southward direction, and as a result MFS5 coincides with the maximum regressive surface of the sequence above (MRS6) from 15/9-B-10 southwards to 15/9-7. In 15/9-B-14, MFS5 coincides with MRS6 in the form of a palaeosol that genetically belongs to MRS6. In this case, roots from the palaeosol extend downward into tidal dunes of the T5 unit. The R5 unit extends northward to 15/9-12 and comprises interfingering shoreface and offshore mudstone deposits.

9.2.6. Sequence 6

MRS6 marks the change from the shoreface and mouthbar deposits of the R5 unit into overlying offshore mudstones in 15/9-12 and 15/9-B-7 and tidal dune and tidal flat deposits in 15/9-B-6 to 15/9-7. The stratigraphic level of MRS6 in 15/9-1 is difficult to identify within the offshore mudstones, which have a homogeneous appearance. Therefore the estimated position of MRS6 in 15/9-1 is projected from the level of MRS6 in 15/9-12 with a downward angle into 15/9-1, since the stratigraphic thickness of the offshore mudstones of R5 is assumed to be significantly less than that of both offshore mudstones and shoreface deposits (R5) in 15/9-12. The T6 unit pinches out between 15/9-B-6 and 15/9-B-7 in a northward direction and MFS6 coincides with MRS7 in 15/9-B-7 and northward to 15/9-1. MFS6 caps tidal dunes in all of the wells except for 15/9-B-14, which contains tidal channel deposits, and 15/9-B-10 which contains tidal flat deposits. The T6 unit shows a thickening trend from 15/9-B-7 to 15/9-7. Above MFS6, the R6 unit has mouthbars in wells 15/9-B-10 and 15/9-B-14 but is absent in 15/9-2 indicating a pinch-out of the R6 unit between 15/9-B-10 and 15/9-2. A southward pinch-out is also assumed between 15/9-B-14 and 15/9-B11.

9.2.7. Sequence 7

The maximum regressive surface of sequence 7 (MRS7) is placed on top of the mouthbar deposits of the R6 unit in 15/9-B-10 and 15/9-B-14. In 15/9-B-11 and southward to 15/9-7, MRS7 coincides with MFS6 as the R6 unit has pinched out. Above MRS7, the T7 unit comprises salt marsh deposits in 15/9-B-14 and 15/9-B-11, and a coal layer in 15/9-5 and 15/9-7 that is interpreted to be in association with the marsh deposits in 15/9-B-14 and 15/9-B-11. MFS7 caps the salt marsh deposits in 15/9-B-14 and tidal dunes in 15/9-B-11, 15/9-5 and 15/9-7. The T7 unit is relatively thin from distal to proximal and comprises tidal dunes while MFS7 is capped by offshore mudstones. The southward protrusion of the offshore mudstones, as far south as 15/9-5, and the low thickness of the T7 unit, indicates a pronounced transgression at this level. The strata of R7 coarsen upward from MFS7 with offshore

mudstones overlain by shoreface deposits except for 15/9-7, where offshore mudstones are absent. In 15/9-B-11, -5 and -7, the shoreface deposits are overlain by mouthbar deposits. The R7 unit thins basinward from 15/9-7 to 15/9-B-14 and is absent in 15/9-B-10.

9.2.8. Sequence 8

In the 15/9-7 well, MRS8 marks the boundary between the R7 unit below and tidal dunes in T8 above. The absence of the T8 unit in 15/9-5 and further basinward indicates a pinch-out of the T8 unit between 15/9-7 and 15/9-5.

9.3. Systems tracts and vertical stacking

The well correlation panels approximate dip- and strike-sections through the Hugin Formation (Figs. 8 and 9) and provide insight into the relatively ordered stacking pattern of the sediments. The sequences of the Hugin 2 unit are stacked in an overall transgressive succession with both the transgressive and regressive units showing an aggradational component, indicating a rising shoreline trajectory. Therefore, the transgressive units are interpreted to represent the transgressive systems tract (TST) and the regressive units are interpreted to represent the highstand systems tract (HST) (Van Wagoner et al., 1990; Helland-Hansen and Gjelberg, 1994). Both the TST and HST have depositional-dip thickness trends forming sigmoidal-shaped wedges and are stacked in a skewed manner within the sequences. This stacking is attributed to sediment partitioning during the different phases of a sequence and will be discussed later.

In detail, the sequences of the Hugin 2 unit show a vertical or aggradational stacking pattern from sequences 1 to 2 (Fig. 9). MFS3 indicates a pronounced transgression of the system where offshore mudstones extend south as far as 15/9-B-7 (Fig. 8B). Between MFS3 and MFS5 the sequences show another vertical stacking pattern (or aggradational trend), and MFS5 shows another strong transgression of the system with offshore mudstones extending south to 15/9-B-7. From MFS5 up to MFS8 the sequences and their transgressive and highstand systems tracts show a successively more southerly (retrogradational) stacking. MFS7 represents another strong transgression of the system with offshore mudstones extending as far south as 15/9-5. The MFS8 surface caps the Hugin Formation in the southern part of the study area and records the final drowning of the shallow-marine system. This aggradational to retrogradational stacking pattern of the sequences is interpreted to reflect the opening and drowning of the Viking Graben as illustrated in Fig. 3. The aggradational stacking of the sequences illustrates a general balance between the available accommodation and the supply of sediment on a sequence scale, and the retrogradational stacking pattern is the result of the generation of accommodation outpacing the amount of sediment supplied.

In a depositional strike direction (east–west), the sequence-stratigraphic surfaces are near parallel and each of the transgressive and highstand systems tracts generally has a constant thickness (Fig. 9). Small variations in thickness occur and may be primarily controlled by differences in the amount of sandstone versus shale and associated compaction. However, both the transgressive and highstand systems tracts show distinct variations in thickness distribution, as sigmoidal-shaped wedges, in a proximal to distal profile (depositional-dip direction, south–north) as has been noted above (Fig. 8).

10. Discussion

10.1. Sequence stacking pattern

The individual sequences of Hugin 2 unit are characterised by aggradational and climbing shoreline trajectories of the transgressive and highstand systems tracts. The Hugin 2 unit experienced variable rising relative sea level as a consequence of the large-scale transgression of the southern part of the Viking Graben caused by the rifting, subsidence and fault movements (Sneider et al., 1995). High rates of relative sea-level rise would favour transgressive conditions and formation of the transgressive systems tracts and lower rates of relative sea-level rise would favour regression and the development of the highstand systems tracts. The Hugin 2 unit is similar to successions studied by Mellere and Steel (1996), Carr et al. (2003) and Zecchin et al. (2006). In these studies, the successions are characterised by landward stacked sequences of TST-HST deposited within rift-grabens with active fault movements that facilitated the overall transgressive nature of the successions. Eustatic sea level falls are suppressed in rapidly subsiding basin as the basin subsidence rate outpaces any fall in eustatic sea level (Gawthorpe et al., 1994), thus sequence-stratigraphic architecture for subsiding basins can be very different than those sequence-stratigraphic models proposed for passive margins (Hiscott, 2001; Zecchin et al., 2006).

10.2. Style of depositional environment affected by the Viking Graben

During regressive phases, the mixed wave and fluvial deltaic depositional environment of the highstand systems tract of the Hugin 2 unit shows limited wave influence with only wave-reworking in the distal part of the mouthbars. This demonstrates that the wave action in the southern part of the Viking Graben was limited during the deposition of the Hugin 2 unit. The Viking Graben was elongate in shape at that time, about 30 km wide and 100 km long (Sneider et al., 1995), (Fig. 3) and the shape of the graben dampened the wave action (topographic sheltering of Dalrymple et al., 1992) and prevented longshore drift as a mechanism for sediment supply at the coast. Conversely, during transgressive phases, the elongate shape of the graben funnelled and amplified tidal influence (tidal range and current velocities), (Dalrymple et al., 1992; Yoshida et al., 2007) and promoted the development of tide-dominated estuaries (Fig. 3). This aspect of tidal-enhancement caused by tectonic development of graben-morphology (see also Gawthorpe and Leeder, 2000) was also reported by Richards (1991) in the Bruce-Beryl Embayment in the central Viking Graben. Mellere and Steel (1996) reported in their study graben structures focusing tidal currents with deposition of tidal sediments during transgressive phases, and Porebski (2000) also interpreted tectonic movements at the coast creating grabens that favoured tidal sedimentation in estuaries.

10.3. Sediment partitioning

The thickness trends of the TSTs and the HSTs illustrate differential sediment partitioning and are explained by considering the balance between accommodation and sediment supply (Swift and Thorne, 1991; Schlager, 1993; Shanley and McCabe, 1994; Cant, 1995; Martinsen et al., 1999), through a distal to proximal profile during the different stages of deposition within a sequence (Fig. 8). Typically, regression (in this case the highstand systems tract) occurs due to a lack of available accommodation and an excess in sediment supply in a landward position which then forces the sedimentary system to prograde basinward through time. Thus, the thickness of a regressive segment of a sequence typically thins in a landward direction due to reduced accommodation. It thickens in a basinward direction where accommodation is available, out to a point where the available accommodation consumes the amount of supplied sediment and the regressive unit pinches out. Therefore in the distal parts where offshore shales are deposited, sediment starvation will prevail. This geometry means that the regressive segment has the shape of a sigmoidal wedge in a depositional-dip direction (Fig. 8). The same sigmoidal wedge shape is found for the transgressive segment of a sequence (in this case the TST) but the segment has its greatest thickness more landward of the regressive unit in the same sequence. The transgressive segment is thin in the distal/offshore area due to sediment starvation. However, this segment thickens in a landward direction due to generation of new accommodation in the depositional profile and trapping of supplied

sediments from the landward side during transgression (see also Cattaneo and Steel, 2003). It thickens up to the point where the added accommodation equals the supplied amount of sediment. However, this study does not have sufficient data coverage to describe what happens beyond this point in a landward direction.

10.4. Reservoir implications

The model described here for the Hugin 2 unit (Fig. 10) can be used to understand the spatial and temporal development of the Hugin Formation in the area. It can help to understand the interwell distribution of facies, reservoir thickness and aerial extent of each sequence-stratigraphic unit. This information is important in understanding the drainage pattern of hydrocarbons from the reservoir and optimising the number and placement of wells that will maximize the recovery of hydrocarbons from the reservoir. Within a predictive model, reservoir distribution, reservoir quality and potential compartmentalisation due to horizontal barriers (e.g. shale layers associated with flooding surfaces or coal layers linked to maximum regressive surfaces) can be evaluated to maximize subsurface production. In addition, the model can then be used to help explore undrilled areas in the vicinity in order to find new hydrocarbon reserves.

However, understanding the limitations and uncertainties associated with these models is critical when using them, and when new information is at hand, these models should be tested and may need to be modified. In this study, the Hugin 2 unit is penetrated extensively by wells in the Sleipner Area. However, the well coverage is biased, with wells located near the top of the structures, and generally following a south–north trend (Figs. 1, 8). Hence, little is known about the Hugin Formation in the structurally low areas, and there remains some uncertainty about the precise orientation of the coastline. Other factors that most likely had an influence on deposition of the Hugin Formation in the Sleipner area include syn-sedimentary tectonic activity related to rifting and possible salt tectonics in some areas. The relatively uniform pattern of the sequence-stratigraphic units in the wells studied here indicates that the effects of syn-sedimentary tectonism were limited on the structural crests covered by the dataset. However in other areas, away from the wells, this interpretation is relatively untested.

11. Conclusions

The facies analysis, stratigraphic correlation and palaeogeographical interpretation outlined here leads to the following conclusions:

a) Facies analysis shows that the Hugin 2 strata consist of multiple fining-upward tidal estuary deposits (with channels, dunes and flats) deposited during transgression, each overlain by coarsening-upward, mixed fluvial- and wave-dominated deltaic deposits, with mouthbars and shoreface sandstones, deposited during regression. These strata were deposited in an elongate graben where tidal currents were amplified, and wave-action damped.
b) The transgressive and regressive units of the Hugin 2 strata are arranged into 8 sequences. These transgressive and regressive units are bound by surfaces representing both facies shifts and changes in stacking pattern (illustrating the shoreline trajectory), namely maximum flooding surfaces and maximum regressive surfaces. The transgressive units are interpreted as transgressive systems tracts and the regressive units as highstand systems tracts.
c) Shoreline trajectory exerts a strong control on the thickness, spatial extent, and stacking pattern of the preserved sandbodies. In this study, an aggradational component of the transgressive and highstand systems tracts of the sequences is described. The stacking pattern of the sequences shows an aggradational trend in the lower sequences followed by a retrogradational trend in the upper sequences. This stacking pattern is interpreted to be a result of the drowning of the southern Viking Graben, undergoing rifting and subsidence in Callovian to Oxfordian times. The rifting and subsidence created a setting of continuous rising relative sea level where during low rates of relative sea-level rise a highstand systems tract was deposited and during higher rates a transgressive systems tract was deposited. Any falls in eustatic sea level would be overprinted by the rift-related subsidence and therefore no lowstand systems tract was developed.
d) Correlation and mapping of the transgressive and highstand systems tracts shows that they are sigmoidal-shaped wedges with skewed thickness distributions in a depositional-dip direction. This is explained by changes in the rate of accommodation space versus sediment supply through time. The focus of sedimentation is forced basinward during regression due to a lack of accommodation in landward areas while during transgression the focus of sedimentation is moved landward because of added accommodation in that region. These sigmoidal-shaped geometries of systems tracts have not previously been described in the Hugin Formation.
e) The integration of these results established a new depositional model within a sequence-stratigraphic framework that serves as input to reservoir models to help increase recovery and identify new exploration targets.

Acknowledgments

The authors would like to thank the partners in the Sleipner Licence for permission to publish; StatoilHydro, Esso Norge, and Total. In addition Ronald Steel is thanked for his comments on an early version of this manuscript. Reviews by Sedimentary Geology's editor Chris Fielding, Gary Hampson and an anonymous reviewer greatly improved the quality of this manuscript.

References

Bhattacharya, J., Walker, R.G., 1992. Deltas. In: Walker, R.G., James, N.P. (Eds.), Facies Models: Response to Sea Level Change. Geological Association of Canada, St. John, Newfoundland, Canada, pp. 157–177.
Bhattacharya, J., Giosan, L., 2003. Wave-influenced deltas: geomorphological implications for facies reconstruction. Sedimentology 50, 187–210.
Bromley, R.G., 1996. Trace Fossils: Biology, Taphonomy and Applications, 2nd ed. Chapman and Hall, London, p. 361.
Cant, D.J., 1995. Sequence stratigraphic analysis of individual depositional successions: effects of marine/nonmarine sediment partitioning and longitudinal sediment transport, Mannville Group, Alberta Foreland Basin, Canada. American Association of Petroleum Geologists Bulletin 79, 749–762.
Carr, I.D., Gawthorpe, R.L., Jackson, C.A.L., Sharp, I.R., Sadek, A., 2003. Sedimentology and sequence stratigraphy of early syn-rift tidal sediments: the Nukhul Formation, Suez Rift, Egypt. Journal of Sedimentary Research 73, 407–420.
Cattaneo, A., Steel, R.J., 2003. Transgressive deposits: a review of their variability. Earth-Science Reviews 62, 187–228.
Catuneanu, O., 2002. Sequence stratigraphy of clastic systems: concepts, merit, and pitfalls. Journal of African Earth Science 35, 1–43.
Cockings, J.H., Gifford Kessler II, L., Mazza, T.A., Riley, L.A., 1992. Exploration Britain. In: Hardman, R.F.P. (Ed.), Geological insights for the next decade. Special Publication, vol. 67. Geological Society of London, pp. 65–105.
Coleman, J.M., Prior, D.B., 1982. Deltaic environments. In: Scholle, P.A., Spearing, D.R. (Eds.), Sandstone Depositional Environments. . Memoir, vol. 31. American Association of Petroleum Geologists, pp. 139–178.
Cope, J.C.W., Ingham, J.K., Rawson, P.F., 1992. Atlas of Palaeogeography and Lithofacies. Memoir, vol. 13. The Geological Society of London. 155 pp.
Dalrymple, R.W., Knight, R.J., Zaitlin, B.A., Middleton, G.V., 1990. Dynamics and facies model of a macrotidal sandbar complex, Cobequid bay — Salmon river estuary (Bay of Fundy). Sedimentology 37, 577–612.
Dalrymple, R.W., Zaitlin, B.A., Boyd, R., 1992. Estuarine facies models: conceptual basis and stratigraphic implications. Journal of Sedimentary Petrology 62, 1130–1146.
Elliott, T., 1986. Deltas. In: Reading, H.G. (Ed.), Sedimentary Environments and Facies. Blackwell, Oxford, pp. 113–154.
Fält, L.M., Helland, R., Jacobsen, V.W., Renshaw, D., 1989. Correlation of transgressive–regressive depositional sequences in the Middle Jurassic Brent/Vestland Group megacycle, Viking Graben, Norwegian North Sea. In: Collinson, J.D. (Ed.), Correlation in hydrocarbon exploration. Graham and Trotman, London, pp. 191–200.
Fjellanger, E., Olsen, T., Rubino, J.L., 1996. Sequence stratigraphy and palaeogeography of the Middle Jurassic Brent and Vestland deltaic systems, Northern North Sea. Norwegian Geological Journal 76, 75–106.
Gawthorpe, R.L., Leeder, M.R., 2000. Tectono-sedimentary evolution of active extensional basins. Basin Research 12, 195–218.
Gawthorpe, R.L., Fraser, A.J., Collier, R.E.L., 1994. Sequence stratigraphy in active extensional basins: implications for the interpretation of ancient basin-fills. Marine and Petroleum Geology 11, 642–658.

Gjelberg, J., Dreyer, T., Høie, A., Tjelland, T., Lilleng, T., 1987. Late Triassic to Mid-Jurassic sandbody development on the Barents and Mid-Norwegian shelf. Petroleum Geology of North West Europe. In: Brooks, J., Glennie, K. (Eds.), Petroleum Geology of North West Europe. Graham and Trotman, London, pp. 1105–1129.
Graue, E., Helland-Hansen, W., Johnsen, J.R., Lømo, L., Nøttvedt, A., Rønning, K., Ryseth, A., Steel, R.J., 1987. Advance and retreat of the Brent Delta System, Norwegian North Sea. In: Brooks, J., Glennie, K. (Eds.), Petroleum Geology of North West Europe. Graham and Trotman, London, pp. 915–937.
Hampson, G.J., Sixsmith, P.J., Johnson, H.D., 2004. A sedimentological approach to refining reservoir architecture in a mature hydrocarbon province: the Brent Province, UK North Sea. Marine and Petroleum Geology 21, 457–484.
Helland-Hansen, W., Gjelberg, J.G., 1994. Conceptual basis and variability in sequence stratigraphy; a different perspective. Sedimentary Geology 92, 31–52.
Helland-Hansen, W., Martinsen, O.J., 1996. Shoreline trajectories and sequences; description of variable depositional-dip scenarios. Journal of Sedimentary Research 66, 670–688.
Hiscott, R.N., 2001. Depositional sequences controlled by high rates of sediment supply, sea-level variations, and growth faulting: the Quaternary Baram Delta of northwest Borneo. Marine Geology 175, 67–102.
Hodgson, N.A., Farnsworth, J., Fraser, A.J., 1992. Salt-related tectonics, sedimentation and hydrocarbon plays in the Central Graben, North Sea, UKCS. In: Hardman, R.F.P. (Ed.), Exploration Britain: Geological insights for the next decade. Special Publication, vol. 67. Geological Society of London, pp. 31–63.
Howell, J.A., Flint, S.S., Hunt, C., 1996. Sedimentological aspects of the Humber Group (Upper Jurassic) of the South Central Graben, UK North Sea. Sedimentology 43, 89–114.
Hunter, R.E., Clifton, H.E., 1982. Cyclic deposits and hummocky cross-stratification of probable storm origin in Upper Cretaceous rocks of Cape Sebastian area, southwestern Oregon. Journal of Sedimentary Petrology 52, 127–144.
Husmo, T., Hamar, G.P., Høiland, O., Johannessen, E.P., Rømuld, A., Spencer, A.M., Titterton, R., 2003. Lower and Middle Jurassic. In: Evans, D., Graham, C., Armour, A., Bathurst, P. (Eds.), The millenium atlas: petroleum geology of the central and northern North Sea. Geological Society of London, pp. 129–155.
Hwang, I., Heller, P.L., 2002. Anatomy of a transgressive lag: Panther Tongue Sandstone, Star point Formation, central Utah. Sedimentology, 49, 977–999.
Kuecher, G.J., Woodland, B.G., Broadhurst, F.M., 1990. Evidence of deposition from individual tides and of tidal cycles from the Francis creek Shale (host rock to the Mazon Creek biota), Westphalian D (Pennsylvanian), north-eastern Illinois. Sedimentary Geology 68, 211–221.
MacEachern, J.A., Bann, K.L., Bhattacharya, J.P., Howell, C.D., 2005. Ichnology of deltas: organism responses to the dynamic interplay of rivers, waves, storms, and tides. In: Giosan, L., Bhattacharya, J.P. (Eds.), River Deltas — Concepts, Models, and Examples. Special Publication, vol. 83. Society for Sedimentary Geology, pp. 49–85.
Martinsen, O.J., Ryseth, A.E., Helland-Hansen, W., Flesche, H., Torkildsen, G., Idil, S., 1999. Stratigraphic base level and fluvial architecture: Ericson Sandstone (Campanian), Rock Springs Uplift, SW Wyoming, USA. Sedimentology 46, 235–259.
McCarthy, P.J., Plint, A.G., 2003. Spatial variability of paleosols across Cretaceous interfluves in the Dunvegan Formation, NE British Columbia, Canada: palaeohydrological, palaeogeomorphological and stratigraphic implications. Sedimentology 50, 1187–1220.
Mellere, D., Steel, R.J., 1996. Tidal sedimentation in Inner Hebrides half grabens, Scotland: the Mid-Jurassic Bearreraig Sandstone Formation. In: De Baptist, M., Jacobs, P. (Eds.), Geology of Siliciclastic Seas. Special Publication, vol. 117. Geological Society of London, pp. 49–79.
Milner, P.S., Olsen, T., 1998. Predicted distribution of the Hugin Formation reservoir interval in the Sleipner Øst field, South Viking Graben; the testing of a three-dimensional sequence stratigraphic model. In: Gradstein, F.M., Sandvik, K.O., Milton, N.J. (Eds.), Sequence Stratigraphy; Concepts and Applications. Special Publication, vol. 8. Norwegian Petroleum Society, pp. 337–354.
Mitchener, B.C., Lawrence, D.A., Partington, M.A., Bowman, M.B.J., Gluyas, J., 1992. Brent Group; sequence stratigraphy and regional implications. In: Morton, A.C., Haszeldine, R.S., Giles, M.R., Brown, S. (Eds.), Geology of the Brent Group. Special Publication, vol. 61. Geological Society of London, pp. 45–80.
Pemberton, S.G., MacEachern, J.A., Frey, R.W., 1992. Trace fossil/facies models; environmental and allostratigraphic significance. In: Walker, R.G., James, N.P. (Eds.), Facies Models: Response to Sea Level Change. Geological Association of Canada, St. John, Newfoundland, Canada, pp. 47–72.
Porebski, S.J., 2000. Shelf-valley compound fill produced by fault subsidence and eustatic sea-level changes (Eocene La Meseta Formation, Seymor Island, Antarctica). Geology 28, 147–150.
Posamentier, H.W., Jervey, M.T., Vail, P.R., 1988. Eustatic controls on clastic deposition I – conceptual framework. In: Wilgus, C.K., Hastings, B.S., Kendall, C.G.St.C., Posamentier, H.W., Ross, C.A., Van Wagoner, J.C. (Eds.), Sea Level change: an integrated approach. Special Publication, vol. 42. Society of Economic Palaeontologists and Mineralogists, pp. 109–124.
Rahmani, R.A., 1988. Estuarine tidal channel, and near shore sedimentation of a late Cretaceous epicontinental sea, Drumheller, Alberta, Canada. In: de Boer, P.L., van Gelder, A., Nio, S.D. (Eds.), Tide-influenced Sedimentary Environments and Facies. D. Reidel Publishing Company, pp. 433–471.
Reineck, H.E., Wunderlich, F., 1968. Classification and origin of flaser and lenticular bedding. Sedimentology 11, 99–104.
Reinson, G.E., 1992. Transgressive barrier island and estuarine systems. In: Walker, R.G., James, N.P. (Eds.), Facies models: Response to Sea Level change. Geological Association of Canada, St. Johns, Newfoundland, Canada, pp. 179–194.
Richards, P.C., 1991. An estuarine facies model for the Middle Jurassic Sleipner Formation: Beryl Embayment, North Sea. Journal of the Geological Society of London 148, 459–471.
Saito, Y., 1994. Shelf sequence and characteristic bounding surfaces in a wave-dominated setting: latest Pliocene–Holocene examples from North-east Japan. Marine Geology 120, 105–127.
Schlager, W., 1993. Accommodation and supply — a dual control on stratigraphic sequences. Sedimentary Geology 86, 111–136.
Shanmugam, G., Poffenberger, M., Alava, J.T., 2000. Tide-dominated estuarine facies in the Hollin and Napo ("Tand U") Formations (Cretaceous), Sacha Field, Oriente Basin, Ecuador. American Association of Petroleum Geologists Bulletin 84, 652–682.
Shanley, K.W., McCabe, P.J., 1994. Perspectives on the sequence stratigraphy of continental strata. Report of a Working Group at the 1991 NUNA Conference on High Resolution Sequence Stratigraphy. American Association of Petroleum Geologists Bulletin 78, 544–568.
Skarpnes, O., Hamar, G.P., Jacobssen, K.H., Ormaasen, D.E., 1980. Regional Jurassic setting of the North Sea north of the central highs. The sedimentation of the North Sea reservoir rocks. Special Publication, vol. 13. Norwegian Petroleum Society, pp. 1–8.
Smith, D.G., 1988. Tidal bundles and mud couplets in the McMurray Formation, north-eastern Alberta, Canada. Bulletin of Canadian Petroleum Geology 36, 216–219.
Sneider, J.S., de Clarens, P., Vail, P.R., 1995. Sequence stratigraphy of the Middle and Upper Jurassic, Viking Graben, North Sea. In: Steel, R.J., Felt, V.L., Johannessen, E.P., Mathieu, C. (Eds.), Sequence Stratigraphy on the Northwest European Margin. Special Publication, vol. 5. Norwegian Petroleum Society, pp. 167–198.
Steel, R.J., 1993. Triassic–Jurassic megasequence stratigraphy in the Northern North Sea: rift to post-rift evolution. In: Parker, J.R. (Ed.), Petroleum Geology of Northwest Europe: Proceedings of the 4th Conference. The Geological Society of London, pp. 299–315.
Steel, R.J., Ryseth, A., 1990. The Triassic–Early Jurassic succession in the northern North Sea: megasequence stratigraphy and intra-Triassic tectonics. In: Hardmann, R.F.P., Brooks, J. (Eds.), Tectonic Events responsible for Britain's Oil and Gas Reserves. Special Publication, vol. 55. Geological Society of London, pp. 139–168.
Swift, D.J.P., Thorne, J.A., 1991. Sedimentation on continental margins, I: a general model for shelf sedimentation. In: Swift, D.J.P., Oertel, G.F., Tillman, R.W., Thorne, J.A. (Eds.), Shelf sand and Sandstone Bodies: Geometry, Facies and Sequence Stratigraphy. Special Publication, vol. 14. International Association of Sedimentologists, pp. 3–31.
Taylor, A.M., Gawthorpe, R.L., 1993. Application of sequence stratigraphy and trace fossils analysis to reservoir description; examples from the Jurassic of the North Sea. In: Parker, J.R. (Ed.), Petroleum Geology of Northwest Europe: Proceedings of the 4th Conference. The Geological Society of London, pp. 317–335.
Thomas, D.W., Coward, M.P., 1996. Mesozoic regional tectonics and South Viking Graben formation: evidence for localised thin-skinned detachments during rift development an inversion. Marine and Petroleum Geology 13, 149–177.
Van Wagoner, J.C., Mitchum, R.M., Campion, K.M., Rahmanian, D., 1990. Siliciclastic sequence stratigraphy in well logs, cores and outcrops: Concepts for high-resolution correlation of time and facies. Methods in Exploration Series, vol. 7. American Association of Petroleum Geologists. 55 pp.
Visser, M.J., 1980. Neap–spring cycles reflected in Holocene subtidal large-scale bedform deposits: a preliminary note. Geology 8, 543–546.
Vollset, J., Dòre, A.G., 1984. A revised Triassic and Jurassic lithostratigraphic nomenclature for the Norwegian North Sea. Norwegian Petroleum Directorate Bulletin 3, 1–53.
Walker, R.G., Plint, A.G., 1992. Wave- and storm-dominated shallow marine systems. In: Walker, R.G., James, N.P. (Eds.), Facies models: Response to Sea Level change. Geological Association of Canada, St. Johns, Newfoundland, Canada, pp. 219–238.
Willis, B.J., 1997. Architecture of fluvial-dominated valley-fill deposits in the Cretaceous Fall River Formation. Sedimentology 44, 735–757.
Willis, B.J., 2005. Deposits of tide-influenced river deltas. In: Giosan, L., Bhattacharya, J.P. (Eds.), River Deltas — Concepts, Models, and Examples. Special Publication, vol. 83. Society for Sedimentary Geology, pp. 87–129.
Yielding, G., Badley, M.E., Roberts, A.M., 1992. The structural evolution of the Brent Province. In: Morton, A.C., Haszeldine, R.S., Giles, M.R., Brown, S. (Eds.), Geology of the Brent Group. Special Publication, vol. 61. Geological Society of London, pp. 27–43.
Yoshida, S., Steel, R.J., Dalrymple, R.W., 2007. Changes in depositional processes — an ingredient in a new generation of sequence-stratigraphic models. Journal of Sedimentary Research 77, 447–460.
Zecchin, M., Mellere, D., Roda, C., 2006. Sequence stratigraphy and architectural variability in growth fault-bounded basin fills: a review of Plio-Pleistocene stratal units of the Crotone Basin, southern Italy. Journal of the Geological Society of London 163, 471–486.
Ziegler, P.A., 1990. Geological Atlas of Western and central Europe. Shell International Petroleum Maatschappij, Den Haag, Netherlands.

5. Synthesis

The synthesis is organized into three themes, based on the findings in the five papers and the supporting abstracts. The papers and abstracts report different examples within the themes which strengthens the mutual interpretations and illustrates the diversity within these themes. In addition to the key-findings, each theme is discussed in terms of:

- the geological setting and evolution of the sedimentary basins
- the development of sedimentary models
- with reference to modern examples

The discussion of the three themes is followed by a section focusing on the broader perspective and applicability to other areas.

5.1 Theme 1) Allogenic forces in the basin: tectonics - climatic- eustatic controls

5.1.1 Tectonics

The northern North Sea had a complex tectonic history and illustrates the concept of geological inheritance concerning the building of post-Caledonian sedimentary basins on top of a terrane with many older faults and lineaments. The Devonian basins are linked to the Mesozoic sedimentary basins and rift-phases and affected the younger sedimentary basins by their shape and perhaps also the infill style.

The Devonian Hornelen Basin has been termed a pull-apart basin (Steel, 1976; Blair & Bilodeau, 1988; Titus et al., 2002) or an extensional basin (Seguret et al., 1989; Fossen et al., 2016) or extensional-collapse basin (Steel, 1988). This basin formed after the Caledonian Orogenesis due to post-thrusting collapse of overthickened crust, together with other pull-apart basins within the Caledonian realm. Pull-apart basins are typically formed along major strike-slip faults (Mann et al., 1983) as with the Devonian basins on the west-coast of Norway. They formed due to strike-slip movements on the Caledonian lineaments cutting across the northern North Sea (Fig. 2), where these

lineaments had a lateral movement in the order of 100 km in Devonian time (Fossen et al., 2016). A modern example of the Hornelen Basin is the Death Valley pull-apart basin in California with extensive alluvial infill. This basin was formed due to lateral movement of the bounding strike-slip fault in the range of 40-100 km displacement (Stewart, 1983).

These Devonian pull-apart basins became imprinted onto the Caledonian basement (Beach, 1985) and defines the initial fault-system of the northern North Sea. This had a great impact on the development of the following sedimentary basins where Beach (1985) and Coward (1993) suggested that these Devonian pull-apart basins later became reactivated along old basement shear zones by renewed extensional phases as the Permo-Triassic and Middle-Upper Jurassic rift phases. Odinsen et al., (2000) demonstrated various extension rates within the Mesozoic basins of the northern North Sea and a supporting observation of variable tectonic activity of the northern North Sea in the Mesozoic is indirectly suggested by Larsen et al., (2003) from onshore data. This aligns with the interpretation of Færseth & Ravnås (1998) who interpreted the Mesozoic of the northern North Sea to be tectonic active but with variable intensity through this period. The variable tectonic activity is exemplified by the Mesozoic papers within this dissertation.

Orre & Folkestad (2019) (Paper 2) proposed that the Permo-Triassic rift axis, located under the Horda Platform (Færseth, 1996) (Fig. 2), consists of two pull-apart basins of probably Devonian origin and that the former Devonian pull-apart basins under Tampen Spur became reactivated during the Jurassic extensional phases. This suggestion follows Coward (1995) who interpreted the Viking Graben to reflect reactivation of a Devonian fracture system. This aligns with the interpretation of Dorè et al., (1997) who described how the Caledonian basement fault system (Devonian) became reactivated and modified in Mesozoic and formed, for example, the Early Jurassic Seaway (Dorè et al., 1997). Thus, the Mesozoic sedimentary basins of the northern North Sea are related to the older Devonian basins through reactivation of faults and modification in rift-phases. This give testimony to the concept of geological

inheritance and the dominance of the allogenic tectonically force controlling the Mesozoic sedimentary basins.

5.1.2 Climate

Climate has a strong impact on the Earth's surface and modulates mountain building, ocean circulations, greenhouse gases, where expanding and contracting ice-caps occur in ice-house and green-house periods, respectively. Climate`s impact is reflected by variations in temperature and precipitation (along with tectonic relief) which influence the magnitude of erosion of the sediment source area and the sediment input to the receiving basins (Syvitski & Milliman, 2007). The climatic influence is relevant for all the examples used in this dissertation but appears to be of secondary order in terms of allogenic control.

The break-up of the super-continent Pangaea in the Permo-Triassic was the cause of the Early-Middle Triassic rifting in the northern North Sea. This tectonic event gave a dominant tectonic control on the development of the sedimentary basin during deposition of the Teist and Lomvi formations (Orre & Folkestad, 2019) (Paper 2). However, the tectonics induced a secondary climatic effect with strong winds directed along the axis of the rift graben (north-south) during this rift phase (Mader & Peryt, 1995). It is likely that the rift topography amplified the winds within the grabens as inferred from the aeolian deposits of the Lomvi Formation with fine grain-size, indicating strong winds in order to keep the grains in saltation. It is interesting to view the aeolian deposits in terms of accommodation space as the wind-strength defines how much can be preserved. This deviate from the common notion that accommodation space in continental environments is defined by the lake level (Shanley & McCabe, 1994). The other climatic allogenic effect within the Triassic, as suggested by Orre & Folkestad (2019) (Paper 2), is the uplift of the basin margins. This triggered a monsoonal system in the Triassic that both eroded the mountain range of Norway (and Scotland) and produced the enormous amount of sediments that filled in the basins in the North Sea. The stacked alternation of fluvial channels capped by muddy redbeds of

the Lunde Formation (Nystuen et al., 1989) illustrates the monsoonal effect on the Triassic deposits with alternating phases of fluvial input followed by draught. This shows that the Triassic period in the northern North Sea experienced a strong climatic allogenic control that was secondary to the tectonic allogenic force which induced the climatic effect in the first place.

Sediment supply is itself not an allogenic force but variation in the supply is sometimes interpreted as controlled by climate (Leeder et al., 1998) where high sediment yield is typical for greenhouse conditions (Carvajal et al., 2009). The Triassic Lunde Formation in the northern North Sea show a likely monsoonal effect in the sedimentary strata (Orre & Folkestad, 2019) (Paper 2), but the Triassic succession is mainly controlled by tectonic subsidence. The Jurassic sedimentary units of the northern North Sea, such as the Cook Formation, Brent Group and the Hugin Formation, built out in the basins due to basin-margin (relative) uplift. Any climatic differences within these units where probably suppressed by the basinal subsidence rate, but variation in the rate of sediment supply came probably from differences in rates of basin margin uplift, changes in precipitation, drainage routes and lithological differences in the exhumed rocks.

5.1.3 Eustasy

The third allogenic force to be considered for the Mesozoic sedimentary basin in the northern North Sea is eustasy. The Quaternary and Pliocene are known for their oscillating sea-level linked to glacial cycles (Shackleton, 1987; Rovere et al., 2016) with the glacio-eustatic cycles typically on the order of 60-120Kyr.

Eustasy is not relevant for the Triassic package of the northern North Sea but eustatic cyclicity has been suggested as an allogenic force in the Jurassic package, especially for the Brent Group (Helland-Hansen et al., 1992; Van Wagner et al., 1993; Hampson, 2004; Hampson et al., 2009) based on the widely used global sea-level curve of Haq et al., (1987). The global sea level curve of Haq et al., (1987) was questioned by Underhill & Partington (1994) who pointed out contradictions in the database of the study of Haq et al., (1987). The geological type-section for the Aalenian time-period in Germany,

shows a deepening trend of the basin while Haq et al., (1987) show a sea-level fall for the same time-period. Moreover, as the Jurassic period lacked ice-caps at the polar regions (Ravnås et al., 2000; Nøttvedt et al., 2008; Gomez et al., 2016), an eustatic cyclicity as suggested by Haq et al., (1987) is difficult to argue for this period.

Another contradicting observation regarding an eustatic control is the progradation of the extensive Sognefjord Formation `Delta` on the Horda Platform in Oxfordian (Dreyer et al., 2005) that occurred while the Hugin Formation retreated in the South Viking Graben (pers. com. Erik P. Johannessen, 2019). These two contemporary formations would in terms of eustasy represent sea-level fall or stillstand and sea-level rise, respectively. However, the Jurassic showed an oscillation in temperature of the sea in Europe with cooling in Pliensbachian and a marked warming in Toarcian (Gomez et al., 2016) which is connected to the Toarcian Anoxic event (Bailey et al., 2003). A variable sea temperature in the Jurassic suggest both expansion and contraction of the sea volume which probably gave some eustatic variation but of minor or negligible magnitude.

Haq (2017) presented a revised global sea-level model arguing for Jurassic eustatic changes related to orbital eccentricity and not to glacial ice-sheet variations. Eustasy may have had some influence in the Jurassic in North West Europe but even in tectonically stable basins as in the Jurassic Paris Basin with carbonate platforms, it is difficult to separate eustasy from tectonism (Brigaud et al., 2014). Eustasy is probably of less relevance as an allogenic force for the Mesozoic sedimentary basins of the northern North Sea as variation of eustasy would be suppressed by the tectonism.

5.1.4 Timescale

There is commonly a marked difference in timescales of tectonic forces (>1 Myr) compared with the timescales of climate (>100Kyr). However, if they act on the same time-scale it can be difficult to assess which allogenic force is dominating in some basins. The Paleozoic and Mesozoic time periods in the northern North Sea was tectonically active with variable intensity (Ziegler, 1990; Dorè, 1991; Coward, 1993;

Færseth & Ravnås, 1998; Odinsen et al., 2000; Larsen et al., 2003; Fossen et al., 2016) where the time-scale of the tectonic force was probably also variable, including shorter timescales similar to typical climatic and eustatic timescales (>100Kyr). An example of this is shown in Folkestad & Satur (2008) (Paper 5) where the sequences of the Hugin Formation are on a timescale of <1Myr. With a probably low or insignificant eustatic control of the Jurassic northern North Sea (Underhill & Partington, 1994; Ravnås et al., 2000) the cyclicity of the Jurassic sedimentary strata is caused by tectonics whereas climate probably had a secondary influence.

The allogenic control for the Devonian Hornelen pull-apart basin seems to be clearly related to tectonism as the basin had a high subsidence rate with about 25 km of stratigraphic infill, which is typical for pull-apart basins (Balance & Reading, 1980; Hempton & Dunne, 1984). The cyclic nature of the cyclothems may be the result of changing climate as suggested by Garner (1979) and by Anderson & Cross (2001), but it seems unlikely that climate should shift as regularly according to the ordered cyclicity of the basin. Milankovitch cycles cause regular climatic shifts, but it operates on 40Kyr which seems too short for the 200+ cyclothems of the Devonian basin. However, it is more likely that the cyclicity was caused by repeated stress-release and slip on the basin-bounding faults in repeated succession (Steel, 1988), creating renewed subsidence. Such repeated fault movements are common for pull-apart basins (Rodgers, 1980; van Wjik et al., 2017) and this was most likely the cause that formed the cyclicity of the Devonian Hornelen Basin.

5.2 Theme 2) Basin-wide infill style, rift-stages and sequence- stratigraphic implications

5.2.1 Infill style of the Devonian Hornelen basin

The cyclothems of the Devonian Hornelen Basin stand out as near basin-wide tabular units in the middle to upper part of the stack of about 200 cyclothems (Steel et al., 1977). The lower part of the stack of 200 cycles is covered and they are probably not

tabular shaped as they filled in the initial basin topography. The cyclothems measured in Folkestad & Steel (2001) (Paper 1) belongs to the axial drainage system of the basin and show near-symmetrical A/S ratio cycles. This shows that the basin was a balanced rift basin type during deposition of the middle to upper cyclothems. Such an ordered arrangement of the cyclothems of the Hornelen Basin is probably unusual in the geological record.

The rhythmic coarsening to fining upwards trends of the cyclothems from mudstones to coarse sandstones (Folkestad & Steel, 2001) (Paper 1) suggest an established drainage system feeding into the basin. The basin had internally a broad axial fluvial distribution system. The cyclothems were formed by repeated stress-release of the basin-bounding faults giving added accommodation space and a relative uplift of the hinterland leading to rejuvenation of the drainage system. This resulted in increased sediment supply that was tuned to a near-balance with the added accommodation space which makes this basin unique in the world. Extensional basins show typically progradation of clastic wedges during tectonic quiescence whereas retrogradation occurs due to faulting and subsidence (Frostick & Steel, 1993). This suggest that the rhythmic progradation and retrogradation of the cyclothems of the Hornelen Basin reflects tectonic quiescence and fault movement respectively.

5.2.2 Middle Triassic to Early Jurassic: Post-rift or inter-rift

The period between the Permo-Triassic rift (syn-rift phase in Early Triassic) and the Middle-Late Jurassic rift phase in the northern North Sea has traditionally been regarded as a post-rift phase (Nøttvedt et al., 1995; McLeod et al., 2000; Hampson et al., 2004). This term dictates evenly thick, tabular stratal units without signs of growth strata as wedge-shaped units. An example of using a post-rift approach is shown in Ryseth (2000) who observed thickness differences of the same stratal unit from fault block to fault block in Middle Jurassic strata in the Oseberg area. Ryseth (2000) interpreted these observations as differential subsidence of each fault block but without block rotation in a general post-rift setting.

An opposing view was presented by Færseth & Ravnås (1998) who described minor extensional phases within this interval. Ravnås et al., (2000) suggested that this period should be termed an inter-rift phase (mild tectonic activity between the rift-phases). This aligns with Ziegler (1990) who described the Permo-Triassic rift phase to be followed by a less tectonically active period and with rifting intensifying in the Middle Jurassic. Hence, Ziegler (1990) implied some degree of fault-activity in the Middle Triassic to Early Jurassic interval. The same view has been stated in many studies such as Dorè et al., (1999) who suggested that this period experienced mild extensional tectonics resulting in the Early Jurassic Seaway. Furthermore, fault activity is documented in the Pliensbachian-Toarcian time at the Alwyn-Ninian-Hutton Alignment (Sawyer & Keegan, 1996), in the Statfjord and Gullfaks area (Roberts et al., 1987) and in the Beryl Embayment (Richards, 1991). In the Triassic succession, Aamodt (2015) interpreted syn-sedimentary faulting within the upper part of the Lunde Formation (Late Triassic) and Triassic sedimentary wedges are indicated in Steel & Ryseth (1990). The findings in Folkestad et al., (2012a) (Paper 3) with fault movements and growth strata in the Early Jurassic Cook Formation aligns with the syn-sedimentary faulting within the Cook Formation as reported by Livbjerg & Mjøs (1989).

These examples of syn-sedimentary faulting within the Middle Triassic to Early Jurassic support an inter-rift phase for this interval as argued by Færseth & Ravnås (1998) and Ravnås et al., (2000). Further, an inter-rift-phase in the Middle Triassic to Early Jurassic in the northern North Sea fits with the establishment of the Early Jurassic Seaway (Dorè et al., 1997) which was the precursor of the Viking Graben. This suggests that the late part of the Early Jurassic probably represented a proto-rift stage in the northern North Sea before the rift initiation within the Brent Group (Folkestad et al., 2014) (Paper 4).

5.2.3 Rift stages in the Brent Group and Hugin Formation

The Jurassic Brent Group experienced both rift initiation and syn-rift stage (Folkestad et al., 2014) (Paper 4) and show therefore subtle and varying infill-style. Prior to and

at the rift initiation, the wave-dominated Brent `Delta` prograded northward due to a sediment supply rate that exceeded the available accommodation space. Thus, the sedimentary basin of the Brent `Delta` represents an over-filled basin. In the early syn-rift phase, the rotation of fault blocks generated sufficient accommodation space which led to a balance with the sediment supply. This balance between accommodation space and sediment supply, ended the progradation of the Brent `Delta`. Continued high rates of fault-induced subsidence, promoted transgression (Nøttvedt et al., 1995; Folkestad et al., 2014) (Paper 4) and a shoreline retreat of the Brent `Delta`. The accommodation space generation outpaced the sediment supply and thus the infill-style of the rift basin became underfilled. The transgressive nature of the underfilled basin gave a dominance of tidal depositional environments, as recorded in the Tarbert Formation (Folkestad et al., 2014) (Paper 4). This paper illustrates that the flooded hanging walls gave a funnel effect and thereby enhanced the tidal currents. Shallow-marine rift basins are commonly dominated by tidal deposits (Leckie & Rumpel, 2003) with an amplification of tidal currents (Reynaud & Dalrymple, 2012) as recorded in the Tarbert Formation.

The rifting during deposition of the Brent Group led to a southward retreat of the Tarbert Formation within the Viking Graben from the North Viking Graben and about 200 km south into the South Viking Graben (Fig. 2). In the South Viking Graben, the deposition of the Hugin Formation commenced in Late Bathonian (Husmo et al., 2003; Folkestad & Satur, 2008, Paper 5; Folkestad et al., 2012b, Appen. 2) and the Hugin Formation is the southern equivalent of the Tarbert Formation (Vollset & Dorè, 1984) (Fig. 4). The rapid retreat of the Tarbert Formation southward within the Viking Graben gave an underfilled rift basin where the generated accommodation space outpaced by far the rate of sediment supply. This indicates high subsidence rates due to rifting during the southward retreat of the Tarbert and Hugin formations.

The Jurassic South Viking Graben is bounded to the south by the triple junction of the Viking Graben, Moray Firth and Central Graben (Ziegler, 1990; Underhill & Partington, 1994) (Fig. 2). In the South Viking Graben, the Hugin Formation (Callovian-Early Oxfordian) show a near vertical and slightly southwards stacking of the sequences (see Fig. 8 in Folkestad & Satur, 2008) (Paper 5) towards the end of the

graben. This stacking pattern indicates equal rates of accommodation space versus sediment supply which illustrates a balanced- to slightly underfilled- rift basin. Such a stacking pattern can be caused by a reduction in rift-intensity or by an increase in sediment supply. An increase in sediment supply may have occurred in the South Viking Graben as the western margin of the South Viking Graben experienced uplift and inversion in the Late Jurassic (Zanella & Coward, 2003). On the other hand, the rift-intensity may have decreased or died out in the Late Jurassic. The South Viking Graben is part of the triple junction (Underhill & Partington, 1994) and it is likely that the tectonic activity was transferred to the Moray Firth and Central Graben (Fig. 2). The Central Graben and Moray Firth graben systems appear more pronounced than the South Viking Graben in Late Jurassic, as shown in Fraser et al., (2003) (Fig. 2). This is probably related to the Jurassic northern North Sea rift became a failed rift (Rattey & Hayard, 1993). A marine connection between the South Viking Graben and the Moray Firth was established in the Late Oxfordian (Underhill & Partington, 1994) and marks the end of the southward retreat of the Hugin Formation.

The Brent Group and the younger Hugin Formation represents three different infill styles that can form in a sedimentary basin experiencing rifting. The change in infill style is the result of the rift-initiation and increase in rift-intensity through time coupled with an initial large sediment supply. A modern example of the Middle-Late Jurassic rift in the northern North Sea is the Red Sea to Suez rift (Khalil & McClay, 2001) which also is a failed rift (Jackson et al., 2005). The Suez rift shows today rotated fault blocks flooded by the sea and with isolated footwall islands above the sea-level and represents an underfilled basin, similar to the final stage of the Brent Group (Folkestad et al., 2014) (Paper 4).

5.2.4 Sediment supply in under-filled rifts

The sediment supply issue of the Middle-Late Jurassic Viking Graben rift basin has some interesting aspects. The balanced infill of the rift basin in the South Viking Graben, illustrated by the vertically stacked Hugin Formation in the Sleipner Field (Folkestad & Satur, 2008) (Paper 5), shows sequences of alternating deltas and estuaries where the deltas are fed from the hinterland. However, in the (older)

underfilled Viking Graben farther north in North Viking Graben (Fig. 2) (Folkestad et al., 2014) (Paper 4), the tidal-dominated Tarbert Formation was deposited under transgressive conditions. Longshore drift is a common sediment supply mechanism along wave-dominated coasts (Carvajal et al., 2009) and tidal systems typically erode in the coastal areas and transport sediment landward with tidal currents. This type of sediment supply mechanism of the transgressive system was demonstrated by Chang et al., (2006) in their study of the Holocene Wadden Zee (Netherland). Here, the bulk part of the sediments of the back-barrier or lagoonal environment, is fed from the North Sea. Hence, it is likely that a considerable part of the Tarbert Formation was sourced from coastal areas by tidal erosion with sands brought into the estuaries and dragged southwards within the Viking Graben by tidal currents. Such a sediment supply mechanism may explain the well-sorted and clean character of the Tarbert Formation (Folkestad et al., 2014) (Paper 4) as the tidal currents will sort and clean-up the eroded sand (Leva Lopez et al., 2016). This explanation can probably be applied to the transgressive Stø Formation in the Barents Sea being dominated by tidal facies (Folkestad et al., 2005, Appen. 1a; Hess et al., 2014) as one of the characters of the Stø Formation is the well-sorted and mature sandstones (Walderhaug & Bjørklund, 2003). The Tarbert Formation has commonly been interpreted as a shoreface depositional environment (Mjøs, 2009: Løseth et al., 2009) which stand in contrast to a tidal interpretation. This might be related to a tendency to interpret transgressive tidal deposits as shoreface (Devine, 1991). The identification of mud-drapes in cross-bedded sandstones are often used as the main criteria to interpret tidal sandstones. Tidal sands supplied from the coastal area lack river-supplied terrigenous sediments as suspended mud, which produce slack-water mud-drapes during tides. Hence, mud-drapes are not a common feature of mature and well-sorted tidal sandstones fed from shoreline erosion.

The Tarbert Formation is about 70 m thick in the area of the Kvitebjørn-Gullfaks fields, whereas it is about 240 m thick in the Tune Field (Løseth et al., 2009) 75 km farther south in the North Viking Graben. The southward thickness increase of the Tarbert Formation indicates a higher rate of accommodation space and sediment supply to the

south. The increase in accommodation space can be explained by the accelerated rifting as the rift propagated southwards in the Middle Jurassic. If the increase in sediment supply was caused by a major graben axial feeder system, this would have given a thickening trend of the Tarbert and Hugin formations farther south in the South Viking Graben. However, such a thickening trend of the Tarbert and Hugin formations to the south is not recorded (Hampson et al., 2009). Instead, the sediment supply came most likely from the north within the North Viking Graben (Fig. 2) with tidal currents bringing in eroded sand from the coastal areas. The reduced amount of sand in the Tarbert-Hugin formations southwards (Hampson et al., 2009) is probably caused by the exhaustion of the sediment budget in the northern areas (NVG in Fig. 2). This can be summed up as underfilled shallow-marine rift basins favors tidal processes whereas overfilled basins have a tendency to be more dominated by wave or fluvial processes.

A modern example of a tidal-dominated rift basin as discussed above, is the Gironde Estuary (Jouanne & Latoche, 1981; Allen, 1991). This estuary is fed from the Dordogne and Garonne rivers from the landside and from coastal erosion at the seaside fed into the inlet as well-sorted tidal sandstones (Allen, 1991. The estuary appears to be in a balanced infill mode as it has the typical tripartite sand-mud-sand distribution in the estuary (Allen, 1991). A different aspect of the sediment supply versus subsidence in modern depositional environments, is the effect of man-made river diversions. River diversion may reduce the sediment supply to the coastal area, as in estuaries, and thereby enhance coastal erosion with supply from the seaside into the estuaries to restore the balance of the sediment budget. The effects of man-made-river diversions can also be seen at the Louisiana coast. Here, the diversion of the Mississippi river by the Corps of Engineers deprives the region of New Orleans of yearly flood-sediments that would have kept the floodplain at sea level (Kesel, 2003). Instead, the river-diversion contributes to the subsidence of the city of New Orleans by sediment-starvation. A similar effect can be seen in Venice, Italy, with sediment-starvation of the lagoonal islands where the city is located. In the Nile Valley, the man-made river interference of the Nile threatens to drown the valley itself due to subsidence and sediment-starvation (Aly et al., 2009).

5.2.5 Sequence stratigraphy in rifts

Sequence stratigraphic models are often shown as depositional dip oriented stratal sections whereas along-strike stratal sections are not demonstrated (Fielding, 2011). Stratal packages within shallow-marine rifts illustrate an interesting limitation of the sequence stratigraphic method, which may explain why they tend to be shown in dip-section. An example is the study of the shallow-marine Nukhul Formation in the Suez rift of Jackson et al., (2005) showing sequence stratigraphic correlations constructed in a dip-direction within a fault block.

In order to apply the sequence stratigraphic method to a sedimentary formation, it requires uniform subsidence within the basin as for example a shelf. A basin undergoing rifting with rotation of fault blocks creates an un-even distribution of accommodation space on local scale and therefore prevents sequence stratigraphy to be applied on basin-scale. However, it is possible to apply this method to individual rift blocks as demonstrated in Folkestad & Satur (2008) (Paper 5). Near uniform subsidence within a fault block exist at the footwall high or in the hanging wall in a dip-direction, whereas in a strike-direction the rotation of the fault block creates difference in accommodation space. During the rotation of a fault block, the footwall crest will be dominated by low accommodation whereas the hangingwall low will have high accommodation rates, which gives different facies expressions (Folkestad et al., 2014) (Paper 4). In Folkestad & Satur (2008) (Paper 5) the Hugin Formation is interpreted along the footwall high of a fault block at the Sleipner Field. Here, the Hugin Formation is represented by a stack of deltaic and estuary couplets representing regressive and transgressive units that defines the sequence stratigraphic surfaces of maximum regression and transgression, respectively. The alternating stack of regressive and transgressive units may be related to tectonic activity and quiescence (in this case on shorter timescales than normal for tectonics) as progradation typical occurs during tectonic quiescence in extensional basin (Frostick & Steel, 1993). Figure 9 in Folkestad & Satur (2008) (Paper 5) indicates differences in generation of accommodation space between fault blocks, which illustrate the uncertainty in using the sequence stratigraphic surfaces regionally. However, it is possible to correlate

sequence stratigraphic surfaces in a strike-direction within a fault block as the A/S ratio can be used relatively.

Folkestad & Satur (2008) (Paper 5) highlights the importance of identifying the transgressive unit as it is of volumetric significance, especially in a landward direction in a balanced infilled rift basin. By interpreting the transgressive phases as flooding surfaces, the recognition of the volumetrically transgressive strata can be missed out and instead be incorporated into the proximal strata of regressive units (Kieft et al., 2010). In Folkestad & Satur (2008) (Paper 5) the transgressive and regressive units show a skewed thickness distribution in a sequence, where the transgressive units thicken landward and the regressive units thicken basinward. This illustrates the concept of sedimentary partitioning (Cant, 1995) within a sequence (Fig. 5) which describes where the locus of sedimentation occurs in a proximal-distal profile, defined by the accommodation space versus sediment supply. The skewed thickness pattern, where both the regressive and transgressive units are of somewhat similar magnitude, is probably a consequence of a balanced infilled rift basin. The regressive and transgressive units may have different reservoir properties that can be of importance to map out in subsurface studies.

It appears to be a lack of papers addressing the sedimentary partitioning aspect in underfilled and overfilled rift basins. To speculate, an overfilled rift basin will have sediment supply exceeding the accommodation space generation and the regressive units will dominate volumetrically within the sequences. In an underfilled rift basin the opposite will probably occur with the transgressive unit being more pronounced volumetrically compared to the regressive unit.

5.3 Theme 3) Intra-basinal fault induced depositional environments

Uplift or subsidence as a response to extensional faulting results in spatial variations in generation of accommodation space and thereby induce differences, affecting the

depositional pattern. Examples of this kind of effect on the depositional environments are given in Papers 2-3-4. In Orre & Folkestad (2019) (Paper 2), the Triassic Lomvi Formation is interpreted as aeolian sandstones confined to the footwall highs at the end of the syn-rift phase. The syn-rift Teist Formation located below, consists of lake and playa deposits without aeolian deposits, suggesting that the footwall highs were submerged at that time. Increased syn-rift fault block rotation caused the fault block crests to be elevated above the lake-level and thereby, induced deposition of aeolian sandstones at the drained area. In the continental environments, it is common to regard the lake-level as the controlling surface with deposition below and erosion above (Posamentier & Allen, 1993). The characteristics of the aeolian deposits of the Lomvi Formation contradicts this model and suggest that the wind strength created the accommodation space for the aeolian deposits and controlled the sediment supply.

In Folkestad et al., (2012a) (Paper 3), the Cook Formation show syn-sedimentary faulting during deposition of tidal deltas in the study area. A beach-barrier depositional environment is inferred to exists at the footwall high as part of a large shoreface dominated environment according to the interpretation of Dreyer & Wiig (1995). Such a barrier attached to the fault crest would have protected the tidal-dominated delta from wave-reworking given the interpretation of the larger Cook Formation depositional system presented by Dreyer & Wiig (1995) and Charnock et al., (2001).

Dalrymple & Zaitlin (1994) interpreted estuaries to occur within incised valley that had been drowned by sea level rise and filled with tidal facies. Even though this interpretation has been popular among sedimentologists to assign to tidal facies, rift basins or fault-induced depressions offer the same setting with high rates of accommodation space versus sediment supply. Jackson et al., (2005) interpreted the Nukhul Formation in the Suez Rift as a tide-dominated formation formed due to the transgressive nature of the shallow-marine rift. This is a similar interpretation to both the Tarbert and Hugin formations (Folkestad & Satur, 2008, Paper 5; Folkestad et al., 2014) (Paper 4) and in the study of Leckie & Rumpel (2003) on shallow-marine rift.

The Tarbert Formation in the Brent Group represents a subsurface example of fault-induced depositional environment with estuaries formed in a syn-rift setting due to fault-block rotation with an increase in accommodation space in the hangingwall (Folkestad et al., 2014) (Paper 4). The Tarbert Formation experienced retrogradation of the shoreline due to rotating fault-blocks, with dominance of tidal currents due to the funnel-shape of the hangingwall part. This configuration caused an amplification of the tidal currents with deposition of tidal bars and estuarine facies. At the footwall high, wave-reworked strata interpreted as deposited in a spit-environment prevailed due to uplift of the fault crest and reduction in accommodation space. This facies distribution of the Tarbert Formation gave an undulating to almost a zig-zag pattern of a coastline morphology. This was represented by the spit depositional environment at the footwall highs extended farther out into the sea than the subsiding hangingwall areas with estuaries. This stand in contrast to the interpretation of the Tarbert Formation by Hampson et al., (2004) or Mjøs (2009) who depicts the coastline as a linear east-west feature. Folkestad et al., (2014) (Paper 4) illustrated a facies segregation of the rotating rift block during deposition of the Ness-Tarbert formations with more frequent fluvial channels and swamp deposits in the hangingwall (high accommodation space) and a general lack of these deposits towards the footwall high (low accommodation space).

A different sub-surface example of fault-induced estuary is the Early Jurassic Stø Formation in the Hammerfest Basin (Barents Sea). The Stø Formation shows a transgressive stacking pattern (Hess et al., 2014) of mature sandstones of the Stø Formation (Walderhaug & Bjørkum, 2003) indicating re-deposition of sediments which is typical for tidal deposits (Chang et al., 2006). In the study of Folkestad et al., (2005) (Appen. 1a) (see also Folkestad, 2008, Appen. 1c), the Stø Formation was interpreted as deposited within a fault-induced depression, formed by a blind fault with deposition of tidal facies in an estuarine setting. In the literature, it appears to be scarcity of subsurface examples of fault-induced estuaries. However, in the modern environment fault-bounded estuaries have been reported by Simms et al., (2016) on the coast of California. In the western part of the Gulf of Mexico, the Rio Grande rift-graben includes estuaries induced by faults (Isla et al., 2004) and Hijma et al., (2009)

interpreted the evolution of the Holocene Rhine-Meuse estuary to be associated with fault movements.

5.3.1 Broader perspectives

The aspects of the Norwegian sedimentary basins raised in this dissertation can be considered in terms of:

- the mature northern North Sea rift basin versus other rift basins in the world
- if the Suez and Corinth rift models are analogue to the northern North Sea rift basin
- current thinking within the sequence stratigraphic methodology in rift basins
- the difference between the contemporary Jurassic Paris Basin in the southern part of the North Sea and the Jurassic northern North Sea

1). The Mesozoic northern North Sea rift basin versus others rift basins in the world.
Numerous rift basins and failed rifts exist around the world and many of them are related to the break-up of the Pangaea mega-continent from Mesozoic and into Cenozoic (Hadlari et al., 2016). The Artic rift system commenced in late Permian and formed several Mesozoic shallow-marine rift basins (Dorè, 1991) such as the Sverdrup rift basin in Canada (Hadlari et al., 2016; Sømme et al., 2018),), Bay of Biscay rift-basin (Tugend et al., 2014) and the Jeanne d`Arc Basin (Driscoll et al., 1995) to name a few.

These basins are typically described on a broad scale with the sedimentary response to rifting, addressed on formation scale. The Mesozoic Bay of Biscay formed through a series of extensional and compressional phases with depositions ranging from clastic sedimentary units, carbonate platforms and evaporites with a general drowning of the basin (Tugend et a., 2014). The Mesozoic Sverdrup Basin represents a single-rift basin and the sedimentary infill appears sand-starved with a dominance of both continental and marine mud deposits (Hadlari et al., 2016: Sømme et al., 2018). These two basins are, to a lesser extent, analogue to the Mesozoic northern North Sea Basin in terms of rift style and arrangement of depositional environments. Instead, the Jeanne d`Arc Basin offshore Newfoundland appears more similar to the Mesozoic northern North

Sea rift basin. This basin developed through multiple rift-phases and shows a sedimentary infill style grossly similar to the northern North Sea with sand-dominated continental facies in the lower part, followed by shallow-marine strata and with deep-marine deposits above (Driscoll et al., 1995). Unfortunately, it appears to be a lack of papers following up the study of Driscoll et al., (1995) on the Jeanne d`Arc Basin.

According to Ichaso et al., (2016), the best documented examples of marine rift basins in the world are the Jurassic basins of the northern North Sea and Haltenbanken in the Norwegian Sea. This is due to the fact that they are mature basins in terms of exploration with extensive seismic data and well coverage. Therefore, the interpretation and presented models of the sedimentary response in the basins shown in the papers of this dissertation may be used as examples and guides for other sedimentary studies in extensional basins.

2). *The Suez and Corinth rift models.*

In terms of rift basin models, both the Suez rift basin (Gupta et al., 1999; Lewis et al., 2017) and the Corinth rift basin (Gawthorpe & Leeder, 2000; Ford et al., 2017) are popular examples to illustrate the development of rift basins. However, these examples are single-rift basins, i.e. they have experienced one rift phase, and they initiated as continental rifts that later became flooded by the sea. The sediment supply into these basins came from exposed rocks being either crystalline or lithified fault blocks or rift shoulder/margin. These two famous rift basin examples deviate from the Jurassic period of the northern North Sea multi-rift basin as the latter initiated within the shallow-marine environment during deposition of the Middle Jurassic Brent Group (Folkestad et al., 2014) (Paper 4). The poorly consolidated sedimentary strata within the rotating fault blocks (of the recently deposited Brent Group) became sub-arial exposed along the footwall highs and acted as local sediment source. Thus, the sedimentary response was most likely faster in the northern North Sea rift basin compared to the Suez or Corinth rift basins with lithified rocks, resilient to erosion. The Suez or Corinth rift basins have a topography-controlled drainage system whereas

in the Jurassic northern North Sea such a drainage system was probably absent or poorly developed within the eroded Brent Group. The Corinth and Suez rift examples are probably more analogue to the Triassic northern North Sea rift basin that formed in the continental environment. The Triassic rift phase was the first rift phase in the Mesozoic and can in that sense, be regarded as a single rift. The Death Valley extensional basin (Stewart, 1983) is probably the best analogue for the Triassic northern North Sea rift basin.

3). *Current thinking within the sequence stratigraphic methodology in rifts.*

The current status of the sequence stratigraphic methodology was summarized in the studies of Catuneanu et al., (2009) and Catuneanu (2019). It appears that the methodology is much the same as has been presented in the papers from the 90`s. The study of Catuneanu (2019) shows strong similarities with the study of Helland-Hansen & Gjelberg (1994) with focus locked onto the shoreline trajectory in basins with uniform tectonic subsidence. There seems to be a lack of advances in improving the sequence stratigraphic methodology in tectonic active areas as well as in rifts. Martins-Neto & Catuneanu (2010) proposed a sequence stratigraphic model for rift basins using Prosser (1993) sedimentary infill styles (under-balance and overfilled basins) as descriptive terms. They believed that a rift basin had an internal uniform subsidence pattern and thereby missed out on recognizing the key element of the rift system being the extension forces causing fault block rotation, resulting in large variations in accommodation space across the basin. A different example of applying this method to a rift basin is the study of Jackson et al., (2005) who applied the sequence stratigraphic method to the Suez rift system by describing the sequence stratigraphic framework of sedimentary strata within a fault block in a dip direction, i.e. in a section of near uniform subsidence. This approach is similar to the study of Folkestad & Satur (2008) (Paper 5) in the Hugin Formation in South Viking Graben.

In the sequence stratigraphic summary study of Catuneanu (2019) the accommodation space is defined by the sea or lake level. In Orre & Folkestad (2019) (Paper 2), the

deposition of aeolian sandstones of the Lomvi Formation were controlled by the wind strength within the Triassic rift basin and thereby define the accommodation space. This stand in contrast to the commonly used relative sea-level or the idea of base-level equal to lake or sea-level (see Catuneanu, 2019). Some could argue that the aeolian deposits are only preserved temporarily and depends on tectonic subsidence and burial, but that argument can be turned to any kind of sedimentary deposits. Instead, it is more interesting to accept the idea of the base-level, as proposed by Wheeler (1964), where erosion occurs above an imaginary line and deposition below. This is best described by the accommodation space versus sediment supply ratio as proposed by Schlager (1993) which is not dependent on either sea-level or lake level. By using sea-level or lake-level as a reference point (Helland-Hansen & Hampson, 2009; Catuneanu, 2019) the focus is on the lake margin or shoreline with the danger of ignoring whatever forces that acts on the sedimentary strata farther inland. In this sense, the A/S ratio is an objective and descriptive approach to describe deposition and preservation within the clastic sedimentary environments. Accommodation space is extensively used in carbonate sedimentology to describe growth and decay of carbonate platforms. It is interesting that the sequence stratigraphic method for carbonate sedimentology dictates deposition during rising sea-level whereas clastic sedimentology dictates drowning and abandonment with a shut-off of the depositional process, which illustrate a paradox in the sequence stratigraphic method.

4). *Difference between the contemporary Jurassic Paris and the northern North Sea basins.*

The Jurassic basins in Northern Europe shows pronounced difference. To the south, the Jurassic Paris Basin experienced tectonic quiescence and development of carbonate platforms during a general sea-level rise (Brigaud et al., 2014). Carbonate platforms are absent in the Jurassic northern North Sea due to a very different geological setting. The best modern example of such a discrepancy is the east coast of South America where carbonate platforms as reefs, fringe the coastline except seaward of the Amazon River. Here, the clastic output and currents suppress coral reef growths in front of the

Amazon river mouth. Coral reefs need clean waters to live whereas marine waters with clastic sediments as silt and mud from river-floods, choke the carbonate organism (Tebbet et al., 2017). The lack of carbonate platforms in the Jurassic northern North Sea indicates a tectonic active basin with variable rates of subsidence and drowning combined with generally high rates of clastic input. Factors such as rift and inter-rift phases, greenhouse conditions with extensive precipitation and exhumation of the repeatedly elevated basin margins, explain the sedimentary infill of the basin. Perhaps a study linking subsidence rates, sediment input rate and sediment volume of the Jurassic northern North Sea should be done in the future. The study of Gabrielsen et al., (2010) gives a good illustration of the relative uplift rates of Norway at the different geological ages, which would be a natural starting point for such studies.

6. Conclusions and suggestion for further work

This dissertation has brought forward several important points on the subject of sedimentary response to tectonism and rifting in basins. The main conclusions are:

Theme 1 – Allogenic forces:

- The Devonian and Mesozoic sedimentary basins onshore and offshore Norway were formed and controlled by tectonism due to post-Caledonian extensional phases.
- The Permo-Triassic and the Jurassic-Early Cretaceous rift phases reactivated the old post-Caledonian lineaments and the Devonian pull-apart basins in the northern North Sea. This influenced the subsidence pattern in the different sub-basins. The Triassic rift axis was located at the Horda Platform whereas the Jurassic rift axis was located in the Viking Graben.
- Climate had probably a secondary influence but affected the rates of sediment supply. The climatic impact is probably best seen in the Triassic succession with a likely monsoonal effect.
- Eustasy seems to have had a lesser role in the Mesozoic northern North Sea due to Greenhouse conditions at that time with lack of ice-caps. Changes in eustasy would had been suppressed by tectonic movements if they were rapid.
- The variable tectonic activity of the Jurassic northern North Sea led the tectonic forces to sometimes act on shorter time scales similar to climatic time scales.

Theme 2 – Basin infill style:

- The Brent Group shows three different infill styles: underfilled, balanced and overfilled. The overfilled stage was characterized by progradation with a wave-dominated delta-front whereas the underfilled stage was characterized by retrogradation and tidal processes.
- The Suez and Corinth single-rift basins differ from the Jurassic northern North Sea multi-rift basin. The former rifts consist of lithified rotated fault blocks whereas the latter consisted of rotated fault blocks of poorly consolidated strata. This gave a much faster sediment supply response in the latter case, and probably without a topography-controlled drainage system.
- Coastlines under transgression experience erosion in the coastal area and a sediment supply from the sea-side into estuaries and barrier lagoon embayments. These sediments are often well-sorted and mature sandstones that are typically found in estuaries and tidal bars.
- Conventional sequence stratigraphy can be applied to sedimentary strata in rift basin in a dip-section of a fault block. However, the method cannot be applied across a rift basin due to fault block rotations.

Theme 3 – Fault-induced depositional environments:

- The aeolian Lomvi Formation (Triassic) was deposited on uplifted and drained footwall highs above the adjacent lakes. This was an effect of the Early Triassic rift phase and the aeolian dunes represent a fault-induced depositional environment.
- The Tarbert Formation (Brent Group) show a variation of fault-induced depositional environments as estuaries (in hangingwall) and spits (at footwall high). The Stø Formation in the Hammerfest Basin show a similar feature with an estuary associated with fault movement. Even though estuaries often have been interpreted to occur in incised valleys, the examples here show that faulting may give the same setting.
- The rifting within the Brent Group formed an uneven coastline defined by the shallow fault crest. This fault-block rotation gave contrasting depositional environments of the coastline along the strike of the fault-blocks. This deviates from the interpreted linear coastline style presented in previous studies of the Brent Group.

The understanding of the Mesozoic multi-rift basin of the northern North Sea and other basins would be improved if new studies could be undertaken focusing on:

- Better understanding of the shifting subsidence pattern of the Mesozoic sub-basins through time of the northern North Sea. The understanding of the Devonian fault configuration and how this affected the younger sedimentary basins through reactivations, is a theme that should be investigated further.
- An approach to apply sequence stratigraphy on basin scale within active rifts should be an aim for the future. This would clarify if it is possible to use sequence stratigraphy in rift basins, or if one must conclude that the sequence stratigraphic method has limitation in such basins.
- A comparison of rift basins in terms of depositional environments in underfilled, balanced and overfilled would help to better characterize rift basins.

7. References:

Aamodt, T.K.M., 2015. Sedimentological study of the Late Triassic Lunde Formation in the Tampen Spur area, northern North Sea. Master thesis, unpublished, University of Bergen, 148pp.

Abbink, O., Van Konijnenburg-Van Cittert, J., Visscher, H. 2004. A sporomorpheco-group model for the Northwest European Jurassic–Lower Cretaceous: concepts and framework. *Netherlands Journal of Geosciences,* **83**, 17–31.

Allen, G.P., 1991. Sedimentary processes and facies in the Gironde estuary: a recent model of macrotidal estuarine systems. *In Smith, G.D., Reinson, G.E., Zaitlin, B.A., and Rahmani, R.A., eds., Clastic Tidal Sedimentology. Canadian Society of Petroleum Geologists Memoir,* **16**, 29-40.

Aly, M.H., Zebker, H.A., Giardino, J.R., Klein A.G. 2009. Permanent Scatter investigation of land subsidence in Greater Cairo, *Egypt Geophys. J. Int.,* **178**,1238-1245.

Anderson, D.S., Cross T.A. 2001. Large-scale cycle architecture in continental strata, Hornelen Basin (Devonian), Norway, *Journal of Sedimentary Research,* **71**, 255-271.

Aschoff, J. L., Steel, R. J. 2011. Anomalous clastic wedge development during the Sevier-Laramide transition, North American Cordilleran foreland basin, USA. *Geological Society of America Bulletin,* **123**, 1822–1835.

Bailey, T. R., Rosenthal., Y., McArthur, J. M., van de Schootbrugge, B., Thirlwall, M. F. 2003. Paleoceanographic changes of the Late Pleinsbachian-Early Toarcian interval: a possible link to genesis of an oceanic anoxic event. *Earth Planet. Sci. Lett.* **212**, 307–-320.

Balance P.F., Reading H.G. 1980. Sedimentation in oblique slip mobile zones, *International Association Sedimentology,* Special Publication, **4,** 337.

Baroni, I.R., Pohl, A., van Helmond, N.A.G.M., Papadomanolaki, N.M., Coe, A.L., Cohen, A.S., van de Schootbrugge, B., Donnadieu, Y., Slomp, C.P. 2018. Ocean circulation in the Toarcian (Early Jurassic): a key control on deoxygenation and carbon burial on the European Shelf. *Paleoceanogr. Paleoclimatol.,* **33**, 994-1012

Beach, A. 1985. Some comments on sedimentary basin development in the Northern North Sea. *Scottish Journal of Geology,* **21**, 493–512.

Blair, T. C & Bilodeau, W. L. 1988. Development of tectonic cyclothems in rift, pull-apart, and foreland basins: sedimentary response to episodic tectonism. *Geology,* **16**, 517-520.

Blatt, H., Tracy, R. 1996. Petrology, Igneous, Sedimentary and Metamorphic. W.H. Freeman, New York. 529pp.

Brekke, H. 2000. The tectonic evolution of the Norwegian Sea Continental Margin with emphasis on the Vøring and Møre Basins. *In: Dynamics of the Norwegian margin (Eds: A. Nøttvedt, B.T. Larsen, S. Olaussen, B. Tørudbakken, J. Skogseid, R.H. Gabrielsen, H. Brekke and Ø. Birkeland),* Geol. Soc. Spec. Publ., **167**, 327–378.

Brigaud, B., Vincent, B., Carpentier, C., Robin, C., Guillocheau, F., Yven, B., Huret, E., 2014. Growth and demise of the Jurassic carbonate platform in the intracratonic Paris Basin (France): Interplay of climate change, eustasy and tectonics. *Marine and Petroleum Geology,* **53**, 3–29.

Bullimore, S.A., Helland-Hansen, W. 2009. Trajectory analysis of the lower Brent Group (Jurassic), Northern North Sea: Contrasting depositional patterns during the advance of a major deltaic system. *Basin Research*, **21**, 559–572.

Cant, D.J., 1995. Sequence stratigraphic analysis of individual depositional successions: Effects of marine-nonmarine sediment partitioning, and longitudinal sediment transport, Mannville Group, Alberta foreland basin, Canada. *American Association of Petroleum Geologists Bulletin*, **79**, 749-762.

Carroll, A.R., Bochas, K.M., 1999. Stratigraphic classification of ancient lakes: Balancing tectonic and climatic controls. *Geology,* **27**, 99-102.

Carvajal., C., Steel R., Petter A. 2009. Sediment supply: the main driver of shelf-margin growth. *Earth-Science Reviews,* **96**, 221-248.

Catuneanu, O., 2002. Sequence stratigraphy of clastic systems: concepts, merits, and pitfalls. *Journal of African Earth Sciences,* **35**, 1–43.

Catuneanu, O., Abreu V., Bhattacharya, J.P., Blum, M.D., Dalrymple, R.W., Eriksson, P.G., Fielding, C.R., Fisher, W.L., Galloway W.E., Gibling M.R., Giles, K.A., Holbrook, J.M., Jordan, R., Kendall, C.G.St.C., Macurda, B., Martinsen, O.J., Miall, A.D., Neal, J.E., Nummedal, D., Pomar, L., Posamentier, H.W., Pratt, B.R., Sarg, J.F., Shanley, K.W., Steel, R.J., Strasser, A., Tucker, M.E., Winker, C. 2009. Towards the standardization of sequence stratigraphy. *Earth Science Review,* **92**, 1-33.

Catuneanu, O. 2019. Model-independent sequence stratigraphy. *Earth Science Review,* **188**, 312-388.

Chang T. S., Bartholoma A., Flemming B. W. 2006. Seasonal dynamics of fine-grained sediments in a back-barrier tidal basin of the German Wadden Sea (Southern North Sea). *Journal of Coastal Research,* **22**, 328–338.

Charnock, M.A., Kristiansen, I.L., Ryseth, A., Fenton, J.P.G., 2001. Sequence stratigraphy of the Lower Jurassic Dunlin Group, northern North Sea. *In: Martinsen, O.J., Dreyer, T. (Eds.), Sedimentary Environments Offshore Norway - Palaeozoic to Recent.* Norwegian Petroleum Society, Special Publication, **10**, 145-174.

Chen, X., Wang, C., Wu, H., Kunht, W., Jia, J., Holbourn, A., Zhang, L., Ma, C., 2015. Orbitally forced sea-level changes in the Upper Turonian–Lower Coniacian of the Tethyan Himalaya, Southern Tibet. *Cretaceous Research,* **56**, 691–701.

Coward, M.P. 1993. The effect of Late Caledonian and Variscan continental escape tectonics in basements structures, Palaeozoic basin kinematics and subsequent

Mesozoic basin development in NW Europe. *In: Parker, J.R. (ed.) Petroleum Geology of Northwest Europe: Proceedings of the 4th Conference.* Geological Society, London, 1095–1108.

Coward M. P. 1995. Structural and tectonic setting of the Permo-Triassic basins of northwest Europe. *In: Boldy S. A. R. (ed.) Permian and Triassic Rifting in Northwest Europe.* Geological Society, London, Special Publications, **91**, 7–39.

Coward, M.P., Dewey, J.F., Hempton, J.F., Holroyd, J. 2003. Tectonic evolution. *In: Evans, D., Graham, C., Armour, A. & Bathurst, P. (eds). The Millennium Atlas: Petroleum Geology of the Central and Northern North Sea.* Geological Society of London, 17–33.

Davies, S.J., Gibling, M.R. 2003. Architecture of coastal and alluvial deposits in an extensional basin: the Carboniferous Joggins Formation of eastern Canada. *Sedimentology,* **50**, 1–25.

Devine, P.E. 1991. Transgressive origin of channeled estuarine deposits in the Point Lookout Sandstone, Northwestern New Mexico: a model for Upper Cretaceous, cyclic regressive parasequences of the U.S. Western Interior. *American Association of Petroleum Geologists Bulletin,* **75**, 1039-1063.

Dokka, R. K., 2006. Modern-day tectonic subsidence in coastal Louisiana. *Geology*, **34**, 281–284.

Doré, A.G., 1991. The structural foundation and evolution of Mesozoic seaways between Europe and the Arctic. *Palaeogeograhy, Palaeoclimatology, Palaeoecology,* **87**, 441–492.

Doré, A.G., Lundin, E.R., Fichler, C., Olesen, O. 1997. Patterns of basement structure and reactivation along the NE Atlantic margin. *Journal of the Geological Society,* London, **154**, 85–92.

Doré A.G., Lundin, E.R., Jensen, L.N., Birkeland, Ø., Eliassen, P.E., Fichler, C., 1999. Principal tectonic events in the evolution of the northwest European Atlantic

margin. *In: Fleet, A.J. and Boldy, S.A.R., (eds.), Petroleum Geology of Northwest Europe: Proceedings of the 5th Conference.* Geological Society, London, 41–61.

Dreyer, T., Wiig, M., 1995. Reservoir architecture of the Cook Formation on theGullfaks field based on sequence stratigraphic concepts. *In: Steel, R.J., Felt, V., Johannessen, E.P., Mathieu, C. (Eds.),* Sequence Stratigraphy of The Northwest European Margin. Norwegian Petroleum Society, Special Publication, **5**, 109-142.

Dreyer, T., Whitaker, M., Dexter, J., Flesche, H., Larsen E. 2005. From spit system to tide dominated delta: integrated reservoir model of the upper Jurassic Sognefjord Formation on the Troll West Field. *In: A.G. Doré, B. Vining (Eds.), Petroleum Geology of North-West Europe and Global Perspectives, Proceedings of the 6th Petroleum Geology Conference*, Geological Society of London, London, 1-26.

Driscoll N. W., Hogg J. R., Christie-Blick N., Karner G. D. 1995. Extensional tectonics in the Jeanne d'Arc Basin, offshore Newfoundland: Implications for the timing of breakup between Grand Banks and Iberia. *In: The Tectonics, Sedimentation and Palaeoceanography of the North Atlantic Region. Scrutton R. A., Stoker M. S., Shimmield G. B., Tudhope A. W. (eds).* Geological Society, London, Special Publications, **90**, 1–28.

Duffy, O. B., Bell, R. E., Jackson, C. A. L., Gawthorpe, R. L., Whipp, P. S. 2015. Fault growth and interactions in a multiphase rift fault network: the Horda Platform, Norwegian North Sea. Journal of Structural Geology, **80**, 99– 119.

Fielding, C.R., 2011. Foreland basin structural growth recorded in the Turonian Ferron Sandstone of the Western Interior Seaway Basin, U.S.A. *Geology,* **39**, 1107–1110.

Fjellanger. E., Olsen T. R., Rubino, J. L. 1996. Sequence stratigraphy and palaeogeography of the Middle Jurassic Brent and Vestland deltaic systems, northern North Sea. *Norwegian Geological Journal,* **76**, 75–106.

Folkestad, A., Steel, R. J. 2001. The alluvial cyclicity in Hornelen basin (Devonian Western Norway) revisited: a multiparameter sedimentary analysis and stratigraphic implications. *Norwegian Petroleum Society,* Special Publications, **10**, 39-50.

Folkestad, A., Ottesen, S., Rømuld, A. 2005. Reservoirs in a structurally controlled estuary: the Jurassic Snøhvit gas condensate Field, Barents Sea, Norway. Abstract presented at the American Association of Petroleum Geologists Annual Meeting Calgary, Alberta, 19–22 June.

Folkestad, A. 2008. The Snøhvit Field. *In: Ramberg I.B., Brynhni I., Nøttvedt A. & Rangnes K. (eds.). The making of a land—geology of Norway.* Trondheim: Geological Society of Norway, 380p.

Folkestad, A., Satur, N. 2008. Regressive and transgressive cycles in a rift-basin: depositional model and sedimentary partitioning of the Middle Jurassic Hugin Formation, Southern Viking Graben, North Sea. *Sedimentary Geology,* **207**, 1-21.

Folkestad, A., Veselovsky, Z., Roberts, P. 2012a. Utilising borehole image logs to interpret delta to estuarine system: a case study of the subsurface Lower Jurassic Cook Formation in the Norwegian northern North Sea. *Marine and Petroleum Geology,* **29**, 255-275.

Folkestad, A., Skar, T., Pearce, M., A., 2012b. Using sedimentology, biostratigrapy and tectonics to interpret a complex rift-graben: The Middle-Late Jurassic South Viking Graben, North Sea. Abstract presented at the American Association of Petroleum Geologists Annual Meeting Long Beach, California, 22-25 April.

Folkestad, A., Odinsen T. H. Fossen, Pearce, M.A. 2014. Tectonic influence on the Jurassic sedimentary architecture in the northern North Sea with focus on the Brent Group. *International Association of Sedimentologists,* Special Publication, **46**, 389–416.

Folkestad, A., Johannessen, E.P., Steel, R.J., 2015. Variation in stacking style of delta-estuary couplets and associated deep-marine fans: An example from the Eocene Central Basin

of Spitsbergen. Abstract presented at the American Association of Petroleum Geologists Annual Meeting Denver, Colorado, 1-3 June.

Ford, M., Hemelsdael, R., Mancini, M., Palyvos, N. 2016. Rift migration and lateral propagation: evolution of normal faults and sediment-routing systems of the western Corinth rift (Greece). *In: Childs, C., Holdswort, R.E., Jackson, C.A.L., Manzocchi, T., Walsh, J.J., Yieling, G. (eds). The Geometry and Growth of Normal Faults.* Geological Society of London, Special Publications, 439pp.

Fossen, H., Khani, H.F., Faleide, J.I., Ksienzyk, A.K., Dunlap, W.J. 2017. Post-Caledonian extension in the West Norway – northern North Sea region: The role of structural inheritance. *In: Childs, C., Holdswort, R.E., Jackson, C.A.L., Manzocchi, T., Walsh, J.J., Yieling, G. (eds). The Geometry and Growth of Normal Faults.* Geological Society of London, Special Publications, **439**, 465–486.

Fraser, S. I., Robinson, A. M., Johnson, H. D., Underhill, J. R., Kadolsky, D. G. A., Connell, R., Johannesson, P., Ravnås, R. 2003. *In: Evans, D., and Graham, C. G. (eds),* Upper Jurassic, The Millennium Atlas: Petroleum Geology of the central and northern North Sea, Geological Society of London, 157–189.

Frazier, D. E., 1974. Depositional episodes: their relationship to the Quaternary stratigraphic framework in the northwestern portion of the Gulf basin. Austin, TX, Bureau of Economic Geology, , 74-l, 28p.

Frostick, L. E., Steel, R. J. 1993. Sedimentation in divergent plate-margin basins. Special Publication, *International Association Sedimentology,* **20**, 111-128

Færseth, R. B. 1996. Interaction of Permo-Triassic and Jurassic fault blocks during the development of the Northern North Sea. *Journal of the Geological Society,* London, **153**, 931-944.

Færseth, R.B., Ravnås, R. 1998. Evolution of the Oseberg fault-block in context of the Northern North Sea structural framework. *Marine and Petroleum Geology,* **15**, 467–490.

Gabrielsen, R.H., Faleide, J.I., Pascal, C., Braathen, A., Nystuen, J.P., Etzelmuller, B. O'donnel, S. 2010. Latest Caledonian to present tectono-morphological development of southern Norway. *Marine and Petroleum Geology,* **27**, 709–723.

Garner, H. F. 1979. Coarsening-upwards cycles in the alluvium of Hornelen Basin (Devonian), Noway. Sedimentary response to tectonic events: Discussion. *Geological Society of America Bulletin,* **90**, 121-124.

Gawthorpe, R. L., Fraser, A. J., Collier, R. E. L. I. 1994. Sequence stratigraphy in active extensional basins: implications for the interpretation of ancient basin-fills. *Marine Petroleum Geology,* **11**, 642-658.

Gawthorpe, R.L. Leeder M.R. 2000. Tectono-sedimentary evolution of active extensional basins. *Basin Research,* **12**, 195-218.

Gjelberg, J., Dreyer, T., Holes, A., Tjelland, T., Lilleng, T. 1987. Late Triassic to Mid Jurassic sandbody development on the Barents and mid- Norwegian shelf. *In: Brooks, J., Glennie, K. W. (eds), Petroleum Geology of Northwest Europe.* Graham & Trotman, London, 1105-1129.

Gómez, J. J., Comas-Rengifo, M. J., Goy, A. 2016. Palaeoclimatic oscillations in the Pliensbachian (Early Jurassic) of the Asturian Basin (Northern Spain), *Clim. Past,* **12**, 1199–1214.

Gomez-Veroiza, C.A., Steel. R.J. 2010. Iles clastic wedge development and sediment partitioning within a 300-km fluvial to marine Campanian transect (3 m.y.), Western Interior seaway, southwestern Wyoming and northern Colorado. *American Association Petroleum Geology Bulletin,* **94**, 1349-1377.

Gradstein, F.M., Anthonissen, E., Brunstad, H., Charnock, M., Hammer, O. Hellem, T., Lervik, K.S. 2010. Norwegian offshore stratigraphic lexicon (NORLEX). Newsletters on Stratigraphy, **44**, 73-86.

Gressley, A. 1838. Observations geologiques sur le Jura Soleurois. *Schweizer Gesellgesamten Naturwiss*. Neue Demkschr, **2**, 1-112.

Gupta, S., Underhill, J.R., Sharp, I.R., Gawthorpe, R.L., 1999. Role of fault interactions in controlling synrift sediment dispersal patterns: Miocene, Abu Alaqa Group, Suez Rift, Sinai, Egypt. *Basin Research,* **11**, 167-189.

Hadlari, T., Midwinter, D., Galloway, J.M., Dewing, K., Durbano, A.M., 2016. Mesozoic rift to post-rift tectonostratigraphy of the Sverdrup Basin, Canadian Arctic. *Marine and Petroleum Geology,* **76**, 148–158.

Hampson, G.J. 2000. Discontinuity surfaces, clinoforms, and facies architecture in a wave-dominated, shoreface-shelf parasequence. *Journal of Sedimentary Research,* **70**, 325-340.

Hampson, G.J., Sixsmith, P.J., Johnson, H.D. 2004. A sedimentological approach to refining reservoir architecture in a mature hydrocarbon province: The Brent Province, UK North Sea. *Marine and Petroleum Geology,* **21**, 457–484.

Hampson, G., Sixsmith, P.J., Kieft, R.L., Jackson, C.A.L., Johnson, H.D. 2009. Quantitative analysis of net transgressive shoreline trajectories and stratigraphic architectures: mid to late Jurassic of the North Sea Basin. *Basin Research,* **21**, 528-558.

Haq, B.U., Hardenbol, J., Vail, P.R. 1987. Chronology of fluctuating sea levels since the Triassic. *Science,* **235**, 1156–1167.

Haq, U.B., 2017. Jurassic Sea-Level Variations: A Reappraisal., *Geological Society of America Today*, **28**, 1–7.

Helland-Hansen W., Aston, M., Lomo, L., Steel, R. J. 1992. Advance and retreat of the Brent delta: regent contributions to the depositional model. *In: Geology of the Brent Group (Eds A. C. Morton, R. S., Haszeldine, M. R. Giles and S. Brown)*, Special Publication Geological Society of London, **61**, 109-127.

Helland-Hansen, W., Gjelberg, J. G. 1994. Conceptual basis and variability in sequence stratigraphy: a different perspective. *Sedimentary Geology,* **92**, 31-52.

Helland-Hansen, W., Hampson G.J. 2009. Trajectory analysis: concepts and applications. *Basin Research,* **21**, 454-483.

Hempton, M.R., Dunne, L.A. 1984. Sedimentation in pull-apart basins: active examples in eastern Turkey. *The Journal of Geology,* **92**, 513–530.

Hess, S., Nagy, J., Laursen, G.V., 2014. Benthic foraminifera from the Lower Jurassic transgressive mudstones of the south-western Barents Sea—a possible high latitude expression of the global Pliensbachian-Toarcian turnover. *Polar Research*, 33.

Hijma, M.P., Cohen, K.M., Hoffmann, G., Van der Spek, A.J.F., Stouthamer, E. 2009. From river valley to estuary: the evolution of the Rhine mouth in the early to middle Holocene (western Netherlands, Rhine-Meuse delta): *Geologie en Mijnbouw,* **88**,13–53.

Hunt, D., Tucker, M.E., 1992. Stranded parasequences and the forced regressive wedge systems tract: deposition during base-level fall. *Sedimentary Geology,* **81**, 1–9.

Husmo, T., Hamar, G., Høiland, O., Johannessen, E.P., Rømuld, A., Spencer, A., Titterton, R. 2003. Lower and Middle Jurassic. *In: Evans, D. (ed.) The Millennium Atlas: Petroleum Geology of the Central and Northern North Sea.* Geological Society, London, 129–155.

Isla, F.I., Bujalesky, G.G., 2004. Morphodynamics of a gravel-dominated macrotidal estuary: Rio Grande, Tierra del Fuego. *Association of Geologists Argentina,* **59**, 220-228.

Jackson, C.A-L., Gawthorpe, R.L., Carr, I.D., Sharp, I.R. 2005. Normal faulting as a control on the stratigraphic development of shallow marine syn-rift sequences: the Nukhul and Lower Rudeis Formations, Hammam Faraun fault block, Suez Rift, Egypt. *Sedimentology,* **52**, 313– 338.

Jouanneau, J.M., Latouche, C., 1981. The Gironde Estuary, *Contributions to Sedimentology,* Stuttgart, E. Sehweizerbartsche Verlagsbuchhandlung, **10**, 115pp.

Kesel, R.H. 2003. Human modifications to the sediment regime of the Lower Mississippi River flood plain. *Geomorphology,* **56**, 326–334.

Khalil, S.M., McClay, K.R., 2001. Tectonic evolution of the northwestern Red Sea–Gulf of Suez rift system. *In: Wilson, C.J, Whitmarsh, R. (Eds.),* Non-Volcanic Rifted Margins, Geological Society of London Special Publication, **187**, 453-473.

Kieft, R. L, Jackson,C. A.-L., Hampson, G. J., Larsen, E. 2010. Sedimentology and sequence stratigraphy of the Hugin Formation, Quadrant 15, Norwegian sector, South Viking Graben. *In: B. A. Vining and S. C. Pickering, eds., Petroleum Geology: From mature basins to new frontiers—Proceedings of the 7th Petroleum Geology Conference*. Geological Society of London, 157–176.

Larsen, Ø., Fossen, H., Langeland, K., Pedersen, R. B. 2003. Kinematics and timing of polyphase post-Caledonian deformation in the Bergen area, SW Norway. *Norwegian Journal of Geology,* **83**, 149–165.

Leckie D. A., Rumpel, T. 2003. Tide-influenced sedimentation in a rift basin—Cretaceous Qishn Formation, Masila Block, Yemen: a billion-barrel oil field. *American Association of Petroleum Geologists Bulletin,* **87**, 987–1013.

Lee, M.J., Hwang, Y.J. 1993. Tectonic evolution and structural styles of the East Shetland Basin. *In: Parker, J.R. (ed.) Petroleum Geology of Northwest Europe: Proceedings of the 4th Conference.* Geological Society, London, 1137–1149.

Leeder, M. R., Gawthorpe, R. L. 1987. Sedimentary models for extensional tilt-block/half-graben basins. *In: Continental Extensional Tectonics (Eds M. P. Coward, J. F. Dewey and P. L. Hancock),* Special Publication, Geological Society of London, **28**, 139- 152.

Leeder, M.R., Harris, T., Kirkby, M.J., 1998. Sediment supply and climate change: implications for basin stratigraphy. *Basin Research*, **10,** 7-18.

Leva Lopez, J., Rossi, V., Olariu, C., Steel, R., 2016. Architecture and recognition criteria of ancient shelf ridges: an example from Campanian Almond Formation in Hanna Basin, USA: *Sedimentology,* **63,** 1651–1676.

Lewis, M.M., Jackson, C.A., Gawthorpe, R.L. 2017. Tectono- sedimentary development of early syn-rift deposits: the Abura Graben, Suez Rift. Egypt. *Basin Research,* **29**, 327-351.

Livbjerg, F., Mjøs, R. 1989. The Cook Formation, an offshore sand ridge in the Oseberg area, northern North Sea. *In: Collinson, J. D. (ed.) Correlation in Hydrocarbon Exploration.* Norwegian Petroleum Society, Graham & Trotman, London, 299-312.

Liu, S.F., Nummedal, D., 2004. Late Cretaceous subsidence in Wyoming: Quantifying the dynamic component. *Geology,* **32**, 397–400.

Lyell, C., 1830. *Principles of Geology.* John Murray publishing, London, **1**, 511pp.

Løseth, T.M., Ryseth, A.E., Young, M., 2009. Sedimentology and sequence stratigraphy of the Middle Jurassic Tarbert Formation, Oseberg South area (northern North Sea). *Basin Research,* **21**, 597–619.

Mader, D., Peryt, T. 1995. Evolution of palaeoecology and palaeoenvironment of Permian and Triassic fluvial basins in Europe. Vol. 1: Western and Eastern Europe, Vol. 2: Southeastern Europe and index: by D. Mader, Gustav Fischer, Stuttgart, 1992. *Palaeogeography Palaeoclimatology Palaeoecology,* **111**, 181–181.

Mann, P., Hempton, M.R., Bradley, D.C., Burke, K. 1983. Development of pull-apart basins. *Journal of Geology,* **91**, 529–534.

Martinius, A.W., Kaas, I., Næss, A., Helgesen, G., Kjærefjord, J.M., Leith, D.A. 2001. Sedimentology of the heterolithic and tide-dominated Tilje Formation (Early Jurassic, Halten Terrace offshore mid Norway). *In: Martinsen, O.J., and Dreyer, T., (eds.), Sedimentary Environments Offshore Norway—Paleozoic to Recent.* Norwegian Petroleum Society, Special Publication, **10**, 103–144.

Martins-Neto, M.A., O. Catuneanu, 2010. Rift sequence stratigraphy. *Marine and Petroleum Geology,* **27**, 247-253

McKie, T., Williams, B. 2009. Triassic palaeogeography and fluvial dispersal across the northwest European Basins. *Geological Journal,* **44**, 711–741.

McLeod, A.E., Dawers, N.H., Underhill, J.R., 2000. The propagation and linkage of normal faults: insights from the Strathspey–Brent–Statfjord fault array, northern North Sea. *Basin Research,* **12**, 263–284.

Miller, K. G., Mountain, G. S., Browning, J. V., Kominz, M., Sugarman, P. J., Christie-Blick, N., Katz, M. E., Wright, J. D., 1998. Cenozoic global sea-level, sequences, and the New Jersey Transect. Results from coastal plain and slope drilling. *Reviews of Geophysics,* **36**, 569–601.

Mjøs, R. 2009. Anatomy of the seaward steps and seaward termination of the Brent clastic wedge. *Basin Research*, **21**, 573–596.

Muto, T., Steel R.J., 1992. Retreat of the front in a prograding delta, *Geology,* **20**, 967-970.

Nystuen, J.P., Knarud, R., Jorde, K., Stanley, K.O. 1989. Correlation of Triassic to Lower Jurassic sequences, Snorre field and adjacent areas, Northern North Sea. *In: Collison, J.D. (ed.) Correlation in Hydrocarbon Exploration.* Norwegian Petroleum Society, Graham & Trotman, London, 273–289.

Nystuen, J.P., Fält, L.-M. 1995. Upper Triassic–Lower Jurassic reservoir rocks in the Tampen Spur area, Norwegian North Sea. *In: Hanslien, S. (ed.) Petroleum Exploration and Exploitation in Norway.* Norwegian Petroleum Society Special Publications, **4**, 135–179.

Nøttvedt, A., Gabrielsen, R. H., Steel, R. J. 1995. Tectonostratigraphy and sedimentary architecture of rift basins, with reference to the northern North Sea. *Marine and Petroleum Geology,* **8**, 881–901.

Nøttvedt A., Johannessen E. P., Surlyk F. 2008. The Mesozoic of western Scandinavia and East Greenland. *Episodes,* **31**, 59–65.

Odinsen, T., Reemst, P., Van Der Beek, P., Gabrielsen, R.H., Faleide, J.I., 2000. Permo-Triassic and Jurassic extension in the northern North Sea: results from tectonostraigraphic forward modelling. *Geological Society, London,* Special Publication, **167**, 83-104.

Orre, L.T.E., Folkestad A. 2019. Depositional environments of the Early to Middle Triassic Northern North Sea in a syn-rift to a post-rift setting. *Geological Society, London,* Special Publications, **64**. 21pp.

Ottesen, S., Folkestad, A., Gawthorpe, R., 2005. Tectono-stratigraphic development of the Hammerfest Basin (Northern Norway) during the Jurassic to Cretaceous. Abstract presented at the American Association of Petroleum Geologists Annual Meeting Houston, Texas, 9-12 April.

Plint, A. G., Kreitner, M. A., 2007. Extensive, thin sequence spanning Cretaceous foredeep suggest high-frequency eustatic control: Late Cenomanian, Western Canada foreland basin. *Geology,* **35**, 735–738.

Posamentier, H. W., Jervey M. T., Vail, P. R. 1988. Eustatic controls on clastic deposition I — conceptual framework. *In: C. K. Wilgus, B. S. Hastings, C. G. St. C. Kendall, H. W. Posamentier, C. A. Ross and J. C. Van Wagoner, (eds). Sea Level Changes — An Integrated Approach*, Special Publication, Society of Economic Paleontologists and Mineralogists, **42,** 110–124.

Posamentier, H., Allen, G. P. 1993. Variability of the sequence stratigraphic model: effects of local basin factors. *Sedimentary Geology,* **91**, 91-109.

Prosser, S. 1993. Rift-related linked depositional systems and their seismic expression. *In: Tectonics and Seismic Sequence Stratigraphy (Eds: G. D. Williams and A. Dobb)*, Special Publication, Geological Society of London, **71**, 35-66.

Pyrcz, M., Deutsch, C. 2014. Geostatistical Reservoir Modeling, 2nd Edition, Oxford University Press, New York, USA, 429pp.

Ravnås, R., Nøttvedt, A., Steel, R.G., Windelstad, J. 2000. Syn-rift sedimentary architectures in the Northern North Sea. *In: Nøttvedt, A. (eds) Dynamics of the Norwegian Margin.* Geological Society, London, Special Publications, **167**, 133–177.

Ramberg, I.B., Solli A., Nordgulen, Ø., 2008. *The Making of a Land: Geology of Norway.* The Norwegian Geological Association, Trondheim, 624pp.

Rattey, R. P., Hayward A. B., 1993. Sequence stratigraphy of a failed rift system: The Middle Jurassic to Early Cretaceous basin evolution of the central and northern North Sea. *In J. R. Parker, ed., Petroleum geology of northwest Europe: Proceedings of the 4th Conference,* London, The Geological Society, 215–249.

Reynaud, J. Y., Dalrymple, R. W. 2012. Shallow-marine tidal deposits. *In: R.A. Davis, Jr. and R.W. Dalrymple (eds.), Principles of Tidal SedimentoloSpringerDavis, S., Dalrymple, R.W., (eds.), Principles of Tidal Sedimentation*. Springer Verlag, Berlin, 335-369.

Richards, P. C. 1991. An estuarine facies model for the Middle Jurassic Sleipner Formation, Beryl Embayment, North Sea. *Journal of the Geological Society of London,* **148**, 459-471.

Roberts, J. D., Marthieson, A. S., Hampson, J. M. 1987. Statfjord. *In: Spencer, A. M. et al. (eds) Geology of the Norwegian Oil and Gas Fields.* Graham & Trotman, London, 319-340.

Roberts, D. G., Thompson, M., Mitchhener, B., Hossack, J., Carmichael, S. M. M., Bjørnseth, H. M. 1999. Palaeozoic to Tertiary rift and basin dynamics; mid-Norway to the Bay of Biscay; a new context for hydrocarbon prospectivity in the deepwater frontier. *In: Fleet, A. J., Boldy, S. A. R. (eds) Petroleum Geology of Northwest Europe: Proceedings of the 5th Conference.* Geological Society, London, 7–40.

Roberts, A. M., Kusznir, N.J., Yielding, G., Beely, H., 2019. Mapping the bathymetric evolution of the northern North Sea: From Jurassic syn-rift archipelago through Cretaceous-Tertiary post post-rift subsidence. *Petroleum Geoscience,* **25**, 306-321.

Rodgers, D. A. 1980. Analysis of pull-apart basin development produced by enchelon strike-slip faults. *In: Sedimentation in Oblique-slip Mobile Zones (Bailance, P. F. & Reading, H. G., eds).* Spec. Publ. Int. Assoc. Sedimentology. **4**, 27-41.

Rovere, A., Stocchi P., Vacchi M. 2016. Eustatic and relative sea-level changes. *Curr. Clim. Change Rep.,* **2**, 221-231.

Ryseth, A., 2000. Differential subsidence in the Ness Formation (Bajocian), Oseberg area, northern North Sea: facies variation, accommodation space and sequence stratigraphy in a deltaic distributary system. *Norwegian Geological Journal,* **80**, 9-25.

Sarah D., Soebowo E., 2018. Land Subsidence Threats and Its Management in the North Coast of Java. *Global Colloquium on GeoSciences and Engineering, IOP Conference Series*, Earth and Environmental Science.

Sawyer, M., Keegan, J. 1996. Use of palynofacies characterization in sand-dominated sequences, Brent Group, Ninian Field, UK North Sea. *Petroleum Geoscience,* **2**, 289-297.

Schlager, W. 1993. Accommodation and supply - a dual control on stratigraphic sequences. *In: Cloetingh, S., Sassi, W., Horvath, F., Puigdefabregas, C. (Eds), Basin Analysis and Dynamics of Sedimentary Basin Evolution.* Sedimentary Geology, **86**, 111-136.

Seguret, M., Seranne, M., Chauvet, A., Brunel, M., 1989. Collapse basin: a new type of extensional sedimentary basin from the Devonian of Norway. *Geology,* **17**, 127–130.

Shackelton, N.J. 1987. Oxygen isotopes, ice Volume and sea Magnetostratigraphy of the Plio-Pleistocene Camp Rice and level. *Quaternary Science Review,* **6**, 183–190.

Shanley, K.W., McCabe, P.J., 1994. Perspectives on the sequence stratigraphy of continental strata. *American Association of Petroleum Geology Bulletin,* **78**, 544–568.

Simms, A., L.C. Reynolds, M. Bentz, A. Roman, T. Rockwell, Peters. R. 2016. Tectonic subsidence of California estuaries increases forecasts of relative sea-level rise. *Estuaries and Coasts,* **39**, 1571-1581.

Simpson, G., Castelltort, S., 2012. Model shows that rivers transmit high-frequency climate cycles to the sedimentary record. *Geology,* **40**, 1131–1134.

Sloss, L. L., 1963, Sequences in the cratonic interior of North America: *Geological Society of America Bulletin,* **74**, 93-114.

Steckler, M.S., Reynolds, D.J., Coakley, B.J., Swift, B.A., Jarrard, R., 1993. Modelling passive margin sequence stratigraphy. *International Association of Sedimentologists,* Special Publication, **18**, 19–41.

Steel, R. 1976. Devonian basins of western Norway – sedimentary response to tectonism and to varying tectonic context. *Tectonophysics,* **36**, 207–224.

Steel, R.J., Mæhle, S., Nilsen, H., Røe, S.L., Spinnangr, A. 1977. Coarsening-upward cycles in the alluvium of Hornelen Basin (Devonian), Norway. Sedimentary response to tectonic events. *Geological Society of America Bulletin,* **88**, 1124-1134.

Steel, R. J., Gloppen, T.O., 1980. Late Caledonian (Devonian) basin formation, western Norway: signs of strike-slip tectonics during infilling. *In: Reading, H., and Ballance, P. F., (Eds.), Sedimentation in Oblique-Slip Mobile Zones.* Special Publication, International Association of Sedimentologists, **4**, 79-103.

Steel, R.J. 1988. Coarsening-upward and skewed fan bodies: symptoms of strike-slip and transfer fault movement in sedimentary basins. *In: Nemec, W., Steel, R.J., (Eds.), Fan Deltas: Sedimentology and Tectonic Settings.* Glasgow, Blackie & Sons, 77–83.

Steel, R., Ryseth, A. 1990. The Triassic-Early Jurassic succession in the northern North Sea: megasequence stratigraphy and intra-Triassic tectonics. *In: Hardman, R. F.*

P., Brooks, J. (eds.), Tectonic Events Responsible for Britain' s Oil and Gas Reserves. Geological Society of London Special Publication, **55**, 139-168.

Steel, R.J. 1993. Triassic–Jurassic megasequence stratigraphy in the Northern North Sea: rift to post-rift evolution. *In: Parker, J.R. (ed.) Petroleum Geology of Northwest Europe: Proceedings of the 4th Conference.* Geological Society, London, 299–315.

Steel, R.J., Milliken, K.L. 2013. Major advances in siliciclastic sedimentary geology, 1960–2012. *In: Bickford, M.E., (ed.), The Web of Geosciences: Advances, impacts and interactions.* Geological Society of America, Special Paper, **500**, 121–167.

Stewart, J.H., 1983. Extensional tectonics in the Death Valley area, California: Transport of the Panamint Range structural block 80 km northwestward: *Geology*, **11**, 153–157.

Swenson, J. B., Paola, C., Pratson, L., Voller, V. R., Murray, A. B. 2005. Fluvial and marine controls on combined subaerial and subaqueous delta progradation: Morphodynamic modeling of compound-clinoform development. *Journal of Geophysical Research: Earth Surface,* 110.

Syvitski, J. P. M., Milliman, J. D. 2007. Geology, geography and humans battle for dominance over the delivery of sediment to the coastal ocean. *Journal of Geology,* **115,** 1–19.

Sømme, T.O., Doré, A.G., Lundin, E.R., and Tørudbakken, B.O., 2018. Triassic–Paleogene paleogeography of the Arctic: Implications for sediment routing and basin fill. *American Association of Petroleum Geologists Bulletin,* **102**, 2481– 2517.

Teatini, P., Tosi, L., T. Strozzi, 2011. Quantitative evidence that compaction of Holocene sediments drives the present land subsidence of the Po Delta, Italy, *Journal of Geophysical Research,* 116.

Tebbett, S. B., Goatley, C. H. R., Bellwood, D. R. 2017. Fine sediments suppress detritivory on coral reefs. *Marine Pollution Bulletin,* **114**, 934–940.

Titus, S. J., Fossen, H., Pedersen, R. B., Vigneresse, J. L., Tikoff, B. 2002. Pull-apart formation and strike-slip partitioning in an obliquely divergent setting, Leka ophiolite, Norway. *Tectonophysics,* **354**, 101–119.

Tugend, J., Manatschal, G., Kusznir, N.J., Masini, E., Mohn, G., Thinon, I., 2014. Formation and deformation of hyperextended rift systems: insights from rift domain mapping in the Bay of Biscay–Pyrenees. *Tectonics,* **33**, 1239–1276.

Underhill, J.R., Partington, M.A. 1994. Use of maximum flooding surfaces in determine a regional control on the Intra-Aalenian Mid Cimmerian sequence boundary: implications of North Sea basin development and Exxon's sea-level chart. *In: Posamentier, H.W., Wiemer, P.J. (eds) Recent Advances in Siliciclastic Sequence Stratigraphy.* American Association of Petroleum Geologists, Memoirs, **58**, 449–484.

Vail, P.R., Mitchum Jr., R.M., Thompson III, S., 1977. Seismic stratigraphy and global changes of sea level, part 3: relative changes of sea level from coastal onlap. *In: Payton, C.E. (Ed.), Seismic Stratigraphy — Applications to Hydrocarbon Exploration. Memoir*. American Association of Petroleum Geologists, **26,** 63–81.

Van Houten, F. B., 1974. Northern Alpine molasse and similar Cenozoic sequences of southern Europe. *In: Dott, R. H., Jr., Shaver, R. H., eds., Modern and ancient geosynclinal sedimentation*. Soc. Econ. Paleontologists and Mineralogists Spec. Pub. **19**, 260-273.

Van Wagoner, J. C., D. C. Jeannette., P. Tsang, G. P. Hamar, Kaas, I. 1993. Applications of high-resolution sequence stratigraphy and facies architecture in mapping potential additional hydrocarbon reserves in the Brent Group, Statfjord field. International conference on sequence stratigraphy: advances and applications for exploration and production in northwest Europe, February 1–3, Norwegian Petroleum Society.

Van Wagoner, J.C., 1995. Overview of sequence stratigraphy of foreland basin deposits: terminology, summary of papers, and glossary of sequence stratigraphy. *In: Van Wagoner, J.C., Bertram, G.T. (Eds.), Sequence Stratigraphy of Foreland Basin*

Deposits: Outcrop and Subsurface Examples from the Cretaceous of North America. American Association of Petroleum Geologists, Memoir, **64**, 9-21.

Van Wagoner, J.C. 1998. Sequence stratigraphy and marine to nonmarine facies architecture of foreland basin strata, Book Cliffs, Utah, U.S.A. Reply. *American Association of Petroleum Geology Bulletin,* **82**, 1607– 1618.

Van Wijk, J., Axen, G., Abera, R., 2017. Initiation, evolution and extinction of pull-apart basins. Implications for opening of the Gulf of California. *Tectonophysics,* **719**, 37–50.

Vollset, J., Doré A. G., 1984. A revised Triassic and Jurassic lithostratigraphic nomenclature for the Norwegian North Sea. *Norwegian Petroleum Directorate Bulletin,* **3**, 2–53.

Walderhaug, O., Bjørkum, P.A. 2003. The effect of stylolite spacing on quartz cementation in the Lower Jurassic Stø Formation in well 7120/6-1, southern Barents Sea. *Journal of Sedimentary Research,* **73**, 145-155.

Walker, R.G., 1984. Facies models, Toronto, Geoscience Canada Reprint Series, **1**, 141-175.

Wennberg, O.P., Malm, O., Needham, T., Edwards, E., Ottesen, S., Karlsen, F., Rennan, L., Knipe R. 2008. On the occurrence and formation of open fractures in the Jurassic reservoir sandstones of the Snøhvit Field. SW Barents Sea. *Petroleum Geoscience,* **14**, 139-150.

Went, D. J., Hamilton, R. V., Platt, N. H., Underhill, J. R. 2013. Role of forced regression in controlling Brent Group reservoir architecture and perspectivity in the northern North Sea. *Petroleum Geoscience,* **19**, 307-328.

Wheeler, H. E., 1964. Baselevel, lithosphere surface, and time-stratigraphy. *Geological Society of America Bulletin,* **75**, 599–610.

Zanella, E., Coward, M.P., 2003. Structural framework. *In: Evans, D., Graham, C., Armour, A., and Bathurst, P., (eds.),* The Millennium Atlas. Petroleum geology of the central and Northern North Sea. Geological Society of London, 45-59.

Ziegler, P.A., Van Hoorn, B. 1989. Evolution of North Sea rift system. *In: Tankard, A.J., Balkwill, H.R. (eds), Extensional Tectonics and Stratigraphy of the North Atlantic Margins.* Amer can Association of Petroleum Geologists, 471–500.

Ziegler, P.A., 1990. Collision related intra-plate compression deformations in Western and Central Europe. *Journal of Geo-dynamics,* **11**, 357–388.

Yoshida, S., Willis, A., Miall, A. D., 1996. Tectonic control of nested sequence architecture in the Castlegate Sandstone (Upper Cretaceous), Book Cliffs, Utah. *Journal of Sedimentary Research,* **66**, 737–748.

8. Appendix

8.1 Appendix 1a.

Folkestad, A., Ottesen, S., Rømuld, A. 2005. Reservoirs in a structurally controlled estuary: the Jurassic Snøhvit gas condensate Field, Barents Sea, Norway. Abstract presented at the American Association of Petroleum Geologists Annual Meeting Calgary, Alberta, 19–22 June. Abstract reprinted with permission from AAPG, whose permission is required for further use.

Reservoirs in a Structurally Controlled Estuary: The Jurassic Snøhvit Gas-Condensate Field, Barents Sea, Norway

Atle Folkestad, Signe Ottesen, and Arnfinn Rømuld
STATOIL, Stavanger, Norway

Development planning for gas-condensate production from the Snøhvit Field in the continental, rifted Hammerfest Basin, has provided an opportunity for revisiting the key sedimentary and tectonic controls on this important region of the Barents Shelf. Analysis of 2D and 3D seismic data together with some 17 exploration and appraisal wells and 1600 meters of cores now shows the importance of tectonically-enhanced accommodation creation during deposition of the Upper Triassic-Middle Jurassic succession.

The study interval of strata consists of a fluvial/coastal plain clastic wedge (Tubåen and Nordmela formations) overlain by a thick estuarine succession (Stø Formation). The latter consists of (in stratigraphic younging order) (a) inner-estuary tidal/fluvial sandstones, (b) lagoonal/central basin mudstones and sandstones, (c) beach-barrier sandstones and (d) offshore mudstones (Fuglen Formation). This succession is overall transgressive, and is unusually thick to be estuary-infill. It is interpreted as estuarine because of the two clear fluvial and marine sediment-input points, its tidal facies, and because of the landward-stepping stacking pattern of the strata. Syn-sedimentary tectonic movement on a fault zone centrally in the basin and on the northern margin fault complex apparently provided a rapidly subsiding trough in this northwestern part of the Hammerfest Basin. This, in turn, created ideal conditions for large-scale transgression and for the thick accumulation of the linked fluvial-brackish water- shallow marine deposits. This type of tectonically controlled estuarine valley fill differs significantly from the conventional incised-valley estuaries.

AAPG Search and Discovery Article #90039©2005 AAPG Calgary, Alberta, June 16-19, 2005

8.2 Appendix 1b.

Ottesen, S., Folkestad, A., Gawthorpe, R., 2005. Tectono-stratigraphic development of the Hammerfest Basin (Northern Norway) during the Jurassic to Cretaceous. Abstract presented at the American Association of Petroleum Geologists Annual Meeting Houston, Texas, 9-12 April. Abstract reprinted with permission from AAPG, whose permission is required for further use.

[First Hit]

Tectono-Stratigraphic Development of the Hammerfest Basin (Northern Norway) During the Jurassic to Cretaceous

Signe Ottesen[1], Atle Folkestad[2], and Robert Gawthorpe[3]

[1] Statoil, Stavanger, Norway

[2] Statoil, Bergen, Norway

[3] University of Manchester, Manchester, England

The development of the Snøhvit gas-condensate field has led to a renewed interest in the Hammerfest Basin in the Barents Sea. This study emphasized the linkage between tectonics and stratigraphy, and produced a series of paleogeographic maps over the area from Jurassic to Cretaceous time. Analysis of 2D and 3D seismic data combined with a total of 48 wells with cored material shows the importance of tectonically-enhanced accommodation creation during deposition of the studied succession.

The Early Jurassic Stø Fm, the main reservoir on the Snøhvit Field, represents a tectonically controlled wave-dominated estuary that was transgressed while deep marine conditions prevailed in the axial part of the Hammerfest basin. In middle to upper Jurassic time, sedimentation was restricted to both shallow and deep marine deltas along the northern and southern margins of the basin, with mudstone deposits in the central/axial part of the basin. During the Cretaceous, the depositional style changed to include deep marine fans extending far into the basin along structural elements. Subsequently, deep marine fans were also formed by sediments eroded from elevated structural elements in the central/axial part of the basin and slight relative tectonic uplifts of the margins. In the later part of the Early Cretaceous, tectonic activity diminished both in the central part and the southern margin of the basin with some deep marine fan developments on the northern margin. These paleogeographic maps have proven valuable as inputs to prospect evaluation of the Jurassic to Cretaceous succession in the Hammerfest Basin.

8.3 Appendix 1c.

Folkestad, A. 2008. The Snøhvit Field. *In: Ramberg I.B., Brynhni I., Nøttvedt A. & Rangnes K. (eds.). The making of a land—geology of Norway.* Trondheim: Geological Society of Norway, p. 380. Plate reprinted with permission from NGF, whose permission is required for further use.

THE SNØHVIT FIELD *By Atle Folkestad*

The Snøhvit Field comprises the Askeladd, Albatross and Snøhvit discoveries and is located in the centre of the Hammerfest Basin. The field contains gas and small volumes of light oil. The Stø Formation represents the main reservoir, where the estuarine sandstones that make up about half of the succession exhibit the best flow properties for gas. These excellent flow characteristics are the result of the action of waves and tidal currents that sorted the sandstone and washed away all finer-grained material. A lesser proportion of the Stø Formation is made up of beach deposits, which also exhibit adequate reservoir properties, but are not of the same quality as the estuarine deposits. Finer-grained sandstones situated seaward and leeward of the barrier islands exhibit somewhat poorer flow properties as a result of the increased proportion of silt and clay particles in the sandstone, and some of the sandstone pores have been blocked by calcite cement derived from dissolved oyster shells.

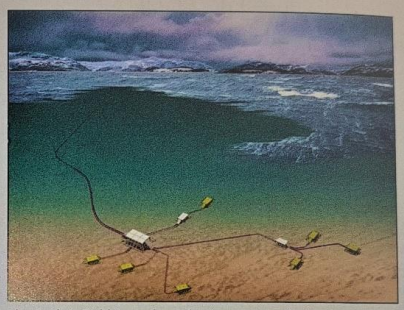

The Snøhvit Field is a subsea development producing gas to the processing plant on Melkøya in Finnmark. (Illustration: Statoil)

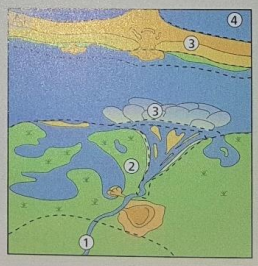

A) Schematic depositional model for the Stø Formation. The different depositional environments are numbered as follows: 1) alluvial plain, 2) tidal flats, 3) estuary, lagoon, beach, and barrier islands, 4) marine.

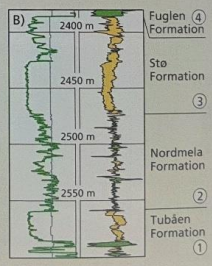

B) Sedimentary log from the Snøhvit field. The Tubåen, Nordmela, Stø and Fuglen Formations were deposited in contrasting coastal depositional environments. The numerals refer to the same environments as shown in A.

8.4 Appendix 2.

Folkestad, A., Skar, T., Pearce, M., A., 2012b. Using sedimentology, biostratigrapy and tectonics to interpret a complex rift-graben: The Middle-Late Jurassic South Viking Graben, North Sea. Abstract presented at the American Association of Petroleum Geologists Annual Meeting Long Beach, California, 22-25 April. Abstract reprinted with permission from AAPG, whose permission is required for further use.

Using Sedimentology, Biostratigraphy and Tectonics to Interpret a Complex Rift-Graben: The Middle-Late Jurassic South Viking Graben, North Sea

Folkestad, Atle [*1]; Skar, Tore [2]; Pearce, Martin A.[1]
(1) Stratigraphy, STATOIL ASA, Bergen, Norway.
(2) Structural Geology, STATOIL ASA, Stavanger, Norway.

The Jurassic Viking Graben in the North Sea is one of the important HC provinces in Europe. The main play model in the southern part of the graben has been used for more than 20 years. In such a setting an improvement in the depositional model will open up for sub-optimal or untested targets. Examination of basic data in terms of sedimentology, biostratigraphy and tectonics was undertaken to reach this ambition.

The Bathonian rifting in the North Viking Graben (NVG) accompanied and influenced the drowning of the HC-rich Brent Delta. The rifting propagated southwards into the Southern Viking Graben (SVG) where the shallow marine and HC bearing Hugin Fm was deposited. The SVG experienced initial rifting in the M Jurassic (Bathonian - Callovian) and the rift-activity escalated through Middle Jurassic and into the Late Jurassic.

The Hugin Fm was deposited during differential subsidence and early part of the rift-phase and show in places sedimentary wedges that suggests rotated fault blocks, especially in the upper half of the formation. The increase in tectonic signatures upwards in the formation illustrates the escalation of rift-activity and formation of low-relief half-graben topography. The sedimentary wedges show characteristic facies pattern with dominance of wave-reworked facies at the fault crest and tidal facies and a general decrease in net to gross in deeper parts of the half-grabens. The rift topography amplified the tidal currents and preservation of mudstones and tidally-dominated heterolithics due to wave-sheltering at the elevated fault crests. Such a complex basin topography caused by the rifting led to pronounced environmental differences with a large span in water-chemistry that is reflected in the biostratigraphic data.

The continued rifting of the SVG into the Late Jurassic led to pronounced rift topography. The rifting and an eustatic sea level fall operating at the same time (Kimmeridge) led to a geological setting facilitating the formation of source rock - the hot shale Draupne Formation. The SVG was at this time characterised by rotated half grabens with exposed footwall islands, giving restricted basins where anoxic shale formed. Locally derived gravity flows from the eroded crests of the footwall islands were in places shed into the sub-basins. These sub-basins therefore also acted as sedimentary traps for local sands delivered from the surrounding elevated areas.

AAPG Search and Discovery Article #90142 © 2012 AAPG Annual Convention and Exhibition, April 22-25, 2012, Long Beach, California

8.5 Appendix 3.

Folkestad, A., Johannessen, E.P., Steel, R.J., 2015. Variation in stacking style of delta-estuary couplets and associated deep-marine fans: An example from the Eocene Central Basin of Spitsbergen. Abstract presented at the American Association of Petroleum Geologists Annual Meeting Denver, Colorado, 1-3 June. Abstract reprinted with permission from AAPG, whose permission is required for further use.

Variation in Stacking Style of Delta-Estuary Couplets and Associated Deep-Marine Fans: An Example From the Eocene Central Basin of Spitsbergen

Atle Folkestad[1], Erik P. Johannessen[2] and Ron Steel[3]

[1]EXP NOR NORTH SEA, STATOIL ASA, Bergen, Norway
[2]EXP EE GCQ, STATOIL ASA, Stavanger, Norway
[3]Jackson School of Geoscience, University of Texas, Austin, Texas, United States
June 3, 2015 Wednesday 3:45 P.M. AAPG Annual Convention and Exhibition, Denver, CO.

Abstract

The Eocene of the Central Basin of Spitsbergen shows a series of eastward building clinothems deposited in a foreland basin. This basin was formed by a westerly active fold and thrust-belt which also acted as provenance area for these shallow-marine sand-wedges. Some of these shallow-marine wedges prograded onto the shelf, whereas some of them reached the shelf-edge and have associated deep-marine sand-lobes. Three of these clinothems have been studied with focus on depositional environment, lateral facies variations, internal stacking pattern and shoreline trajectory pattern. All of them show a regressive deltaic to transgressive estuary/tidal couplet. Internally, there are clear differences between the three clinothems in terms of the style of the regressive deltaic part and the transgressive estuary part. The deltaic parts range from a) fluvial and punctuated mass-flow style; b) wave reworked and delta front collapse style; and c) mixed tide and fluvial influenced delta. The transgressive parts of the clinothems show a variation of the thickness of estuary sandstones and coastal plain fines developments conditioned on the degree of aggradation. Previous studies of these Eocene clinothems have interpreted the associated deep-marine sand-lobes as due to: a) sea-level fall with shelf-incision and basinward movement of the deltaic system beyond the shelf-break; b) high sediment-supply mechanism as hyperpycnal flow within shelf-edge deltas feeding the basin-fans during sustained flow; and c) having a narrow shelf that easily gets prograded across with high sediment supply. On individual basis each of these clinothems can be interpreted with these mechanisms above. However, it is interesting to see how the shape and size of each clinothem has a direct effect on the next clinothem that occurs above. As a clinothem consist of a dominant muddy part, the mud-volume can be stored: at the shelf-edge and expand the width of the shelf, on the shelf and building up the shelf height or even be stored more landward within the lagoonal and coastal areas, starving the shelf. This study show how a volumetrically-limited clinothem enables the next clinothem above, to easily cross the shelf and feed sediments down the shelf slope from a fluvial delta. The two following clinothem faced a wider shelf that first gave a wave-dominated delta and finally a mixed tidal and fluvial delta capped by an estuary.

AAPG Datapages/Search and Discovery Article #90216 ©2015 AAPG Annual Convention and Exhibition, Denver, CO., May 31 - June 3, 2015

Graphic design: Communication Division, UiB / Print: Skipnes Kommunikasjon AS

uib.no

ISBN: 9788230851241 (print)
9788230861684 (PDF)